A

AGARD-AR-36-71

AGARD-AR-36-71

AGARD

ADVISORY GROUP FOR AEROSPACE RESEARCH & DEVELOPMENT

7 RUE ANCELLE 92 NEUILLY-SUR-SEINE FRANCE

AGARD ADVISORY REPORT No. 36

Report of the AGARD Ad Hoc Committee on

Engine-Airplane Interference and Wall Corrections in Transonic Wind Tunnel Tests

NORTH ATLANTIC TREATY ORGANIZATION

DISTRIBUTION AND AVAILABILITY ON BACK COVER

AGARD Advisory Report No.36-71

NORTH ATLANTIC TREATY ORGANIZATION

ADVISORY GROUP FOR AEROSPACE RESEARCH AND DEVELOPMENT

(ORGANISATION DU TRAITE DE L'ATLANTIQUE NORD)

REPORT OF THE AGARD AD HOC COMMITTEE

on

ENGINE-AIRPLANE INTERFERENCE AND WALL CORRECTIONS IN TRANSONIC WIND TUNNEL TESTS

UNLIMITED

This Ad Hoc Study was conducted as part of the AGARD Research and Development Activities Programme

THE MISSION OF AGARD

The mission of AGARD is to bring together the leading personalities of the NATO nations in the fields of science and technology relating to aerospace for the following purposes:

- Recommending effective ways for the member nations to use their research and development capabilities for the common benefit of the NATO community;
- Providing scientific and technical advice and assistance to the North Atlantic Military Committee in the field of aerospace research and development;
- Continuously stimulating advances in the aerospace sciences relevant to strengthening the common defence posture;
- Improving the co-operation among member nations in aerospace research and development;
- Exchanging of scientific and technical information;
- Providing assistance to member nations for the purpose of increasing their scientific and technical potential;
- Rendering scientific and technical assistance, as requested, to other NATO bodies and to member nations in connection with research and development problems in the aerospace field.

The highest authority within AGARD is the National Delegates Board consisting of officially appointed senior representatives from each Member Nation. The mission of AGARD is carried out through the Panels which are composed of experts appointed by the National Delegates, the Consultant and Exchange Program and the Aerospace Applications Studies Program. The results of AGARD work are reported to the Member Nations and the NATO Authorities through the AGARD series of publications of which this is one.

Participation in AGARD activities is by invitation only and is normally limited to citizens of the NATO nations.

Published August 1971

533.6.071.4

Printed by Technical Editing and Reproduction Ltd
Harford House, 7–9 Charlotte St. London. W1P 1HD

FOREWORD

Within AGARD, particularly within the Propulsion and Energetics, and the Fluid Dynamics Panels, it is felt that large uncertainties exist with respect to the present techniques for predicting aircraft performance at transonic speed, particularly with respect to engine installation and high lift. In order to review the present techniques as used in the various NATO countries and to gain insight into their specific merits and shortcomings, an Ad Hoc Committee under the leadership of Prof A.Ferri, was proposed by the Director of AGARD, and approved by the National Delegates at the 1970 Annual Meeting. The purpose was to study the above problems and, if possible, to make recommendations for further studies.

The selection of committee members by the National Delegates was completed in April 1970. The members of the Committee are as follows:

For France:
I.Berger, J.M.Hardy, B.Masure, P.Poisson-Quinton.

For Germany:
W.Alvermann, A.Heyser, E.Riester.

For Italy:
C.Casci, R.Monti.

For the Netherlands:
M.E.E.Enthoven, F.Jaarsma.

For the United Kingdom:
E.C.Carter, E.L.Goldsmith.

For the United States of America:
P.Antonatos, A.Ferri (Chairman), A.E.Fuhs, J.Jones, D.Zonars.

The Committee selected a list of technical organizations interested in the accuracy of wind tunnel data derived from three groups: (a) Wind tunnel operators and experimental research workers, (b) Airplane designers and airplane manufacturers, and (c) Airplane users and design evaluators.

As an initial step for the preparation of a meeting of the specialists, the Committee prepared a questionnaire for the selected organizations interested in this problem in each country; this was distributed by the members of the Committee of that country. The objective of the questionnaire was to obtain consistent and comparable sets of information on the approaches used to simulate engine interference and to evaluate the effects of incomplete simulation in wind tunnel tests of engine flow. A second questionnaire requested information on the type of corrections used for evaluating wall interference at high lift, on the criteria used for justifying the lack of corrections where corrections were not performed, and on the wind tunnel turbulence and its effects. Such questionnaires were prepared and finalized at the first meeting of the Ad Hoc Committee which took place at AGARD Headquarters on July 15–17, 1970. The questionnaire was distributed to all components of the three groups. A meeting of the interested specialists was planned at that time. It was decided that the results of the different contributions would be presented in an organized form and discussed, and that a set of conclusions and recommendations would then be generated. The Committee decided that at this second meeting only one representative of each organization that responded to the questionnaire would be invited, and that observers would be excluded.

The following companies, agencies and establishments cooperated in the study:

For France:
SNECMA, ONERA, SNIAS, Dassault.

For Germany:
DFVLR – AVA, Hamburger Flugzeugbau, Messerschmitt-Bölkow-Blohm, Vereinigte Flugtechnische Werke.

For Italy:
Fiat.

For the Netherlands:
N.L.R., Fokker.

For the United Kingdom:
A.R.A.
RAE (Farnborough and Bedford)
Rolls Royce (Hucknall and Bristol)
British Aircraft Corporation (Filton, Warton, Weybridge)
Hawker Siddeley Aviation (Brough, Hatfield, Kingston, Woodford).

For the United States of America:

NASA (Ames, Langley, Lewis), USAF,(ASD, FDL, APL, AEDC), ARO, Inc., Boeing
Fairchild Hiller (Republic Aviation Division)
Fluidyne
General Dynamics (Convair Division)
General Dynamics (Fort Worth Division)
General Motors (Allison Division)
Grumman Aerospace
Lockheed-Georgia Co.
LTV-Vought Aeronautics Division
McDonnell Douglas Corp.
Northrop, United Aircraft (Pratt and Whitney Division).

The second meeting was scheduled for 21–23 September 1970 in Florence, Italy at the Scuola di Guerra Aerea. The participants at the second meeting totalled 42; this list is available at AGARD. The discussions and presentations of the summaries took place on the first two days, September 21 and 22. On the third day the Committee members outlined the conclusions and recommendations to be transmitted to the organizations active in this field, and to the National Research Laboratories of the NATO Nations.

aircraft performance at transonic speeds, with particular respect to the installation of engines and the use of wind-tunnels for testing models at high lift.

Technical organisations interested in the accuracy of wind-tunnel data were selected from (a) wind-tunnel operators and experimental workers, (b) airplane designers and airplane manufacturers, and (c) airplane users and design evaluators. Questionnaires were sent to obtain consistent sets of information on the simulation of engine interference, evaluation of effects due to incomplete simulation in wind-tunnels of engine flow, wall corrections used for models at high lift, criteria justifying the lack of such corrections, and the effects of wind-tunnel turbulence.

The report
Advisory ~~Report No.36~~ presents edited versions of the data given in replies to the Questionnaires, and the conclusions and recommendations of the Ad Hoc Committee.
+1 GR

aircraft performance at transonic speeds, with particular respect to the installation of engines and the use of wind-tunnels for testing models at high lift.

Technical organisations interested in the accuracy of wind-tunnel data were selected from (a) wind-tunnel operators and experimental workers, (b) airplane designers and airplane manufacturers, and (c) airplane users and design evaluators. Questionnaires were sent to obtain consistent sets of information on the simulation of engine interference, evaluation of effects due to incomplete simulation in wind-tunnels of engine flow, wall corrections used for models at high lift, criteria justifying the lack of such corrections, and the effects of wind-tunnel turbulence.

Advisory Report No.36 presents edited versions of the data given in replies to the Questionnaires, and the conclusions and recommendations of the Ad Hoc Committee.

aircraft performance at transonic speeds, with particular respect to the installation of engines and the use of wind-tunnels for testing models at high lift.

Technical organisations interested in the accuracy of wind-tunnel data were selected from (a) wind-tunnel operators and experimental workers, (b) airplane designers and airplane manufacturers, and (c) airplane users and design evaluators. Questionnaires were sent to obtain consistent sets of information on the simulation of engine interference, evaluation of effects due to incomplete simulation in wind-tunnels of engine flow, wall corrections used for models at high lift, criteria justifying the lack of such corrections, and the effects of wind-tunnel turbulence.

Advisory Report No.36 presents edited versions of the data given in replies to the Questionnaires, and the conclusions and recommendations of the Ad Hoc Committee.

AGARD Advisory Report No.36 North Atlantic Treaty Organization, Advisory Group for Aerospace Research and Development REPORT OF THE AGARD AD HOC COMMITTEE ON ENGINE–AIRPLANE INTERFERENCE AND WALL CORRECTIONS IN TRANSONIC WIND TUNNEL TESTS Published August 1971 148 pages, including figures. The Ad Hoc Committee, under the Chairmanship of Professor A.Ferri, was proposed by the Director of AGARD and approved by the AGARD National Delegates in 1970. The purpose was to study present techniques used by NATO Nations for predicting P.T.O.	533.6.071.4	AGARD Advisory Report No.36 North Atlantic Treaty Organization, Advisory Group for Aerospace Research and Development REPORT OF THE AGARD AD HOC COMMITTEE ON ENGINE–AIRPLANE INTERFERENCE AND WALL CORRECTIONS IN TRANSONIC WIND TUNNEL TESTS Published August 1971 148 pages, including figures. The Ad Hoc Committee, under the Chairmanship of Professor A.Ferri, was proposed by the Director of AGARD and approved by the AGARD National Delegates in 1970. The purpose was to study present techniques used by NATO Nations for predicting P.T.O.	533.6.071.4
AGARD Advisory Report No.36 North Atlantic Treaty Organization, Advisory Group for Aerospace Research and Development REPORT OF THE AGARD AD HOC COMMITTEE ON ENGINE–AIRPLANE INTERFERENCE AND WALL CORRECTIONS IN TRANSONIC WIND TUNNEL TESTS Published August 1971 148 pages, including figures. The Ad Hoc Committee, under the Chairmanship of Professor A.Ferri, was proposed by the Director of AGARD and approved by the AGARD National Delegates in 1970. The purpose was to study present techniques used by NATO Nations for predicting P.T.O.	533.6.071.4	AGARD Advisory Report No.36 North Atlantic Treaty Organization, Advisory Group for Aerospace Research and Development REPORT OF THE AGARD AD HOC COMMITTEE ON ENGINE–AIRPLANE INTERFERENCE AND WALL CORRECTIONS IN TRANSONIC WIND TUNNEL TESTS Published August 1971 148 pages, including figures. The Ad Hoc Committee, under the Chairmanship of Professor A.Ferri, was proposed by the Director of AGARD and approved by the AGARD National Delegates in 1970. The purpose was to study present techniques used by NATO Nations for predicting P.T.O.	533.6.071.4

CONTENTS

ACKNOWLEDGEMENTS

On behalf of AGARD, the Chairman of the Ad Hoc Committee and the editors (see above) wish to thank all the participants in the study and all the agencies, companies and laboratories which gave the information and time which made the study possible.

Particular thanks are due to Mr E.C.Carter and Dr A.E.Fuhs, who reviewed the manuscripts.

PART I

CONCLUSIONS AND RECOMMENDATIONS

on

ENGINE AIRPLANE INTERFERENCE AND WALL CORRECTIONS IN TRANSONIC WIND TUNNEL TESTS

by

Antonio Ferri

Director, Aerospace Laboratory,
Astor Professor of Aerospace Sciences,
New York University, Bronx, New York 10453

1. INTRODUCTION

Recent developments of high performance airplanes have generated requirements for the prediction of the aerodynamic performance of airplane designs with extremely high accuracy, certainly better than that which is presently possible with available experimental techniques. As a result, a critical review of present experimental methods is taking place, and development of new experimental techniques is in progress. Such activity is primarily carried on at a national level; however, substantial activity in this field exists to some degree in several of the NATO nations. For this reason, the Director of AGARD, supported by the National Delegates, has initiated an Ad Hoc Committee for the purpose of generating a direct exchange of information and technical opinions, and where feasible, to stimulate joint programs in this field. As a first step in this program, two separate efforts were initiated by AGARD related to experiments in transonic flows: (a) one was sponsored by the Fluid Dynamics Panel and, as reported in AGARD–AR–35–71, related to the effects of Reynolds number on aircraft performance and to the design of high Reynolds number wind tunnels; (b) the second related to correct representation in wind tunnel tests of the interaction between engine flow and airplane characteristics, and on wall interference at high lift. The second task, because of its specialized nature, was assigned to an Ad Hoc Committee recommended by the Propulsion and Energetics Panel, reporting to the AGARD Director and consisting of specialists from different nations who were nominated by the National Delegates. The Committee has performed the first phase of the technical activities and has prepared a technical report which contains a description of the techniques used, and as summarised in Sections 2 and 3 below, the comments, conclusions and recommendations of the Ad Hoc Committee.

2. ENGINE-AIRFRAME INTERFERENCE IN TRANSONIC TESTS

The review of the experimental methods used for determining correctly engine airplane interference in transonic tests has been divided into the following topics:

1. Inlet airplane interference.
2. Definition of engine thrust consistent with the definition of the airplane drag and nozzle characteristics.
3. Exhaust flow and airplane interference.
4. Determination of interference of the engine flow on the aerodynamic characteristics of the complete configuration.

The justification for such a division was based on the fact that the inlet and nozzle are developed in experimental investigations which are separate from the investigation of a complete configuration, while the thrust of the engine is measured independently and the definition is based on the experimental approach used for the measurement of thrust by engine manufacturers.

The Committee found that the present methods used by different groups have substantial similarity and some differences. However, the panel has concluded that all of the approaches used have important unknowns and shortcomings that are not necessarily satisfactory when thrust-minus-drag is to be predicted with one or two percent accuracy. Better and more satisfactory approaches are required. Such approaches are not completely available; therefore action on the part of the research groups involved is required in order to develop new techniques and to improve existing experimental techniques.

Listed here are specific comments and recommendations by the Committee.

2.1 Inlet

(1) In inlet tests, only a small part of the airplane configuration is usually represented, this being usually limited to the part ahead or in the proximity of the inlet. Usually the flow somewhat downstream of the inlet is not correctly represented in the tests. In many cases, the characteristics of the downstream flow affects substantially the flow field entering the inlets, and the flow of the boundary layer scoops or boundary layer bleeds. The Committee recommends that the first step of an inlet test in transonic flow be devoted to ascertaining that the downstream effects either are small, or are correctly represented. The results of this part of the investigation should be attached to any report documenting experimental results on inlets. This practice is not generally followed in the present programs. The panel feels that such a problem can be solved more easily for engine installations attached to the fuselage, while it is extremely difficult for podded engine installations. Here methods to add energy to the inlet flow are required. An approach recently developed along this line is the use of the engine simulators. The panel recommends that this direction be encouraged. However, it is important that in the development of engine simulators careful attention be given to represent correctly the scaling parameters that define the pumping characteristics and therefore the mixing of the engine jet with the outside flow. Unless such characteristics are correctly represented, the use of the engine simulator does not assure correct representation of the downstream influence. Analytical and experimental work is required in this field.

(2) The boundary layer scoops, boundary layer bleeds, and the dimensions of the inlet entrance cannot be truly represented geometrically in the model unless the experiments are made at full scale Reynolds numbers. Usually in present tests, the geometry is either conserved or changed in such a way that the air entering the inlet is free from nonrepresentative low energy boundary layers produced by the front part of the airplane. This is obtained either by increasing the size of the boundary layer scoops, or by modifying the airplane shape.

The problem of correct aerodynamic representation of the airplane configuration is a very important one, and exists for all airplane components. Such problems, until now, have not received the required attention. Not only should the airplane shape be changed because of differences in boundary layer displacement thickness, but also because of differences in aeroelastic deformations. In inlet design, a compromise is usually required between drag of the boundary layer scoops and inlet performances. Such a compromise tends to select a solution where the outer part of the boundary layer enters the inlet. This compromise is usually not simulated in inlet tests. Present methods for evaluating scoops and bleed drag for representation of the boundary layer flow field in front of the inlet, and for selecting the required

changes in the airplane configuration in order to account for the different Reynolds numbers, are neither standard nor satisfactory. The approach used with respect to this simulation is usually not described in inlet reports. The Committee recommends that an activity be initiated, possibly sponsored by AGARD, for the purpose of defining an acceptable standard method for attacking such a problem, and to outline acceptable experimental techniques required to determine more accurately the performance of the inlet and to evaluate the drag of the inlet and boundary layer scoop of the airplane.

(3) One of the important quantities to be measured in the inlet and exhaust nozzle test is the mass flow. Systems capable of obtaining accuracy on the order of 1 to 0.5% can be produced, provided that the distortion of stagnation pressure and temperature profiles are negligible. In inlet tests, this stagnation temperature distribution is usually not measured. When the model is at a different temperature from the stagnation temperature of the tunnel, and heat transfer takes place in the inlet duct, the stagnation temperature distribution should be measured in front of the flow meter in order to obtain the required accuracy. In addition, calibration rigs should be used for the calibration of the flow meter where the actual distortion of stagnation pressure and temperature measured in the inlet can be represented. When possible, the distortion should be minimized in front of the flow meter; better accuracy can then be obtained, this being required in order to have more accurate information on external drag. For good accuracy of results, precision on the order of 0.5 is required. Reports on experiments should describe the approach used to define the accuracy quoted for the flow meter.

(4) The measurement of dynamic characteristics of the inlet is important for some flight conditions and engine designs so as to allow analysis of the compatibility of inlet and engine near stalling.

The dynamic characteristics depend on the acoustic characteristics of the main flow, and on the dynamic characteristics of the boundary layer. Disturbances generated downstream can produce local separation of the inlet boundary layer, or move the separation point of the boundary layer. Such effects can amplify the intensity of nonsteady disturbances. The Committee recommends that such a phenomenon be investigated in order to define the scaling laws, and the experimental techniques to be used. Some activity already exists in this field; however, the scaling criteria for the experiments are not yet available. Additional basic research in this field is necessary. Such research should be carried on at the national level.

2.2 Engine Thrust

The definition of engine thrust as given by the engine manufacturer is based on the method used to measure engine thrust in the test cells. The impulse of the entering flow is measured accurately, and the tangential force produced by the engine is measured in a balance. In this measurement a convergent nozzle usually is utilized to throttle the engine. The nozzle discharging into a chamber where the average flow velocity is zero, the static pressure at some distance from the engine is measured during the tests.

Mass average values of the stagnation pressure and temperature are measured and quoted and the nozzle coefficient of the nozzle used in the test is also given. Such a value is determined experimentally in separate nozzle tests where the average stagnation pressure and temperature measured in the engine are used as stagnation conditions. Such quantities are also used to define the thrust of the engine for different flight conditions.

The Committee feels that the use of average stagnation quantities to define the engine performance is not satisfactory for advanced engines. In addition, the use of converging conical nozzles for the calibration of the engine is not the best approach for an accurate thrust definition. These two approaches can introduce errors in the definition of the actual thrust of the engine to be used in the determination of thrust minus drag.

In advanced turbojet engines of the bypass type or those having partial afterburners, large nonuniformities in stagnation pressure and temperature can exist. The nonuniformities have several effects; because of velocity and temperature gradients, viscosity and heat conduction are important. Such effects produce entropy rises in the flow; therefore, the nozzle flow is not isentropic. The use of nozzle coefficients obtained from tests where the nonuniformity is not represented introduces errors in the evaluation of thrust minus drag. Because of the nonuniformity in stagnation pressure and temperature, the flow field at the exit of the nozzle is different from that obtained in a flow having uniform stagnation pressure and temperature equal to the mass average values. The pressure distribution at the exit of a convergent nozzle is different (and higher) than the average value of the static pressure in the discharge chamber. The sonic line and the Mach number at the exit of a converging nozzle are affected by the presence of nonuniformities in stagnation conditions. Thus the nozzle coefficient obtained by using uniform quantities is not equal to that obtained in the engine. For converging nozzles at transonic speed, errors as high as 2% in thrust have been calculated due to these differences.

The second objection is related to the use of a convergent conical nozzle as a reference nozzle. The flow field at the exit of a convergent conical nozzle is not unequivocally defined even if the pressure ratio through the nozzle is above critical. The sonic line starts at the end of the nozzle; however, the flow at the section at the end of the nozzle is subsonic. The sonic line is affected by the static pressure disturbances along the streamline that divides external and internal flow until the flow is completely supersonic. Such pressure in flight depends on the flight Mach number and airplane configuration. In the test cell, such distribution depends on the mixing phenomena between external and internal flows. Such phenomena are strongly affected by local conditions and cannot be defined completely by simple parameters. Therefore, in order to obtain consistent calibrations, the Committee recommends that a nozzle having a small diverging region downstream of the throat be used for the definition of thrust so that the external conditions will not be important. This problem is of special importance for bypass engines that discharge the two flows separately. In this case an incorrect representation of the nozzle flow for the bypass air affects the split between main flow and bypass flow. In this case it is important that the flow at the exit of a bypass engine be carefully analyzed and if required, correctly represented. Analytical and experimental work is recommended in this topic to determine the importance of these effects and methods for eliminating such errors.

2.3 Nozzle

The Committee feels that substantial additional analytical and experimental work is required for the selection of optimum nozzle shape and for the experimental determination of the nozzle performances. The specific recommendations are:

1. Simple nozzles where only engine flow is injected should be investigated by taking into account actual distortions in stagnation temperature and pressure. Nozzle coefficients determined from tests without distortion are not representative when distortion is present. Analytical methods that consider the effects of distortion and transport properties should be generated and made easily available to industry.

2. Recognition should be given to the fact that external flow can substantially affect the nozzle performance. Tests performed for the determination of such effects are unsatisfactory because they do not correctly simulate the mixing phenomena at the exit of the nozzle. Such phenomena influence nozzle performances and external drag. Similarity laws should be developed to permit the performance of accurate tests to determine such efforts.

3. Nozzles where secondary flows such as bypass flows, cooling flow, or external flows are utilized, have in principle the possibility of increasing the performance or flexibility of present nozzle installations; however, methods for designing such nozzles are lacking. Present methods of analysis usually neglect important parameters such as mixing, boundary layer flows, or three-dimensional effects. The Committee recommends that analytical and experimental research be increased in this field, at the national level.

4. Very little information is available on the nozzle performances when leakage is present, or when the nozzle discharges in a nonuniform field. The importance of such a problem should be investigated.

5. The interaction between internal and external flows depends on the details of the flows in the region of the mixing between them. Such details are affected by the boundary layer properties of the two flows. Velocity, stagnation temperature and pressure should be correctly simulated in the tests. The investigation of such interaction requires correct representation of the external flow. Extensive research on analytical and experimental techniques to investigate such phenomena is recommended. The analytical work should be directed toward determining methods for correcting tests performed with incomplete simulation, and to determine the parameters that should be correctly represented in the tests.

2.4 Complete Model Tests

Many different aspects are to be considered today in order to interpret the results of complete model tests. Many of the problems involved in such interpretations are related to the general limitations of experimental techniques and are not specific to engine airplane interference. Some of the most important are: Reynolds number, support interference, aeroelastic effects on the model, tunnel calibration, etc. However, the engine airplane interference simulation plays a major role also on the interpretation of data. In the actual airplane, the internal variation of stream tube area from the entrance of the inlet to the exit of the nozzle is such that for many engines the exit area when the flow is expanded to ambient pressure is slightly smaller or about equal to the entrance area. If the model is tested without energy addition in the internal flow, then the exit area required in order to pass the correct mass flow through the inlet is of the order of twice the area required for correct simulation. For bypass engines, this difference in streamtube representation is so large that serious errors are introduced in the determination of the drag of the airplane.

The variation of the streamtube of the flow leaving the engine is also important for the drag determination when the airplane extends downstream of the engine exhaust. This variation depends on the pressure field produced by the airplane and on the mixing process between internal and external flows. The mixing process depends on the ratio of products of density and velocity in the two mixing streams. For given external conditions, large differences in variation of the streamtube along the length occurs depending on the stagnation temperature and pressure of the internal stream. When this is important, the ratio of the product of the velocity and density of jet to that of the outside flow should be simulated. In addition, the mixing should be turbulent. At the present time, the use of engine simulators appears to be a good solution to such a problem, which is very serious for podded type engines placed under the wing. However, the use of engine simulators that use rotating components complicates the testing programs and makes the program more expensive. In addition, it introduces serious difficulties in the model design because the thrust of the engine simulator must be determined independently during the tests in order to measure accurately the drag of the model. Such requirements increase the complexity. For tests of this type attempts should be made to simulate correctly the mass flow and stagnation temperature at the exit of the nozzle. Schemes where the stagnation pressure and Mach number are simulated, and where an increase of mass flow is used to balance a decrease of stagnation temperature, could introduce errors because of the difference in mixing at the exit of the nozzle and during mixing downstream of the discharge plane, due to the incorrect jet velocity and density. The problem of testing configurations having engines installed in pods under the wing is different from the problem of testing airplanes having engines installed near the fuselage or in the rear part of the fuselage. For the second family of configurations, the possibility of changing the model support or of tests of a half model with reflecting plates should be investigated. Such methods have been attempted in the past by several groups without much success; however, some of the difficulties encountered could probably be eliminated if a systematic investigation of the problems could be made before such steps are taken.

The conclusion of the Committee is that substantial additional work is justified in this field.

2.5 Future Plans

Because of the magnitude of the research programs required to solve the problems described above, the Committee suggests that AGARD consider the advisability of outlining a program of research to be supported on a voluntary basis by several NATO nations at a national level but integrated at an international level by AGARD. This coordination, if possible, would permit an exchange of information, correlation of results, and would avoid unnecessary duplication of effort, thereby decreasing for each nation the overall costs required to obtain positive results. In addition, the Committee supports the request expressed by the representatives of industry present at the meeting, that a second meeting be planned to review the progress on such problems and to be held one year from the first meeting.

3. WIND TUNNEL WALL INTERFERENCE IN TRANSONIC TESTS WITH HIGH LIFT

The Committee reviewed the methods used by different groups for taking into account the effects of wall interferences for models with high lift.

Usually, the wall interference parameter used has been the blockage parameter, that is the ratio of the cross-sectional area of the model to the wind tunnel cross-sectional area. In the past the tendency has been to use sufficiently low blockage in order to avoid the necessity of performing corrections because presently, uncertainty exists on the possibility of making such corrections. A single criterion has been used at all angles of attack. If the value is satisfactory at high lift, then probably the value is too small at small lift. The same parameter is used for zero lift and for lifting models.

The main observations and recommendations of the Committee in this field are as follows:

1. While up until now corrections used for considering wall interference have been minimal and used only when large porosity exists at the wall, some experimental activities are in progress today in several laboratories to try to improve results by developing correction criteria, and to determine the most satisfactory value of the wall permeability to be used. It must be noted that the value of wall permeability presently used varies in different wind tunnels. The results of these efforts will generate a better understanding of the problem.

2. The Committee feels that the blockage criterion used, which is related only to the maximum cross-sectional area, is not a satisfactory criterion for models with high lift. The assumption that corrections are small and can be neglected is justified only when the disturbances at the boundary of the wind tunnel are small, and therefore are represented with good accuracy by porous or slotted walls. The intensity of such disturbances is related to the model size as well as to the variation of cross-sectional area of the model and to lift and not only to the value of the maximum area; therefore, better criteria should be developed. Several parameters have been suggested by the participants at the meeting to be added to the blockage parameter such as separation parameter, wake parameter, blockage due to lift, etc. The panel feels that better criteria should be developed in order to determine a practical criterion for defining when wall effects are small. Possibly such criteria should be based on the values of the pressure disturbances occuring at the wall. Such values can be, and should be measured during the tests; therefore, the accuracy of the criterion can be checked.

3. In order to generate a better understanding of wall interference and its dependence on model characteristics, systematic investigations are required. The Committee recommends that a panel be formed by AGARD to define simple suitable models to be tested when possible in a suitable size in all transonic wind tunnels in the NATO nations. This panel should also outline details of the experiments. Possibly several scales of models should be tested in each wind tunnel, and when possible different porosities should be used. An alternate approach is to control the flow outside of the test section. Several existing wind tunnels have such capabilities. Such types of control should be investigated. In all of these tests, careful definition of the flow field in the test section in the absence of models should be made available and detailed information of the pressure field and flow field at the walls in the region of the model should be obtained. In addition, the Committee recommends that flight data of the same configuration be obtained. The Committee recommends the following members for such a task:

France	Netherlands	U.S.A.
Mr. Poisson-Quinton	Mr. Enthoven	Dr. Zonars
		Mr. Jones
Germany	United Kingdom	
Dr. Lorenz-Meyer	Mr. Carter	

This investigation will furnish the required information necessary for any introduction of wall corrections. The Committee, of course, realizes that such a recommendation involves a substantial amount of work. However, from the discussions among the participants, it appears that substantial work in this direction is already planned at the national scale in many countries. The main point of the Committee's recommendation is that the AGARD attempt to organize in practical form these activities at an international level. Then all groups will benefit substantially with the increased sources of information.

4. The basic concept of porous or slotted wind tunnels is based on the superimposition of solid and open wind tunnel wall corrections. However, substantial differences exist between slotted and porous wind tunnels. In addition, the best porosity distribution required is a function of disturbances produced by the model. Presently, several groups are investigating the possibility of using variable porosity. The Committee recommends that substantial additional efforts be committed to analytical work to support such an investigation, particularly with regard to the appropriate downstream conditions that simulate the downwash for the case of a model with lift. Only a good integration of experimental and analytical work can produce good results.

5. The Committee feels that by directing the experimental program by means of analysis, there exists the possibility of improving experimental results and testing larger models where suitable wall corrections could be introduced. Therefore, the availability of advanced analysis is urgent because it could have an input on the design of future high Reynolds number wind tunnels. For example, it would affect the shape of the cross section of the wind tunnel, the design of the chambers outside of the porous or slotted walls and the design of the walls.

6. From the review of the contributions obtained, it appears that very little is known on the scale and level of turbulence of different wind tunnels. In addition, the influence of the turbulence level on the aerodynamic characteristics of the boundary layer is also unknown. Usually, because of the low Reynolds number of the tests, transition from laminar to turbulent flow is obtained artificially. The length of the transitional region is not certain, and nor is the interaction of the tunnel turbulence with these phenomena. The Committee recommends that the effect of stream turbulence in experimental results be investigated and measured. The scale and level of turbulence is probably affected by the type of wall used and of the wind tunnel design. The effect of turbulence level can be important for the development of supercritical wings.

3.1 Future Plans

Presently, substantial efforts are under way in many countries to try to determine the effect of Reynolds number at transonic speed. AGARD could try to organize a systematic exchange of data and information in this field. If such an effort is contemplated by AGARD, the Committee recommends that an invitation to participate in this effort be extended to Canada.

PART II

ENGINE-AIRPLANE INTERFERENCE IN TRANSONIC TESTS

by

F.Jaarsma

National Aerospace Laboratory, N.L.R., Amsterdam, The Netherlands.

ABSTRACT

This part of the report is a compilation of the response to a distributed questionnaire on engine-airframe interference in transonic tests among aeronautical laboratories operating transonic wind tunnels, aircraft manufacturers, engine companies, and airplane users in the AGARD countries.

The experimental techniques, correction procedures, advantages and limitations of inlet, nozzle/afterbody and complete model testing and of engine thrust determination are discussed in a technical order without reference to the source of the information.

BACKGROUND STATEMENT

The basic method for the prediction of aircraft flight performance from ground tests involves independent assessment of the airframe aerodynamic performance from wind tunnel tests and the engine thrust performance from static thrust stand tests. The degree to which these primary vehicle components interact with each other has not been adequately investigated in the past by either the aerodynamicists or the propulsion specialists. Standardized techniques do not exist for proper simulation of these interaction effects at transonic speeds, nor have correction procedures been well established. It can be argued that for certain aircraft configurations, such as transports, which stress the independent mounting of engine pods substantially free from the wing-body flow fields, the two components are essentially independent with only minor interactions. Equally true is the fact that for well integrated airframe-engine configurations (e.g. fighters) a high degree of mutual interaction exists which must be accurately assessed during wind tunnel and static thrust engine tests to substantiate total vehicle flight capability. Many examples exist, both military and commercial, of vehicles with flight capabilities inaccurately assessed because of the inability to simulate and properly account for the aerodynamic interactions between the airframe and engine flow fields. This inability has been due in a large part to the practice of utilizing small-scale models for the purpose of obtaining vehicle external aerodynamic performance, and to the application of marginal, unrefined analytical procedures to the problem of scale corrections necessary in predicting full-scale flight performance. These methods, although appropriate in the early stages of feasibility and preliminary design study, are not consistant with the accuracy required for projections of performance for prototype vehicles. As a result of this experience, the more recent programs of air vehicle development include detailed wind tunnel testing whereby several large-scale wind tunnel models are tested in a manner to allow an accurate bookkeeping of all the airframe-propulsion system aerodynamic interactions. Likewise, flight-size engine systems are being evaluated under conditions which closely simulate the spatial and dynamic environment to which the engine is exposed in flight. These procedures are both discussed in detail in this part of the report using inputs from a working group of aerodynamic and propulsion specialists. Emphasis has been placed on the engine-airplane interference at transonic conditions where inaccuracies can have a significant influence on predicted flight performance.

To this end a questionnaire was distributed in order to obtain information on specific questions and doing so obtaining a complete review of the techniques used in the various AGARD countries. Appendix A is the questionnaire as distributed. It contains three topics: inlets, engine thrust and exhausts, and generally asks for information on test procedures, techniques, applied corrections, obtained and required accuracies and, if available, comparisons between wind tunnel and flight data. The response to this questionnaire was very good, although not each topic was or could be equally well covered.

This part of the report is a compilation of the response including the results of a discussion between the propulsion and aerodynamic specialists of the co-operating establishments, agencies and companies. This discussion was part of the study and was held after each group had submitted the answers to the questionnaire.

CONTENTS

I INTRODUCTION

Development of present day high performance airplanes requires prediction of aerodynamic performance with accuracy above what is possible with available techniques. This is especially true for the transonic flight regime, which is important for both civil and military aircraft; the former for economic cruise performance, the latter for low fuel consumption, during transonic ferry and combat missions.

Three parties are involved in the airplane design: the customer or aircraft user, the airframe manufacturer and the engine company. The customer demands such stringent aircraft performance that optimum integration of engine into the airframe is a necessity. The airframe manufacturer is responsible for this optimum integration e.g. for the aerodynamic design. The engine company guarantees the engine performance if the compressor entrance flow conditions are met and if a company-defined reference exhaust nozzle is used. The aerodynamic airframe design should be such that minimum losses are generated at the inlet and at the exhaust. Therefore in the wind tunnel tests conducted for the evaluation of external and internal geometry, emphasis is given to the inlet and exhaust with two objectives in mind. First objective is to determine how the inlet and exhaust flows influence the external aerodynamics, and the second is how the external flow affects the internal flow and engine performance. Due to the scaling and the inability to represent simultaneously the complete inlet and exhaust flows corrections must be introduced to predict the full scale free flight performances. The degree of accuracy depends on the experimental techniques used and the methods for the determining corrections.

Since at transonic speeds the engine thrust felt by the airframe is of primary importance in the analysis of engine airframe integration, most emphasis will be given in this report to thrust and drag components. However, similar analysis and techniques apply for terms such as lift, pitching moment and stability derivatives.

Fig. I.1 is a schematic representation of an highly integrated engine airframe installation. The various drag terms due to the engine installation are indicated and defined below the drawing. These definitions are not standard, however, and are not used in a similar manner by every group. It is felt that the definitions as given represent a suitable average. Fig. I.2 gives the major elements of a wing-pylon-nacelle flow field of an isolated engine installation.

Current practice for the wind tunnel evaluation of vehicle external aerodynamic performance of the combined engine and airframe is to utilize three separate large scale force models. The bookkeeping procedure for combining all test results to provide compatible drag and thrust performance is schematically shown in figure I.3. The basic aero force model shown in figure I.3 (A) duplicates the external geometry of the full-scale vehicle as accurately as possible and is tested with flow-through inlets operating at a reference mass flow ratio. The mounting sting or strut geometry usually results in modified closure lines near the model aft end which requires an afterbody drag correction (B). In addition jet exhaust effects which are usually not simulated contribute to the afterbody drag correction. Basic force coefficients (lift, drag, moments, etc.) are determined using the aero force and moment model. Afterbody drag corrections are obtained from a jet effects model (fig. I.3D). This model is usually strut mounted to minimize interference effects and duplicates the aft-end geometry and jet exhaust flow conditions. An aero reference configuration similar to the modified closure lines (with dummy sting effects included) of the aero force model is sometimes also tested on the nozzle afterbody model. The installed afterbody drag is then equal to the drag for the correct afterbody plus jet effect minus the drag of the aero reference. Both afterbody geometry and power setting effects are obtained with the jet effects model. These are obtained in a manner which allows corrections to both the aero force model aerodynamic data and the installed engine thrust. It is usual practice to fair over the inlets of the jet effects model.

An inlet drag or propulsion model (fig. I.3C) is used to correct for the effect of inlet mass flow ratio on the installed engine net thrust. In some cases external aerodynamic performance is also corrected based on inlet drag model results. The resulting thrust which also contains nozzle afterbody corrections is usually termed the net installed propulsion system thrust, F_N. As was mentioned earlier, the vehicle external aerodynamics are measured on the aero force model which is operated at some specified reference mass flow ratio condition. The inlet drag model, therefore, is necessary to account for the effect of inlet mass flow ratio variation (engine power setting) on the inlet and adjacent vehicle surfaces.

Great care should be taken for each aerodynamic geometry whenever the above mentioned separated model tests are conducted. The wind tunnel experimentalist should be sure that the inlet flow does not have an effect on the afterbody drag and vice versa that the jet flow does not influence the inlet conditions. In transonic flow this experimental setup is usually correct for airplane geometries with widely separated inlets and exhausts e.g. for integrated engine-airframe systems. For a podded engine installation, such as fig. I.2, the non interference between inlet flow and afterbody flow is not so evident. It can be shown that under certain conditions independence occurs. It can be argued that for podded engine installations the engine-airframe interference is less pronounced and less care could therefore be devoted to it. However due to the large mass flow of the newly developed high by-pass ratio engines and due to the fact that the net thrust is only a small fraction of the engine gross thrust, new interference problems arise for such installations. This is true for engines mounted either under the wings or aft on the fuselage. For engine representation in wind tunnels a scaled engine simulator with an externally driven compressor can be utilized providing close simulation of both inlet and exhaust flow. The use of powered engine simulators is rather new. Additional experience is needed to define the best calibration and testing techniques. The main advantage of this technique, besides its good simulation properties, is that the calibration and installation procedures for test benches and the wind tunnel nearly duplicate the procedures for the actual engine in the actual airplane.

However, the difficulty of data reduction and scaling to the flight conditions remains and little is known of the achievable accuracy of performance predictions. After treatment of the inlets, engine thrust, and exhausts in chapters II, III and IV respectively, the problem and necessity of complete model tests will be considered in chapter V.

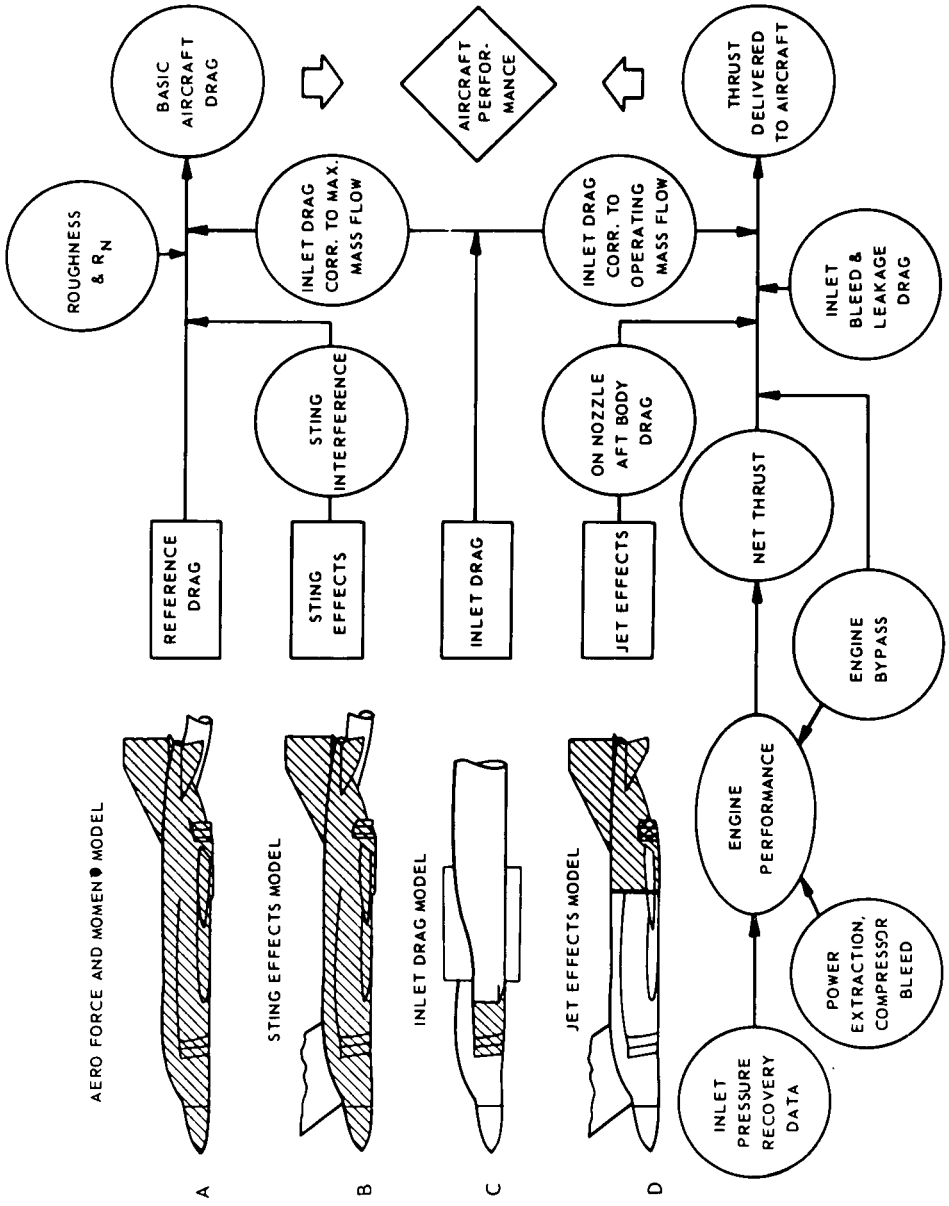

FIG. 1. 3 THRUST AND DRAG ACCOUNTING SYSTEM.

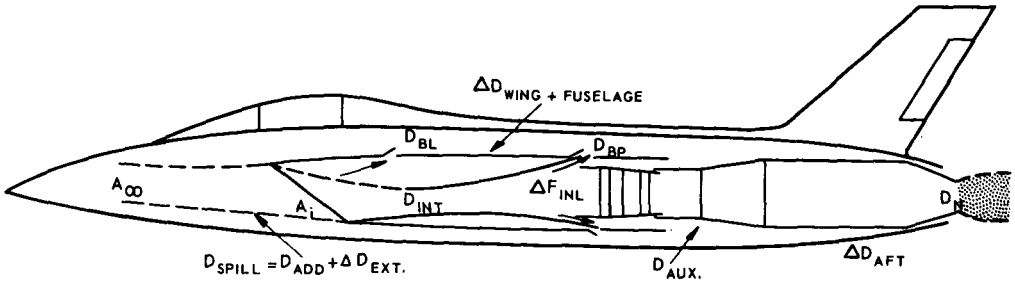

F_U = UNINSTALLED GROSS THRUST AS SPECIFIED BY ENGINE COMPANY WITH REFERENCE NOZZLE

F_i = INSTALLED GROSS THRUST = $F_U + \Delta F_N - D_N + \Delta F_{INL}$.

ΔF_N = DIFFERENCE IN GROSS THRUST OF ACTUAL NOZZLE DIFFERENT FROM REFERENCE NOZZLE EXHAUSTING INTO QUIESCENT ATMOSPHERE.

D_N = DIFFERENCE IN GROSS THRUST OF ACTUAL NOZZLE EXHAUSTING INTO QUIESCENT ATMOSPHERE AND WITH EXTERNAL FLOW

ΔF_{INL} = DIFFERENCE IN GROSS THRUST DUE TO INLET FLOW DISTORTIONS AND NOT COMPLETE PRESSURE RECOVERY

D_{SPILL} = SPILLAGE DRAG DUE TO $A_\infty < A_i$ VS $A_\infty = A_i$
= $D_{ADD} + \Delta D_{EXT}$

D_{ADD} = ADDITIVE OR PRE ENTRY DRAG (PRESSURE FORCES ACTING ON STREAMTUBE)

ΔD_{EXT} = CHANGE IN INLET EXTERNAL DRAG, PRESSURE DRAG, WAVE DRAG, FRICTION DRAG (IDEALLY $D_{ADD} = \Delta D_{EXT}$)

D_{INT} = INTERNAL INLET DRAG

D_{BL} = CHANGE IN AIRPLANE DRAG WITH BOUNDARY LAYER BLEED VS NO BLEED

D_{BP} = CHANGE IN AIRPLANE DRAG WITH BY-PASS INSTALLED VS NO BY-PASS

ΔD_{W+A} = CHANGE IN AIRPLANE DRAG (EXCEPT INLET) DUE TO $A_\infty < A_i$ VS $A_\infty = A_i$ OR $A_\infty = A_{REF}$

D_{AUX} = CHANGE IN AIRPLANE DRAG DUE TO AUXILIARY AIRSYSTEM INSTALLED VS NO AUX. SYSTEM INSTALLED

ΔD_{AFT} = CHANGE IN AIRPLANE DRAG DUE TO ACTUAL NOZZLE FLOW AND REFERENCE NOZZLE FLOW OR REFERENCE NOZZLE GEOMETRY

F_N = NET THRUST = $F_i - \dot{M} V_\infty$ ($\dot{M}$ = ENGINE MASS FLOW)

FIG. I. 1 SCHEMATIC REPRESENTATION OF VARIOUS THRUST AND DRAG TERMS.

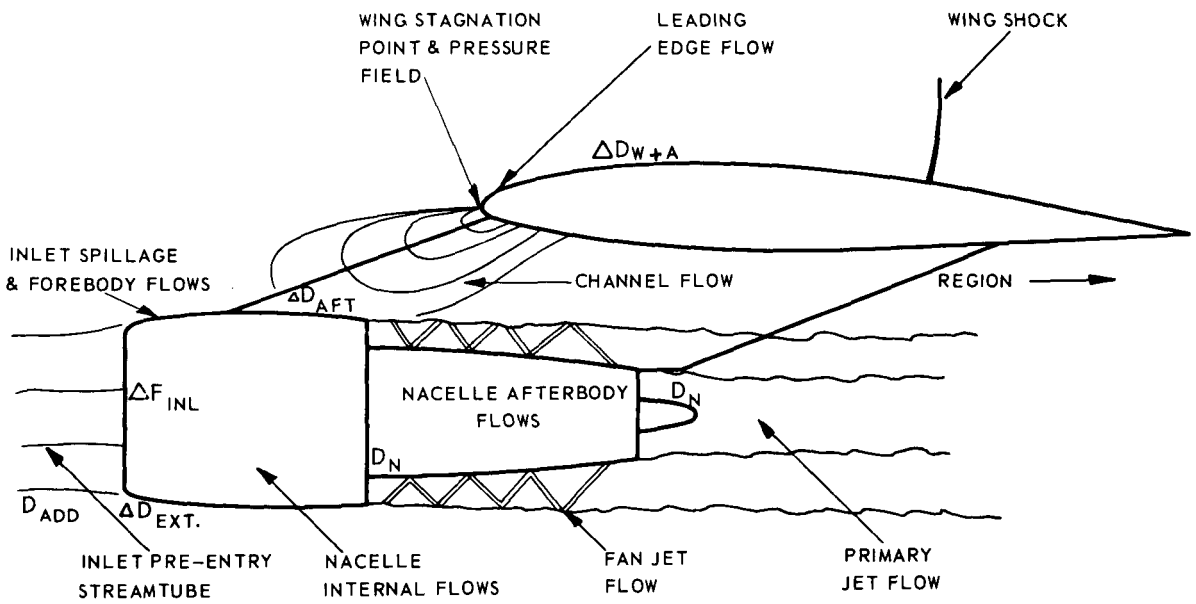

FIG. I. 2 MAJOR ELEMENTS OF WING / PYLON / NACELLE FLOW FIELD.

II INLETS

LIST OF SYMBOLS

A	Area
$\bar{c}$	cord
C_d	Discharge coefficient
C_D	Drag coefficient (the reference area: appropriate engine area or wing area; it must be clear which area is used).
C_L	Lift coefficient (ref. area is wing area)
C_M	Pitching moment coefficient
C_p	Pressure coefficient
C_T	Thrust coefficient
D	Drag
F_N	Installed net thrust
g	Gravitational acceleration
h	Diverter height
$\dot{m}$	Mass flow
M	Mach number
p	Static pressure
p_t	Total pressure
q	Dynamic pressure
r	Coordinate in radial direction
T	Temperature
V	Velocity
x	Coordinate in stream direction
y	Coordinate perpendicular to main flow
α	Angle of incidence
γ	Ratio of specific heats
δ	Boundary-layer thickness
ε	Mass flow ratio = A_∞/A_1 (spillage is zero)
ρ	Density
τ	Shear tension
λ	Ratio of throat curvature to throat radius

SUBSCRIPS

add	Additive
blc	Boundary layer control
bp	Bypass
cr	Critical
div	Diverter
e	At nozzle exit plane
ed	Boundary layer edge
en	Engine
ext	External
f	Due to friction
int	Internal
p	Due to pressure
spill	Spillage
∞	At upstream infinity
1	Inlet entrance plane
2	Compressor entrance plane

2.1 INFLUENCE OF INLET MASS FLOW ON EXTERNAL AERODYNAMICS AND MEASURED FORCES

2.1.1 GENERAL

For aero force models of almost all jet powered aircraft the inlet mass flow is usually completely, or almost completely, simulated. The basic force coefficients (lift, drag, moments, etc.) are determined from such models when the measured data from pressure plotting or balance readings are corrected for the internal flow through the inlet. The correction procedure is discussed in 2.1.2. Use of a reference mass flow is a necessity for large by-pass turbo fan engines since at transonic speeds changes in the inlet flow alters the pressure distribution on wings. This is especially true for rear fuselage mounted engines. Also for supersonic cowl shapes reduction in inlet mass flow of wind tunnels models is very undesirable if the air spillage (e.g. inlet mass reduction from $A_1 \neq A_\infty$) is outside the range of flight requirements.

The external drag is usually the most difficult problem of measurement. Fig. II.1 poses the usual questions and dilemmas that the experimentalist faces when planning a complete aero force aircraft model for wind tunnel testing when one of the objectives is the representation and measurement of the engine nacelle drag. The questions posed are of course only concerned with the inlets and the shape of the model. There are many similar questions associated with the representation of the jet exhaust flow; these questions will be considered in chapter IV.

For measuring the drag terms associated with the inlet (spillage, bleed, diverter, by pass, additive) special inlet models are tested incorporating the external surfaces which might influence the values of inlet drag terms. It is evident that the model inlet mass flow ratio should duplicate the flight envelope. The problem concerning these measurements will be discussed in 2.1.2.

A clear statement defining the conditions when complete inlet mass flow duplication is required is not possible on the basis of past experience. Each program must be reviewed as to its objectives and the general layout of the test configurations. Interference effects are of primary importance in establishing accurate drag levels as said before, although examples exist (reference II-1) where lift and pitching moments were affected by closing inlets with an aerodynamically smooth fairing.

Similar tests were conducted using an F-8 model which utulized the NASA Supercritical Airfoil section. Whereas the aircraft of reference II-1 has twin side-mounted inlets, the F-8 model had a large air intake duct located under the nose of the fuselage. The unpublished data indicate no effect of closing the inlet on lift and drag characteristics of the configuration after appropriate corrections for the internal drag and base drag were applied. Although there was no effect on the aerodynamic center location as a result of closing the inlet, there was a small shift in pitching moment with the inlet closed.

References II-2 and II-3 contain information on the effect of mass flow ratio on external lift, drag and pitching moment for underslung and submerged inlets. The data show the expected increase in external drag as mass flow ratio was reduced. There is a small effect of mass flow ratio on lift and pitching moment.

In general, it is thought desirable to duplicate inlet mass flow ratio when determining model drag. Simulation of mass flow ratio is of doubtful value if details of the airplane geometry (cowl shape and leading edge contours, e.g.) are not duplicated. Even though the airplane geometry is duplicated by the model, Reynolds number effects may significantly affect the relative cowl lip pressures (drag) which occur on the model and airplane. This is particularly true when separation effects predominate. In those cases where experimental external aerodynamics are obtained using nonrepresentative model test conditions, corrections must be applied to the force and moment data. These corrections account for the effect of inlet mass flow ratio on external drag using data acquired on a separate large scale inlet drag model as discussed later. Analytical predictions of the variation of isolated inlet drag with mass flow ratio have been attempted with reasonable success. References II-4 to II-10 cover the most significant contributions in this area.

The interference drag that accounts for the effect of inlet airflow spillage on the external surfaces of the aircraft has not been adequately studied in the past. Thus, installation effects have been virtually omitted from analytical predictions of total external inlet drag coefficients. More effort is needed, particularly at transonic conditions, to identify the interference drag effects for various inlet-airplane combinations. A program is formulated in the USA to study interference drag on a typical fighter aircraft due to the spillage of inlet airflow. Experimental data will be obtained over a range of subsonic, transonic, and supersonic Mach numbers on a wing-body model incorporating a typical two dimensional inlet and nacelle. Inlet location, geometry, and mass flow ratio will be varied. Experimentally determined drag will be compared with theoretical predictions.

Basically, the consensus of opinion on incomplete inlet mass flow duplication is that for finalized predictions of aircraft performance the inlet mass flow must be duplicated during some phase of the experimental tests. As mentioned previously, it is not the practice to simulate the full operational range of inlet mass flow ratios on the aero force model from which the basic external aerodynamic force and moment characteristics are obtained. Rather, these data are corrected on the basis of data obtained on a large scale inlet drag model which provides an accurate simulation of the full range of inlet mass flow ratios. If the scale of the aero force model is too small to prevent duplication of the proper cowl lip flow it is recommended that the inlet be operated at a mass flow ratio as close to unity as possible for purposes of determining the minimum drag reference. Inlet compression surfaces are eliminated to provide this reference flow condition. The drag due to lift and moment characteristics can best be obtained at a representative operational mass flow condition.

Although it appears no hard and fast guideline can be established regarding decisions whether or not models should have complete or partial inlet mass flow or complete inlet fairings, some general observations can be made. When it is possible to simulate the inlet mass flow requirements without adversely affecting the external lines of the configuration, then it is strongly recommended that the aero force model be constructed and tested with flow through nacelles. On the other hand, if it appears that because of model size limitations it is not possible to provide the model with sufficient inlet mass flow ratio for the speed range considered, then the inlets should be faired closed. In that case the representation of small mass flow and the required measurements are more nuisance than they are worth. As is well known, improper inlet mass flow matching could result in adverse separation from the lips of the inlets thus causing erroneous external aerodynamic measurements.

Many bookkeeping procedures are possible under the system which utilizes a number of wind tunnel models to provide the data for prediction of flight performance. The principal requirement for any method is careful attention to providing consistent corrections for inlet mass flow ratio effects between the external aerodynamic forces and the engine thrust forces.

2.1.2 TECHNIQUES FOR OBTAINING EXTERNAL AERODYNAMIC DATA WITH COMPLETE MASS FLOW REPRESENTATION

A COMPLETE OR AERO FORCE MODELS

The utilization of wind tunnel models for transonic tests requires particular attention to the complete simulation of inlet mass flow ratio and to the proper force corrections resulting from inlet mass flow effects. Aircraft which cruise in this speed regime require an accurate accounting for inlet mass flow ratio since both aerodynamic and propulsion performance are sensitive to mass flow ratio operating conditions. Vehicles of the type which require a rapid acceleration through transonic Mach numbers are also affected by the direct and indirect effects of mass flow ratio, since aircraft thrust minus drag is usually a minimum at these conditions. In this Mach number range, inlet drag is relatively large and is sensitive to inlet mass flow ratio operating conditions.

Two techniques exist for inlet mass flow simulation at transonic speeds namely flow-through inlets and use of powered engine simulators. The former is the simplest and is generally used in the early stage of wind tunnel testing. In order to apply this technique three conditions must be met: (a), adequate exit area, (b), low pressure at exit, preferably below ambient, and (c), low total head losses in the internal duct.

Regulation of the inlet airflow below maximum can be accomplished by inserting restrictions in the duct. The advantage of this technique besides its simplicity is its consequent ease of measuring forces. The main disadvantage is the need for increased exit area compared to the real jet exhaust which must involve geometric distortion e.g. incorrect nacelle length or boattail angle or elemination of turbine afterbody in case of podded fans. For complete aircraft models such as with podded engine installations this increased exit area might be unacceptable and geometric scaled engine pod models are used in that case. The value of these pods is then not to simulate inlet flow, but to simulate an entire nacelle-pylon system. Effects of various pod and pylon contours and mounting positions on airplane stability and drag can be evaluated from increments obtained from flow-through pod-on models. Optimum configurations can then be investigated further with more refined techniques such as powered simulators or blown nacelles. Use of turbine driven fan jet simulators is a recent development, which extends the power-off simulation of the flow-through pod to include some effects of both primary and fan exhausts. It is practice nowadays that this technique is applied in the final complete wind tunnel models. Operation of these units has become a technology in itself and deserves a separate section for complete discussion; it is covered later.

Fig. II.2 illustrates one particular choice of answers to the questions as posed in fig. II.1. In this case, that of the Concorde aircraft,(Ref. II-11) the choice of alternatives was dominated by two considerations (1) the maximum scale of a complete model (limited to 1/30) and (2) the need to obtain a very accurate value for drag for sustained cruise flight at M = 2.0 - 2.2. The nacelle was represented on this complete aircraft model either without any or with only a single 7° wedge compression surface and (in the first alternative) without a boundary layer diverter, the exit area was fixed and traversed in great detail to get an accurate value of internal drag so as to obtain the installed wave drag of the nacelle at datum intake flow. Pre-entry drag and lift at full flow was not obtained from these tests because the relatively low Reynolds number of the tests would undoubtedly have meant that with correct representation of the compression surface geometry external shock waves would be in incorrect positions and substantial drag errors would occur. For the geometry of the Concorde nacelle (i.e. an isolated nacelle on a wing with the external shocks from the compression surfaces not impinging directly on adjacent surfaces of the aircraft) this was probably a correct choice. If the compression surfaces had been turned through a right angle as in the B70 for example this choice would probably have been unwise in that vital interactions would have been missed between the intake and airframe flow fields that were dependent on the correct representation of the compression surfaces.

A description is given below of a procedure used to determine the external drag, lift and pitching moment from complete aircraft models corrected for the effect of the internal mass flow.

The external drag is defined as the sum of the longitudinal forces acting on the force boundaries of the pre-entry streamtube and those parts of the body and wing which are wetted by the external flow (but excluding any base area of the nacelles). Drag coefficient of the full scale aircraft is then:

$$C_{D_{aircraft}} = \{ C_{D_{Bal}} - C_{D_{base}} - C_{D_{internal}} - C_{D_{2_{f_{external}}}} \} + C_{D_{f_{external_{aircraft}}}}$$

where $C_{D_{Bal}}$ = drag coefficient of complete configuration (including nacelles) measured in the wind tunnel. (Fig. II.2). This term will include corrections associated with the model support system e.g. forces due to model definition to permit rear sting mounting. This is done by testing a model with a correct rear fuselage shape mounted on a twin sting support (Fig. II.3).

$C_{D_{base}}$ = drag coefficient of any unrepresentative installation base.

$C_{D_{internal}}$ = standard internal drag coefficient (see Fig. II.4 for symbols).

$$= - \text{ net standard thrust.}$$

$$= \frac{2A_\infty}{A_{en}} - [(p_e - p_\infty) \cos \phi + \rho_e V_e^2 \cos \psi \cos \theta] \frac{A_e}{q_\infty A_{en}} \ *$$

(q_∞ = dynamic pressure and A_{en} = reference engine area).

$C_{D_{2_{f_{external}}}}$ = skin friction drag coefficient appropriate to all model surfaces wetted by external flow (from Ref. II.12).

$C_{D_{f_{external_{aircraft}}}}$ = external skin friction drag coefficient of the aircraft at full scale Reynolds number (also from Ref. II.12).

* This is the general expression when the exit plane is canted at an angle ψ to the duct centreline (Fig. II-4)

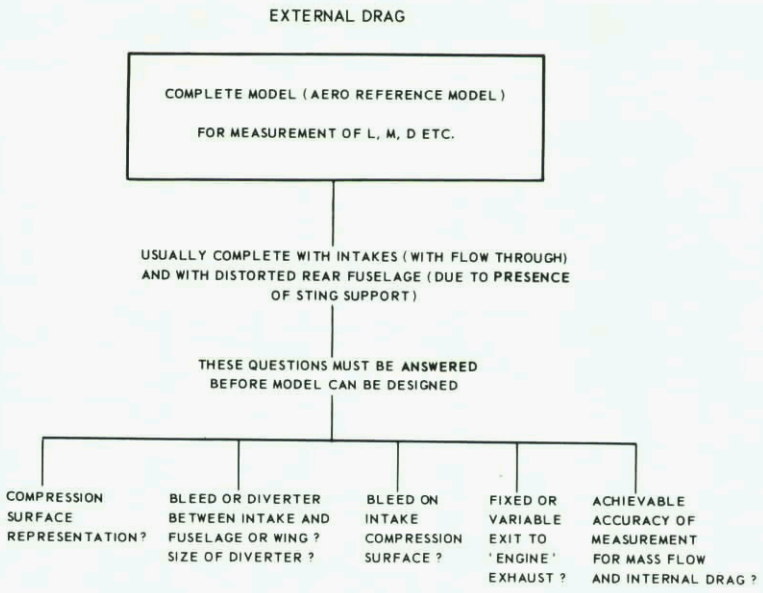

FIG. II. 1 PROBLEMS OF REPRESENTATION OF AIR INTAKES ON COMPLETE AIRCRAFT MODELS.

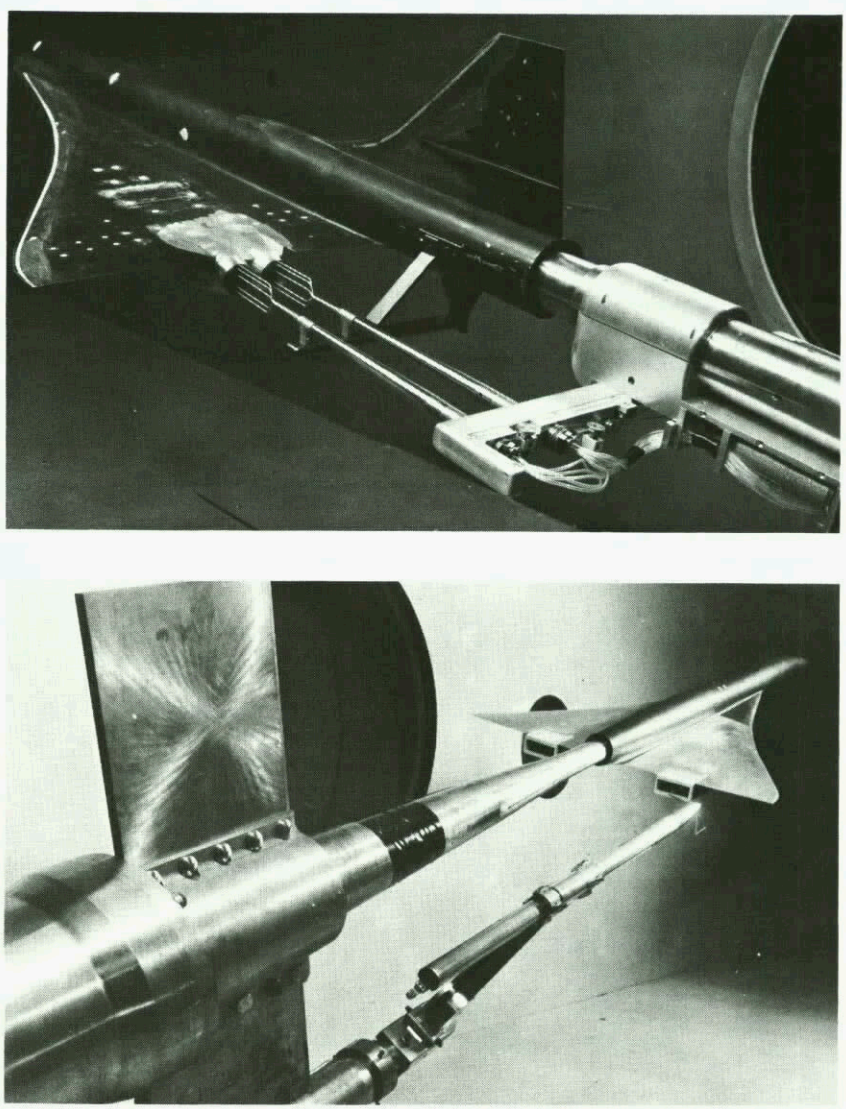

FIG. II. 2 EXAMPLES OF SUPERSONIC TRANSPORT MODEL INSTALLATION IN WIND TUNNELS FOR EXIT FLOW SURVEY.

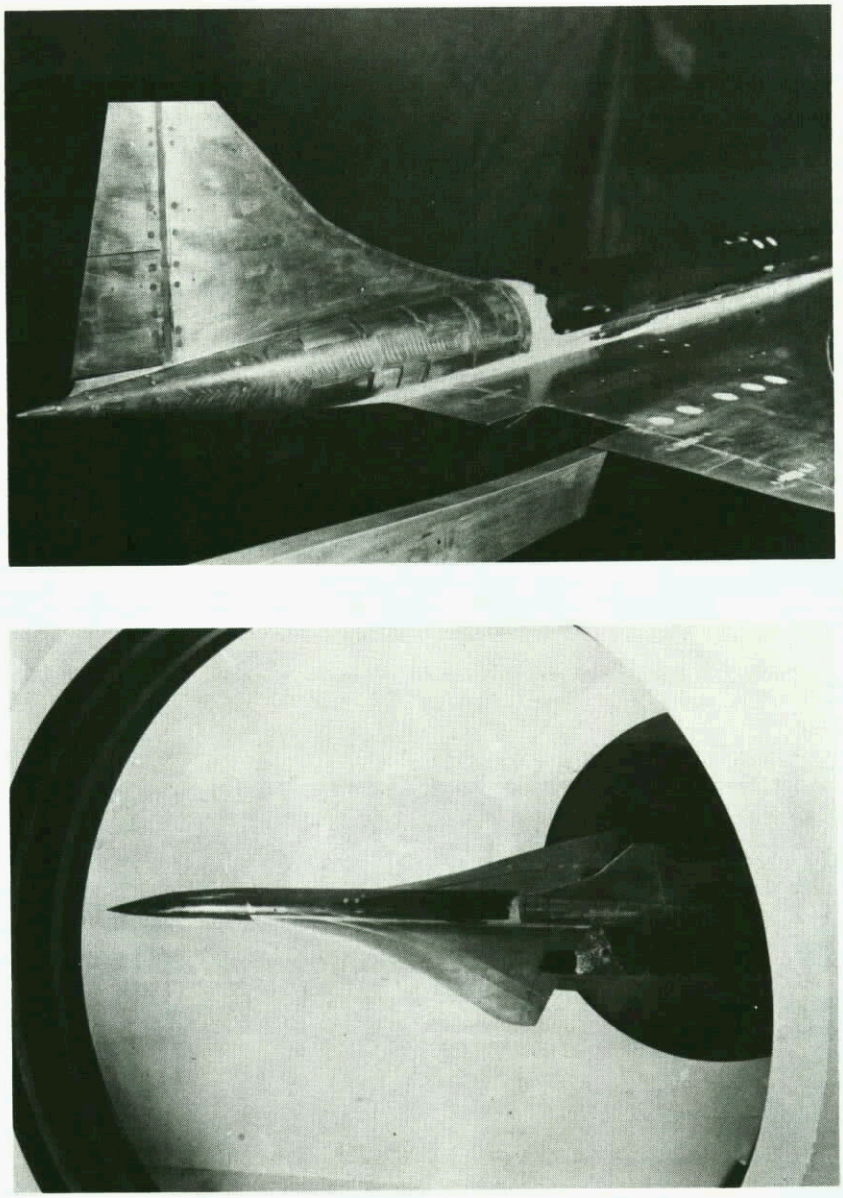

FIG. II. 3 TWIN STING SUPPORT FOR SUPERSONIC TRANSPORT MODEL.

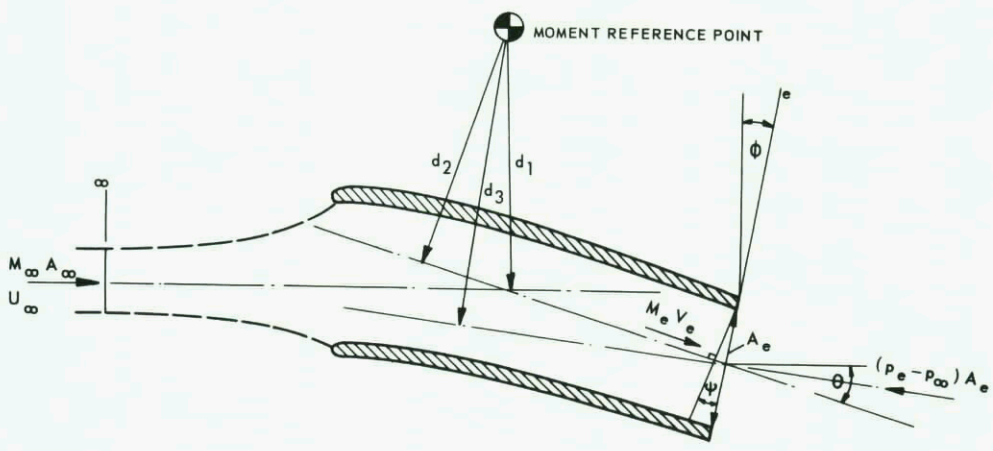

FIG. II. 4 DEFINITION OF DUCT GEOMETRY AND OF MOMENT ARMS ASSOCIATED WITH PITCHING MOMENT.

The full scale aircraft lift and pitching moments can be written similarly as:

$$C_{L_{aircraft}} = C_{L_2} - C_{L_{base}} - C_{L_{internal}}$$

$$C_{M_{aircraft}} = C_{M_2} - C_{M_{base}} - C_{M_{internal}}$$

where C_{L_2} and C_{M_2} are lift and pitching moment of the complete configuration in the wind tunnel,

and $C_{L_{internal}} = [(p_e - p_\infty) \sin \phi + \rho_e V_e^2 \sin \Theta \cos \psi] \frac{A_e}{A_{en} q_\infty}$

and $C_{M_{internal}} = -\frac{2A_\infty}{A_{en}} d_1 + \rho_e V_e^2 \cos \psi \frac{A_e}{A_{en} q_\infty} d_2 + (p_e - p_\infty) \frac{A_e d_3}{A_{en} q_\infty}$

where d_1, d_2 and d_3 are defined in Fig. II.4.

Other forms of external drag coefficient that have been found to be useful are:

External pressure drag coefficient $C_{D_{ext_p}} = C_{D_2} - C_{D_{base}} - C_{D_{internal}} - C_{D_{2_{f_{external}}}}$

and installation drag coefficient

$$C_{D_{instlln}} = (C_{D_2} - C_{D_1}) - (C_{D_{base}} + C_{D_{internal}}) - (C_{D_{2_{f_{external}}}} - C_{D_{1_{f_{external}}}})$$

where C_{D_1} = drag coefficient of wing plus body without nacelles

$C_{D_{1_{f_{external}}}}$ = skin friction drag of wing and body without nacelles .

Four measurements are necessary to determine external drag of a model with free flow through the engine ducts:

(a) overall force measurement
(b) nacelle and body base pressure
(c) static pressure distribution in the internal flow at or close to its exit
(d) pitot pressure distribution in the internal flow at or close to its exit.

The internal drag equation (including additive drag) can be rewritten as (Ref. II-13)

$$D_{int} = \rho_\infty V_\infty^2 A_\infty - \int_{A_e} (p_e - p_\infty + \rho_e V_e^2) \, dA$$

$$= \int_{A_e} p_e \left[\gamma M_e^2 \frac{V_\infty}{V_e} - (1 + \gamma M_e^2) \right] dA + p_\infty A_e$$

$$= \int_{A_e} p_e \, f(M_e) \, dA + p_\infty A_e$$

where $f(M_e) = \left[\gamma M_e^2 \frac{(\frac{V}{a^*})_\infty}{(V/a^*)_e} - (1 + \gamma M_e^2) \right]$

Use of this function is very benifitical at supersonic speeds and shocked exit conditions, especially if $M \simeq 2$, than this function is about zero.

Comprohensive surveys (i.e. 50 static and 120 pitot pressures of say $A_e = 23$ cm^2) are made using a single static pressure four tube pitot rake to evaluate p_e and $f(M_e)$ (Fig. II.5).

At supersonic speeds it is necessary to measure the base pressure (by base statics) at the same time as force measurements are made. The exit flow surveys are made on a separate occasion as of course the presence of the exit survey probe would alter base pressure.

In tests at transonic speeds it is necessary to measure internal flow by means of a few fixed pitot tubes supported from the duct walls at the same time as the base pressure and force measurements are made. These few pitot measurements are then used to assess the absolute level of pitot tube measurements taken when surveying the exit flow in a separate tunnel run.

For tests of subsonic engine installations (Figs. II.6 and II.7) some simplification of the above procedure can be made for the measurement of internal drag. From measurement of duct wall static pressure at the exit plane and a calculation of the boundary layer thickness at the exit plane, internal drag and mass flow can be evaluated. (See Ref. II-14).

Since in those engine installation the internal drag is small, the required accuracy of measurement can be low.

For example the measured mass flow does not need to be measured within 5 °/o, therefore simple rake measurements are sufficient for those cases.

B SPECIAL INLET MODELS

In the early stage of the wind tunnel program of an aircraft design the engine installation in the aero force model is schematically represented. The primary goal for those tests is to determine the complete aircraft characteristics. Corrections are made for the internal airflow through the inlets as indicated in section 2.1.2 A.

Separately special inlet models are tested on a larger scale which give, first the inlet performance

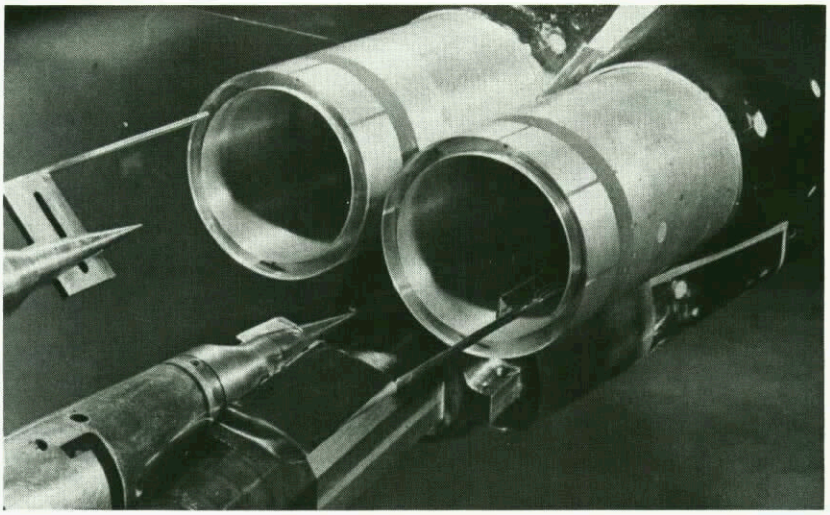

FIG. II. 5 FOUR PITOT TUBE RAKE AND SINGLE STATIC TUBE FOR EXIT FLOW SURVEY.

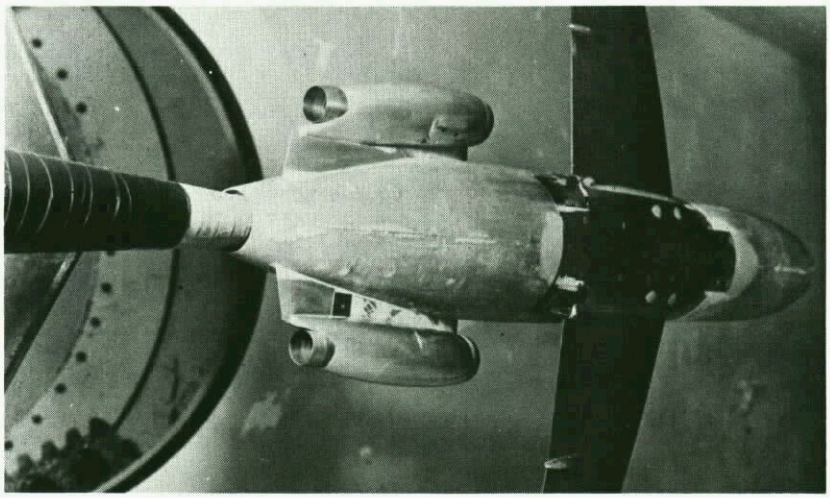

FIG. II. 6 SUBSONIC TRANSPORT MODEL INSTALLED ON SINGLE STING SUPPORT.

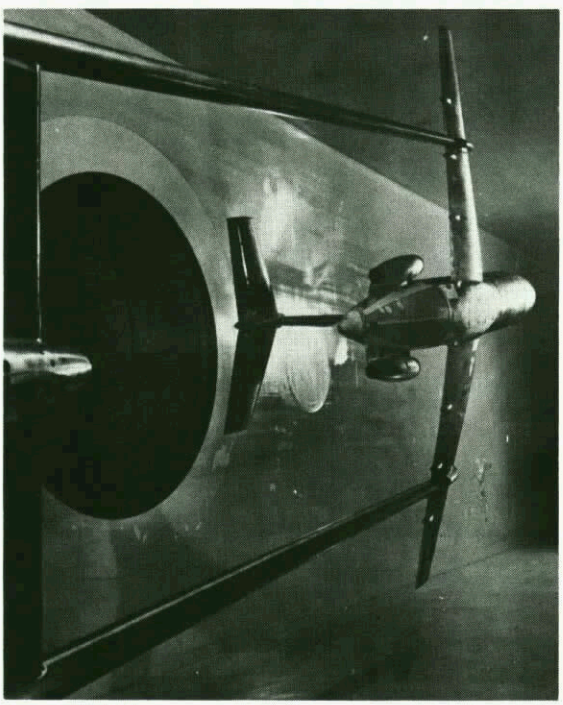

FIG. II. 7 SUBSONIC TRANSPORT MODEL INSTALLED ON TWIN STING SUPPORT.

and, second refined corrections for the aircraft characteristics as determined from the aero force model for the complete envelope of the engine(s) operating regimes. Fig. II.8 gives an example of such a bookkeeping procedure, particularly devoted to the inlet drag terms, which are important for the aircraft performance. In the connotation of this figure the ΔD_{ref} value would be applied to the vehicle drag polar as obtained from the aero force model. Compatibility is maintained between external aerodynamic and propulsion forces by correcting the installed engine thrust, F_N, by the change in inlet drag from the basic inlet to the propulsion reference inlet, ΔD_I (a similar correction is included for the nozzle afterbody, ΔD_N). The ΔD_I correction consists of several incremental components which are specified in this figure. The term $\Delta D_{I_{cr}}$ accounts for the drag differences between the basic inlet operating at its critical (cr) mass flow ratio and the reference inlet which is generally operated at a capture area ratio (mass flow ratio) as close to 1.0 as possible by using minimum inlet compression surfaces. The effects of inlet spillage below the critical mass-flow ratio would be included in the term $\Delta D_{I_{spill}}$. Both $\Delta D_{I_{cr}}$ and $\Delta D_{I_{spill}}$ will necessarily account for changes in local inlet forces such as inlet cowl drag and inlet additive drag.*) Also, interference effects due to interactions between the external flow field and the inlet flow field will be accounted for in these two terms.

The remaining drag quantities $\Delta D_{I_{blc}}$ and $\Delta D_{I_{bp}}$ include the flow momentum loss between free stream and exit conditions for the respective flows plus the installed door or louver drag. The effects of interference between bleed/bypass flow and the external surfaces of the aircraft are also included. Further information on the subject of engine-airplane interference and bookkeeping procedures is contained in references II-15-18.

Fig. II.9 poses similar questions to those in Fig. II.1 for the design for an inlet model specifically to measure the various inlets drag components. These questions primarily concern highly integrated engine-airframe designs such as a fighter. The testing of inlets for podded high bypass ratio fan engine requires a different consideration. Therefore first attention will be given to the integrated systems (B1) and later to the podded systems (B2)

B1 INTEGRATED SYSTEMS

At transonic speeds the upstream airframe surfaces and to a great extent the downstream surfaces must be simulated during inlet tests in the wind tunnel. Usually a compromise must be made between what is practical and what is desirable. At least checks should be made that neglected surface or system simulation does not influence the required results or can be accounted for by some other means. No standard rules are available which can give a priori an indication of the interference effects of downstream surfaces on the flow near the inlet.

Complete simulation for the operating range of inlet mass flow ratios is required for this inlet drag model. It is desirable to size the model to as large a scale as possible and thus provide for simulation of the boundary layer on all inlet and fuselage surfaces. Usually a total Reynolds number equal to flight cannot be achieved and artificial means are needed to scale the boundary layers on the model to equal the geometric scale. In some cases this is accomplished by fixing boundary layer transition forward of the point where transition normally would occur. In other cases where the viscous characteristics are not properly matched to the inlet geometry, the geometry can be adjusted. For example, the inlet can be placed further from the airframe surface to provide the proper aerodynamic scaling of the boundary-layer thickness relative to the diverter height. More attention will be given to it in 2.1.4. Inlet drag models which can be adapted in this manner should be on the order of 1/12 scale or larger.

TECHNIQUES

Some techniques and examples as used by various groups will be discussed next.

Probably the primary choice in the design of a specialized inlet model is whether the whole model (i.e. intake plus fuselage or wing) is mounted on a balance or just the intake itself. Fig. II.10 shows an arrangement where the supersonic intake alone is on the balance. This leads to measurement of smaller forces, with those associated with the intake being predominant. In addition the means of measuring the internal mass flow can be located wherever desired, and whatever means necessary to ensure accurate measurement can be introduced (e.g. screens, venturi, multi tube rakes etc.) easily. The disadvantages are: (a) the sealing problems at the junction between the "live" and "earthed" portions of the duct, (b) the accurate measurement of forces on parts of the fuselage on the balance that could change as intake flow conditions change, (c) the difficulties of measuring momentum of the internal flow at the duct junction position where the flow may still be quite non-uniform, and (d) the general difficulties of interpreting forces measured on only part of a model. Changes of geometry which lead to changes of pressure on non-metric parts of the model can lead to spurious conclusions as to the efficiency of the geometric changes being studied. Inlet flow is discharged through an extended duct far enough downstream to avoid any influence on the inlet.

Inlet mass flow ratio is usually controlled and measured by a variable area nozzle or plug (metric or non-metric). For most wind tunnel conditions the nozzle can be operated at choked flow conditions which makes possible a measurement of mass flow ratio at the minimum flow area station. The "sonic plug" method of measurement assumes uniform choked flow conditions at the exit plug station with minimum flow area (throat). The flow coefficient of the metering system is obtained by inserting calibration flow meters usually downstream of the flow measuring station. Calibration is accomplished under static conditions using an external pump arrangement or, if space permits, under wind tunnel flow conditions using an attachment to the model which is removed after the calibration runs to prevent encumbering the force measurements.

Variation of the throat area is the means by which mass flow ratio is changed, and in those cases using plug systems a remote control drive motor can be used for rapid and precise flow changes. Low transonic Mach number testing requires the use of rakes (total and static pressure measuring probes) or flow meters for mass flow ratio measurement, since sonic flow is difficult to attain. The accuracy of any mass flow measurement decreases with a decrease in velocity at the measuring station. The calibration procedure for the rake method requires precision and must include the full range of flow conditions which will occur at the rake during the wind tunnel tests. More attention to mass flow measurements will be given in 2.1.3.

*) Additive drag is a force correction which accounts for the momentum differences between free stream conditions and conditions at the inlet cowl leading edge.

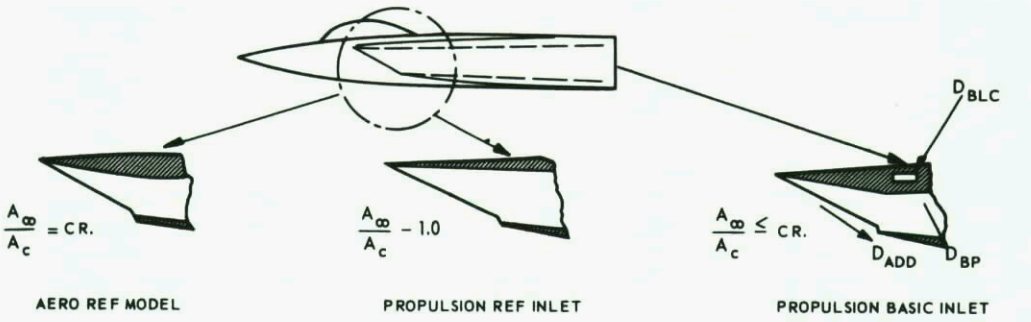

AERO FORCE MODEL

$DRAG_{A/V} = DRAG_{AERO\ MODEL} - \Delta D_{REF}$

$\Delta D_{REF} = D_{AERO\ REF} - D_{PROP\ REF}$

ΔD_{REF} OBTAINED FROM PROPULSION MODEL

ΔD_{REF} OBTAINED FOR RANGE OF α

PROPULSION MODEL

$F_N = F_G - \Delta D_I$

$\Delta D_I = D_{PROP\ BASIC} - D_{PROP\ REF}$
$= \Delta D_{I_{CR}} + \Delta D_{I_{ADD}} + \Delta D_{I_{BLC}} + \Delta D_{I_{BP}}$

ΔD_I OBTAINED FOR RANGE OF α

FIG. II. 8 INLET DRAG BOOKKEEPING.

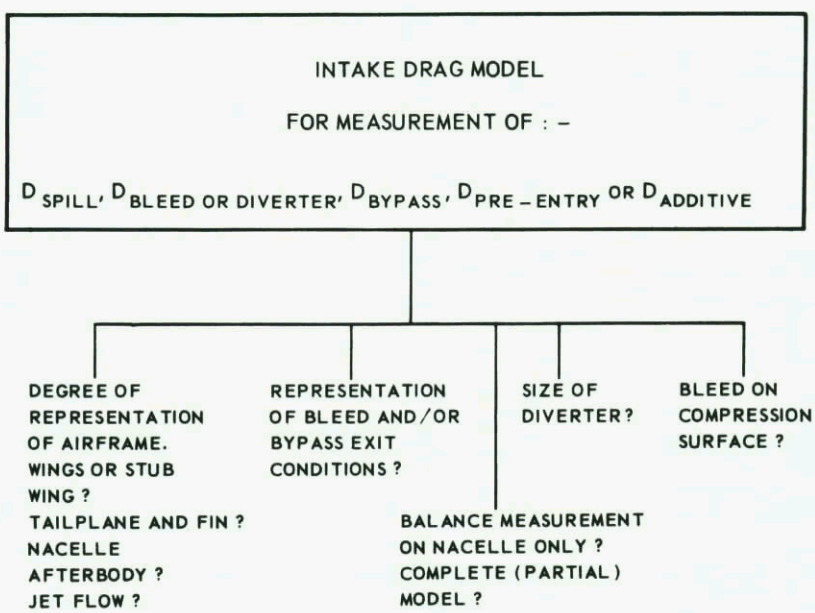

FIG. II. 9 PROBLEMS OF INTAKE DRAG MODELS.

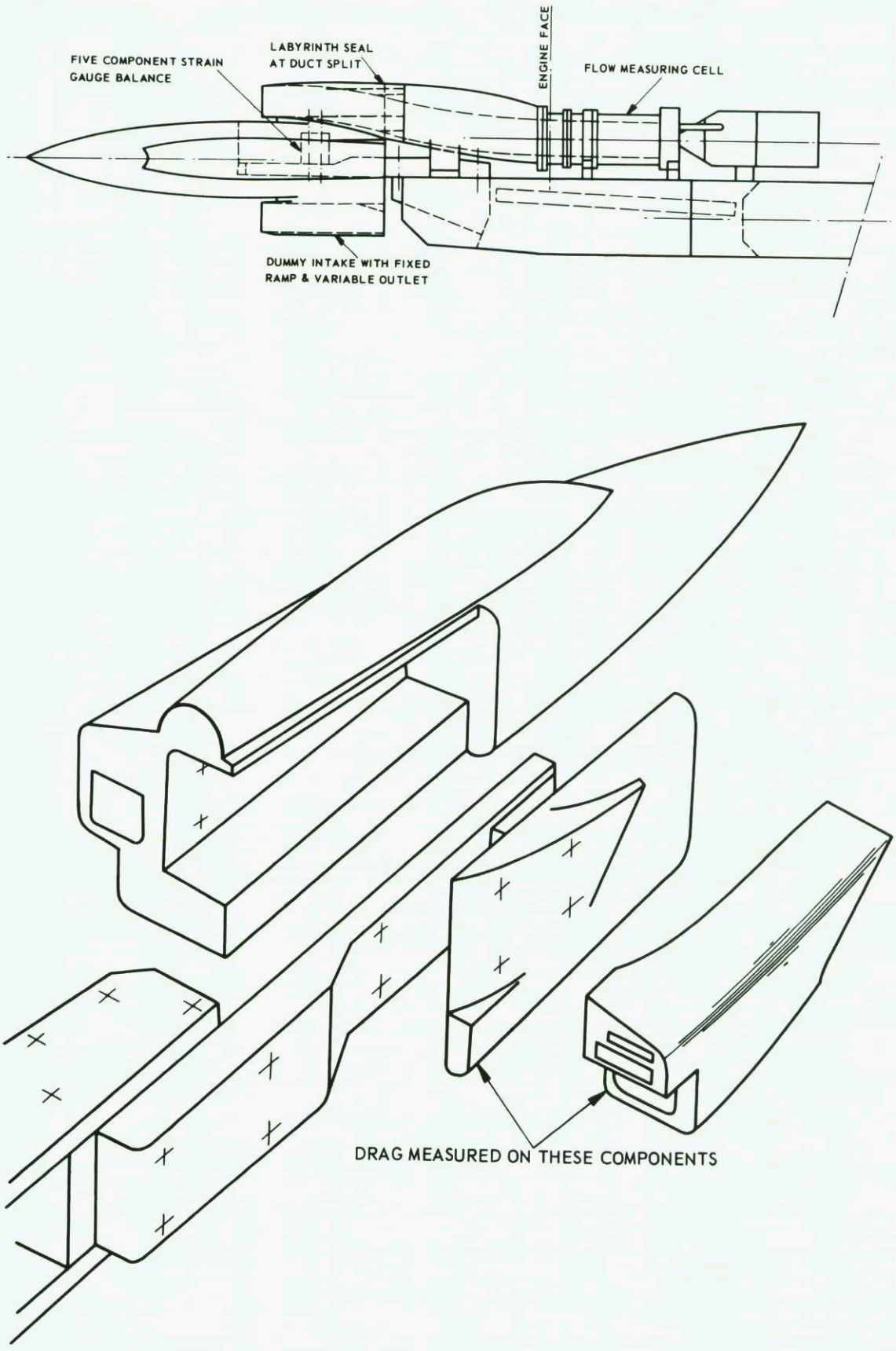

FIG. II. 10 INLET MODEL WITH METRIC INLET ONLY.

A simplier set-up, wall mounting, is used by another group as shown in fig. II.11a for a two dimensional supersonic inlet. The metric part (inlet + boundary layer diverter between wall and inlet) is connected to the balance with struts through the wind tunnel wall. The bleed flow is ejected by a tube with calibrated-stiffness bellows. Internal static pressure, p_2, and base pressures p_{b_i} (30 points) are measured in a first step. Then, the pressure ducts are disconnected, and the forces are measured. The rig yields the intake drag ($D_{add} + D_{ext}$) using some elementary relations; the mass flow is deduced from the measured p_2, with the assumption of a sonic discharge throat. This permits only measurements in high subsonic flow as stated before. A reference cowl drag is also measured, for comparison, according to the figure II.11b.

Validity limits for the measurements have not been derived, because of the lack of cowl pressure survey. Two difficulties are encountered: (a) the imperfection of the mass flow measurement, due to the non-uniformity of the internal flow, and (b) the imperfection of the base drag measurement, due to the non-uniformity of the base pressure. These two difficulties can be solved by connecting the rear part of the model on a mass flow meter and on an ejector, by some calibrated-stiffness rubber seals, sothat a similar set up is obtained as in Fig. II.10. This will also permit measurements at lower Mach numbers. The examination of the drag calculation from the test results showed that the result is very sensitive to the Mach number definition of the wind tunnel; in other words, it is necessary to verify that the wind tunnel Mach number is representative of the upstream Mach number for the model. However, preliminary tests have provided some reliable values of the inlet drag correction with the mass flow rate in spite of the difficulties stated above.

Fig. II.12a and b show another method for measuring the same quantities. In this case the complete model is mounted on the balance, and only the units used for traversing the internal flow for measurement of mass flow and momentum are "earthed". The forces being measured now include fairly large components (eg base, nose and canopy drag) which are not required. This has the effect of inhibiting the reproduction of other components on the model, such as wings, to reduce the overall loads and increase the sensitivity of the balance to the force components which are of interest. Thus the effect of, say, bypass door operation, on the stability of the configuration has to be sacrificed. The model tends to become rather long if the flow measurement station is to be at a position where the flow is fairly uniform. To avoid difficulties due to shock reflections at low supersonic speeds with a long model, the rear half has to be made with constant cross sections; hence, additional true geometrical representation may be lost. However, the sealing problems as in Fig. II.10 and 11 at the duct junction have disappeared and changes in geometry of the nacelles can be studied with the knowledge that their total effect is being measured. The base drag is measured by pitot tubes placed approximately 0,5 mm from the base. The base is shrouded to try to produce uniform base pressure under all conditions (Ref. II-19).

Fig. II.13a and b show a solution to the same problem somewhere between the solutions of Fig. II.11 and II.12. The metric line is provided along the cylindrical part of the model, where the external flow is almost uniform. The seal is rolled on itself if the metric part is translated, sothat the reaction is constant. This sealing technique seems to be very satisfactory.

As seen at the complete model tests, the external drag must be determined from three drag measurements:

$$D_{external} = D_{balance} - D_{base} - D_{internal} .$$

The balance force, $D_{balance}$, needs to be corrected for the base drag, D_{base}, or by the sealing drag, both obtained by pressure plotting, and by the internal drag. The internal drag, D_{int}, is the difference between the freestream momentum minus the impuls at the measuring station or exit

$$D_{int} = \dot{m}\ V_\infty - \int_{A_e} [p_e\ (1 + \gamma M_e^2) - p_\infty\ ]\ dA$$

or expressed as a coefficient

$$C_{D_{int}} = \frac{2A_\infty}{A_{en}} - \frac{A_e}{q_\infty\ A_{en}} [\ (p_e - p_\infty\ ) + \gamma\ p_e\ M_e^2]$$

where the subscripte denotes exit plane or measuring station and A_{en} represents a reference engine area. If the measuring station is upstream or downstream of the internal seal the duct area must be constant and parallel. Then the internal drag can be corrected for estimated internal friction forces. The measured external drag is then the pre-entry or additive drag minus the suction forces on the cowl plus the external skin friction drag. If bleeds and bypasses are provided, these terms are included in the external drag.

B2 PODDED INSTALLATIONS

The installation drag of an high bypass fan engine in pods may be as high as 10 °/o of the net engine thrust. This fact necessitates careful nacelle and pylon design in order to minimize unfavourable interference effects. The goal of the inlet designer is to achieve a reduced pressure on the external inlet cowl such that the axial component of the integrated relative surface pressure results in a thrust force equal to the additive drag. For reversible inviscid flow complete additive drag cancellation would occur. To this end isolated inlet tests are performed to obtain optimum cowl design at all speed ranges within the flight envelope. As with integrated engine installations it is possible to approach the problem of podded engines, at least up to a given Mach number, by studying the force operating on the forebody cowl with an integrated balance combined with precision measurement of the internal flow, alternativily the forces can be obtained from pressure measurements on the forebody cowl and from boundary layer measurements for the skin friction. The advantage of this last combination is that a detailed description of the flow can be obtained. This description is necessary to optimize the shroud shape.

Another technique to measure the inlet drag consists of a complete exploration of the wind tunnel flow around the inlet extended by a cylindrical extension. The drag is then deduced from a momentum balance-sheet between upstream and downstream infinities. This technique will be discussed later in this section.

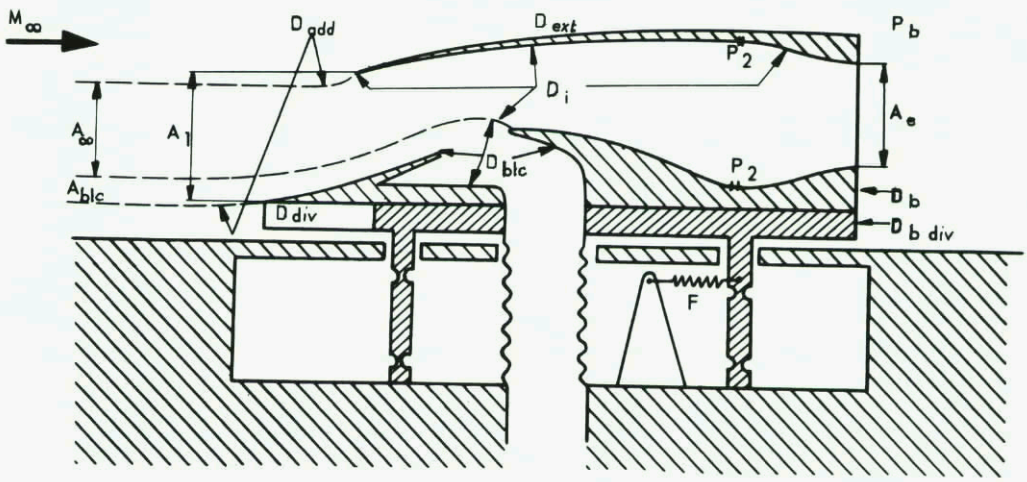

FIG. II. 11a DRAG MEASUREMENT ON COMPLETE AIR INTAKE SCHEMATIC PRINCIPLE.

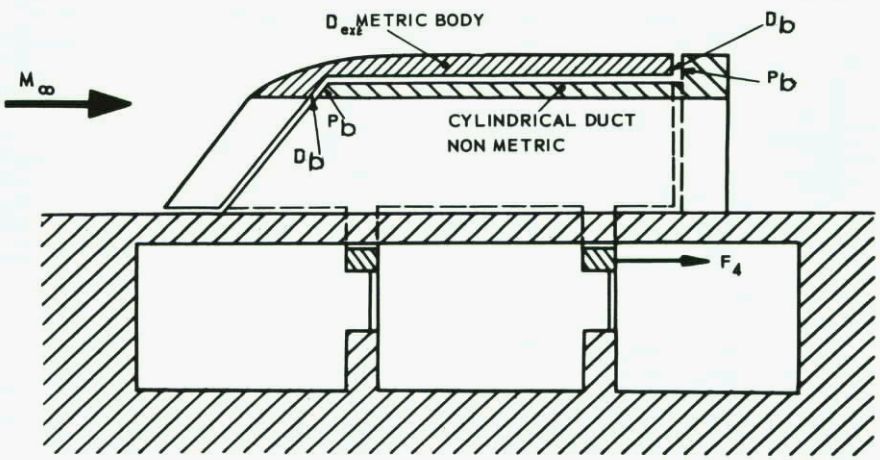

FIG. II. 11b DRAG MEASUREMENT ON A REFERENCE COWL.

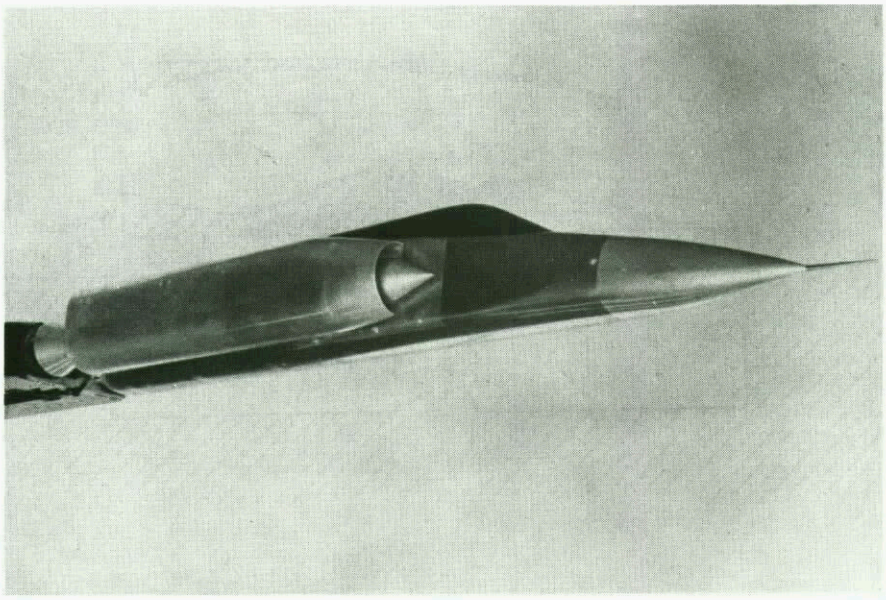

FIG. II. 12a PARTIAL MODEL OF STRIKE – FIGHTER FOR MEASUREMENT OF COWL, SPILLAGE AND DIVERTER DRAG.

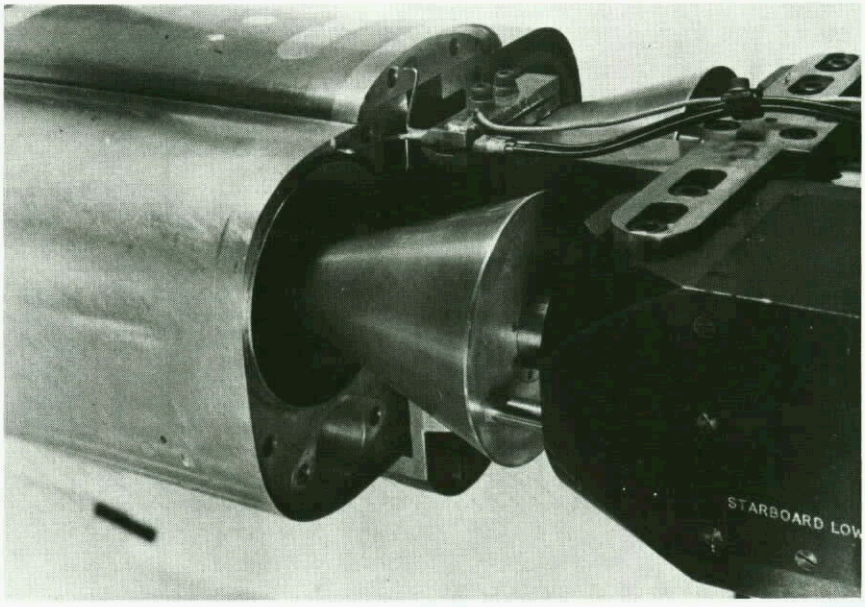

FIG. II. 12b SHROUDED BASE AND BASE PITOT TUBE RAKE.

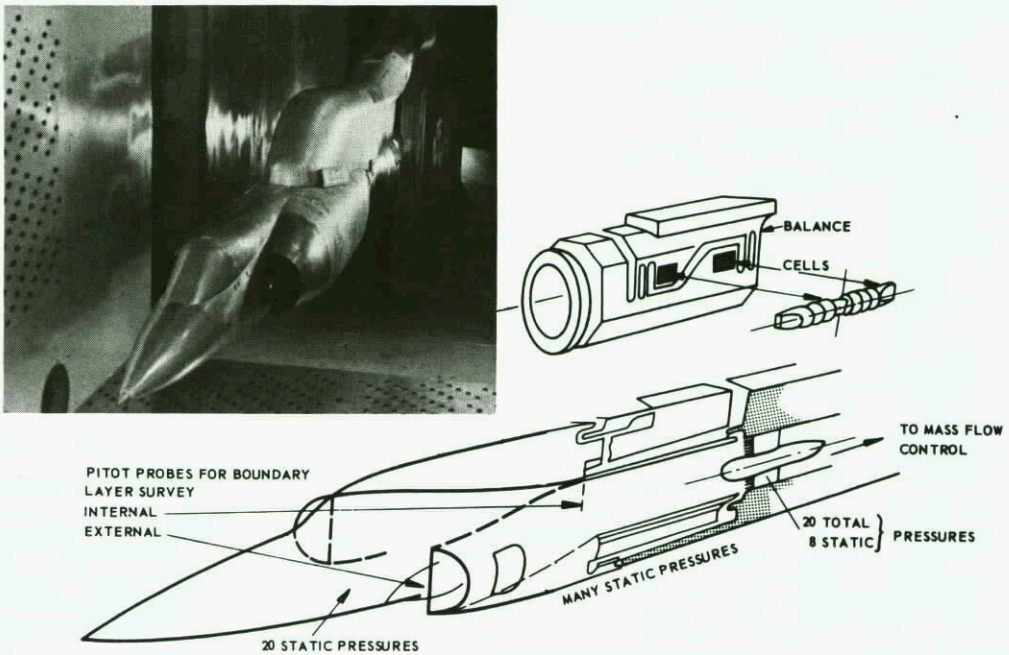

FIG. II. 13a DETAIL OF INLET WIND TUNNEL MODEL.

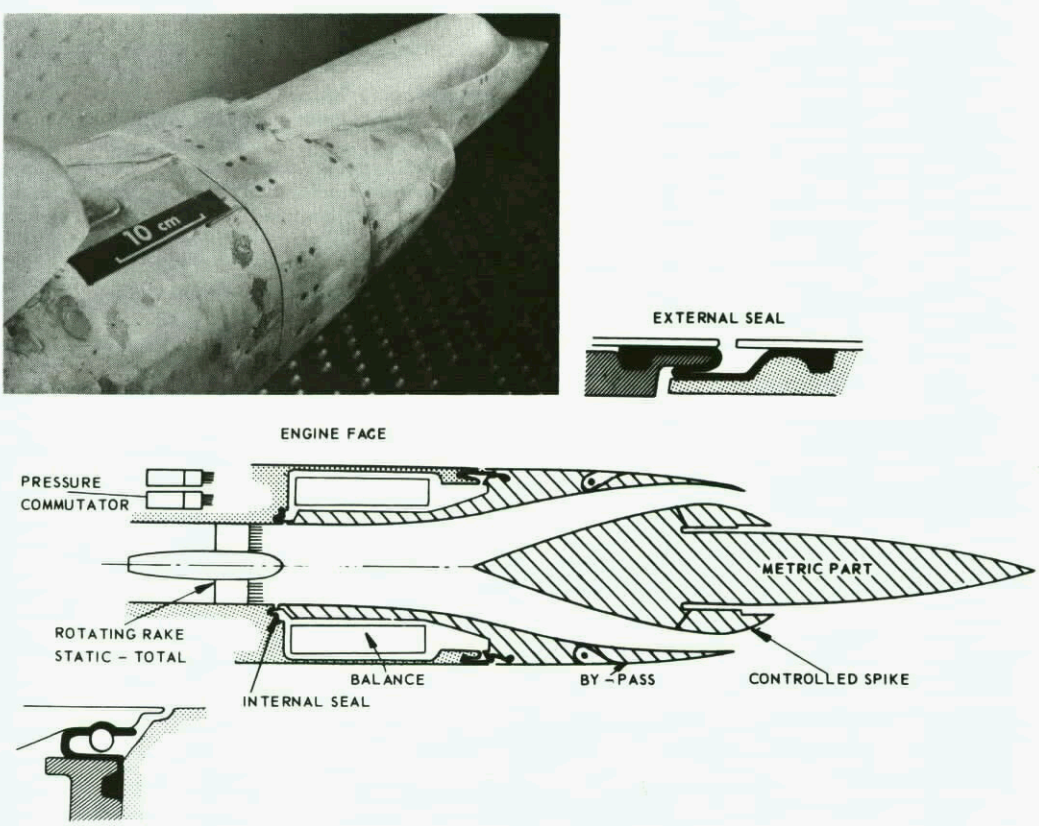

FIG. II. 13b FURTHER DETAILS OF MODEL OF FIG. II. 13a.

Consider first the following sketch:

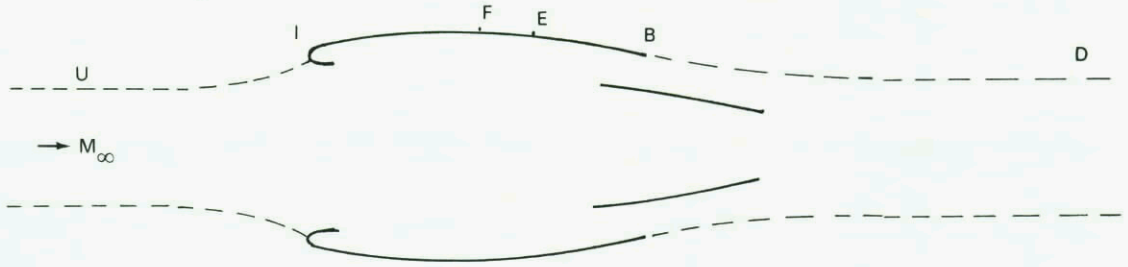

If the external flow, limited by the stream surface UIFBD, presents no irreversibility (shock, separation, vortex...) except for the friction on the wall IB and the shearing according to the surface BD, the resultant of the relative normal pressure forces on the supposed solid contour UIFBD is equal to zero, after a correction for the displacement effect of the boundary layer. If the flow is not reversible, the resultant without correction is, by definition, the engine pressure drag.

The inlet pressure drag coefficient may be defined as the difference of the pressure drag coefficients relative to the UIFE surface, between the case of the considered flow and the case of a reversible potential flow. This difference can usually be determined experimentally. Since it is supposed that downstream has no influence on upstream, these coefficients can be measured with an installation consisting of a cylindrical pipe put in place of the jet and connecting the inlet with an ejector via a mass flow meter.

The experimental arrangement is shown in Figure II.14 (Ref. II-20). All the forebody isolated cowl contains static pressure taps from an internal cylindrical cross-sectional area A_2 up to the external point E. The determination of the pressure drag coefficient on the surface UIE as previously defined results, for a given Mach number, from the pressure and the mass flow measurements, and from the description of the internal boundary layers. The knowledge of the external boundary layer yields the precise skin friction factor and the displacement correction for the smooth flow test.

In order to obtain these results, various applications of the momentum theorem are used. The model is shown in a transonic wind tunnel in Figure II.15, with downstream faired support struts.

Figure II.16 shows an example of the evolution of the pressure drag coefficient (C_{D_p}) deduced from the measurements for different given Mach numbers. It is seen on this figure that for both mass flow coefficients, the drag is equal to zero for $M = 0.5$. For these tests however, at low Mach number and smooth flow around the leading edge, it is only the external drag of the model forebody which is theoretically equal to zero, but the result is explained by the almost null values of the pressure coefficients near E and the vicinity of the downstream cylindrical part. Furthermore, the boundary layer displacement correction has been neglected.

Figure II.17 gives an example of the friction drag coefficient, calculated at $M = 0.85$, as a function of the mass flow coefficient. This drag is calculated in this case from a boundary layer exploration in E. A corrective factor must be calculated to take into account the fact of a non cylindrical forebody shape. Its expression is written on the figure. Its evaluation is uncertain because it is based on a approximate boundary layer calculation which can be very inaccurate when the external flow has shocks, separations etc. The pressure drag coefficient must be added to the friction drag coefficient to obtain the inlet drag coefficient.

This technique has two practical difficulties: (a) the lip suction force is very strongly influenced by any errors in determining the location of the stagnation line, and (b) an accurate solution for the compressible equations of motion of the flow ahead of the inlet must be calculated before the additive drag can be determined and compared with the measured lip suction force.

Both of these difficulties can be avoided if tests are carried out with an axial force measurement on inlet models. An arrangement which is proposed to use in a transonic wind tunnel is shown in Figure 11.18 (Ref. II-21). After making the following definitions,

$$\text{Additive drag } D_{add} = \int_{A_\infty}^{A_1} (p - p_\infty)\, dA$$

$$\text{Suction thrust } T_{ls} = \int_{A_1}^{A_4} (p_\infty - p)\, dA - \int_{S_1}^{S_4} \tau\, dS$$

$$\text{External drag: } D_{Ex} = D_{add} - T_{ls}$$

it will be shown that the external lip drag, D_E, can be calculated from measured quantities on such a test arrangement as:

$$D_{Ex} = \dot{m}\,(V_n - V_\infty) + A_n(p_n - p_s) + A_4(p_c - p_\infty) + A_s'(p_s - p_c) - H\ .$$

If the internal surfaces of the shaded body of Figure II.19 exert a force on the captured streamtube whose axial component, φ, is assumed to be directed downstream, the axial force on the captured streamtube between a station ahead of the model in undisturbed flow and the exit plane of the nozzle, n, is:

$$p_\infty A_\infty + \int_A^{A_1} p\, dA + \varphi - p_n A_n\ .$$

This force may be equated to the increase in the axial component of momentum flux of the captured streamtube between these two reference stations:

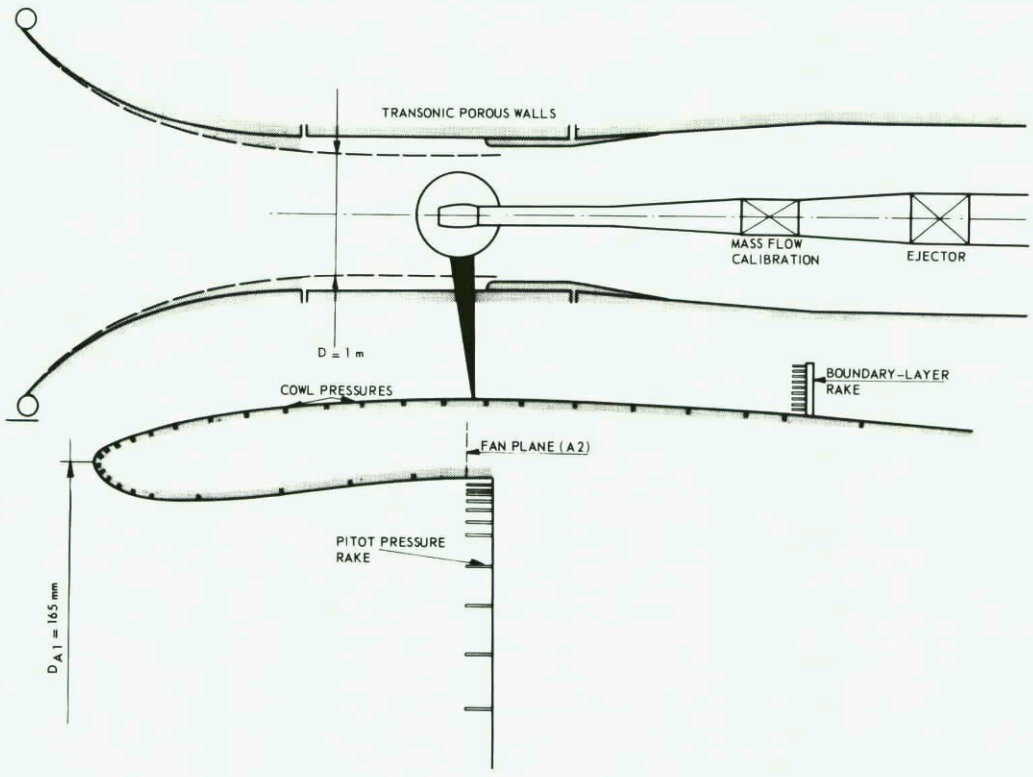

FIG. II. 14 TRANSONIC TESTS ON ISOLATED AIR INTAKE FOR FAN ENGINE.

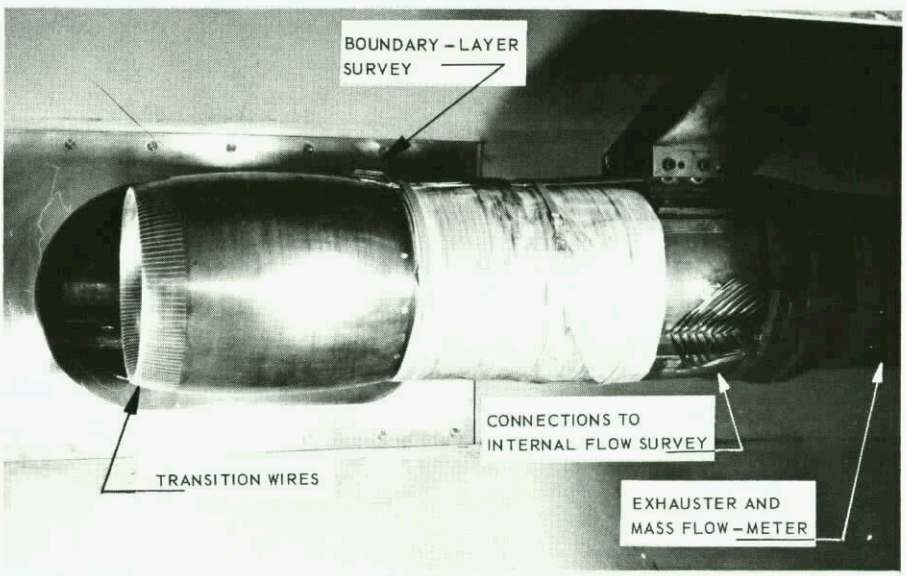

FIG. II. 15 AIR INTAKE STUDY.

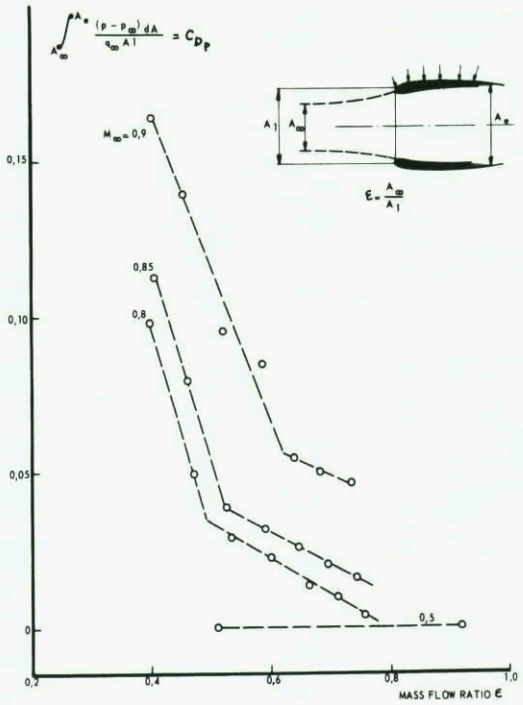

FIG. II. 16 PRESSURE DRAG VERSUS MASS FLOW RATIO FOR AN ISOLATED FAN INLET.

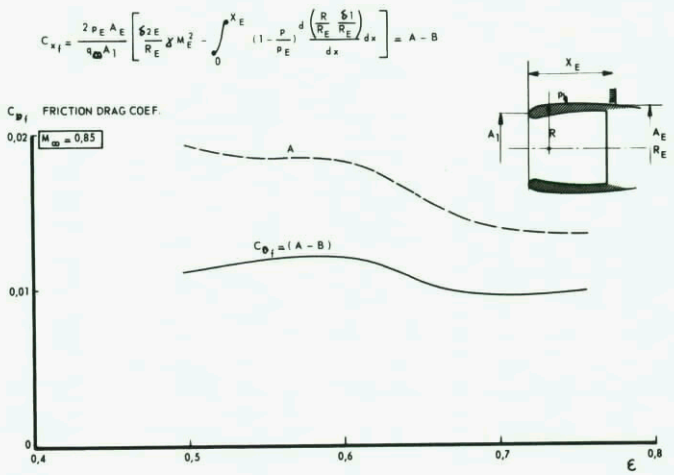

FIG. II. 17 FRICTION DRAG COEFFICIENT VS MASS FLOW RATIO FOR AN ISOLATED FAN INLET.

$$p_\infty A_\infty + \int_{A_\infty}^{A_1} p\,dA + \varphi - p_n A_n = \dot{m} V_n - \dot{m} V_\infty .$$

An equal but opposite force, $-\varphi$, must be exerted by the streamtube on the body. Since the body is in static equilibrium, the total axial force acting on the surface of the body must be zero:

$$-\varphi + \int_{A_1}^{A_4} p\,dA + \int_{S_1}^{S_4} \tau\,dS - p_c (A_4 - A_s') - p_s (A_s' - A_n) + H = 0.$$

Simultaneous solution of the above equations eliminates the force and the expression for D_{Ex} is obtained. Proper corrections can be made to D_{Ex} to account for the change in skin friction, τ, for the higher Reynolds number of the aircraft installation. Such an isolated inlet test can also incorporate studies of inlet total pressure loss and distortion without affecting the external drag.

Another technique to determine the external inlet cowl drag is depicted in fig. II.19 which is in use since 1960. Originally the complete cowl profiles could be varied, but currently the aft end of the nacelle is an integral part of the rig and only the forebodies are interchangeable. Intake mass flow is controlled using a motorised exhaust plug, and is determined from internal rake measurements. Four external rakes positioned aft of the nacelle are used to obtain the drag from the momentum deficit associated with the flow about the nacelle. By varying the taper angle of the rig aft of the rakes and also be removing the rakes, the aft end of the rig was shown to have an insignificant effect on the forecowl surface pressures, although it did of course produce a pressure increase on the rear faces of the nacelle. This test also confirmed Ritter's assessment (Ref.II.22) that interference field effects on boundary layer development have a negligible effect on the magnitude of the profile drag.

Each drag rake is of sufficient extent to measure wake losses at high spill conditions, at incidences of at least 6°. At very high subsonic Mach numbers shock wave losses extend beyond the confines of the rakes, but this is not of concern in determining M_D, and for qualitative assessments of relative nacelle performance. Since the area weighting of the pressure tubes is on an annular basis the very small total head losses that are present at the extremities of the rakes when weak shock waves are present are more significant than in equivalent 2-dimensional rake survey tests. At low Mach numbers and at low incidence the extent of the wake is small even when the intake is spilling and typically does not extend further than 0.2 cowl diameters from the support tube surface at the measurement plane.

The calculation of profile drag from the measurement of total pressure and static pressure distributions at the rakes follows the usual method in which the mass flow and total head loss is determined for a particular stream tube at the measurement rake and this data is then used to calculate the momentum deficit at downstream infinity assuming no further total head losses occur.

Thus,

$$D = \sum \dot{m}_i (V_\infty - V_i)$$

where $\dot{m}_i$ is the air mass flow in the stream tube containing pitot i and V_i is the velocity in this stream tube at downstream infinity. Suffix ∞ refers to freestream conditions.

Now

$$Q_i = \left(\frac{\dot{m}\sqrt{T}}{p_t A}\right)_i = \sqrt{\frac{2\gamma g}{(\gamma-1)R} \frac{\left\{1-\left(\frac{p_{t_i}}{p_i}\right)^{\frac{1-\gamma}{\gamma}}\right\}}{\frac{p_{t_i}}{p_i}^{2/\gamma}}}$$

and

$$\frac{V_i}{\sqrt{T_\infty}} = \sqrt{\frac{2\gamma g R}{(\gamma-1)} \left\{1 - \left(\frac{p_{t_i}}{p_\infty}\right)^{\frac{1-\gamma}{\gamma}}\right\}}$$

where p_i, p_{t_i} are the static and total pressures in the stream tube at the rakes.

Hence,

$$D = \sum Q_i\, p_{t_i}\, A_i \left[\left(\frac{V_\infty}{\sqrt{T_\infty}}\right) - \left(\frac{V_i}{\sqrt{T_\infty}}\right)\right]$$

where A_i is the area allocated to each stream tube at the rakes.

2.1.3 TECHNIQUES FOR MEASURING INLET MASS FLOWS

It is obvious that the inlet mass flow is a primary inlet variable and must be controlled and measured with extreme precision. For example a double ramp intake operating at $M = 2.2$ an effective change of ramp of 1° results in a change of maximum inlet flow $\left(\Delta A_\infty / A_{en}\right)_{max}$ of 1 °/o and a change of pre-entry drag coefficient $\Delta C_{D_{pre}}$ of 0.008. It is therefore generally agreed that if the external drag is being determined from the difference of a drag balance measurement and the internal drag-as described in the previous section - the inlet mass flow should be measured at least within 1/2 °/o. (Ref. II-23). With specially designed mass flow cells-as will be described later - measurement of mass flow to within 1 °/o certainty can be normal routine. If insufficient care is taken errors as large as 5 °/o may result. The least inaccuracy can be expected if the mass flow is computed from rake surveys in the internal duct only and can only be obtained if the distortions at the measuring station are small.

The higher accuracies are obtained if the measuring cell is calibrated against a standard. It is usual that the exit is formed by a sonic or near sonic exhaust with plug. The mass flow can than be written as a function of the discharge coefficient of the exhaust. What is important in quoting the stated accuracies are the numbers on the standard deviations and on the possible error of the mean. The former should be at least less than 1/2 °/o. The presence of noise could cause perturbations of the

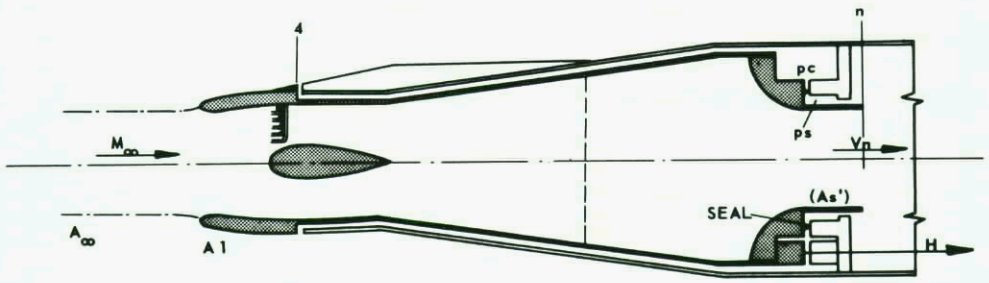

FIG. II. 18 WIND TUNNEL TEST OF INLET MODEL.

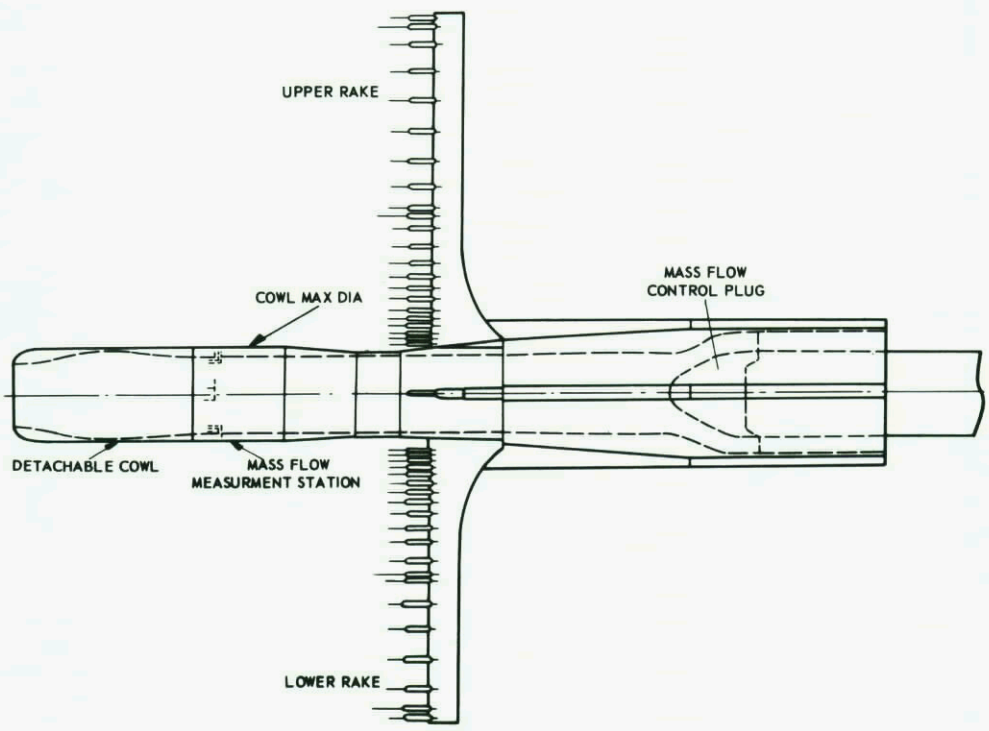

FIG. II. 19 GENERAL ARRANGEMENT OF MODEL FOR COWL DRAG DETERMINATION.

order of 1/2 °/o. By careful calibration the error of the mean of the discharge coefficient can be less than 0,1 °/o. However in inlet tests, usually the stagnation temperature distribution is not measured. When the model is at a different temperature as the stagnation temperature of the tunnel, and heat transfer takes place in the inlet duct, the stagnation temperature distribution should be measured in front of the flow meter in order to obtain the required accuracy. In addition in the calibration rigs the actual distortion of the stagnation pressure and temperature measured in the inlet should be represented. When possible, the distortion should be minimized in front of the flow meter. For example supercritical internal flow will give distortions and therefore rapid deterioration in the accuracy of inlet flow and internal drag measurement, leading to wrong conclusions regarding the external drag. Furthermore, the accuracy of the mass flow measurement decreases with a decrease in velocity at the measuring station. The calibration procedure for the rake method requires extreme precision and must include the full range of flow conditions which will occur at the rake.

Fig. II.20 shows a standard cell for measurement of the mass flow which is also used to measure engine fan pressure recovery and flow distortions. This is a completely self contained piece of equipment which can be made in several sizes (Ref. II-13). Some results of calibration tests are also shown. Fig. II.21 is a photograph of a similar design. In this case the flow is surveyed by a rake of twelve pitot tubes across a diameter plus two static stubes (one located centrally and one at 0.67 of duct radius) which can rotate to any position. This rake and the conical throttles, which vary the exit area, are cantilevered forwards into the duct and survey the flow at a station "f" where the duct is of constant area. This internal rake, model duct and exit are calibrated for accurate measurement of mass flow. Flow through a standard orifice plate is compared with that measured by the rake using the model duct but replacing the intake by a 4 : 1 contraction ratio bellmouth.

The following calibration factors are evaluated from this test:

$$C_{d_{(P_f)}} = \frac{\text{mass flow measured by orifice plate}}{\text{mass flow derived from area weighted mean total pressure at station "f" and the geometric area of the choked exit}}$$

$$K_f = \frac{\text{mass flow measured by orifice plate}}{\text{mass flow derived from mean static pressure and area weighted total pressure at station "f"}}$$

$C_{d_{(p_f)}}$ is applied at supersonic speeds in the form of a correction to the geometric exit area giving:

$$A_{ex_{effective}} = A_{ex_{geometric}} \times C_{d_{(P_f)}} .$$

K_f is used at subsonic speeds where the exit is not choked and as the Mach number M_f is generally less than 0.5 the flow can be considered incompressible so that

$$K_f = \frac{\text{true mean Mach number } M_f}{\text{measured mean Mach number } M_f} .$$

When using the equation for internal drag the true mean value of M_f^2 is required, This is obtained in the following way. For a family of velocity profiles defined by:

$$\frac{V}{V_m} = \left(\frac{1 - r}{1 - z}\right)^{1/n}$$

the two constants:

$$K = \frac{\text{Mean Mach number } M_f \text{ from integration of velocity profile}}{\text{Mean Mach number obtained from six discrete points (the positions of the pitot tubes) on the profile}}$$

and

$$K_M = \frac{\text{Mean } M_f^2 \text{ from integration of velocity profile}}{\text{Mean } M_f^2 \text{ obtained from six discrete points on the profile}}$$

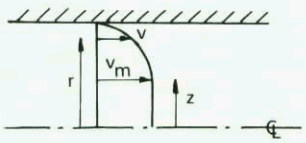

are calculated for the conditions:

$$0.2 \leqslant z \leqslant 0.8$$
$$2 \leqslant n \leqslant 7$$

To a first approximation it is found that a single linear relationship exists between the factors K and K_M. Thus the experimental value of K (i.e. K_f) is used to find a value of K_M which is then used to evaluate the "true" mean value of M_f^2 in equation.
The table below gives an indication of the estimated accuracies of the external drag of the model of Fig. II.12a at various Mach numbers.

M_∞	$\frac{A_\infty}{A_{en}}$	Component accuracies				Absolute value $C_{D_{ext}}$
		$C_{D_{internal}}$	$C_{D_{bal}}$	$C_{D_{base}}$	C_D	
0.5	0.687	± .031	± .003	± .004	± .038	.39
0.9	0.742	± .024			± .031	.41
2.0	0.895	± .024			± .031	1.04

It is noticed that general consistency and repeatability of points is about $C_D = \pm .01$ when the velocity distribution at the survey station is good.

Fig. II-22 shows an example of a rig used to calibrate these mass flow cells. At the present time a standard NGTE choked nozzle (whose discharge coefficient is known to ± 1/4 °/o) is being used to calibrate a large range of standard flow orifices. With the NGTE nozzle removed, these calibrated orifices are then

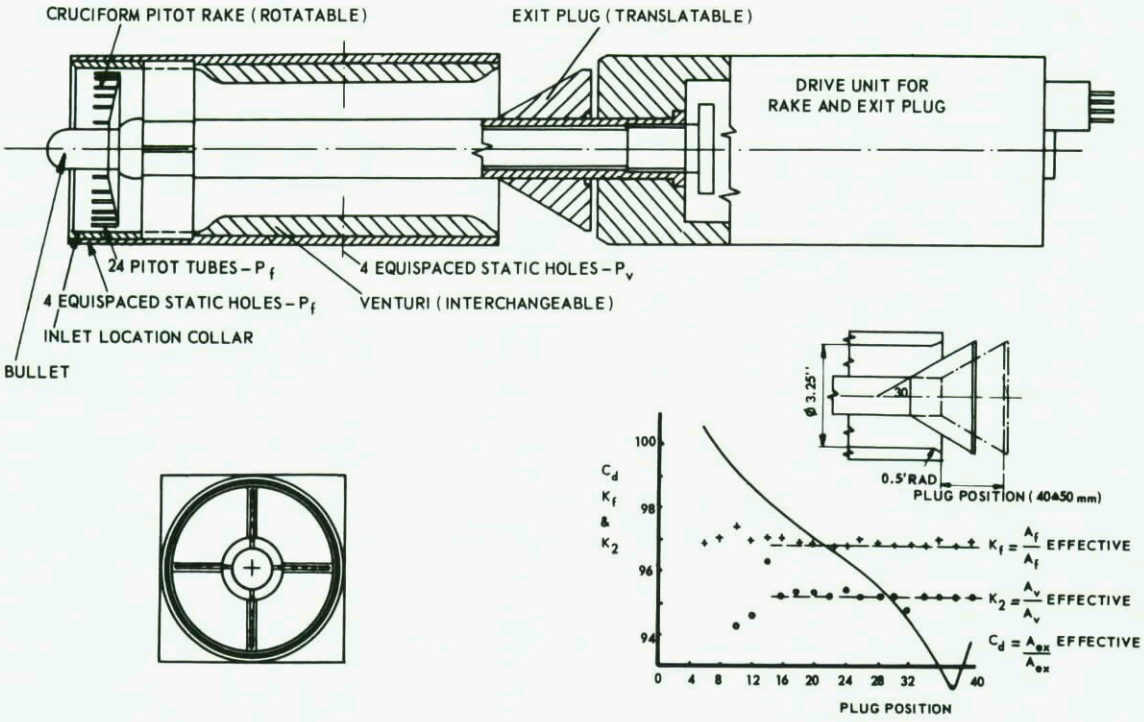

FIG. II. 20 CELL FOR MEASUREMENT OF ENGINE FACE RECOVERY, FLOW DISTORTIONS AND MASS FLOW AND CALIBRATION DATA.

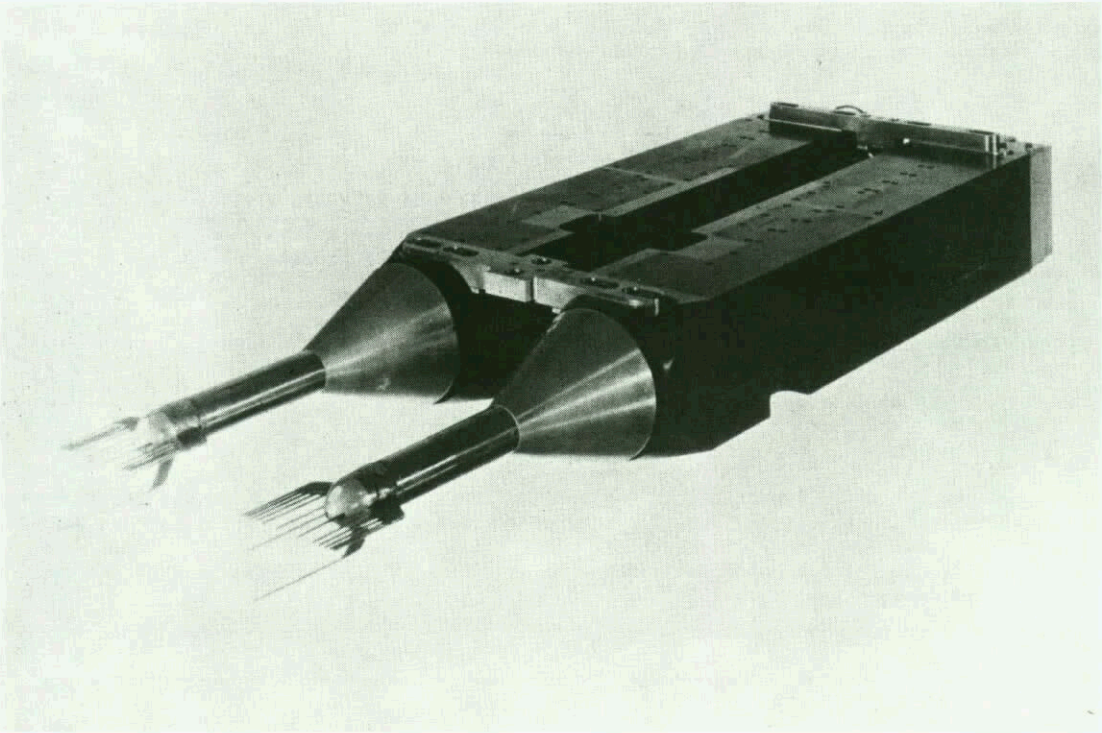

FIG. II. 21 CONICAL THROTTLES AND ROTATING RAKES FOR MASS FLOW MEASUREMENT AND MOMENTUM SURVEY.

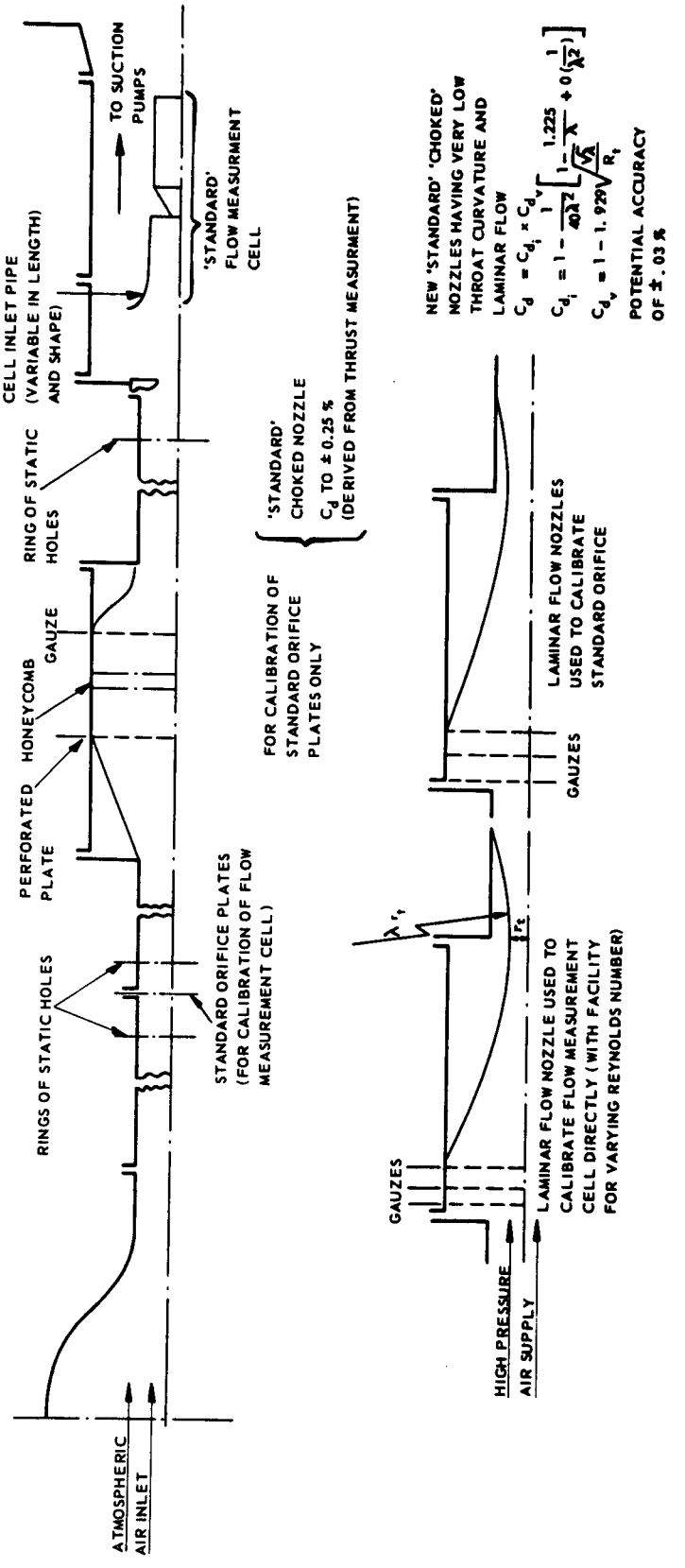

FIG. II. 22 MASS FLOW CALIBRATION TUNNEL.

used to calibrate the mass flow measurement cells which are operated in a choked exit condition. A later development is the design of a new standard choked nozzle having very low throat curvature and laminar flow. This standard will rely on a calculated discharge coefficient which is (a) very close to unity and (b) will have very small error (Ref. II-24). This nozzle will be followed by an efficient diffuser so that it is hoped that it can be used directly to calibrate the cells, both of them operating choked.

2.1.4 BLEED AIR, BYPASS, DIVERTERS, INFLUENCE ON EXTERNAL FLOW

The problem of bleed, diverter and bypass simulation in wind tunnel is only relevant for aircraft with integrated engine-airframe systems and for supersonic aircraft. These items cause interference with both the internal flow and external flow; however, it usually had the most affects on the former. The accurate determination of bleed/bypass and also of spillage drag effects in the transonic range of Mach numbers is an important requirement. It is at these speeds where bypass and spillage mass flows are the greatest and where effects on performance can be large.

Simulation of inlet bleed (including bypass) and spillage effects is accomplished with the inlet drag model. As indicated in Figure II.8 and others, the bleed/bypass geometry is simulated on this model as accurately as possible. Adjacent surfaces such as wings, fuselage, etc., which could interact with the flow from the bleed/bypass exhaust systems must also be duplicated to scale on the inlet model. It is the practice during wind tunnel tests to duplicate a range of bleed/bypass mass flow ratios in combination with a range of operating inlet mass flow ratios. In this manner the proper drag increments can be assessed for a wide variety of matched inlet-engine operating conditions. It is not recommended that any external bleed should be incompletely represented. If the bleed is only internal to the intake, it can be assumed that it will not influence the external flow pattern. At supersonic speeds however, it has been shown - at model Reynolds number - that the amount of bleed can influence the position of the external shock waves. Typically full inlet flow changes 2 - 3 °/o as bleed increases from zero to 2 °/o. In this case the external drag will also change. Therefore for bleed representation in wind tunnels it is a necessity to use as large as possible model Reynolds number, and thus scale, preferably as high as 1/6.

In the cases where the bleed/bypass and spillage mass flow ratios are not duplicated or simulated during wind tunnel model tests, analytical corrections for these effects are made. The calculation usually involve only a momentum balance (drag) for the individual flows being considered and are not amenable to calculation of interference effects.

The major correction from wind tunnel inlet model to full scale aircraft involves the boundary layer on the fuselage forebody. The problem on integrated airframe-engine configurations is the adequate scaling of the boundary layer thickness to the geometric scale of the model for the full range of flight conditions (M_∞) and attitudes (α and β). Corrections for the effect of boundary layer thickness on the inlet flow field are difficult to accomplish with accuracy. Improperly assessed forebody flow field effects have been the major reason for past propulsion deficiencies experienced during full scale flight.

This is particularly true for boundary layer scoops or diverters since at the reduced Reynolds number of the wind tunnel model the ratio of the diverter height(h)and the boundary layer thickness (δ) is smaller than at full scale if the former is scaled geometrically. In inlet design, a compromise is usually required between drag and the diverter performance. Such a compromise tends to select a solution where the outer part of the boundary layer enters the inlet, and it is this compromise that cannot usually adequately obtained from wind tunnel tests. In general the parameter h/δ is used which describes the proportion of boundary layer ingested by the intake. Though convenient, it is obvious that a parameter which is a ratio of the loss of momentum in the boundary layer air ingested to the momentum of the remaining "free stream" air entering the intake would be more appropriate. However, it is obvious that further thought and systematic experimentation is required to elucidate better simulation criteria for model and full scale representation than just identical h/δ values. Whatever parameters do emerge (and in practice they may still amount to something similar to using identical values of h/δ) there remains the problem of how to achieve them physically. As illustrated in Fig. II.23 to obtain identical values of h/δ, model and full scale, there are the following possibilities of geometrical changes to the model:

(a) Move intakes bodily out from the sides of the fuselage.
(b) Move wall of intake adjacent to the fuselage side outwards keeping the rest of the intake identical.
(c) Reduce body size adjacent to the intakes so that fineness ratio of the forward fuselage is increased.
(d) Bleed some of the boundary layer from the fuselage forward of the position of the intakes.

The last of these alternatives would appear to be the best but has difficulties associated with force measurements, establishment of the correct profile turbulent boundary layer before the intake position is reached, etc.

Usually the pressure drag of the diverter $C_{D_{div}}$ is determined based on the diverter frontal area and this coefficient is then applied to the correct size diverters on the full scale aircraft.

When part of the boundary layer from a forebody is allowed to enter the intake the measured standard internal drag includes part of the skin friction drag associated with the flow over the forebody. (Ref. II-25). In these circumstances to arrive at the external drag a separate experiment must be done in which preferably the intake is removed and the boundary layer profile at the compression surface leading edge is measured. If the intake cannot be removed from the model then the traverse has to be done sufficiently far upstream of the leading edge of the intake so that its presence will not effect the results from the traverse. The results of this traverse can then be evaluated in terms of the momentum defect in the boundary layer for the flow that will enter the intake. If the boundary bleed or diverter is "started" then the position of the boundary streamline which divides internal and external flows can be taken as the geometric distance of the cowl lip above the forebody surface. If this bleed or diverter flow is not "started" then this bounding streamline can only be approximated and then only if a very accurate determination of mass flow through the intake is known.

An illustration of the evaluation and final magnitude of the skin friction that is ingested into the intake in a typical case is shown in Figure II-24.

2.1.5 PARTIAL INLET MASS FLOW AND COMPLETE INLET FAIRING

A INTEGRATED SYSTEMS

The general review of wind tunnel test procedures under sections 2.1.1. and 2.1.2 indicated that full inlet mass flow is usually not duplicated on either the aero force model or the nozzle afterbody model. In the aero force model case the reference mass flow ratio is usually the critical mass flow ratio. Since the reference mass flow ratio is also a reference test condition for the inlet drag model, it must be determined

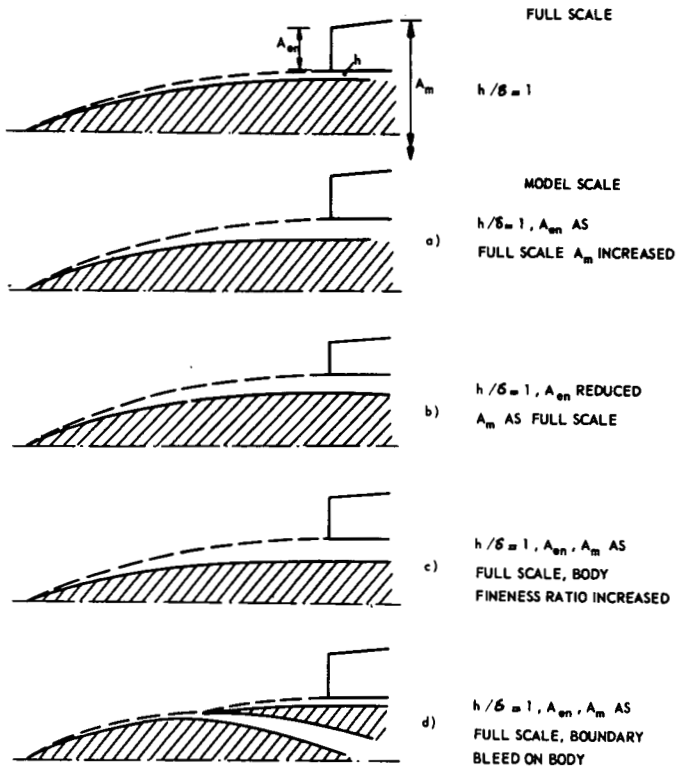

FIG. II. 23 POSSIBLE GEOMETRY CHANCES TO INTAKE MODEL TO KEEP h/δ AT SAME VALUE FOR MODEL SCALE AS FULL SCALE.

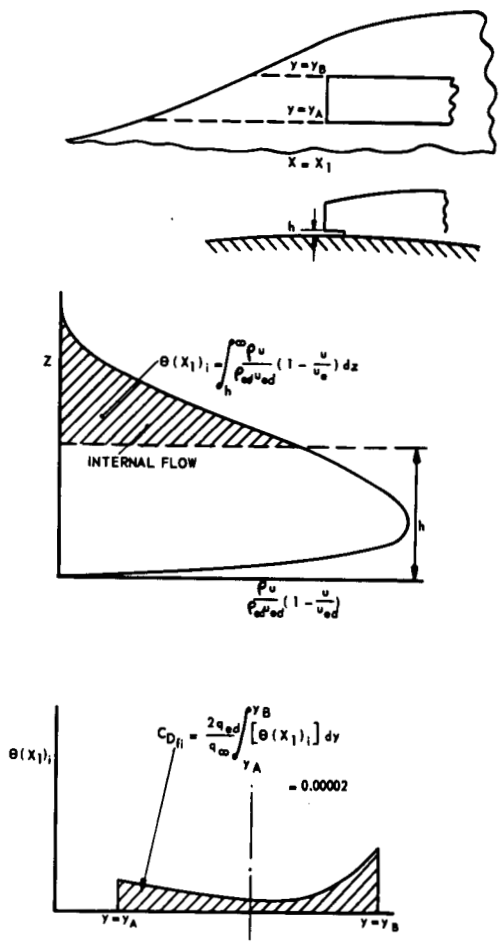

FIG. II. 24 MEASUREMENT OF EXTERNAL SKIN FRICTION THAT IS INCLUDED IN INTAKE INTERNAL FLOW.

with maximum accuracy. Unfortunately, the scale of the aero force model is not generally conducive to providing the instrumentation necessary for such accuracy. For this reason there is a tendency that the more recent aero force models approach the inlet drag model in size (1/12 scale) and have included not only instrumentation for mass flow measurement but also for mass flow control.

However, if the aero force (or complete) model yields only small inlet flows due to model back end distortions and sting size, the inlet flow representation and measurement may be more nuisance than worth. In those cases the inlet may be completely faired, particularly at the complete wind tunnel models in the early stage of aircraft development.

Usually the shapes for intake fairings are arbitrary. Figure II-25 shows an example of such a fairing for a rectangular intake. As an example the corrections to lift and pitching moment slopes due to these intake fairings can be derived in the following manner:
The potential flow contributions due to fairings as derived from slender lifting surfaces are determined from the difference between values calculated for the body with and without fairings. These contributions are as follows:

$$\frac{dC_L}{d\alpha} = \frac{2\pi R_L^2}{A_{ref}}$$

$$\frac{dC_M}{d\alpha} = \frac{2\pi}{A_{ref}\bar{c}} \int_0^L R_X^2 \, dX - \frac{(L - X_m)}{\bar{c}} \frac{dC_L}{d\alpha}$$

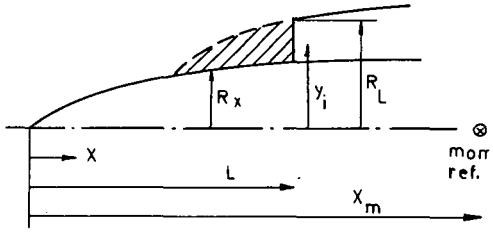

where R_X is the local semi-width of the body

R_L is the body semi-width at the intake entry plane

S_{ref} is the reference area (usually wing planform area)

$\bar{c}$ is the reference (wing) chord.

The contribution due to the intake fairings are subtracted from the measured lift and pitching moment slopes. The calculated contributions due to engine flow are added and are

$$\frac{dC_L}{d\alpha} = \frac{2A_\infty}{A_{ref}} \frac{d\alpha_i}{d\alpha}$$

$$\frac{dC_M}{d\alpha} = -\frac{2A_\infty (L - X_m)}{A_{ref}\bar{c}} \frac{d\alpha_i}{d\alpha}$$

where A_∞ is cross sectional area of the capture streamtube in the free stream and

$\frac{d\alpha_i}{d\alpha}$ is the rate of change of flow incidence at the intake entry plane with respect to free stream.

$$\frac{d\alpha_i}{d\alpha} = 1 + \frac{R_i^2}{y_i^2}$$

where y_i is the distance from the aircraft centreline to the centre of area of the intake entry plane,

and R_i is the semi-width of the fuselage at the intake entry plane.

The interference effects of both fairings and real inlet spillage are ignored.

Nozzle afterbody models use complete inlet fairings at all test conditions. There can be an effect of inlet mass flow ratio on aft surfaces for some aircraft configurations. Since the jet exhaust is also present, the question of possible interactions due to inlet and exhaust flows is raised. Simulation of both flows simultaneously on the same model would be needed to answer this question. Very little, if any, testing of this nature has been attempted. The development of small scale engine simulators could provide a means by which this dual simulation can be accomplished (Chapter V).

B PODDED ENGINE INSTALLATION

If during complete model tests the nacelle aft body of a subsonic transport with podded engines (turbine cowl) should for some reason be geometrically scaled, the natural inlet mass flow is considerably reduced and might cause separation and increased spillage drag. Two methods can be used to avoid such phenomena: (a), the inlet can be reshaped (decreased inlet area) such that similar suction at the cowl can be expected, and (b), within the inlet a bullet shaped body may be inserted such that the pre-entry streamline pattern is akin to that for the intake without body and with the actual scaled mass flow. For both techniques caution should be exercised not to introduce unfavourable secondary interference effects especially at high angle of attack and yaw.

Also if small scale engine simulators are used for simultaneous inlet and exhaust simulation, the inlet mass flow is somewhat reduced compared to the actual engine. In practice the inlet area is proportionally reduced.

When engine simulators are not available or practical (scale, tunnel blockage) the direct blowing technique is applied to evaluate jet effects. The inlet may be completely faired or the captured streamtube may be represented by an upstream body (usually from tunnel plenum chamber) (Ref. II-17, II-20). The latter method causes difficulties when angle of attack is varied, and boundary layer suction at the inlet entry plane is required for reducing the boundary thickness at the fan nozzle.

The former method is not generally applied since the omission of the inlet flow might cause considerable interference effects at the pylon-wing-nacelle location. However, preliminary tests with an underwing fan engine wind tunnel model showed that the closure of the inlet by an elliptical shaped body and simulating the natural flow-through jet with a body of revolution (Fig. II.26) did not disturbe the

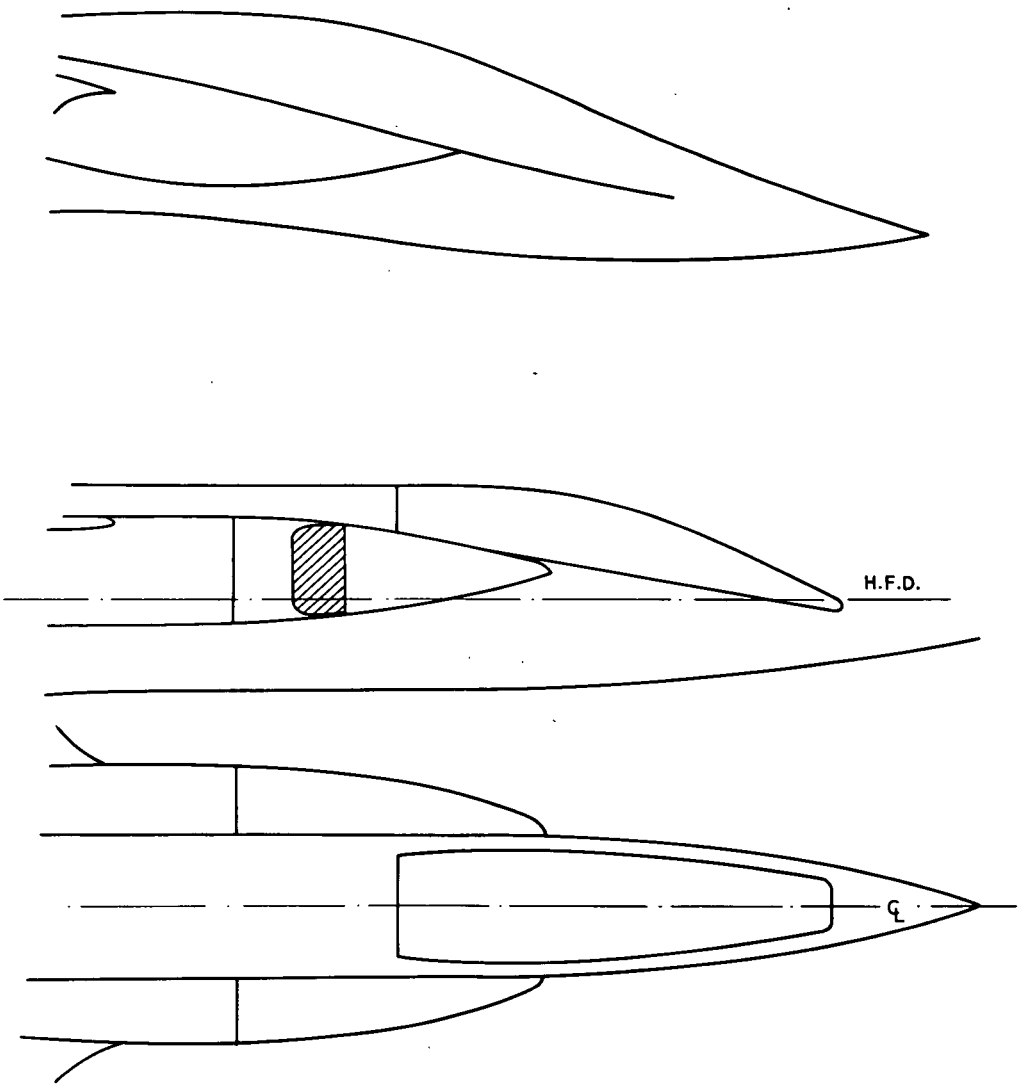

FIG. II. 25 FAIRING FOR A RECTANGULAR INTAKE.

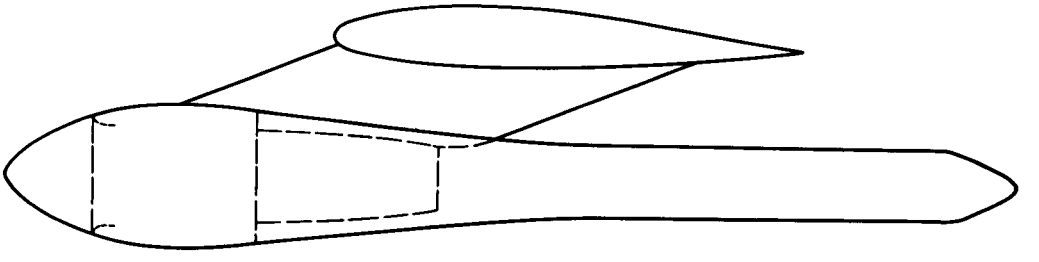

FIG. II. 26 SUBSONIC TRANSPORT MODEL WITH FAIRED INLETS AND SOLID BODY JET SIMULATORS.

flow field on the aft fan cowl, pylon and wing. The pressure levels shifted somewhat but the shape of the pressure distributions remained identical as shown by some examples in Fig. II.27. The argument was given that the thickness of the body representing the jet was chosen too small causing the main deviation between the pressure levels for flow-through and faired nacelle. In any case these tests showed that for this particular configuration the blowing nacelle with closed inlet and with jet properties similar to that for the flow-through nacelle, yields a good reference condition for further tests determining the jet effects. However, no data are available on the boundary, layer condition at the fan nozzle location.

Fortunately recently developed computation techniques which determine theoretically the interference between wings and bodies at subcritical speeds (Ref. II-26, 27) will be of great help for determining the optimum body and cowl shapes for zero and reduced inlet mass flows respectively. Optimum should mean that the velocity and pressure fields at the fuselage wing, pylon and fan aft body are affected to a minimum as compared to the fields of the reference nacelles used.

2.1.6 FINAL REMARKS ON CORRECTIONS

The previously described techniques for determing the inlet effects on external aerodynamics with special inlet models generally yield corrections for the overall aerodynamic data obtained from complete model tests. Translation of these data to full scale might sometimes cause difficulties due to the reduced Reynolds numbers of the wind tunnel tests. The difficulties arise if shock wave-boundary layer interactions and flow separation occur. For example, for podded fan engine installations the spillage effects on wings could be very sensitive to Reynolds number variations, just as the basic wing will be. Cowl separation boundaries are also liable to be sensitive to Reynolds number changes. In many cases the transition is fixed by some artificial means, but this does not give at all any guarantee of flow field and pressure field duplication in the wind tunnel. A complication in deciding how to represent the intake in relation to a fuselage or wing at model scale is particularly obvious for a pitot or half axisymmetric centrebody intake where the intake shock system directly impinges on the adjacent fuselage or wing boundary layer. The scale of the interaction between shock system and boundary layer and the effect of this interaction on the downstream boundary layer properties will then depend on the absolute size of the boundary layer and, hence, will change from model to full scale.

Much work still needs to be done on viscous effects at transonic speeds. Much attention has been given to it already, particularly within AGARD. The results of these studies will undoubtedly have a marked influence on the interpretation of and correction procedures for wind tunnel data concerning engine installation. Presently only guesses can be made for those corrections.

2.2 INTERNAL INLET FLOW

The separation in treatment between external and internal inlet flow and the mutual influencing effects cannot strictly be made. This is particularly true for diverters, bleeds and other bypass systems. In the previous sections most attention has been devoted to the external effects where the primary inlet parameter is the inlet mass flow. The measurement of this variable has also been treated. In the next sections we will consider the internal flow primarily, how the internal flow is simulated, how measurements are performed and which corrections are applied.

The purpose of the inlet is to diffuse the entering air properly, to cause minimum drag penalties, and, to deliver to the engine an air flow that is compatible with the engine requirements both steady and unstationary. Usually such tests are performed in special inlet wind tunnel models, sometimes called propulsion performance models, which are preferably at large scale (1/6). In many cases however the inlet drag and performance model are the same.

2.2.1 TECHNIQUES FOR INLET MASS FLOW SIMULATION

The techniques to achieve mass flow variation in the special inlet models are generally similar to those described in section 2.1.2 with the addition that the duct shape from the inlet plane to the compressor face must be simulated as on the full scale aircraft and the measuring station must be located at the compressor entrance plane (Fig. II.28).
When applicable, it is necessary to have a boundary layer control system (bleed) and a bypass system properly scaled so as to simulate the airflow at the engine compressor face. Pressure measurements at the compressor face station of the inlet performance model should be sufficiently detailed to provide an accurate measurement of total pressure recovery, engine mass flow (see 2.1.3) and the spatial distribution of the local total pressure ratio. Usually this involves a total pressure array of 30 to 40 individual total pressure probes for model scales on the order of 1/6 for the typical fighter aircraft.

For large scale tests, an actual engine may be used to combine flow control with inlet-engine interaction effects. This technique, however, is quite expensive and can result in a doubling of the complexity of the test. Furthermore, the range of inlet mass flow ratio tested is limited by the engine capability. As a rule, therefore, inlets are tested with engines only when the inlet-engine interaction if of paramount importance.

Tests may also be conducted using a small engine with a subscale inlet. For example an off-the-shelf small engine appropriate for, say, a 1/2 scale inlet may be used. The difficulty with these tests are the fact the small engine may be either more or less sensitive to distortion as compared to the actual full scale engine.

At transonic speeds below approximately Mach number 1.0 the full mass flow range through supercritical operation is not usually attainable because of the lack of natural pumping. That is, the base pressure at the inlet exit is not low enough to introduce the maximum flow through the inlet. To reduce the base pressure, ejector systems have been employed as well as extending the duct by a conical diffuser. Another approach has been through direct suction where a flexible bellow and pipe arrangement can be attached to the inlet exit and lead to an outside vacuum source or merely to atmospheric pressure if the tunnel pressure is sufficiently high. For Mach numbers above 1.0, sufficient natural pumping to cover the complete mass flow range is usually available at least for relatively small scale models. For complete or partial airframe inlet tests, small gas driven turbines have been used to simulate the engine mass flow demand.

The means for varying bypass flow depends in part upon the method employed to remove it. If the bypass is taken off at the throat, flow rates will be determined by slot gap width, offset, and back pressure. The back pressure may be determined either by a fixed or by a remotely variable exit. Again, a properly designed variable plug can be used to serve both as a flow control and flow measurement device. (Fig. II-29).

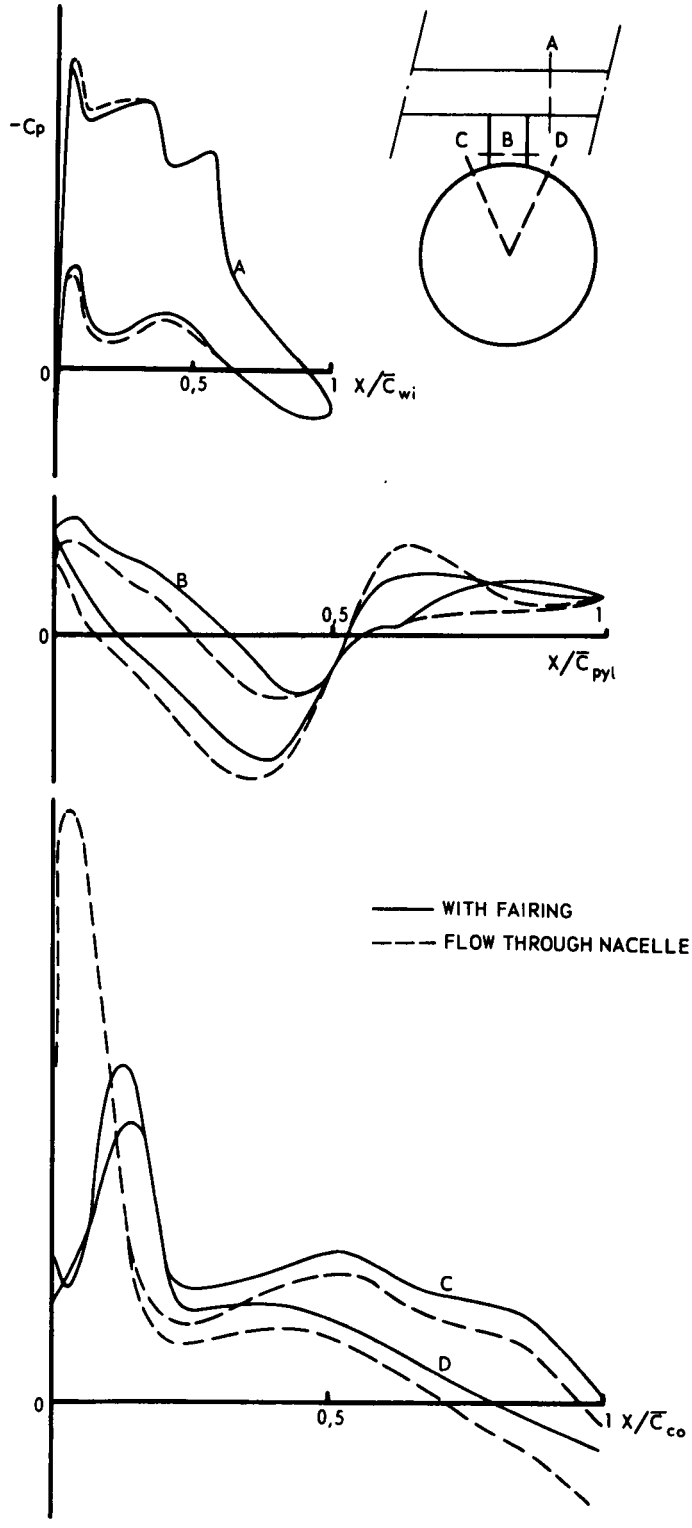

FIG. II. 27 EXAMPLES OF SOME PRESSURE DISTRIBUTIONS AT A SIMILAR MODEL AS FIG. II. 25. M≈0,8

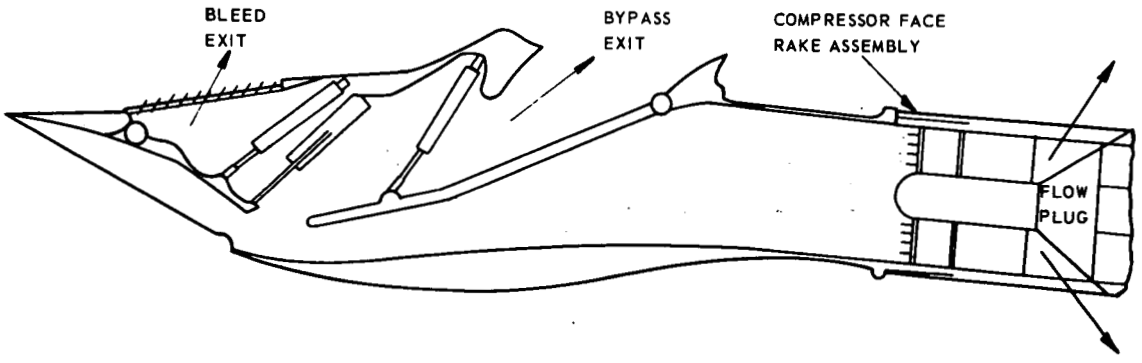

FIG. II. 28 TYPICAL INLET PERFORMANCE TEST ARRANGEMENT BLEED AND BY-PASS TO EXTERNAL FLOW.

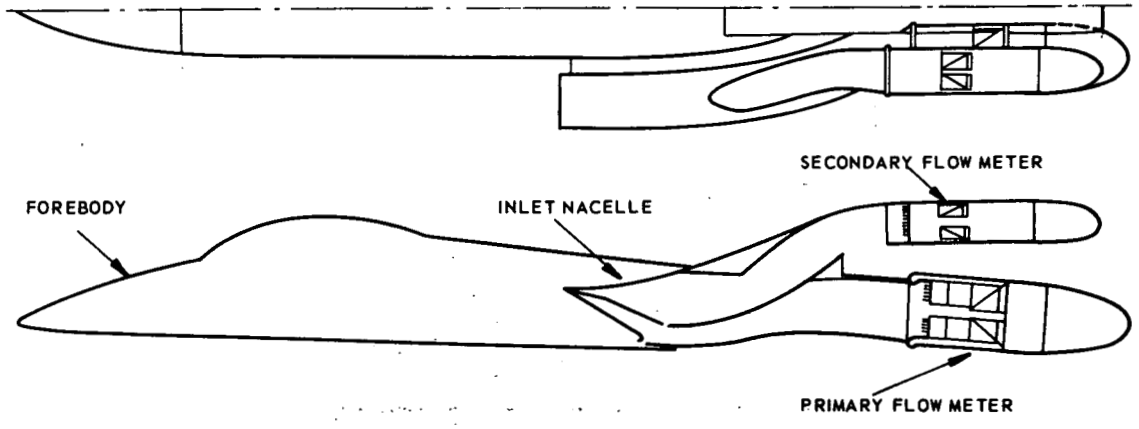

FIG. II. 29 COMPOSITE INLET TEST MODEL.

When a fixed area exit is used, very rough estimates of bypass mass flow can be made from pressure measurements in the exit channel. An alternative method of removing bypass flow places a collector plenum around the duct near the compressor face with flow rate controlled again by a variable exit area. If close approximation of actual bypass flows are to be achieved - within 2 °/o or 3 °/o - the carefully calibrated remotely controlled plug (or its equivalent) is necessary. This type of variation is also necessary for comprehensive investigations of the best balance of spillage and bypass for transonic flight. For small scale investigations where the expense and complexity of a remotely variable bypass exit is not warranted, a series of fixed exits may be used with reasonable success. The approximation of bypass flow should be consistent with the reproduction of other parameters in small scale.

In duplicating bleed systems in a model, the goal is to maintain a viscous layer through the inlet which reacts to inlet pressure gradients similarly to full scale flight operation. It is advisable then to perform some theoretical analysis on the flight vehicle bleed system to determine plenum back pressures and then perform wind tunnel tests over a small range of back pressures near that value in order to be absolutely certain of acquiring representative data. In cases where wind tunnel test conditions do not match flight Re (Reynolds number based on boundary layer height), it may be necessary to make adjustments in the size of bleed holes (or slots) in order to remove the proper amount of flow. In the case of perforated side plates or compression ramps, remotely variable porosity may be effected by means of sliding plates. As with the case of bypass, small scale model tests (on the order of 1/12 scale) do not have a critical requirementfor variation of boundary layer bleed ad transonic Mach numbers in order to be consistent with other areas of duplication.

Proper duplication of the above mass flow ratios for engine $(\dot{m}_{en})/(\dot{m}_{\infty})$, bypass $(\dot{m}_{bp})/(\dot{m}_{\infty})$, and bleed $(\dot{m}_{BD})/(\dot{m}_{\infty})$, coupled with a sufficiently high tunnel pressure to produce Re (Reynolds number based on boundary layer height) near the full scale value provides the most important input to inlet mass flow simulation. Generally speaking, it is not difficult to manage this simulation well enough to obtain a close approximation of average total pressure recovery p_{t_2}/p_{t_∞}, but also total pressure distortion - both steady state and dynamic - be determined to meet engine development demand, a great deal of attention to detail is required. For instance, boundary layer analysis must be accomplished carefully and the boundary layer diverter design based on this analysis should provide, as nearly as possible the same channeling of viscous flow as would the flight vehicle design. If it appears that model boundary layer flows will not have "healthy" velocity profiles, vortex generators may be used to energize viscous flows in regions of relatively high pressure gradient.

Tests should be run over a wide range of vehicle manoeuvre attitudes to determine inlet performance and operational stability at all possible flight conditions.

High frequency fluctuations in the compressor face mass flow may be affected by cowl lip-flow field interactions, shock wave-boundary layer interactions, wakes from struts terminal shock location, and/or flow separations in the inlet duct. Close attention to the inlet geometry then can also help to assure that the patterns of total pressure - even at high frequencies - are duplicated in a wind tunnel inlet model. In fact, a honeycomb near the simulated compressor face or some other device to reproduce proper "organ pipe" duct resonance may be required to define resultant adverse disturbances.

It can be concluded that the more sophisticated testing techniques offer the combined advantages of accuracy and versatility in advanced development whereas the cruder transonic test methods are more consistent with low operating budgets and the rough approximations expected during initial investigations of systems designs.

2.2.2 EXTERNAL FLOW FIELD SIMULATION AND MEASURING

Simulation of the flow field in which an inlet is immersed can be at once, an important and difficult task in transonic wind tunnel tests. If the inlet system is to operate only at high subsonic Mach numbers and/or is located reasonably well ahead of the regions where the flow fields are significantly affected by the proximity of the flight vehicle, isolated inlet tests are acceptable. An ultimate check-out is always necessary with the correct model flow field. When inlets are closely integrated with the flight vehicle and especially when these inlets are designed for moderate to high supersonic Mach number flight, the inlet flow field is mostly defined by the vehicle forebody shape and attitude, but can be affected tangibly by diverter shapes, near by stabilizer surfaces, nose booms, and external stores. If a large part of the airframe must be simulated in the wind tunnel for proper flow field duplication, losses must accepted for the reduced scale, and hence, reduced Reynolds number. It is recommended that the partial model should be extended at least 5 to 8 engine diameters behind the inlet.

In simulating the external flow field at transonic Mach numbers, it is particularly important to reproduce viscous conditions, vortices, and local flow angularities. Local values of Mach number and total pressure also come into play as part of this simulation. The inlet may be rather sensitive to local flow angularities with flow separation (internal or external) resulting from high flow incidence angles with inlet boundary layer diverters, side plates, or cowls. Vortex formation from some of the possible upstream sources mentioned above may be shed into the region where an inlet is to be located and, consequently, should be defined during development wind tunnel tests. Also, in transonic inlet tests it is advisable to consider duplicating some disturbances downstream of the inlet, e.g., downstream portions of the wing when the inlet is shielded by the wing. In this context, the question arises also, does the actual engine exhaust influence the inlet flow field. Usually this question remains unanswered, but might be worthy of consideration in many instances.

During the wind tunnel development of inlets which are located close to the fuselage, careful attention must be given to the relative thickness of the boundary layer on the model and on the airplane in order that the effects of the fuselage flow field on inlet performance may be properly evaluated (see 2.1.4). One aspect of the problem is illustrated in Figure II.30. This figure compares the calculated thickness of the boundary layer on a body of revolution, representing the forebody of an airplane fuselage, with the calculated thickness (converted to full-scale values) on a 1/6 scale wind tunnel model of the same forebody. The thickness was calculated at a station 20 feet (full scale) behind the nose, using the method presented in Ref. II-28. This method accounts for three dimensional and pressure gradient effects. The calculations for the airplane were made for altitudes of 30,000' and 50,000' and for a completely turbulent boundary layer. The calculations on the model were made for several boundary layer transition assumptions: free transition, transition at the distance from the nose which corresponds to the minimum Reynolds number for transition, and at 5' and 10' from the nose. If the diverter height on

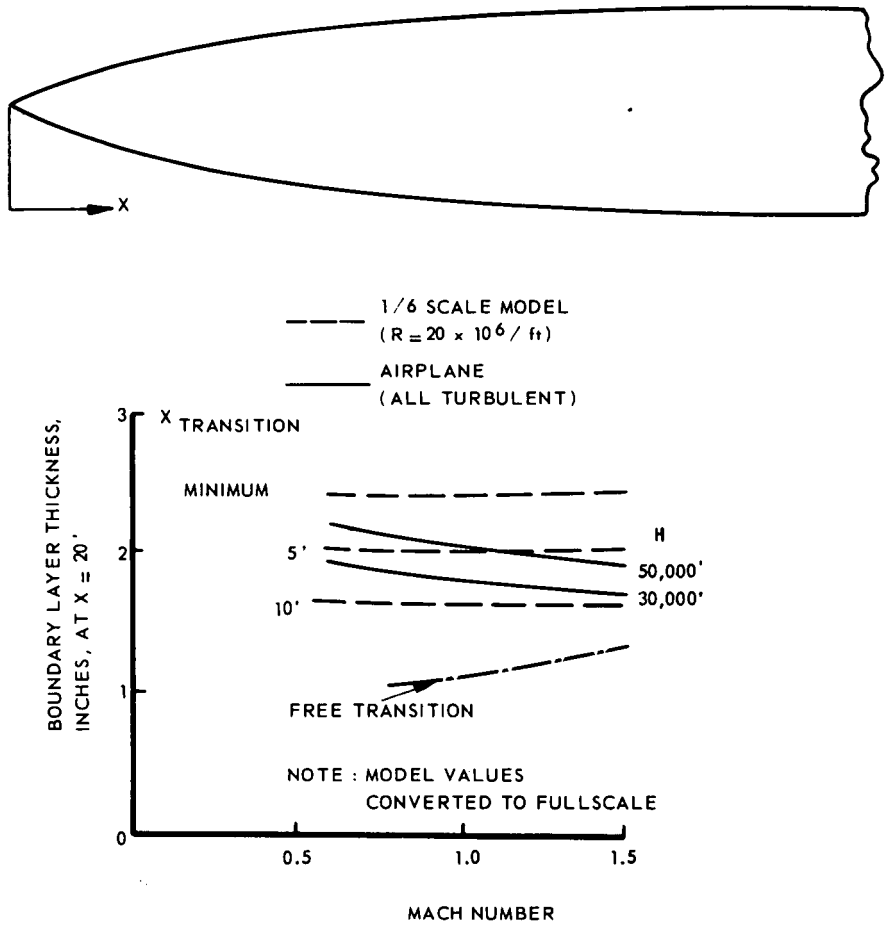

FIG. II. 30 COMPUTED BOUNDARY LAYER THICKNESSES AT FREE FLIGHT AND AT WIND TUNNEL SCALE WITH VARIOUS TRIPPING LOCATIONS.

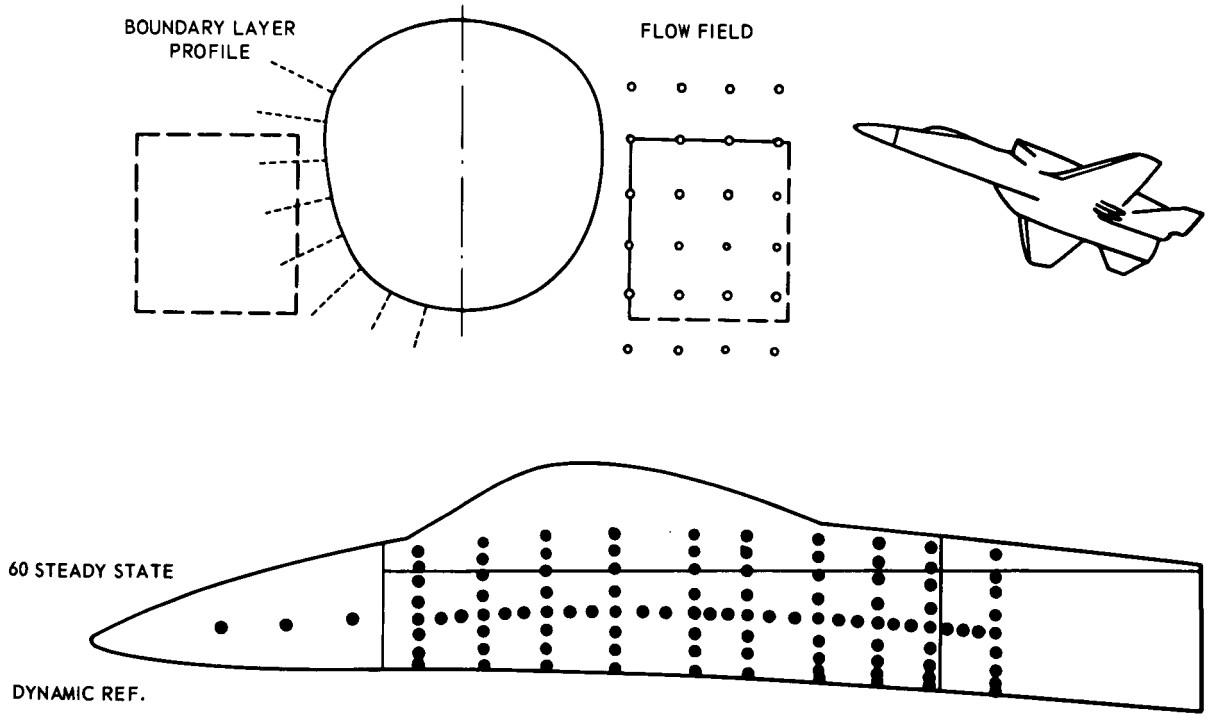

FIG. II. 31 EXAMPLE OF EXTERNAL FLOW FIELD SURVEY.

the model is scaled from the airplane then it would appear that proper boundary layer simulation at $\alpha = 0^{o}$ would be obtained by fixing transition on the model at a station corresponding to 5' or 10' full scale. The trip location will, of course, be affected by the test Reynolds number. Whether or not the other boundary layer characteristics are simulated by this tripping method, remains an open question, e.g. is the shock wave-boundary layer interaction also duplicated? This can give a marked effect on unstarted inlets at supersonic speeds (Ref. II-29). For manoeuvring fighters the growth of the fuselage boundary layer with angle-of-attack is of prime importance. The problem of how well this boundary layer growth can be duplicated in a wind tunnel is worthy of further research. For example, if transition is fixed on the 1/6 scale model at the 10' full-scale station, laminar flow exists over half the linear distance of the model in contrast to a completely turbulent flow on the airplane. With this large extent of laminar flow on the model does the build-up of boundary layer with angle-of-attack correspond to the build-up on the airplane? Or, should the boundary layer on the model be made completely turbulent and the inlet diverter height on the model be increased from the scaled value to account for the relatively thicker boundary layer at $\alpha = 0^{o}$? Another unanswered question is how does unit Reynolds number affect the rate of growth of the turbulent boundary layer with angle-of-attack?

The careful definition of external flow fields at transonic Mach numbers is normally important only for systems designed for higher supersonic flight where the inlet flow field is influenced by the fuselage and/or wing (Ref. II-29, 30, 31). Figure II.31 shows an example of the type of instrumentation which might be provided for such installations including boundary layer profile measurements, wing and fuselage static pressure surveys, and inviscid flow field measurements. The flow field measurements should be made with some type of cone probe arrangement such as that shown in Figure II.32 with which local flow angularity, Mach number and total pressure can be determined.

As mentioned previously, there are some inlets which can be tested alone. These would include nose mounted inlets and low transonic inlets mounted well away from the flight vehicle fuselage. The obvious advantage to such a test is that it allows the use of larger scale inlet models in the same size wind tunnel. Another testing technique to be explored is the use of small scale forebody tests to determine inlet flow fields. If a low blockage aerodynamic device can then be constructed which reproduces the flow field generated by the actual forebody, it would be possible to test the larger scale inlet in the correct flow field generated by this device. The questions to be answered in future investigations of this concept are whether the flow fields can be duplicated, whether varying aircraft angles-of-attack can be reproduced, and whether inlet installation in the simulated flow field has the same effect as its installation in the vicinity of the actual vehicle forebody.

2.2.3 TECHNIQUES FOR INLET PERFORMANCE MEASUREMENTS

For the inlet flow entering the engine four properties are of primary importance namely, the mass flow, the pressure recovery, the stationary distortions and the unsteady or dynamic distortions.

The mass flow measurements have been previously treated in section 2.1.3 and nothing will be added here.

Inlet pressure recovery and distortion are usually obtained from the measurement of 30 to 50 total pressures and several static pressures at the compressor face. Either mass weighted or area weighted recovery may be used. The distortion indices require sufficient probes in order to accurately define the inlet distortion as shown in Figure II.33, while the pressure recovery is less sensitive. In practice the area mean pressure recovery is obtained within $\pm$ 1/2 %. It seems that corrections of the pressure recovery due to scale effects can usually be neglected.

Different engine manufacturers use different distortion parameters for engine surge. One company favours the DC_{60} parameter:

$$DC_{60} = \frac{\bar{P}_{60} - \bar{P}}{(1/2\ \rho V^2)_{\text{mean at engine face}}}$$

(where $\bar{P}_{60}$ is the mean total pressure in the worst 60^{o} section; $\bar{P}$ is the mean total pressure overall). Another company uses the K_D factor which has several slightly differing forms one of them being:

$$K_{DM} = \frac{1}{2} \frac{\sum_{i = \text{ring } 1}^{\text{ring } n} \left[\left(\frac{P_{max} - P_{min}}{\bar{P}} \right)_i \bar{\theta_i} C_i \right] \times 100}{\sum_{i = \text{ring } 1}^{n} C_i}$$

This is a summation of conditions on a number of rings of pitots at differing radii where P_{max}, P_{min} and $\bar{P}$ are maximum, minimum, and mean values of total pressure on the ring

$$C_{ring} = \frac{\text{Engine radius}}{\text{ring radius}} \quad \text{and}$$

$\bar{\theta}$ is the largest continuous arc of the ring over which the total pressure is below the ring average. In general the measurement of all or any of these factors should present no problem. The only problem is the ever present one of the relevance of model tests at much lower than full scale Reynolds numbers, where the incorrect representation of the external flow probably is the main cause.

The recent advance of the turbo fan engine cycle for application in high performance supersonic vehicles has required more detailed study for engine-interface dynamic interactions. The engine might randomly surge after perhaps sometime spent at a steady state condition which initially appeared to be acceptable to the engine. Indications at present are that the engine is insensitive to inflow dynamics in the lower transonic regime.

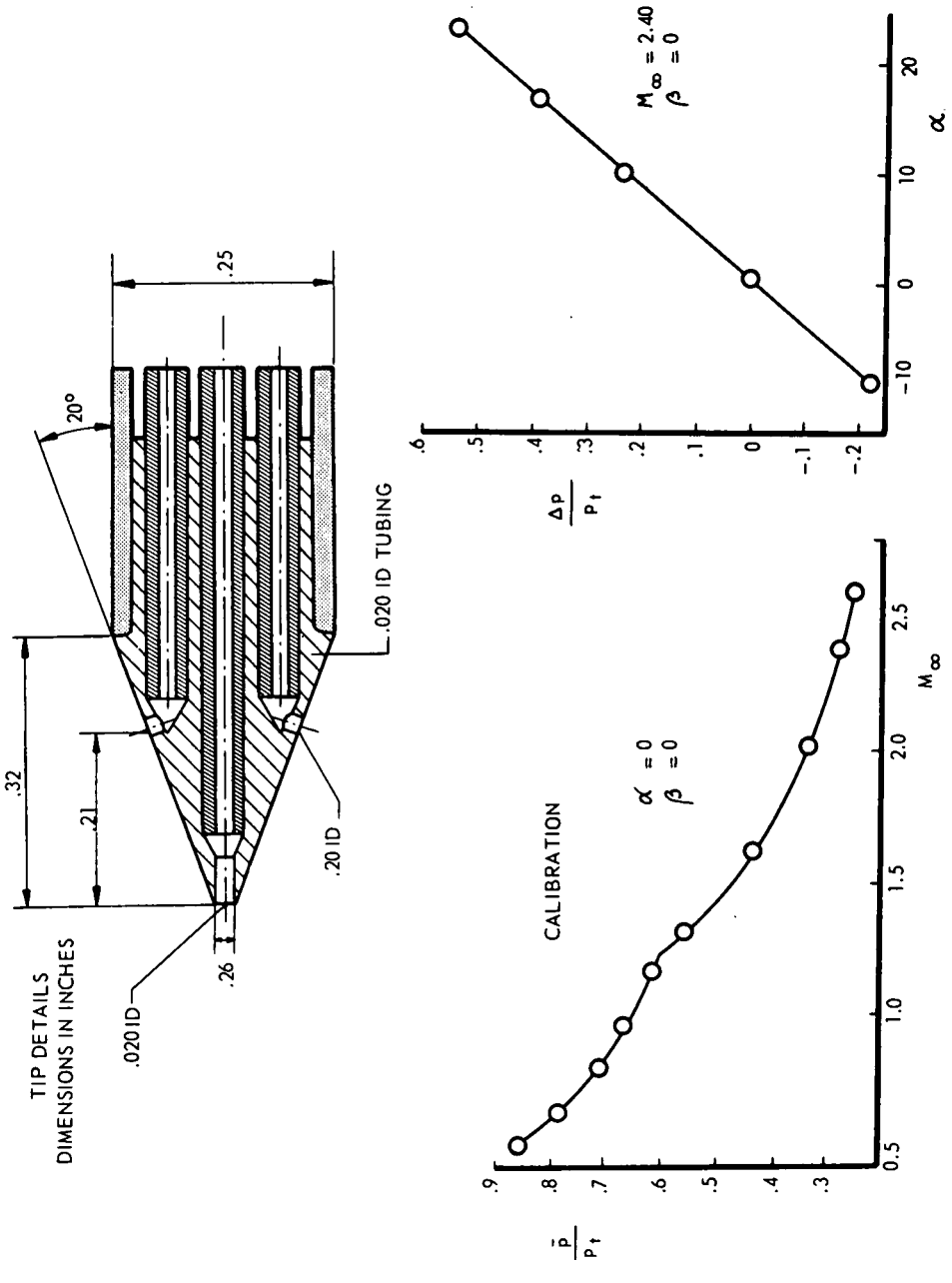

FIG. II. 32 CONE PROBE YAW METER DESIGN AND SOME CALIBRATIONS.

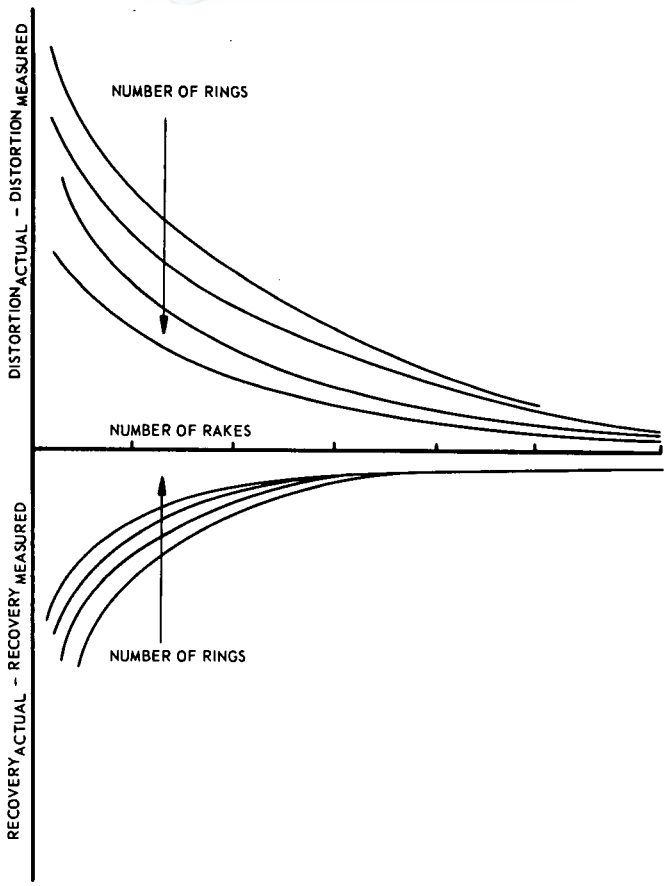

FIG. II. 33 INDICATION OF OBTAINABLE ACCURACY VERSUS NUMBER OF TOTAL PRESSURE RAKES AND RINGS IN THE INLET.

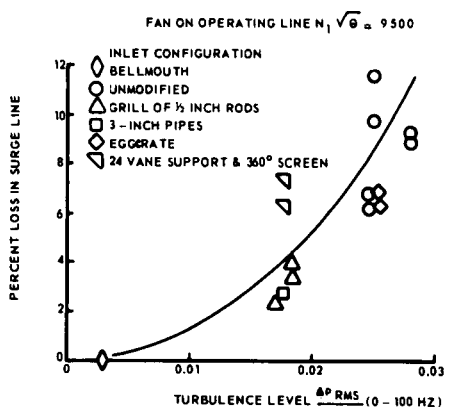

FIG. II. 34a

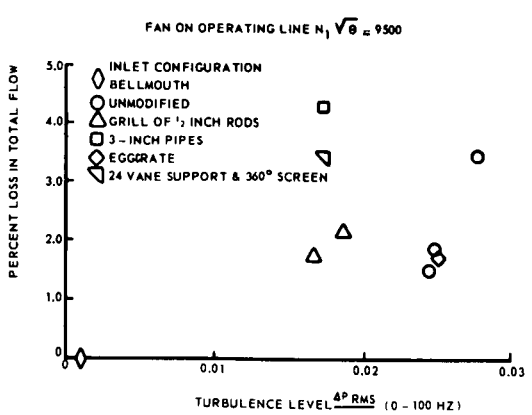

FIG. II. 34b

FIG. II. 34 SURGE LINE REDUCTION AND LOSS IN FLOW VS TURBULENCE LEVEL FROM 0 TO 100 Hz.

However, during supersonic operation, starting at $M_\infty \simeq 1.1$, the engine is susceptible to the dynamic distortions as can be seen by the indicated diagram, where the supersonic working region is at the lower left and the stall margin is the smallest.

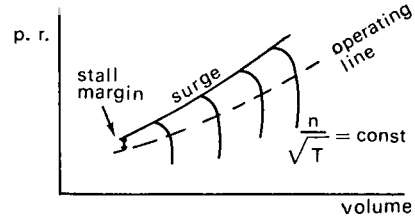

Fig. II.34a gives an example of the reduction in stall margin of a turbo fan engine (where 10 °/o loss in surge line ≃ 100 °/o reduction in stall margin) versus the low frequency turbulence level, generated by various means. Fig. II-34b shows the percent loss in total flow for the same condition. In the first case a correlation can be found; in the latter correlation is completely lost. It is clear from these figures that more work is needed to establish better correlations which describe the influence of the dynamic distortion properties on the engine characteristics. Ref. II-32, describes a theoretical treatment of this problem.

Recent experience suggests that the initiation of surge can probably be linked to the steady state distortion index provided the deviation from steady distortion can be sampled quickly enough i.e. if the steady state distortion factors is exceeded while the compressor is rotating for one revolution then surge can be initiated (Ref. II-33). If this is true then the measuring problem in the wind tunnel reduces to dynamic measurement of pressures through the use of miniature high response transducers, (e.g. Kulite) which are usually located in conjunction with a steady state transducer. These transducers are quite sensitive and must be protected from damage by foreign objects in the tunnel. The calibration, data acquisition and subsequent data analysis then requires extensive electronic recording and play back equipment. Stochastic analysis techniques must be employed to analyze the test results. Steady state probes have a frequency response of a few hertz, while the high response transducers have a frequency response of the order of 5000 cycles per second, depending on the scale.

However after these measurements the problem arises how to translate the wind tunnel data to full scale with the actual engine. The cause of this distortions can be numerous and probably mutual interference exists. Important factors in this phenomenum are turbulence caused by separations, turbulence level and frequency, acoustic characteristics of the main flow, compressor dynamics and acoustic characteristics. This means that Reynolds number, scale and engine characteristics are primary parameters. The dependence of scaling laws on these parameters is unknown (see further section 2.2.4). More information on dynamic distortions can be found in Ref. II-34 - 36.

Transonically, very few attempts have been made to measure temperature distortions at the compressor face, and, in particular, no high frequency response temperature measurements have been made. Measurement of compressor face flow angularity or swirl have not been thoroughly considered although a few attempts have been made using hot wire anemometers to measure stream velocities as well as turbulence.

2.2.4 SCALE EFFECTS

As long as large scale models are used, no significant scale effect on the static internal performance is expected. Dynamic flow measurements must be scaled, however, since the dynamic response of the flow is a function of length. For small scale models (1/12 scale and less) some loss in indicated performance can be expected, especially if the Reynolds number is low and the bleed patterns, slots or scoops, are not properly scaled.

No set rules for the corrections to internal performance are known since each inlet tends to be an individual problem. But comparison of large and small scale inlet test results indicates a small loss in pressure recovery (1 °/o) is experienced going from large to small scale models. The corrections for dynamic scaling are not well established at present, but will be developed by comparison of wind tunnel measurements with flight measurements.

Preliminary results of turbulence scaling procedures have established some of the following results. The turbulence process has been considered to consist of two phases, turbulence generation and turbulence decay. The turbulence decay process is further divided into turbulence dispersion and turbulence dissipation. As used here, dispersion is the process in which the frequency distribution but not the quantity of turbulence energy changes with distance downstream of the turbulence generation station. Dissipation is the process in which the quantity of turbulence energy decreases with distance downstream of the turbulence source. Figure II.35 is a conceptual diagram of this turbulence process.

Three turbulence generating mechanisms are envisioned: boundary layer-shock interaction, boundary layer shear, and sharp lip separation. These mechanisms are inter-related and can coexist. Depending on the inlet operating condition, any one of the three mechanisms may be predominant.

Previous analyses of test data indicate that boundary layer-shock interaction is the primary source of high-amplitude turbulence. Other test results indicate that (a) the center and normally highest recovery streamtubes undergo the highest frequency and highest amplitude changes in total pressure, (b) there are local flow oscillations of higher frequency than the basic boundary layer separation and reattachment cycle, (c) near the walls, maximum excursions from the average local total pressure were of relatively short duration and towards the high-pressure side, and (d) there were large changes in total pressure in a given streamtube.

A second mechanism for generating turbulence is the classic boundary layer shock mechanism in which viscous forces at the duct wall result in a turbulent boundary layer. Turbulence generated by this mechanism is higher near the duct walls than in the center of the flow; and, the energy distribution with frequency is relatively uniform. Scale will primarily affect the generated turbulence as a Reynolds number function. A second order effect might be the relatively greater roughness of smaller models.

A third mechanism for turbulence generation is flow separation and vortex formation over the sharp lips of an inlet. Conditions favoring this mechanism include large angles-of-attack and yaw, and high airflows at low flight speeds (mass flow ratios above unity). From similarity to flow through sharp edged orifices, scale effects might be expected to be most apparent for quite small scales and Reynolds numbers.

Turbulence decay is considered to be largely a mixing process. In this mixing process, large-scale, low-frequency turbulence is progressively reduced to smaller-scale, higher frequency turbulence. As the turbulence scale decreases, the mixing process accelerates, and the turbulence energy is dissipated more rapidly.

Although the mixing process is assumed to be geometrically similar with inlet scale, two factors tend to accelerate the process as scale decreases more than would be indicated by geometric similitude.

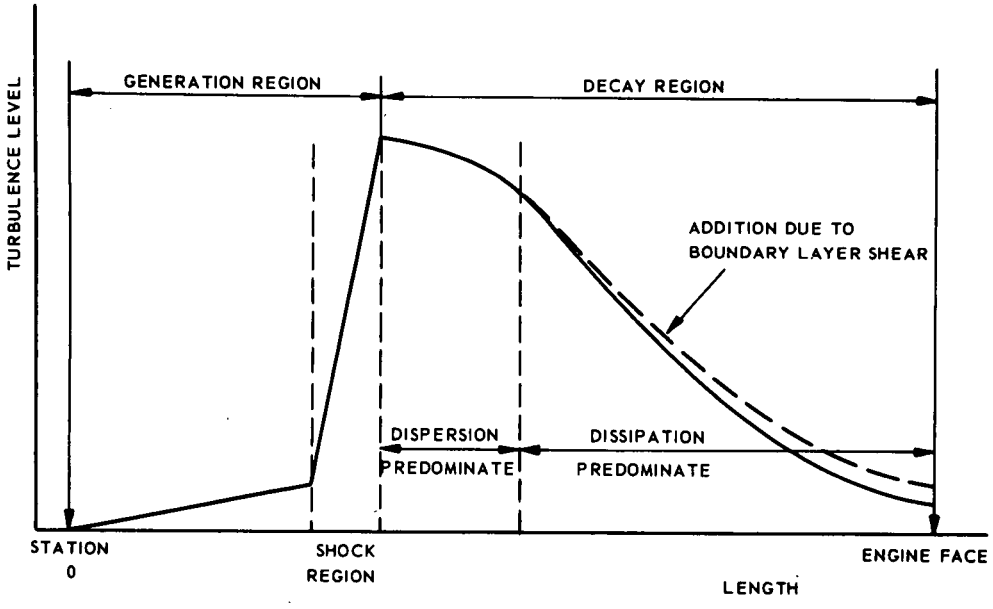

FIG. II. 35 TURBULENCE GENERATION AND DECAY IN INLET FLOW.

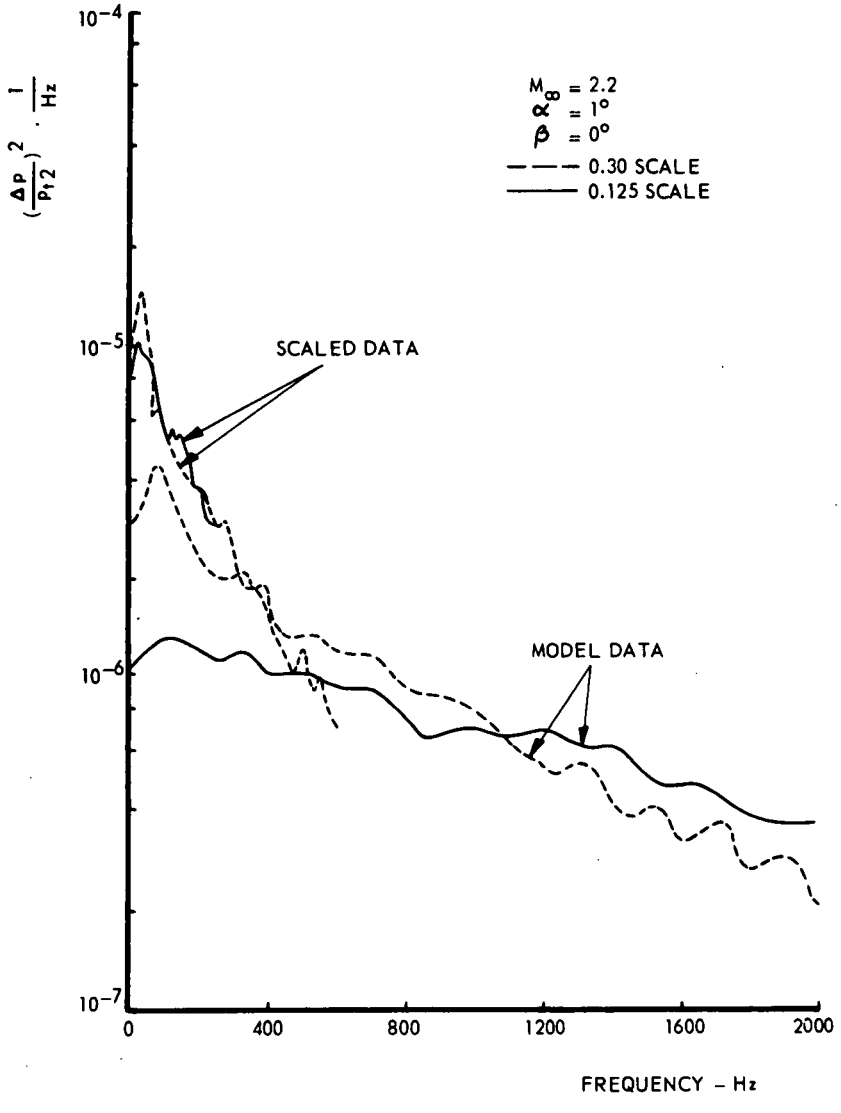

FIG. II. 36 EFFECT OF ACOUSTIC SCALING ON POWER SPECTRAL DENSITY.

One, analogous to the Reynolds number concept, is that, for unit of absolute mixing length, the ratio of the mixing boundary area to the momentum in each of mixing stream tubes is inversely proportional to scale. The second factor is that the dissipation rate is proportional to the square of the frequency which in turn is inversely proportional to scale.

The turbulence model suggests the following effects of scale for geometrically similar inlets.

(a) Just downstream of the turbulence generating region, turbulence amplitudes will be relatively independent of inlet scale. Turbulence frequencies will vary inversely with scale and directly with the square root of the absolute temperature of the flow.

(b) Turbulence decay per unit length downstream of the generating station will vary more than inversely proportional to the inlet scale. Conversion of lower frequency turbulence to higher frequency turbulence per unit length downstream of the generating station will be equal to or more than inversely proportional to the scale factor.

(c) The frequencies at which turbulence energy peaks occur will vary inversely with scale factor and proportional to the square root of the absolute temperature.

Comparisons of the data from the geometrically similar 0.30 and 0.125 scale model showed the following:

(a) The frequency distribution of the turbulence energy differs with model scale. Typically, turbulence energy levels are higher at low frequencies and lower at high frequencies for the larger scale inlet, as shown in Figure II.36. Where resonant peaks occur in the power spectral density curves, the peaking frequencies differ, but are inversely proportional to scale.

(b) Spatial distribution and turbulence patterns and variations of the patterns with angle-of-attack, angle of yaw and Mach number are similar for the 0.30 and the 0.125 scale inlets.

(c) Average engine face turbulence differs both with Reynolds number and with scale. Both the Reynolds number effect on turbulence and the difference due to model scale at a given Reynolds number are apparent from the data of Figure II.36. There differences are largest when turbulence levels are high (low recovery, supercritical operation), and decreases with increasing pressure recovery and decreasing turbulence levels.

The initial scaling correction for RMS turbulence is accomplished by using a cut-off filter prior to processing the data. The cut-off filter frequency is selected in accordance with acoustic theory. That is, to obtain full-scale turbulence values for frequencies up to, say, 300 H_z, a cut-off frequency of 1000 is used in processing the 0.30 scale inlet data. Similarly, a cut-off frequency of 2400 is used for the 0.125 scale inlet data. If model test and full-scale temperatures differ, the filter cut-off frequency is further corrected by the square root of the ratios of the absolute total temperatures. In Figure II.36, it can be seen that this correction makes the turbulence data from the two models more nearly identical. Had this been the only correction required, the data would be superimposed. However, differences due both to size and Reynolds number still exist.

The second correction consists of extrapolating the model data both relative to scale and to Reynolds number. The extrapolations, ideally, are based on data for the configuration of concern obtained from two or more models of different scale tested at several Reynolds number.

2.2.5 COMPARISON BETWEEN WIND TUNNEL TESTS AND FLIGHT TESTS

Several recent and proposed programs have been directed towards the end of being able to correlate and correct wind tunnel scale data to the full-scale flight vehicle conditions.

Figure II.37 presents some typical results obtained from a large scale inlet tested with and without a turbojet engine. The data indicate that there is little differences in inlet flow properties between the two test series. Furthermore, no significant differences (except for rotor harmonics) in the energy spectra were found indicating little upstream influence of the compressor on the inlet flow. Another test series provided some data for comparing inlet performance from a small scale, large scale, and flight test vehicle with identical instrumentation. The data shown in Figure II.38 for a supersonic test condition at low α indicates that there was little difference in the data between the two scaled models in terms of either recovery, distortion, or turbulence. In general, the flight test data pressure recovery was in good agreement but both the distortion and turbulence measured in flight are somewhat lower. The difference in steady-state distortion, however, can be attributed at least in part to the effects of Reynolds number. The outer ring of probes on both models was immersed in the duct wall boundary layer while the flight Reynolds number was sufficiently higher that the boundary layer did not reach out to the outer ring of probes. If another distortion indicator had been used the differences may not have been as significant. The compressor face turbulence is also somewhat higher in wind tunnel tests than flight and may be due in part to Reynolds number effects as well as the level of tunnel turbulence relative to free flight. A comparison of the steady-state distortion patterns are presented in Figure II.39 and show the great degree of similarity between the wind tunnel and flight test results. It should be pointed out here that the similarity between scale data decreases as the model scale is reduced. As the model scale is reduced below approximately 1/10 differences may appear in both distortion and pressure recovery. This again supports the requirement for testing using as large a model as possible consistent with the facilities available.

2.3 REFERENCES AND GENERAL BIBLIOGRAPHY

REFERENCES

II-1	R.S. Osborne D.E. Wornom	Aerodynamic Characteristics Including Effects of Wing Fixes of a 1/20-Scale Model of the Convair F-102 Airplane at Transonic Speeds; NACA RM SL54C23 Confidential.
II-2	P.K. Pierpont J.A. Braden	Investigation at Transonic Speeds of a Forward-Located Underslung Air Inlet on a Body of Revolution. NACA RM L52K17.
II-3	J.A.Braden and P.K.Pierpont	Pressure and Force Characteristics at Transonic Speeds of a Submerged Divergent-Walled Air Inlet on a Body of Revolution. NACA RM L53C13.
II-4	R.V. Osmon	Improved Methods of Spillage Drag Prediction for Two-Dimensional Supersonic Inlets. AIAA paper No. 67-449, July 1967.
II-5	T.M. Savage	A Prediction of the Normal Shock Location for Axi-symmetric and Two-Dimensional Inlets, and a Method for Calculating Supersonic Additive Drag. General Dynamics, Fort Worth Division, MR-P-277, 7 March 1969.

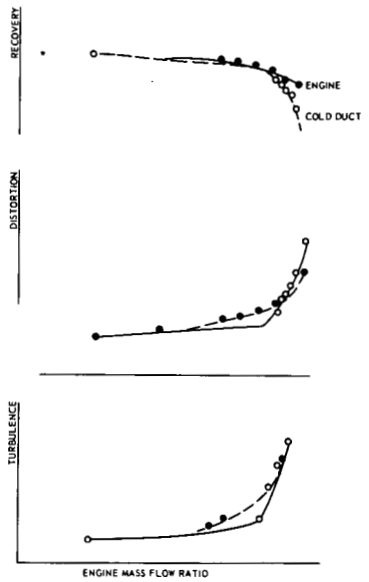

FIG. II. 37 LARGE SCALE INLET TESTS WITH AND WITHOUT ENGINE.

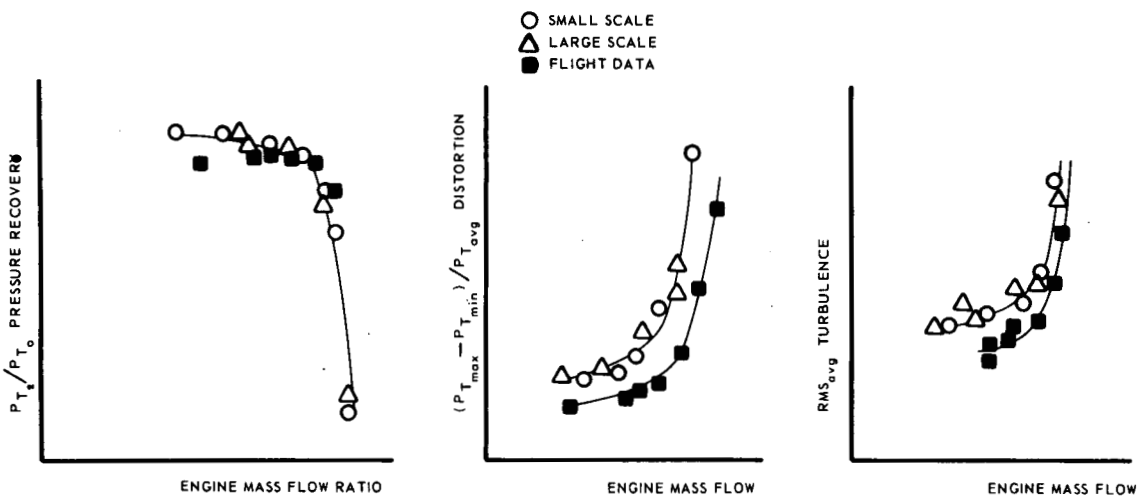

FIG. II. 38 COMPARISONS BETWEEN INLET FLOWS AT SMALL SCALE, FULL SCALE AND FLIGHT.

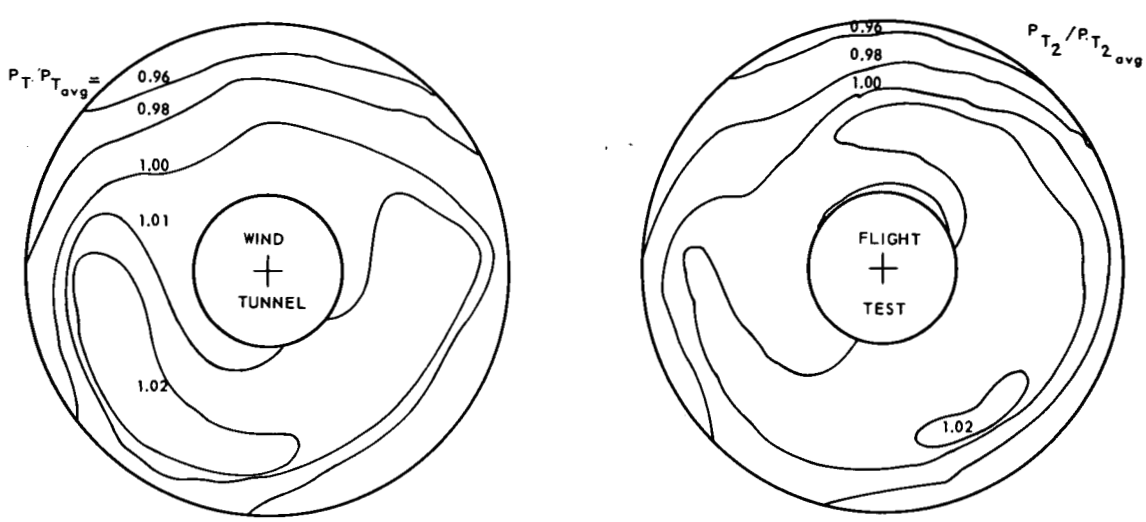

FIG. II. 39 COMPARISON OF STEADY – STATE DISTORTIONS.

II-6	G.L. Muller and W.F. Gasko	Subsonic-Transonic Drag of Supersonic Inlets. Pratt and Whitney Aircraft, TDM-1973, May 1966.
II-7	F.D. McVey J.V. Rejeske E.J. Phillips, et al	Experimental Evaluation of Inlet Drag Characteristics in the Transonic Mach Number Range; McDonnell Douglas Corporation, AFAPL-TR-68-119, November 1968.
II-8	F.D. McVey J.V. Rejeske and E.J. Phillips	Experimental Evaluation of Inlet Drag Characteristics in the Transonic Mach number Regime; McDonnell Douglas Corporation; AFAPL-TR-68-119, Supplement 1, November 1969.
II-9	M.W. Petersen G.C. Ramplin	Experimental Review of Transonic Spillage Drag of Rectangular Inlets; North American Aviation, Inc., Technical Report AFAPL-TR-66-30, May 1966.
II-10	O.W. Smith II	Generalized Method of Predicting Lip-Suction and Spillage Drag Force Coefficients of Isolated, Axi-symmetric Inlets; General Dynamics Fort Worth Division, AIM No. 185, 7 May 1969.
II-11	J.W. Britton	Measurements of the internal drag of air breathing installations on slender wing-body combinations at supersonic speeds. RAE Tech Report 65275. ARC CP 914.
II-12	K.G. Smith	Methods and charts for estimating skin friction drag in wind tunnel tests with zero heat transfer. RAE Tech Note Aero 2980.
II-13	E.L. Goldsmith	Variable Geometry Intakes at Supersonic Speeds - Some techniques and some Test Results. AGARD CP 34, Sept. 1968.
II-14	C.R. Taylor J.R. Hall R.W. Hayward	Super VC10 cruise drag - a wind tunnel investigation, Part I experimental techniques. RAE Tech Report 69188.
II-15	L.H. Schreiber	A plan for Bookkeeping on the Propulsion and Aerodynamic Elements of Airplane Performance; General Dynamics, Fort Worth. Proceedings of the Air Force Airframe-Propulsion Compatibility Symposium, 24 - 26 June 1969. Air Force Technical Report AFAPL-TR-69-103.
II-16	J.S. Holdhusen	Analysis and Demonstration Techniques for Installation Aerodynamic Effects on High-Bypass Ratio Turbofans. FluiDyne Engineering Corporation; Air Force Technical Report AFAPL-TR-69-103.
II-17	D.J. Raney A.G. Kurn V.A. Bagley	Wind Tunnel Investigation of Jet Interference for Underwing Installation of High Bypass Ratio Engines. Royal Aircraft Establishment Technical Report 68049, March 1969.
II-18	D.T. Poland V.C. Schwanebeck	Turbofan Thrust Determination for the C-5A; Lockheed Aircraft; AIAA paper 70-611, June 1970. AIAA 6th Propulsion Joint Specialists Conference, San Diego, Calif., 15 - 19 June 1970.
II-19	M.D. Dobson E.L. Goldsmith	The external drag at subsonic and supersonic speeds of fuselage side intakes for strike-fighter aircraft. ICAS Paper Rome, September 1970.
II-20	J. Leynaert and G. Meauze	Quelques Problemes Transsoniques du Fuseau Moteur d'un Avion du Type "Airbus". AGARD CP.35 "Transonic Aerodynamics".
II-21	J.S. Holdhusen	Analysis and Demonstration Techniques for Installation Aerodynamics Effects on High Bypass Turbofans. AGARD CP.34, Sept. 1968.
II-22	H. Ritter	Wake Traverse in the Presence of Tunnel Blockage. ARL/G/N4, Febr. 1963.
II-24	J.E. Green	A design of sonic nozzle for the precise measurement of mass flow. RAE Tech Report 70201.
II-25	J.W. Britton	Some notes on the analysis of forces on ducted models with fuselage or wing mounted side intakes. RAE report to be published.
II-26	Th.E. Labrujere W. Loeve and J.W. Slooff	An approximate method for the calculation of the pressure distribution on wing-body combinations at subcritical speeds. AGARD CP. No. 71, Aerodynamic Interference, Sept. 1970.
II-27	J.L. Hess and S.M. Faulkner	Determination of low speed interference effects by superposition. AGARD C.P. No. 71, Aerodynamic Interference, Sept. 1970.
II-28	C.M. Jackson Jr. R.S. Smith	A method for determining the total drag of a pointed body of revolution in supersonic flow with turbulent boundary layer. NASA TN D-5046, 1969.
II-29	A.A. VanDuine W.W. Rhoades W.C. Swan	Configuration aspects of propulsion installation on supersonic transports. AGARD C.P. No. 71, Aerodynamic Interference, Sept. 1970.

II-30 D.J. Peake, D.J. Jones and W.J. Rainbird — The half-cone pressure field and its significanse to side-mounted intakes. AGARD C.P. No. 71, Aerodynamical Interference, Sept. 1970.

II-31 L.S. King and T.W. Schmidt — Studies of aircraft flow fields at inlet locations. AGARD C.P. No. 71, Aerodynamical Interference, Sept. 1970.

II-32 B.H. Goethart and K.C. Reddy — Unsteady Aerodynamics of Rotor Blades of a compressor under Distorted Flow Condition. AGARD CP-71, Aerodynamic Interference, Sept. 1970.

II-33 F.W. Burcham and D.L. Hughes — Analysis of in-flight pressure fluctuations leading to engine compressor surge in an F-111A airplane for Mach numbers to 2.17. AIAA Paper No. 70.624.

II-34 M.B. Sussman, G.W.M. Lampard, D.V. Hill, R.R. Bowen, et al — A Study of Inlet/Engine Interaction in a Transonic Wind Tunnel. D6-60116, January 1970, Boeing Report.

II-35 C.E. Langston — Distortion Tolerance - By Design Instead of By Accident. Pratt and Whitney Aircraft; ASME paper 69-GT-115; ASME International Gas Turbine Conference and Products Show, Cleveland, Ohio, March 1969.

II-36 G.S. Plourde and B. Brimelow — Pressure Fluctuations Cause Compressor Instability; 69-9055. Air Force Aero Propulsion Laboratory, Airframe/Propulsion Compatibility Symposium, June 1969.

GENERAL BIBLIOGRAPHY

INFLUENCE OF INLET MASS FLOW ON EXTERNAL AERODYNAMICS AND MEASURED FORCES

E.L. Crosthwait, I.G. Kennon Jr., H.L. Roland et al — Preliminary Design Methodology for Air Induction Systems. Air Force Systems Command, Report SEG-TR-67-1, January 1967.

- — Experience in the Application of Recognized Aerodynamic Estimation Techniques for the Prediction of Aircraft Stability and Control Parameters Including Contributions to the USAF Stability and Control Handbook. Crumman Aircraft Engineering Corporation Report.

INTERNAL INLET FLOW DETERMINATION IN TRANSONIC WIND TUNNEL TESTS

D.W. Brees — Analysis of Flow Distortion Effects in Two-Dimensional Offset Diffusers. SAE Paper 586E, October 1962.

E.A. Frandenburgh and D.C. Wyatt — Theoretical Performance Characteristics of Sharp-Lip Inlets at Subsonic Speeds. NACA TN 3004, September, 1953.

R. Henry, C.C. Wood and S.W. Wilbur — Summary of Subsonic-Diffuser Data. NACA RM L56F05, Washington, D.C. February 8, 1963.

L.D. Miller — Predicting Compressible Turbulent Boundary Layers with Strong Pressure Gradients. Lockheed Report LR-20701, to be published.

TECHNIQUES FOR INLET MASS FLOW SIMULATION

A.C. Brown, H.F. Nawrocki and P.N. Paley — Subsonic Diffusers Designed Integrally with Vortex Generators. AIAA Paper No. 67-464, presented at AIAA 3rd Propulsion Joint Specialist Conference, Washington, D.C., July, 1967.

J.R. Henry, C.C. Wood and S.W. Wilbur — Summary of Subsonic Diffuser Data. NACA RM L56F05, October 1956.

A.W. Martin — Propulsion System Dynamics Simulation Theory and Equations. NASA CR-928, March, 1968.

G. McLafferty — A study of Perforation Configurations for Supersonic Diffusers. United Aircraft Research Report R-53372-7, December 1950.

Th.G. Piercy — Factors Affecting Flow Distortions Produced by Supersonic Inlets. NACA RM E55219.

S.T. Pinckney — Semi-empirical Method for Predicting Effects of Incident-Reflecting Shocks on the Turbulent Boundary Layer. NASA Technical Note TN D-3029, October 1965.

J.B. Rice — Flow Calibration Studies of Seventeen Perforated Plates with Air Flow Parallel to the Plates. United Aircraft Research Report M-95630-16, May, 1954.

M. Sibulkin — Theoretical and Experimental Investigation of Additive Drag. NACA Report 1187, 1954.

B.L. Sorensen — Computer Program for Calculating Flow Fields in Supersonic Inlets. NASA TN D-2897, July, 1965.

A.H. Spring — Upstream Influence of Axial Compressor on Distorted Subsonic Duct Flows. Fort Worth Division Report ERR-FW-755, 26 August 1968.

EXTERNAL FLOW FIELD SIMULATION

R.J. Cresci and P.K. Sasman — Compressible Turbulent Boundary Layer with Pressure Gradient and Heat Transfer. AIAA Journal, Vol. 4, No. 1, January, 1966.

L.E. Hasel and W.L. Kouyoumjian — Investigations of Static Pressures and Boundary Layer Characteristics on the Forward Parts of Nine Fuselages of Various Cross-Sectional Shapes at $M_\infty = 2.01$, NACA RM L 56I13, January, 1957.

E.J. Kremzier and R.C. Campbell — Effect on Fuselage Fences on the Angle-of-Attack Supersonic Performance of a Top-Inlet-Fuselage Configuration. NACA RM E54J04, 1955.

E.J. Kremzier and J. Wasserbauer — Effect of Fuselage Circumferential Inlet Location on Diffuser-Discharge Total - Pressure Profiles at Supersonic Speeds. NACA RM E56G26, October, 1956.

J.L. Lankford — Preliminary Results of Flow Surveys About an Inclined Body of Revolution (Mach Number of 3.5), NAVORD Report 6708, January 1960.

E.T. Marley and H. Ginsberg — Supersonic Pressure Distribution and Axial-Force Characteristics of Axisymmetric Noses at Angle-of-Attack, presented at the Seventh U.S. Navy Symposium on Aeroballistics, 7 - 9 June, 1966.

C. Prokop and R.J. Sanator — Investigation of Airframe-Inlet Interaction for Supersonic Tactical Fighter Aircraft, Air Force Flight Dynamics Laboratory Report, AFFDL-TR-70-66, January, 1970.

E. Reshotko and M. Tucker — Approximate Calculation of the Compressible Turbulent Boundary Layer with Heat Transfer and Arbitrary Pressure Gradient, NACA TN 4154, 1957.

B.M. Sharp and T.C. Rochow — Axisymmetric Rotational Inviscid Supersonic Inlet Flow Field Calculations, McDonnell Report EN 550, June, 1967.

R.A. Smith — An Experimental Inlet Boundary-Layer Removal Research Program, Fort Worth Division Report ERR-FW-637 (to be published).

BOUNDARY LAYER DIVERTER DESIGN

R.C. Campbell and E.J. Kremzier — Performance of wedge-type boundary-layer diverters for side inlets at supersonic speeds, NACA RM E54C23, May, 1954.

H.F. Goelzer and E.M. Cortright, Jr. — Investigations at Mach number 1.88 of half a conical-spike diffuser mounted as a side inlet with boundary-layer control. NACA RM E51G06, September 1951.

T.G. Piercy and H.W. Johnson — Experimental Investigation at Mach numbers 1.88, 3.16 and 3.83 of Pressure Drag of Wedge Diverters simulating Boundary-layer-Removal Systems for Side Inlets, NACA RM E53L14b, February, 1954.

T.G. Piercy and H.W. Johnson — Investigation at Mach number 2.93 of half a conical-spike diffuser mounted as a side inlet with boundary-layer control. NACA RM E52G23, September, 1952.

L.E. Stitt and B.H. Anderson — NASA TM X-147, January, 1960.

SPLITTER PLATES

F.L. Seashore and J.M. Farley — Preliminary performance data obtained in a full-scale free-jet investigation of a side-inlet supersonic diffuser, NACA RM E57E24, January, 1958.

EFFECTS OF CANARDS AND OTHER AERO SURFACES ON FLOW FIELDS

L.J. Obery and H.S. Krasnow — NASA RM E52F26, August, 1952.

MEASURING TECHNIQUES

W.E. Anderson and E.W. Perkins — Effects of Unsymmetrical Air-Flow Characteristics of Twin-Intake Air-Induction Systems on Airplane Static Stability at Supersonic Speeds, NASA TM X-94, December, 1959.

J.S. Bendat and A.G. Piersol — Measurement and Analysis of Random Data, New York: John Wiley and Sons, 1966.

M.R. Bottorff — Wind Tunnel Tests of a 5 % A3J-1 Horizontal Ramp Inlet Model at Mach Numbers From Transonic to 2.25 , Aerodynamic Test Division, USNAMTC, USCEC Report 32-1-21, 29 April, 1958.

D.W. Clutter and K. Kaups — Wind Tunnel Investigation of Turbulent Boundary-Layers on Axially Symmetric Bodies at Supersonic Speeds, Douglas Aircraft Division Report LB 31429, 1964.

G.M. Corcos — Resolution of Pressure in Turbulence, Journal of Acoustical Society of America, Vol. 35, No. 2, 192-199, 1963.

M.G. Hall and H.B. Dickens — Measurements in a Three-Dimensional Turbulent Boundary-Layer in Supersonic Flow, RAE TR 66214, 1966.

M.W. Petersen and G.C. Tamplin — Experimental Review of Transonic Spillage Drag of Rectangular Inlets, Air Force Aero Propulsion Laboratory Report, AFAPL-TR-66-30, May, 1966.

M.B. Sussman, G.W.N. Lampard, D.J. Hill, R.R. Bowen et al — A study of Inlet/Engine Interaction in a Transonic Propulsion Wind Tunnel, Boeing Report D6-60116, January, 1970.

– — Air Induction System and Installed Performance, ASD-TDR-63-165, Part II, Series III, Volume 3, March, 1963.

– — Thermodynamics Group "Performance Analysis of B-70 Subsonic Diffusers, North American Aviation, Inc. Report NA-58-1282, November, 1958.

SCALE EFFECTS

J.S. Doyle — Series 11A Model Tests to Determine Flight Performance of Several Aft-Fuselage Ejector Nozzle Configurations, FluiDyne Engineering Corporation Project 0562, October, 1967.

L.L. Pasiuk, S.M. Hastings and R. Chatham — Experimental Reynolds Analogy Factor for a Compressible Turbulent Boundary-Layer with a Pressure Gradient, Naval Ordnance Laboratory Report NOLTR 64-200, 1965.

SPILLAGE AND BLEED AIR

F.A.L. Winternitz and W.J. Ransay — Effects of Inlet Boundary-Layer on Pressure Recovery, Energy Conversion and Losses in Conical Diffusers, Journ. Roy.Aero.Soc., 61: 116, February, 1957.

R.A. Smith — An Experimental Inlet Boundary-Layer Removal Research Program, Fort Worth Division Report ERR-FW-637 (to be published).

EFFECTS OF INLET B.L. BLEED

L.E. Stitt and R.J. Salmi — Performance of a Mach 3.0 External-Internal Compression Axisymmetric Inlet at Mach Numbers from 2.0 to 3.5, NASA TM X-145, January, 1960.

COMPARISON BETWEEN WIND TUNNEL TESTS AND FLIGHT DATA

G.C. Billips, C.D. Boman, W.R. Haagenson and J.E. Wolfe — XB-70A Flight Test Summary Report, Air Induction System and Air Induction Control System, Contract AF33 (657) - 12395, North American Aviation, Inc., Report NA-66-876, October 4, 1966.

F.T. Rall — Aircraft and Propulsion Operation Considerations Related to Inlet Design, Flight Mechanics Panel - AGARD, September, 1967.

T.A. Sedgwick, A.C. Brown and J.F. Stroud — Correlation of Wind Tunnel and Flight Test Data on the Air Induction System of the F-104 Aircraft, WADC-TR-59-176, July, 1959.

T.R. Slaten — Investigation of the Airframe-Inlet Interaction Effects on the F-111, Fort Worth Division Report ERR-FW-750, 1 August 1968.

III ENGINE THRUST

LIST OF SYMBOLS

a	Speed of sound
A	Area
C_d	Discharge coefficient
C_P	Specific heat at constant pressure
C_T	Thrust coefficient
C_V	Specific heat at constant volume
F_M	Measured force on engine test bench
ΔF_B	Engine test bench correction force
$\dot{m}$	Mass flow
M	Mach number
n	Shaft r.p.m.
p	Static pressure
p_t	Total pressure
R	Gas constant
T	Static temperature
T_t	Total temperature
V	Velocity
x	Coordinate in thrust direction
X_g	Engine gross thrust
X_{id}	Isentropic gross thrust
y	Coordinate perpendicular to thrust axis
γ	Ratio of specific heats
δ	Half angle of conical nozzle
θ	Angle between velocity vector and thrust axis
ρ	Density

SUBSCRIPTS

cr	Critical
e	At nozzle exit plane
id	Isentropic, ideal
j	Of the jet
s	Sealing
t	Total, reservoir conditions
2	At engine entrance
∞	At upstream infinity
*	At throat

If an aircraft manufacturer designs new aircraft, he has to look for the appropriate engine to propel his aircraft. Sometimes he specifies the required thrust and other characteristics which should be met by the engine company. Other times he can make use of existing engines or engines under development. The engine company will define and specify the thrust under certain conditions based on company defined reference inlets and nozzles. The aircraft manufacturer, however, plans to use the engine with a different inlet and nozzle and external conditions typical for that aircraft design. The problem for the aircraft company is to incorporate the defined and specified engine performance in his particular design and to establish a wind tunnel test program compatible with the thrust definitions.

This chapter will first review the various thrust definitions and nozzle coefficients, after which the techniques used to measure the thrust will be considered. The advantages and limitations of these definitions and techniques will be critically reviewed. Also the applied corrections will be considered and some information on obtained and required accuracies of the engine thrust will be given.

3.1 ENGINE THRUST DEFINITION

The engine net thrust as it felt by the aircraft is the engine gross thrust minus the ram drag, vectorally substracted. The ram drag is simply, the engine mass flow times flight velocity, $\dot{m}.V_\infty$. This means that in flight $\dot{m}$ must be defined accurately. The mass flow can generally be obtained in flight from the known compressor characteristics.

Since the gross thrust is some factors larger than the net thrust, it is of great importance to know the gross thrust at a high degree of accuracy. The ratio of gross thrust to net thrust tends to increase with flight Mach number.

Usually the engine manufacturer presents the engine gross thrust in non-dimensional form in tables and/or in curves. For example the gross thrust is presented as

$$\frac{p_\infty}{p_{t_2}} \left(\frac{X_g}{p_\infty . A_e} + 1\right) \text{ given as a function of } n\sqrt{T_{t_2}} \text{ where}$$

p_∞ = static ambient pressure, p_{t_2} = total compressor entrance pressure, T_{t_2} = total compressor entrance temperature, A_e = nozzle exit area, X_g = gross thrust, and n = shaft r.p.m.

In order to use those engine data for airplane performance estimates it is important to know the way the engine manufacturer defined the actual thrust X_g. For defining the gross thrust a reference nozzle is used, which is usual conical and convergent.

The actual gross thrust is

$$X_g = \int_{A_e} \rho_e V_e^2 \, dA + \int_{A_e} (p_e - p_\infty) \, dA$$

where V_e is the axial jet velocity at the exit plane and ρ_e the density. However this X_g cannot easily be obtained from integration of the experimental quantities across the exit plane, and therefore a thrust coefficient is used, defined as

$$C_T = \frac{X_g}{X_{id}} .$$

Here X_{id} is the one dimensional isentropic gross thrust.

The isentropic gross thrust can be defined in several ways based on the quantities measured when the measured quantities are engine mass flow $\dot{m}$, fuel consumption and power- and air subtraction from the engine. X_{id} can be calculated from the thermodynamic engine cycle relations and the known minimum exhaust area A^* (throat). X_{id} can than be defined as

$$X_{id} = \dot{m} V_{id}$$

or

$$X_{id} = \dot{m} V_e + A_e (p_e - p_\infty)$$

where V_{id} is the jet velocity after isentropic expansion from the computed value of the jet total pressure p_{t_j} and jet total temperature T_{t_j} to the ambient pressure p_∞, and V_e is the isentropic expansion to the p_e as belonging to A_e/A^* (usually $A_e/A^* = 1$). A distinction should be made for computed choked, $p_{t_j}/p_\infty \geq (p_{t_j}/p_\infty)_{cr}$, and not choked nozzle flows, $p_{t_j}/p_\infty < (p_{t_j}/p_\infty)_{cr}$.

The isentropic expansion process can be computed using the γ-relationships or more accurately using the entropy-enthalpy diagrams or tables for the gas mixture ($\gamma = C_P/C_V$ for the gas mixture at p_t and T_t or at p and T average during the expansion process).

On the other hand if X_{id} is based on the measured average values of $\bar{p}_{t_j}$ and $\bar{T}_{t_j}$, the computed X_{id} values need to be corrected for the nozzle discharge coefficient C_d defined as

$$C_d = \frac{\dot{m}_{actual}}{\dot{m}_{id}}$$

where $\dot{m}_{id}$ is the ideal mass flow through the nozzle as determined from the mass average values of the upstream total $\bar{p}_{t_j}$ and $\bar{T}_{t_j}$.

For example for a choked convergent nozzle

$$\dot{m}_{id} = \frac{p_e}{p_{t_j}} \frac{a_e}{a_{t_j}} \frac{p_{t_j}}{RT_{t_j}} \sqrt{\gamma RT_{t_j}}\ A_e$$

and using the γ relations also $\dot{m}_{id}$ becomes

$$\dot{m}_{id} = \left(\frac{2}{\gamma+1}\right)^{\frac{\gamma+1}{2(\gamma-1)}} p_{t_j} \sqrt{\frac{\gamma}{RT_{t_j}}}\ A_e$$

(The density ratio $\frac{p_e}{p_{t_j}}$ and the speed of sound ratio $\frac{a_e}{a_{t_j}}$ can be more accurately obtained from the Molier diagram of the average gas mixture). Thus, if the thrust coefficient C_T uses an ideal gross thrust based on jet stagnation measurements, the actual gross is equal to

$$X_g = C_T C_d X_{id}$$

or

$$X_g = C_T C_d \dot{m}_{id}\ V_{id}$$

or the gross thrust of a convergent nozzle can be defined as

$$X_g = C_T C_d\ [\dot{m}_{id}\ V^* + (p^* - p_\infty)\ A_e]$$

where * refers to the sonic values.

One might wonder why the last term within the main brackets should be multiplied by C_d also. This is correct since the one-dimensional momentum relation at the nozzle exit yields

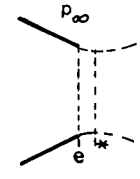

$$X_{id} = p_e A_e + p_e V_e^2\ A_e - p_\infty A_e = p^* A^* + \rho^* V^{*2} A^* + p_\infty (A_e - A^*) - p_\infty A_e$$

$$= [\dot{m}_{id}\ V^* \frac{A^*}{A_e} + \frac{A^*}{A_e} (p^* - p_\infty)\ ]\ A_e \quad .$$

Since one-dimensionally $A^*/A_e = C_d$ the above mentioned equation is obtained. The gross thrust can than also be written as

$$X_g = C_d C_T A_e\ p_\infty\ (K\ p_{t_j}/p_\infty - 1)$$

where K is a constant (using the γ relationships) depending on γ. Typically K = 1,26 for γ = 1,33.

The definition of the engine thrust as given by the engine manufacturer is based on the method used to measure the engine thrust in the test cells, and this thrust is usually called the uninstalled gross thrust. This value is based on the reference nozzle which is normally not the same as will be used in the aircraft. Furthermore, the external flow field will cause a different pressure field at the nozzle exit which will make the installed gross thrust different from the uninstalled value as specified by the engine company. The difference can be defined as the internal nozzle drag, or the ratio of the installed gross thrust and the appropriate isotropic thrust can be defined as the installed thrust coefficient.

The installed thrust values are the airframe manufacturer's responsibility and should be obtained from an extensive wind tunnel testing program of engine-airframe integration.

Sometimes the term flange thrust is found in the literature which is defined as the ideal thrust obtainable from a flow as leaving the engine exit (flange between engine and nozzle) including the flow distortions.

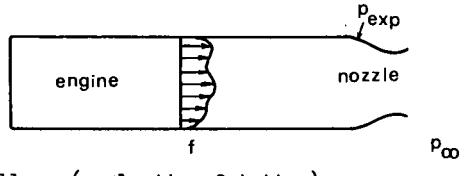

From the momentum equation it follows (neglecting friction)

$$\int_{A_f} V_f dm_f + \int_{A_f} p_f dA - \int_{A_f - A_e} p_{exp}\ dA_{ax} = \int_{A_e} V_e\ dm_e + \int_{A_e} p_e\ dA\ ,$$

where V_f and V_e are the velocity components in the axial direction and dA_{ax} is the projection of the nozzle surface increments parallel to the axis. P_{exp} is the static pressure along the nozzle contour. Since $dm_f = p_f V_f\ dA_f$ and similar for station e, it follows that the gross thrust is equal to

$$X_g = \int_{A_e} (p_e V_e^2 + p_e - p_\infty) dA = \int_{A_f} [(1 + \gamma_f M_f^2)\ p_f - p_\infty]\ dA - \int_{A_f - A_e} (p_{exp} - p_\infty)\ dA_{ax}$$

(M_f = the Mach number in the axial direction).

From the measured static and stagnant pressures at the flange station the first integral at the right hand side can be evaluated, and giving the throat or exit area, the minimum value of the second integral can be computed, using an appropriate flow field computing program taking into account the distortion and energy dissipation due to mixing. The nozzle contour and exit area can be chosen to give optimum gross thrust. The resulting maximum thrust may than be quoted as the flange thrust.

3.2 TECHNIQUES FOR DETERMINING ACTUAL ENGINE THRUST

The definition of the engine thrust as given by the engine manufacturer depends on the method used to measure the engine thrust. The engine company can measure or determine the net and gross thrust in an atmospheric test cell, a so called altitude test cell, or with an experimental aircraft in flight. In the test cells two methods can be used: namely, the scale method and the traversing probe method.

A ATMOSPHERIC TESTS

These tests are important after the early development phase of the engine. The results are useful for take-off and landing conditions. Though the results are not directly useful for the thrust determination at transonic speeds, the procedure will be considered briefly in order to be complete.

The engine is surrounded by infinite or near-infinite atmosphere at ambient pressure, p_∞. Figure III.1 shows schematically the engine installation on a bench. The engine is mounted on a base plate which is slung on flexure strips.

In the case of a bell mouth tied to the engine inlet, the actual gross thrust X_g of the engine, (defined as

$$X_{g_{actual}} = \int_{A_e} (p_e + \rho_e V_e^2 \cos^2 \theta_e)\, 2\pi y dy - p_\infty A_e = \text{Impulse at exhaust} - p_\infty A_e$$

with θ_e is flow angle in the exit plane between velocity vector and the thrust axis), is given by:

$$X_{g_{actual}} = F_M + \Delta F_B \ ,$$

where F_M is the measured force given by thrust measuring system, the scale, and ΔF_B is the bench correction force due to jet entrainment (altering pressure on external surfaces of both bell mouth and engine).

In the case of bell mouth separated from the engine front face, the actual gross thrust defined as before is obtained as follows:

$$- \text{Impulse at exhaust} = \int_{A_e} (p_e + \rho_e V_e^2 \cos^2 \theta_e)\, 2\pi y dy$$

$$- \text{Impulse at inlet (engine front face)} = \int_{A_2} (p_2 + \rho_2 V_2^2)\, 2\pi y dy$$

$$- \text{External forces} = p_\infty (A_2 - A_e)$$

$$- \text{Force acting on sliding seal or labyrinth} : (p_2 - p_\infty) A_s \ .$$

Then:

$$\int_{A_e} (p_e + \rho_e V_e^2 \cos^2 \theta_e)\, 2\pi y dy - \int_{A_2} (p_2 + \rho_2 V_2^2)\, 2\pi y dy + p_\infty (A_2 - A_e) - (p_2 - p_\infty) A_s = F_M \ ,$$

but

$$X_g = \int_{A_e} (p_e + \rho_e V_e^2)\, 2\pi y dy - p_\infty A_e \ ,$$

therefore:

$$X_g = F_M + \int_{A_2} (p_2 + \rho_2 V_2^2)\, 2\pi y dy - p_\infty A_2 + (p_2 - p_\infty) A_s \ .$$

Here it is assumed that the surface pressure is p_∞ ; if not, a bench correction force ΔF_B, as seen before, must be included in the above equation.

The calculation of the impuls of the entering flow:

$$\int_{A_2} (p_2 + \rho_2 V_2^2)\, 2\pi y dy = p_2 A_2 + \dot{m} V_2$$

is obtained from static and stagnation pressures probes both inside the boundary layer and in the free stream flow. If the intake bell mouth is standard the engine mass flow $\dot{m}_{actual}$ can be measured precisely (better than 1 %), and, thereby the impuls is measured precisely also.The measured gross thrust should be divided by the ideal thrust as based on the measured mass flow and fuel consumption, in order to obtain a proper thrust coefficient.

The nozzle survey method, which determines the jet exit momentum, is not used in routine sea level tests. This method is, however, jointly used in altitude tests and will therefore be discussed in B.

B ALTITUDE SIMULATED TESTS

In an altitude simulated test facility, flight simulation is achieved by producing the aircraft intake conditions for a given flight speed and altitude in the forward plenum chamber. The rear part of the cell in which the engine is installed is exhausted to the altitude pressure required. Figure III.2 shows an altitude test cell for the SST Concorde "Olympus" engine thrust measurement. From the accompanying sketch, the thrust equation can be easily derived, in the same form as in A.

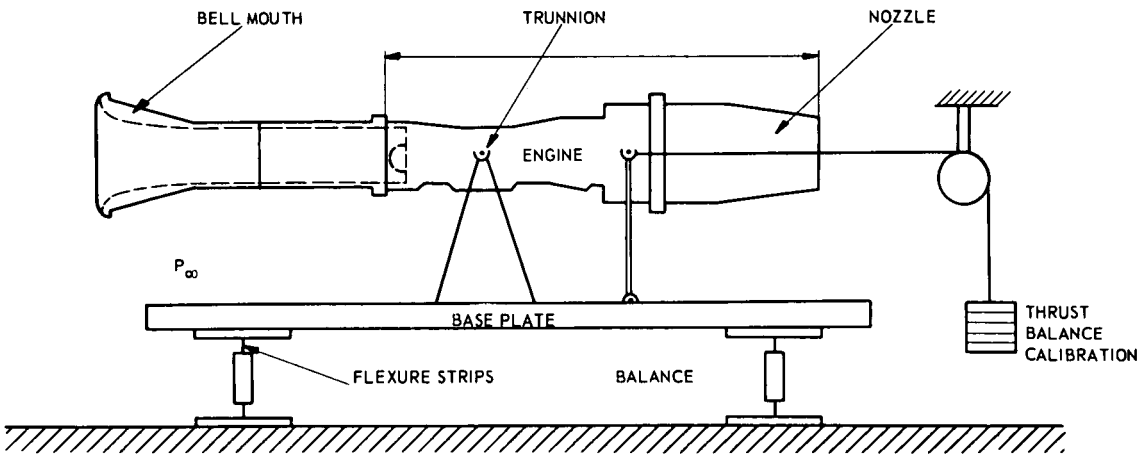

FIG. III. 1 ENGINE STATIC THRUST MEASUREMENT AT SEA LEVEL CONDITIONS.

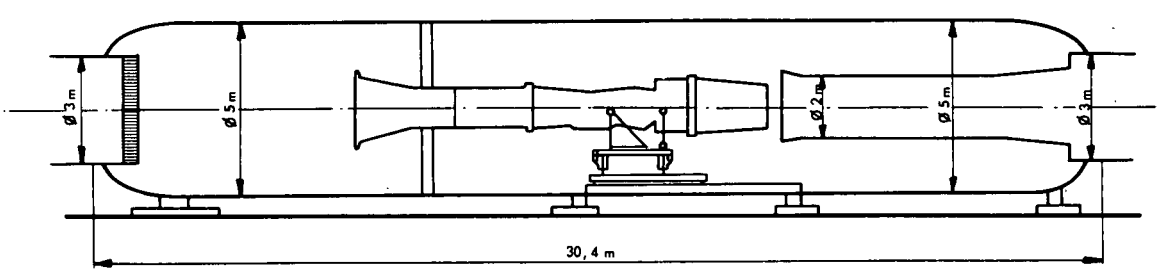

FIG. III. 2 ALTITUDE STATIC TEST FACILITY.

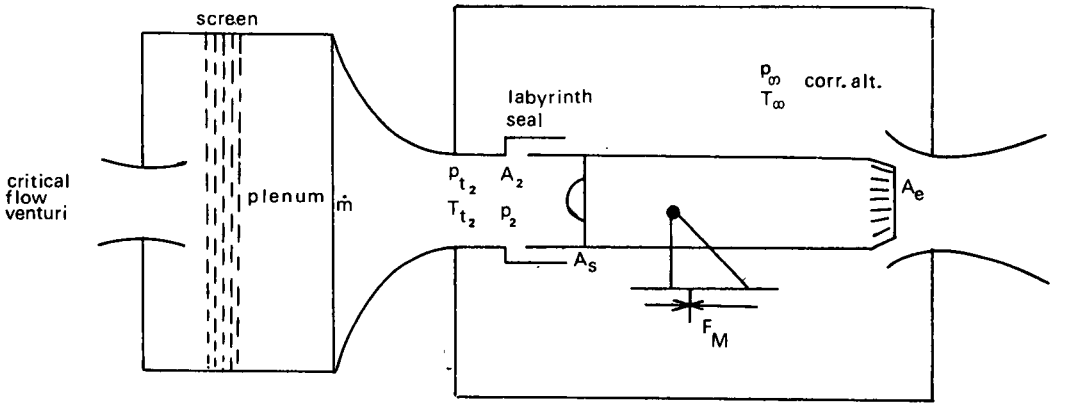

Since the inlet total pressure is larger than the ambient pressure at the exhaust the plenum must be coupled to the engine via a labyrinth (usually automatic balancing) seal, sothat the engine acts as a free body. The load cell that measures F_M must be calibrated for the tare forces due to instrumentation and fuel line hook-ups.

The nozzle survey method utilizes a traversing probe containing total pressure and temperature instrumentation. If the nozzle is convergent only, the survey plane will be the exit plane and direct determination of the integral of the gross thrust equation:

$$X_g = \int_{A_e} (p_e + \rho_e V_e^2) dA - p_\infty A_e \text{ can be accomplished,}$$

though the type of averaging process can lead to difficulties. If a convergent-divergent nozzle is used in the altitude test cell, the survey plane is located just upstream of the geometric nozzle throat in order to avoid measurements in a supersonic flow. A determination of skin friction and static pressure on any internal nozzle geometry downstream of the survey plane allows computation of the engine actual gross thrust.

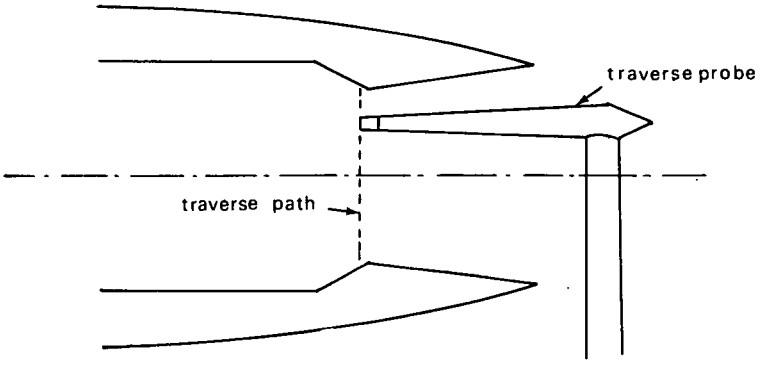

Needless to say the thrust coefficient determined from those data should be based on the ideal thrust as determined from the average total jet properties incorporating the measured nozzle dischange coefficient.

Usually the scale force method and nozzle survey method are jointly used in altitude test cells. This procedure allows for two separate but related thrust determination methods to be utilized in performance assessment. It is stated that values of gross thrust calculated by these methods routinely agree within the accuracy of the two methods.

C FLIGHT TESTS

In the final engine development phase sometimes flight tests are performed. One of the main reason for those tests is to check whether the engine meets environmental condition requirements, especially the free flight stagnation temperature. This temperature can be achieved in altitude test cells only after considerable investments, and is therefore usually not simulated or only partially simulated in altitude test cells. If flight tests are performed thrust is measured by instrumentation within the engine (gas generator method) or by an externally mounted swinging probe. Both techniques are involved with a great amount of flight measurement and ground test calibration. Accuracy of both approaches are considered to be ± 5 percent or better. Since this technique is somewhat out off the scope of this review it will not be discussed further. In all engine test methods and particularly for variable area nozzles in flight tests, it is difficult to accurate determine the nozzle area, due to the following sources of error: (a) rigging inaccuracy on nozzle position, (b) leaves deflection, due to flow pressure (depending from altitude/rating/speed), (c) thermal growth, due to local heating (affected by cooling conditions), (d) thermal growth of the feedback sensor of the nozzle position (difficult to calibrate and affected by the local cooling), and (e) leakage through the master and slave leaves.

3.3 LIMITATION AND ADVANTAGES OF THRUST DEFINITIONS AND MEASURING TECHNIQUES

The installed engine thrust of a particular engine depends on three items:
(a) the nozzle type and geometry, (b) the external flow, and (c) the flow distortion at the nozzle entrance.

If the actual aircraft nozzle is attached to the engine in the test cell, the data obtained are directly related to the uninstalled engine thrust. The degree to which the installed values can be predicted depends on the nozzle system, and the influence the external flow has on the nozzle performance.

In certain types of nozzles such as blow in door ejectors and plug nozzles, no clear distinction can be made between the external and internal performance, sothat no reliable prediction can be made for the installed thrust values.

Gross thrust (and thrust coefficient) as obtained in scale force test cell measurements without nozzle surveys, is useless when a different nozzle system is used in the aircraft, since the effects of the internal flow distortions cannot be predicted, even though a reference nozzle (usual conical) has been used. The thrust coefficient and discharge coefficient of a nozzle are usually determined from separate nozzle tests where the average stagnation pressure and temperature as measured in the engine are used as uniform stagnation conditions. Those average (some average) stagnation quantities are always given in the Engine Bulletins, but in advanced turbojet engines of the bypass type or having partial afterburners, a large nonuniformity of stagnation pressure and temperature can exist. The nonuniformities have several effects, because of velocity and temperature gradients, viscosity and heat conduction are important. Such effects increase entropy of the flow; therefore the nozzle flow is not isentropic. Furthermore, the location of the sonic line is strongly effected by the upstream stagnation pressure and temperature distribution, and, therefore, the Mach number and pressure distribution in the exit plane of a convergent nozzle is affected. Figures III.3a and b show these effects as computed from analysis for a convergent nozzle. These figures give the distribution of the Mach number at the exit of the nozzle shown for the case of variable stagnation temperature and variable or constant stagnation pressure, as well as the shape of the sonic line. The differences in thrust of the engine with respect to uniform flow expanded to M = 1 uniformly are 1.8 °/o and 2.5 °/o respectively. As an example, the distribution for a conical nozzle is also shown in Fig. III.3a. In the following table, the losses related to transport properties are also given. The conditions are for flight Mach number 0.75, altitude 36,000 ft.

	Loss due to nonuniformity	Loss due to shear	Total
Average T_{t_j}, p_{t_j} constant	0	0.02	0.02 °/o
Case 1 nonuniform T_{t_j}, uniform p_{t_j}	1.2	0.7	2.00 °/o
Case 2 nonuniform p_{t_j}, T_{t_j}	1.6	1.1	2.7 °/o

These results agree qualitatively with experiments as shown in Fig. III.4. It can therefore be concluded that the nozzle coefficients are not a single property of a nozzle system. The degree of flow nonuniformity (also swirl and turbulence) at the nozzle entrance strongly influences the nozzle performance. The same conclusion can be drawn for ejector nozzle systems, where ejector action is controlled by the mixing process between the primary and secondary air. The use of nozzle coefficients obtained from uniform flow tests introduces errors in the evaluation of the thrust of an actual engine.

Also several limitations should be noted concerning the calculation of gross thrust from nozzle surveys. The actual engine flow conditions at the survey station are three-dimensional, and radial as well as circumferential pressure and temperature gradients are present. Since unique one-dimensional reference pressures and temperatures are calculated in the cycle analysis, these values must be representative of the actual flow conditions. However, one-dimensional values obtained from three-dimensional data are dependent upon the type of averaging process.

The question of how to correctly calculate the thrust for a flow with a temperature and pressure profile must be considered. The problem is especially significant when it is necessary to compare a nozzle thrust based on a pressure and temperature profile with an engine cycle deck calculation which does not acknowledge such profiles. The problem lies in the fact that different values of thrust can be obtained depending on the calculation method used.

The prime flow quantities can be divided into those which may be identified by unique values without recourse to some sort of averaging process (cross-sectional area, mass flow, stream thrust, and stream kinetic energy) and those which depend upon an averaging process (pressure and temperature). These six prime flow quantities satisfy the three basic equations of motion in terms of integrals across the stream tube. With the addition of other flow quantities such as velocity, total pressure, and total temperature, additional equations can be employed to relate the stagnation and static properties to velocity. Except for the special case where there is an uniform profile across the stream tube, there is no unique value of velocity which will satisfy the three flow equations simultaneously. That is, substituting averaged flow quantities into the flow equations yields two prime quantities which are incorrect.

The problem can be approached by satisfying the continuity and momentum equations and taking the required compromise in the energy equation. This permits use of quantities which may be measured relatively accurately, such as flow and area. The type of averaging process used for the pressure and temperature profiles to obtain unique flow quantities must also be considered. Area weighted pressures and temperatures are often used since these appear to be most representative of one-dimensional values.

Another limitation is related to the use of convergent conical nozzles as a reference nozzle. The flow field at the exit of a convergent conical nozzle is not unequivocally defined even if the pressure ratio through the nozzle is above critical one-dimensionally. The sonic line starts at the end of the nozzle; however, the flow at the section at the end of the nozzle is subsonic. The sonic line is affected by the static pressure disturbances along the streamline that divides external and internal flow until the flow is completely supersonic. Such pressure in flight depends on the flight Mach number and airplane configuration. In the test cell such distribution depends on the mixing phenomena between external and internal flow. These phenomena are strongly affected by local conditions and cannot be defined completely by simple parameters. Fig. III.5 gives a comparison of the effective critical expansion ratio of purely conical nozzles versus nozzles angle, theoretically and experimentally. Therefore, in order to obtain consistent calibration, a nozzle having a small diverging region downstream of the throat should be of advantage for the definition of thrust; then the external conditions are not important. This problem is of special importance for bypass engines that discharge the two flows separately. In this case an incorrect representation of the nozzle flow for the bypass air affects the split between main flow and bypass flow. In this case it is important that the flow at the exit of a bypass engine be carefully analyzed and if required, correctly represented.

The method that has the least limitations is the method bases on the flange thrust definitions. In

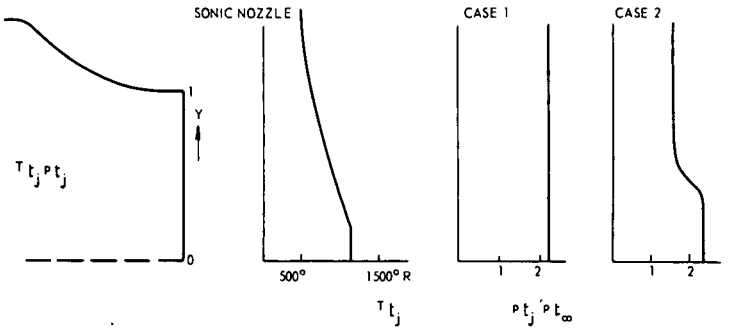

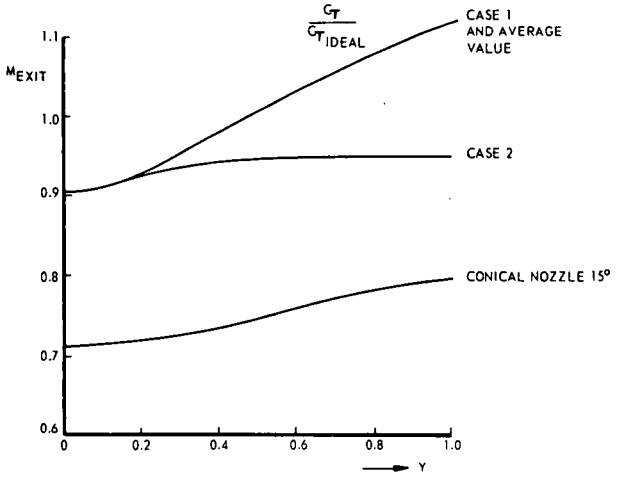

FIG. III. 3a MACH NUMBER DISTRIBUTION AT THE EXIT OF A NOZZLE FOR NON UNIFORM STAGNATION CONDITIONS.

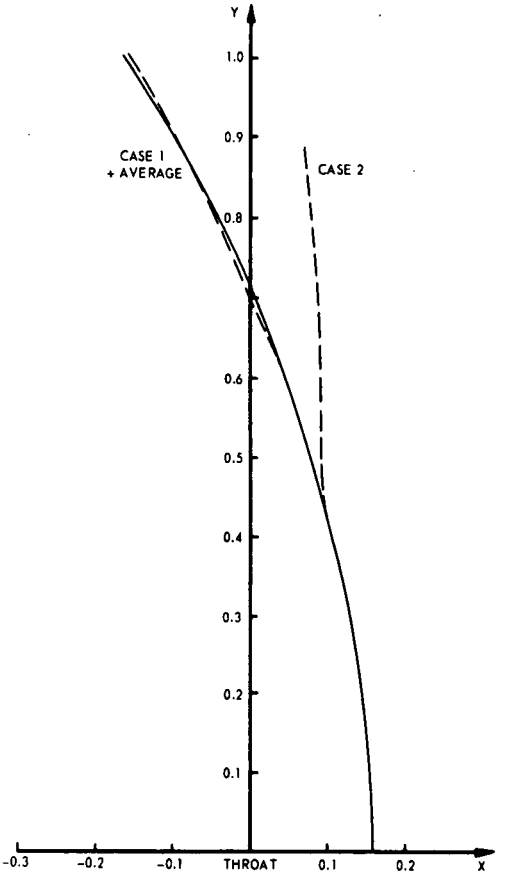

FIG. III. 3b SONIC LINE SHAPES.

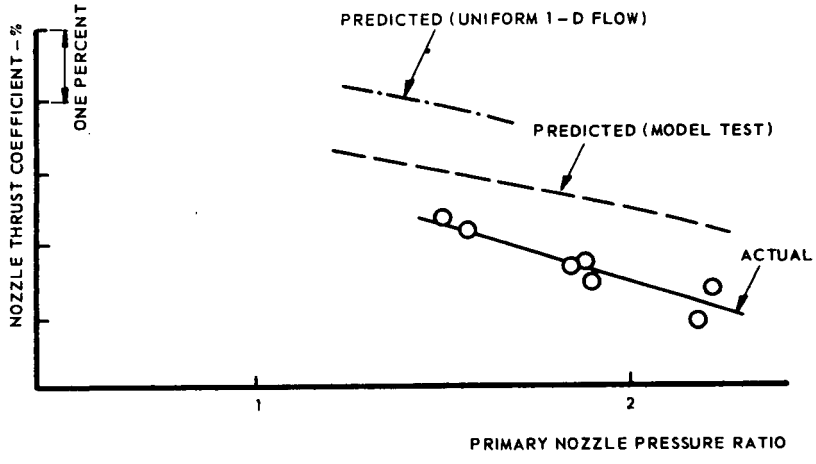

FIG. III. 4 COMPARISON OF THEORETICAL AND EXPERIMENTAL LOSSES IN A NOZZLE.

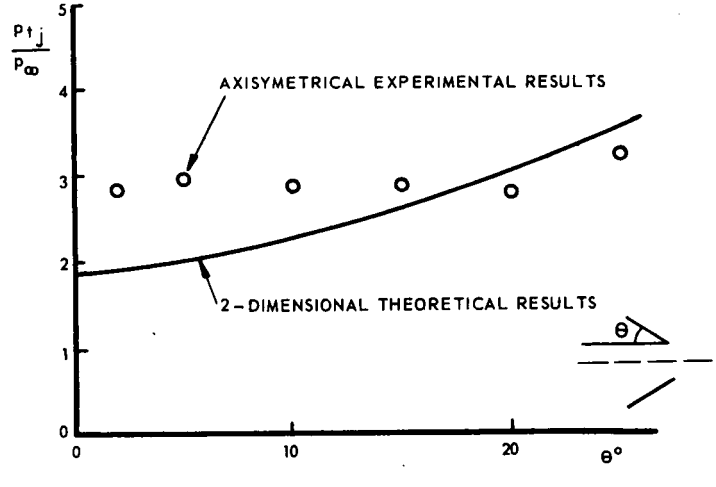

FIG. III. 5 CRITICAL EXPANSION RATIO VERSUS CONICAL ANGLE OF THE NOZZLE.

this case the flow field at the engine exit or nozzle entrance is surveyed yielding the complete flow properties that the traversing cross section. These quantities are input to a gasdynamic computer program, which iterates the three-dimensional variation of the required flow quantities along the nozzle length and integrates them at the exit plane to determine the gross thrust which can be compared with the measured scale gross thrust. Furthermore the internal pressure distribution along the nozzle length can be computed and compared with the measurements. If the computed and actual data agree within the expected accuracies, the program can be applied to other nozzle systems or geometrics, probably yielding accurate results. The computer program may be extended to account for the external flow field (installed thrust) and for incorporating secondary flows in ejector nozzles. However, much work should still be done to make those computer programs useful for actual gross thrust optimization which will heavily rely on empirical quantities. However, determination of the sonic line will be difficult with conical convergent nozzles which are at or just above the critical pressure ratio. In case of large by-pass, low fan pressure ratio, engines, which are currently located under wings of large transports, the pressure field into which the by-pass exhaust is very different from the far field static value. Therefore the fan exhaust sonic line location is influenced by this pressure field which will change the discharge coefficient and affect the fan mass flow. Since the engine net thrust is a strong function of the engine mass flow, information is needed on the degree the back end pressure field affects the engine performance.

3.4 CORRECTIONS

Three types of corrections for actual engine installation can be considered: namely, (a) Corrections during the engine evaluation phase, (b) Corrections due to differences between actual production engines and reference engines, and (c) Corrections due to installation.

If the engine performance is determined on a test bench minor corrections must be applied to account for the actual test conditions different from the desired or reference test conditions. The actual test conditions should be however within close tolerancies with the desired values in order to keep the applied corrections small. These corrections are applied to the actual (physical) air flow ($\dot{m}$) and for the reduced air flow ($\dot{m}\sqrt{\theta}/\delta$, where θ and δ are normalized values of the total temperature and pressure at the compressor face respectively), the fuel flow, gross thrust (which is affected by the nozzle pressure ratio, and fuel-air ratio) and computed ram drag.

These corrections must also be applied in order to determine the actual performance of production engines versus the performance of the reference engine. The engine performance as specified in the Engine Bulletin is based on average or minimum engines; the differences for the actual production engine performance can be of the order of $\pm$ 3 °/o or 0 to + 6 °/o respectively. The airframe manufacturer who installs the engines should be aware which performance is specified (minimum or average). This does not give important discrepancies in multiengine aircraft since from a statistical point of view performance very close to the average can be expected.

The corrections due to actual inlet air flow for the installed engine can be determined in two ways (analytical and experimental) and should consider both stationary and dynamic distortions (corrections due to incomplete inlet pressure recovery is automatically accounted for since the engine performance is defined in terms of the total pressure and temperature at the compressor face). In the analytical case the engine manufacturer should specify the variations versus a distortion parameter (see 2.3.3). These variations should concern gross thrust, surge margin and air flow - the latter for ram drag evaluation. This procedure is applicable for small and stationary distortions. For large distortions the procedure will be inadequate, particularly for supersonic inlets. In those cases the response of the engine to the inlet flow should be determined experimentally. For the stationary distortions screens of varying gage sizes and porosity and distortion plates are placed in the cell intake duct to simulate the spatial distortion characteristics as determined from wind tunnel inlet measurements, after appropriate corrections. Representation of the dynamic distortions actually occuring in flight is a difficult task as described in section 2.2.3.

The corrections which must be applied if the actual flight nozzle is different from the reference nozzle, at which the engine performance is specified, are treated in the previous section. The best procedure is to determine theoretically the variation in thrust coefficient for the various nozzle conditions taking into account losses due to nonuniformities in total pressure, total temperature, turbulence and swirl. However, these analyses are still far from complete, and corrections due to different nozzles including the influence of external flow must be obtained from experiment. Wind tunnel testing of nozzle systems will be treated in chapter IV.

The engine manufacturer gives in the Engine Bulletin curves of correction for auxiliary power and air bleeds. These corrections are deduced from theoretical cycle calculations or direct measurements and are usually rather accurate. For a direct measurement, accessories are mounted on the engine in the test cell (electrical generator, hydraulic pump). All air bleeds must be exhausted at right angle to the thrust axis.

The accuracy required for gross thrust predictions depends upon the ratio of net to gross thrust. For example for a supersonic transport in cruise flight,

$\frac{F_N}{X_g} \simeq 0.5$ and the accuracy in thrust measurement should be $\Delta X_g/X_g$ = 0.1 to 0.2 °/o for given values of ambient and stagnantion condition and engine r.p.m's. The obtainable accuracy depends upon test conditions and test cells; as an example for the net thrust, F_N, the mean figures of accuracy are:

$$\Delta F_N/F_N = \pm 0.5 \text{ °/o to } 1 \text{ °/o (sea level bench testing)}$$

$$\Delta F_N/F_N = \pm 1 \text{ to } 2 \text{ °/o (tests in an altitude test facility).}$$

3.5 BIBLIOGRAPHY

—	AGARDograph 103 "Aerodynamics of Power Plant Installation", October, 1965.
—	AGARD-CP-27 "Integration of Propulsion Systems in Airframes", 31st Meeting of AGARD Flight Mechanics Panel, 1966.
W. Beaulieu, R. Campbell and W. Burchan	Measurement of the XB-70 Propulsion Performance, Journal of Aircraft, Vol. 6, No. 4, July - August, 1969.

Development of a Satisfactory Method for Measuring In-Flight Thrust of Turbojet Aircraft- Gas Generator Method.
Flight Test T.M. 1-61 Naval Air Test Center (March 8, 1961).

T.W. Davidson — Measurement of Net Thrust in Flight.
Journal of Aircraft, Vol. 1, No. 3, May-June, 1964.

J.R. Montgomery — Engine Altitude Test Procedure.
Air Force Aero Propulsion Laboratory, Tech. Memo, APTP-TM-69-20, May 1969.

D.T. Poland and J.C. Schwanebeck — Turbofan Thrust Determination for the C-5A.
AIAA Paper, 70-611, 1970.

E.E. Turner and C.E. Chamblee — An Altitude Military Qualification Test of the J85-GE-13 Turbojet Engine.
AEDC-TDR-64-27, February, 1964.

A.A. Woodfield — Thrust Measurement in Flight.
The Requirements, Current Situation and Future Possibilities,
The Aeronautical Journal of the Royal Aeronautical Society, Vol. 74, April, 1970.

W.R. Hawthorne and W.T. Olson — Design and Performance of Gas Turbine Power Plants,
Princeton Series High Speed Aerodynamics and Jet Propulsion, Vol. XI
Princeton University Press, 1959.

O.E. Lancaster — Jet Propulsion Engines,
Princeton Series High Speed Aerodynamics and Jet Propulsion, Vol. XII.
Princeton University Press, 1959.

Advanced Aero Engine Testing.
AGARDograph 37, Pergamon Press, 1961.

IV EXHAUSTS

LIST OF SYMBOLS

a	speed of sound
A	area
c_p	specific heat at constant pressure
c_v	specific heat at constant volume
C_d	discharge coefficients
C_D	drag coefficient
C_L	lift coefficient
C_M	pitching moment coefficient
C_p	pressure coefficient
C_T	thrust coefficient
D	drag or diameter
F	measured, actual thrust
$\dot{m}$	mass flow
M	Mach number
p	pressure
r	radius
R	gas constant
Re	Reynolds number
S_i^o	entropy of species i
T	temperature
v	velocity
x_i	mole fraction of species i
X_{id}	ideal, isentropic thrust
α	angle of incidence
β	angle of yaw or boattail angle
γ	ratio of specific heats, isentropic exponent
δ	boundary layer thickness
ρ	density

SUBSCRIPTS

AB	afterbody
b	base
β	boattail
ex	exhaust
i	entering fluid
inst	installed
int	interference
j	jet
ℓ	local
m	model
n	nozzle
ref	reference
s	secondary
st	static
t	total, rerservoir conditions
∞	undisturbed infinity

If the airframe manufacturer has chosen an engine for his aircraft design he is in fact free to choose the nozzle system best suitable for the required mission. He can make a choice between ejector nozzles, variable flap ejector nozzles, blow-in-door ejector nozzles, iris nozzles, plug nozzles, short convergent nozzles or two dimensional variable throat nozzles. In this chapter no emphasis will be given to the relative performance and short comings of various nozzle designs under certain conditions, but the attention will be directed to the methods used to predict the nozzle performance from wind tunnel measurements and the methods used to determine jet interference effects at transonic speeds. At transonic speeds the nozzle drag and afterbody drag is usually maximum, therefore critical evaluation of the jet effects in wind tunnels at these speed range is required. The flight conditions to which the aircraft can be subjected to and which should be tested transonically are (a) cruise, (b) transonic acceleration, (c) transonic deceleration, and (d) high-g manoeuvre. These conditions yield various values to the nozzle area ratio, temperature ratio and pressure ratio. Fig. IV.1 gives typical exhaust conditions at transonic speeds; other engines give different envelopes.

As indicated in fig. I.3 and described in chapter I the complete or aeroforce model tests are completed by a special afterbody and jet interference tests in the transonic wind tunnel as is done with special inlet models. If optimum nozzle-afterbody matching is not achieved a considerable penalty on aircraft performance may result, as had been the case in many instances in the past. The actual afterbody drag, may be as large as 20 °/o to 40 °/o of the complete aircraft drag. Therefore most attention of afterbody-nozzle tests at transonic speeds concerns the nozzle gross thrust minus the nozzle and afterbody drag. Fig. IV.2 gives a general impression how afterbody models complete the results of aeroforce models.

As indicated before a large variety of nozzle systems exists now-a-days, each having its particular features. Fig. IV.3 gives a survey of various designs, since in this chapter reference will be made many times to a particular nozzle system. The fixed convergent nozzle is used with airplanes for subsonic flight, such as with civil transports, only without thrust augmentation by afterburning. The ejector nozzles might give thrust augmentation due to the ejector effect, the efficiency of this augmentation has generally been disappointing however. The secondary flow provides for the required cooling of the nozzle leaves. Ejector nozzles are used in early fighter type aircraft. The introduction of the fan and bypass engines made the nozzle design easier with respect to cooling since sufficient cooling air from the fan at the same pressure ratio as the turbine flow, came available which can be ducted to the nozzle, making the other nozzle designs possible. However for optimum use, the fan engines ask for larger nozzle area variations with afterburning. Hence in the past literature most attention was paid to the ejector nozzle installation requiring secondary flows, whereas in the recent literature more experiments are described concerning the other nozzle systems, particularly the iris and plug nozzles. See for further information on nozzles Ref. H18, C23, C24, G2, G4, M12, for example.*

Before initiating nozzle and afterbody tests with or without jet simulation in the wind tunnel, questions must be answered first concerning the variables involved related the nozzle conditions. Fig.IV-4 gives a review of these variables and their possible values or features. After the latter have been established the next step is to define which jet and nozzle parameters should be simulated in the wind tunnel experiments. Usually a compromise is found between what is desirable and what is feasible in practice. From this part on the wind tunnel model can be designed based on local possibilities and on past experience.

The general bibliography at the end of this chapter may be of assistance in establishing the wind tunnel exhaust experiment not only for transonic speeds, but also for the other speed regimes. This bibliography follows a nozzle and jet parameter code similar to that of Fig. IV.4.

In this chapter the jet parameters will be briefly described and it will be indicated as far as possible when these parameters should be simulated in the wind tunnel at transonic speeds. Further the various testing schemes and techniques as used will be described both for the thrust-drag assessment and other jet interference problems.

4.1 ENGINE GROSS THRUST MINUS DRAG AT TRANSONIC SPEEDS

4.1.1 REQUIRED ACCURACY

The required accuracy for the thrust-drag measurements should be compatible with that obtained for the drag (i.e. net thrust) of the basic airframe. This accuracy required for the gross thrust measurement depends on the ratio of the net to gross thrust, which in general will be a function of the engine bypass ratio. The following set of values can be regarded as typical

	Subsonic transport	Fighters	Supersonic transport
Cruise C_D	0,023	0,030	0,018
Accuracy of cruise drag	± 0,0001	± 0,0003	± 0,0005
°/o " " " "	± 0,45	± 1,0	± 0,3
Average $\frac{\text{gross thrust}}{\text{net thrust}}$	3	2,5	2,5
Required °/o gross thrust acc.	± 0,15	± 0,4	± 0,12

This survey shows that an accuracy of better than ± 1/2 °/o of the cruise of critical transonic gross thrust value is desired. Achieved accuracy is difficult to assess because overall accuracy includes the combination of many instruments such as force balances, pressure transducers, thermocouples and mass flow meters, in addition to wind tunnel speed and model attitude indicators. Each model test apparatus presents individual problems in sizing, restricted internal space, pressure tares, metric break seal restraint, thermal expansion, clearances and other items which make any general statement on achievable accuracy inappropriate.

* The Reference code follows the General Bibliography at the end of this chapter.

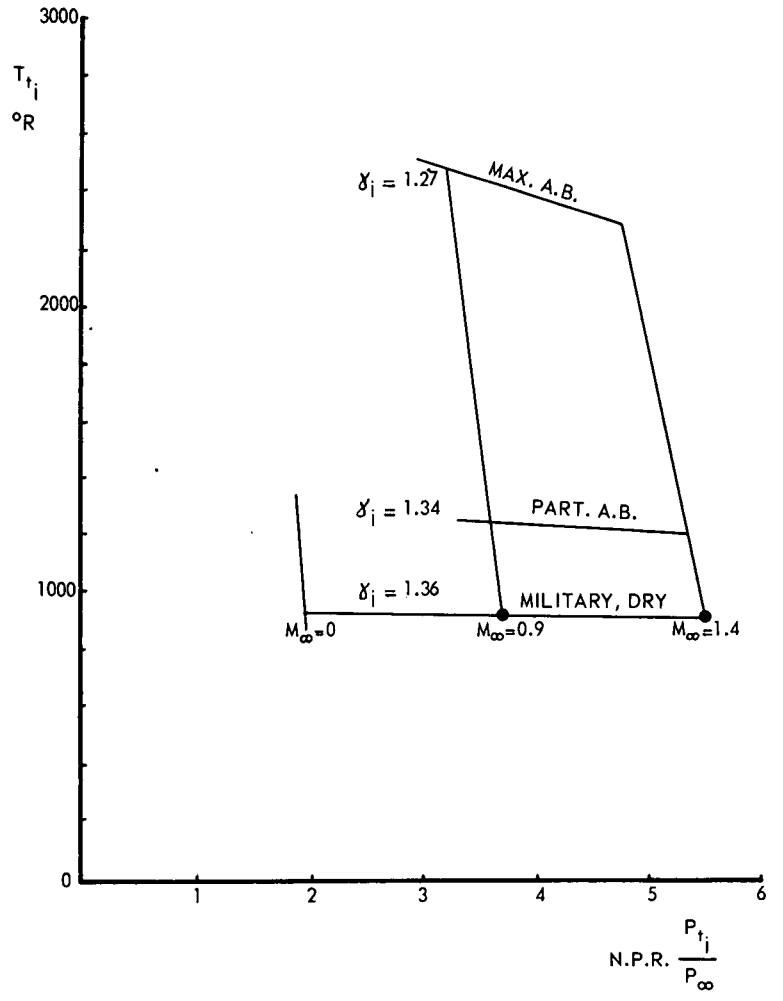

FIG. IV. 1 TYPICAL TRANSONIC EXHAUST CONDITIONS
(γ_j AT STAGNATION CONDITIONS)

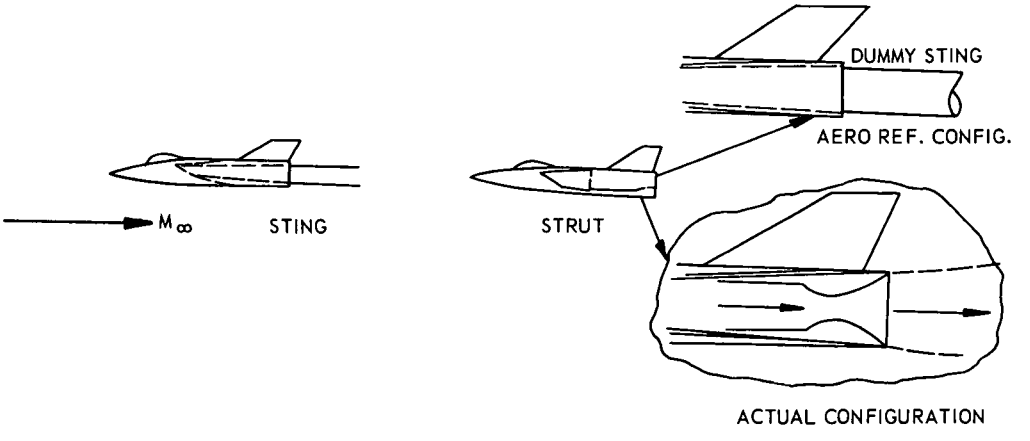

AERO FORCE MODEL
- FLOW – THROUGH NACELLE
- CLOSURE LINES MODIFIED BY STING
- DATA FOR A RANGE OF α & β

NOZZLE AFTERBODY MODEL
- STRUT MOUNTED
- SIMULATES JET EFFECTS
- MEASURES DRAG SEPARATE FROM THRUST (IF POSSIBLE)

INSTALLED NOZZLE DRAG = DRAG CONF. – DRAG AERO REF. CONF.

FIG. IV. 2 NOZZLE / AFTERBODY BOOKKEEPING

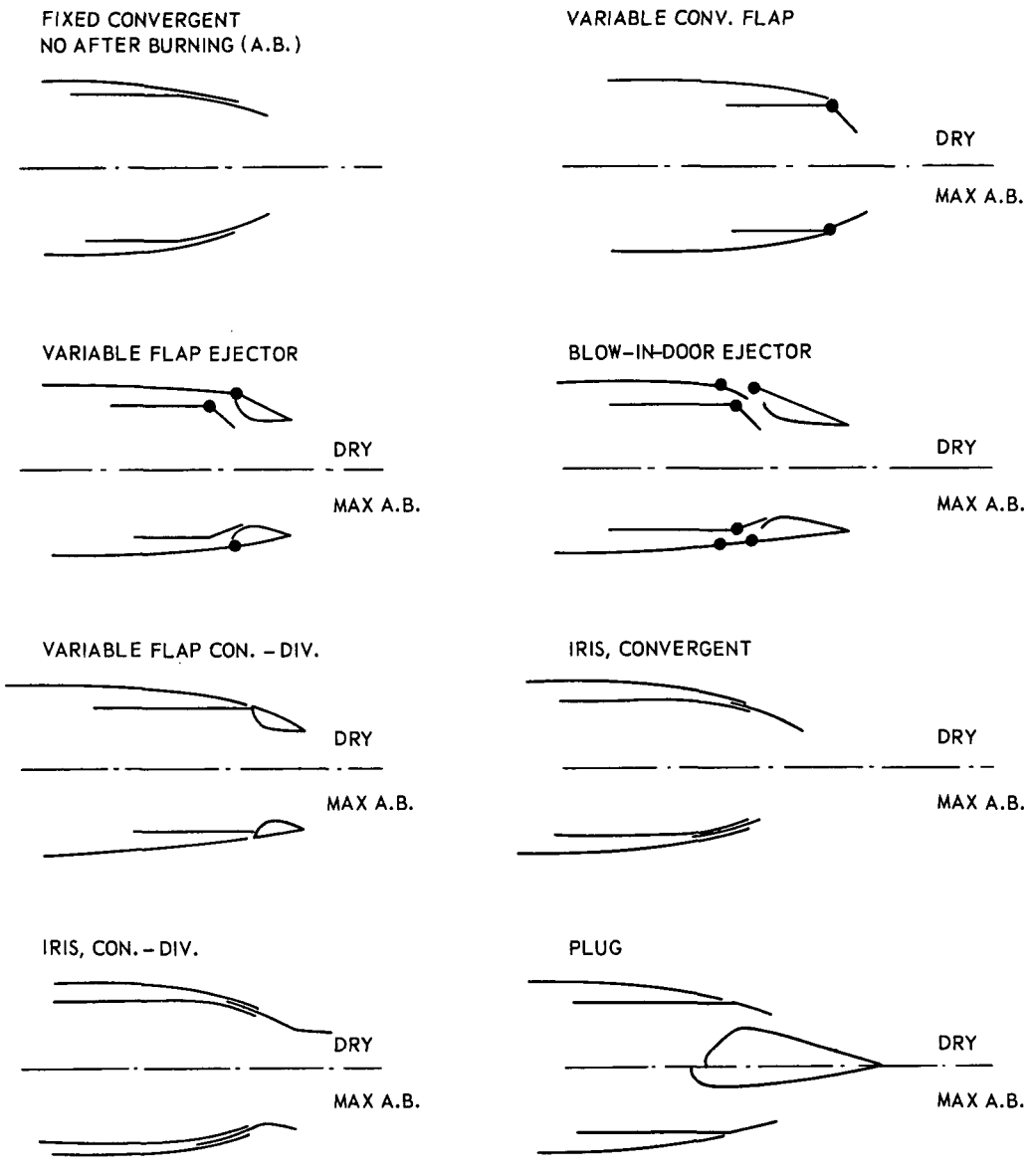

FIG. IV. 3 VARIOUS NOZZLE DESIGNS, SCHEMATIC

VARIABLE	POSSIBLE VALUES OR FEATURE
MAINSTREAM MACH NUMBER	SUBSONIC – TRANSONIC – SUPERSONIC – HYPERSONIC
JET MACH NUMBER	SUBSONIC – TRANSONIC – SUPERSONIC – HYPERSONIC
NOZZLE PRESSURE RATIO	OVEREXPANDED – OPTIMUM – UNDEREXPANDED
DIRECTION OF JET	PARALLEL – ACUTE ANGLE – NORMAL
NUMBER OF EXIT PORTS	SINGLE – DUAL – MULTIPLE
SPACING OF MULTIPLE JETS	NARROW – ONE JET DIAMETER – WIDE
NUMBER OF NOZZLE STREAMS	PRIMARY – PRIMARY & SECONDARY – PRIMARY, SECONDARY & TERTIARY
GEOMETRY OF AFTERBODY	AXISYMMETRIC – NONAXISYMMETRIC
SHAPE OF AFTERBODY	BLUNT BASE – SMOOTH CONTOUR
BOUNDARY LAYER, INTERNAL	LAMINAR – TURBULENT
BOUNDARY LAYER, EXTERNAL	LAMINAR – TURBULENT
RATIO δ^* TO JET DIAMETER	(SMOOTH VARIATION OF THIS PARAMETER)
SENSITIVITY TO EXTERNAL FLOW	NONE – INFLUENCED

FIG. IV. 4 VARIABLES RELATED TO EXHAUSTS

4.1.2 ISOLATED NOZZLE TESTS VERSUS COMPLETE MODEL NOZZLE TESTS

As with inlet tests the question arises as to the extent the external flow field should be simulated for performing reliable nozzle measurements. Usually the answer involves two possibilities. The first possibility is to simulate the external flow field as good as possible by testing the afterbody and nozzle together with the complete aircraft representation for which the inlet is usually completely faired and for which the model support system causes little interference at the exhaust. The second possibility is to simulate only the afterbody geometry and determine from the relative differences the nozzle-afterbody performance. The latter test procedure is usually applied to determine nozzle performances in transonic flows regardless of aircraft fore-body shape. It is performed in the early stage of aircraft development in order to obtain an early estimate of the nozzle-afterbody performance. The complete model nozzle test is usually accomplished for final checks.

It is obvious that both test procedures have advantages and limitations which will be listed below.

For isolated nozzle tests.

(a) For a given size test facility, isolated nozzle tests permit larger scale models to be used with correspondingly higher Reynold's numbers.
(b) Due to a possible reduced length of the forebody, the relative external boundary layer thickness at the nozzle can be properly scaled with respect to full scale.
(c) Higher degree of accuracy as complete model nozzle tests.
(d) Larger models make the design easier and allow more instrumentation (pressures) to be included and secondary airflow systems are more easily accomodated.
(e) More exact detailing of the nozzle shaping is possible, i.e., roughness of variable geometry leaves and joints can be simulated and nozzle base thickness can be scaled.
(f) Isolated nozzle tests are better for basic investigations, e.g., effect of jet temperature ratio, specific heat ratio, internal flow distortions.
(g) Isolated nozzle investigations are a necessary step in the development of new exhaust system concepts. Parametric studies can be conducted at less cost on external geometric variables, internal performance and initial thrust reverser and noise suppressor designs.
(h) The isolated nozzle test apparatus may be used by engine manufacturers to provide the baseline for the nozzle "uninstalled performance" presented in his engine performance deck.
(i) The pressure and force data obtained from isolated data can be used to substantiate or improve theoretical and empirical calculation methods.
(j) Disadvantages include a cylindrical approach section to the nozzle (near free stream flow conditions) which hardly ever occurs in practice.
(k) Airframe installation effects can be very large so that a redesign of the nozzle may be required to obtain the desired installed performance.
(l) Because of the wide variety of nozzle locations possible in an aircraft design, mutual nozzle-airframe interactions cannot be predicted from isolated nozzle tests.
(m) In many large wind tunnel facilities, it is difficult to obtain the true isolated performance of the nozzle since the model requires support structure and ducting to supply the exhaust gas.

For complete model nozzle tests.

(a) Complete model tests provide better external flow simulation and provide a more exact duplication of the nozzle environment that will exist on the full scale airplane (generally except for boundary layer thickness).
(b) Complete model tests are the only means of predicting installed nozzle performance since mutual airframe-nozzle interference exists and forebody-wing influences on the afterbody-nozzle configuration are simulated.
(c) Installation of the isolated nozzle in an airframe may produce either favourable or unfavourable effects depending on the type of nozzle and the flight speed. Results such as these are strongly dependent on the overall aircraft design.
(d) Complete model investigations of generalized research configurations with exhaust and slipstream simulation permit evaluation of effects on aircraft aerodynamics and installed nozzle performance such as exhaust nozzle axial and lateral location, effect of afterbody angle to nozzle, engine interfairing shape, and effects of empennage on nozzle performance.
(e) The additional effect of the exhaust plumes on control surface effectiveness and loading can be determined.
(f) Plume interference on adjacent surfaces may be evaluated including both pressure and temperature increments if hot jet exhausts are employed.
(g) Flow visualization studies (e.g., shadowgraph or schlieren methods) can be conducted on the complete model to aid in theanalysis of results.
(h) For a given size facility the complete model nozzle size will be much smaller than the isolated nozzle, making detailed scaling more difficult (lower Reynolds number etc.).
(i) Complete models generally require more instrumentation, including perhaps more than one strain gauge balance, pressure instrumentation on the afterbody and other portions as well as the nozzle, requiring careful design to provide the propulsion simulation without interference of the measuring instruments of the metric section (fouling).
(j) Space requirements in a complete model make the simulation of secondary and tertiary flows in the nozzle or base regions more difficult.
(k) Model size is limited by the test section available length and cross section at the most critical Mach operating condition and also by the propulsion system flow capacity.
(l) Support system interference must be evaluated for the complete model in order not to invalidate all of portions of the results (Effect at all Mach numbers).

4.1.3 JET SIMULATION PARAMETERS AT TRANSONIC SPEEDS

The degree to which the jet should be simulated in the wind tunnel depends primarily on the nozzle design used, on the type of installation and on the required degree of accuracy of nozzle performance assessment. Different from the inlet performance evaluation, the nozzle is operating in a highly viscous flow field as it is generated by the forebody, wings, tail planes and/or pylons. This makes the flow field computation complicated and only a reasonable degree of succes of predicting the nozzle flow field environment can be achieved for smooth forebodies, for example podded engine installations. Fig. IV.5a and b give indications of the three dimensional flow environment for nozzles in a typical installation and how the viscous actual flow field differs from the ideal, inviscid field.

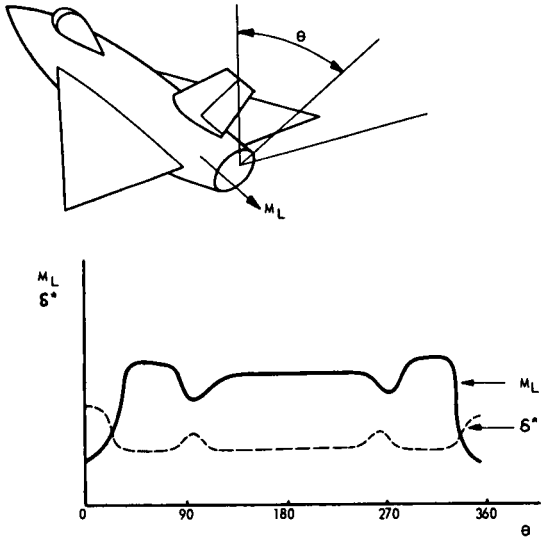

FIG. IV. 5a THREE-DIMENSIONAL FLOW ENVIRONMENT FOR NOZZLE

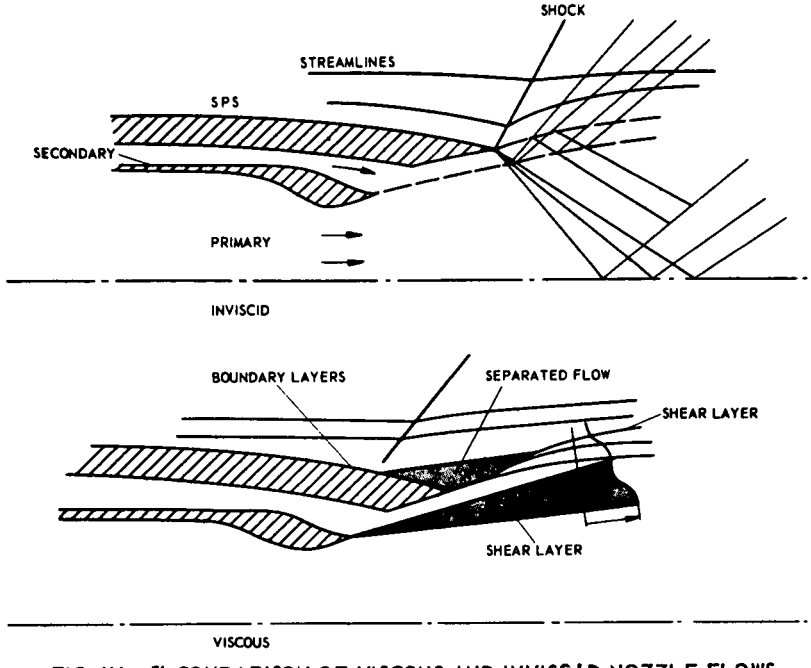

FIG. IV. 5b COMPARISON OF VISCOUS AND INVISCID NOZZLE FLOWS

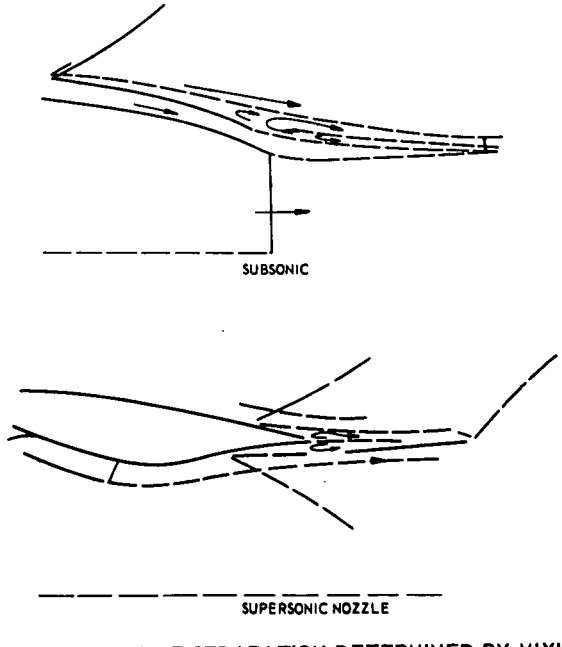

FIG. IV. 6 POINTS OF SEPARATION DETERMINED BY MIXING

In common with inlet tests, the nozzle tests in the wind tunnel are performed at reduced scale and hence, usually at reduced Reynolds number. The degree of scaling depends on the available tunnel and testing rigs, as well as on the degree of external flow field simulation. Large scales can be obtained with isolated nozzle tests omitting the external environment partially or completely, whereas complete external flow field simulation requires small scales. In any event scaling is required necessitating many scaling laws. Ref. P-2 gives an excellent review of these scaling rules for inviscid flows; however, it does not indicate the importance of the particular rules. Furthermore, in general little is known about the similarity laws for the mixing phenomenon as it effects the flow at the exhaust.

INTERNAL THRUST COEFFICIENT

As is indicated in chapter III the static thrust coefficient of a particular nozzle depends primarily on the nozzle pressure ratio and ratio of specific heats as well as on the total temperature and total pressure distortion upstream of the nozzle. In the case of a conical nozzle C_T depends also on the jet boundary contour downstream of the nozzle edge. As is seen in figure IV.3, conical convergent nozzles are frequently used requiring proper simulation of mixing at the downstream boundary between the jet and the external flow in case of a simple convergent nozzle, and between the primary jet and secondary flow in case of ejector nozzles. However little is known about the actual influence of mixing downstream of a (primary) nozzle on the nozzle thrust and discharge coefficients; more analytical and experimental work is needed. The rate of mixing depends on the ratio of the mass density flows (ρv) on both sides of the mixing boundary and on the initial upstream turbulence. In the case of ejector nozzles this means also that the secondary mass flow must be simulated. This simulation is hard to achievefor blow-in-door ejectors since the secondary mass flow depends primarily on the outer boundary layer and flow field conditions. To a lesser extent this can also be said for plug nozzles.

In present wind tunnel nozzle test rigs the internal flow distortions and turbulence are not simulated. More information is needed on when (at which nozzle types and installations) these distortions can be omitted in the nozzle performance assessment, when analytical or experimental corrections can be used (and how) and when these distortions should be simulated in the wind tunnel. Information is needed on the applicability of specific scaling laws.

For nozzles with internal supersonic expansion the ratio of specific heats has an influence on the characteristic lines, which means, for example, that for an ejector nozzle the initial inclination angle of the primary jet is different if γ_j is not simulated. The primary jet contour can be simulated by adjusting the nozzle pressure ratio, resulting in an incorrect simulation of jet momentum. Therefore γ_j should be simulated as close as possible.

EXTERNAL NOZZLE DRAG, BASE DRAG, BOAT TAIL DRAG

These drag terms depend on the jet properties, the external inviscid flow and on the external boundary layer condition at a given free stream Mach number and angle of attack. If the outer flow separates, as it often does near the nozzle exit, the separation point and pressure level in the separated region is fully determined by the viscous interaction between the jet and the ambient flow and hence on the jet boundary (shape) and mixing process (see fig. IV.6). The inviscid jet shape is fully determined by the nozzle pressure ratio $p_j^*/p_\infty, \gamma_j$ and Mach number at the exit M_j. The jet shape (initial inclination angle)is approximately constant for convergent nozzles if $(p_j^*/p_\infty)^{1/\gamma_j}$ = constant. This relation is given in figure IV.7 for $M_j = 1$ which shows that p_j^*/p_∞ must be appr.10 °/o higher if a jet with $\gamma_j = 1{,}3$ is simulated with cold air ($\gamma = 1{,}4$). (If the n.p.r. is less, the corrections become relatively smaller). The base pressure or the pressure in the separated region is a function among others of the jet momentum. This quantity is determined by the nozzle pressure ratio and γ_j also. Two limiting cases can be considered; jet momentum per unit area at the exit and jet momentum per unit area along the jet boundary (fully expanded). The first yields $(p_j^*/p_\infty)\gamma_j$ = constant, the second case gives $M^2_{\text{boundary}}\ \gamma_j$ is constant. Both criteria are shown in fig. IV.7 also. It is concluded from this figure that correction in p_j^*/p_∞ for correct momentum simulation is opposite from correct jet shape simulation if $\gamma_{j\text{model}} \neq \gamma_{j\text{turbo-jet}}$. Few experiments are known which verify a base pressure dependence on γ_j, but from the above analysis a γ_j dependence is expected, which means that γ_j should be simulated as close as possible.

The mixing process along the jet boundary is determined by the jet properties at the boundary and by the external boundary layer characteristics at the nozzle exit. The jet properties depend on the nozzle used, particularly on the cooling system and the secondary air flow, if precent (see fig. IV.6). If smooth uniform jet flows are assumed, the mixing parameter is $(\rho v)_j / (\rho v)_\infty$ (Ref. Z1, S7, S9). This mixing process alters the effective jet boundary shape so that the inviscid flow is affected, particularly at transonic speeds. At a given nozzle pressure ratio the mixing parameter is primarily dependent on $R_j T_{tj} / R_\infty T_{t\infty}$.

Some experiments are available on the influence of the jet temperature on base pressure using hot air (so $\gamma \simeq 1{,}4$). Figure IV.8 is deduced from Ref. M10 yielding base pressure (C_{p_b}), base drag (C_{D_b}) and boat tail drag (C_{D_β}) for a typical afterbody shape at $M_\infty = 0{,}9$ versus the total jet pressure P_{t_j}. It is clearly seen that the afterbody drag ($C_{D_\beta} + C_{D_b}$) is some 20 °/o decreased if a hot jet is used for jet simulation instead of a cold jet. A similar conclusion is reached in Ref. R8, where it is found that the base drag at a temperature ratio of 2,8 is 25 °/o less than it is with an unheated jet at $M_\infty = 0{,}9$, utilizing a propane-air combustion system with a convergent nozzle at a pressure ratio of 2.

The external boundary layer characteristics which have an large effect on the mixing process, also determine the degree the jet and mixing is felt upstream from the nozzle exit. One of the more important non-dimensional parameters is the boundary layer thickness (δ) relative to a reference nozzle radius (r_n) (or diameter). The increase of δ/r_n, as is the case for testing a complete model at reduced Reynolds number, implies that the nozzle is immersed in a larger boundary layer field, making the viscous effects larger. An example of how this parameter affects the total afterbody and nozzle drag is shown in fig. IV.8b for two nozzle systems (Ref. M13). It is seen that the effect of the boundary layer depends largely on the nozzle type.

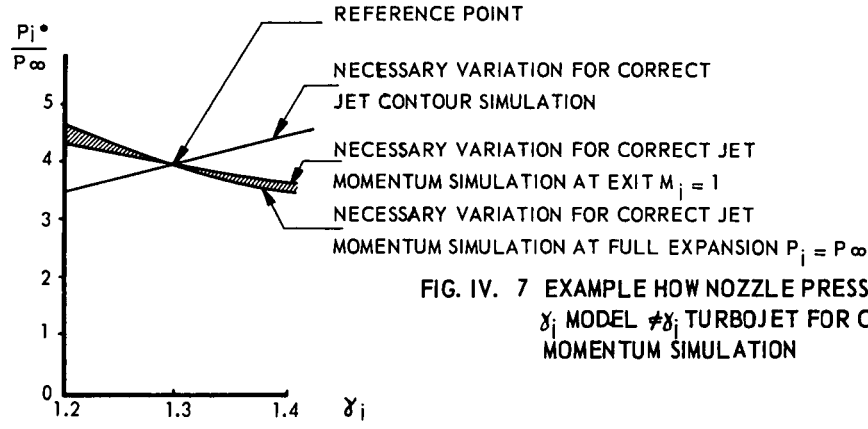

FIG. IV. 7 EXAMPLE HOW NOZZLE PRESSURE RATIO SHOULD BE VARIED IF γ_j MODEL $\neq \gamma_j$ TURBOJET FOR CORRECT JET CONTOUR OR JET MOMENTUM SIMULATION

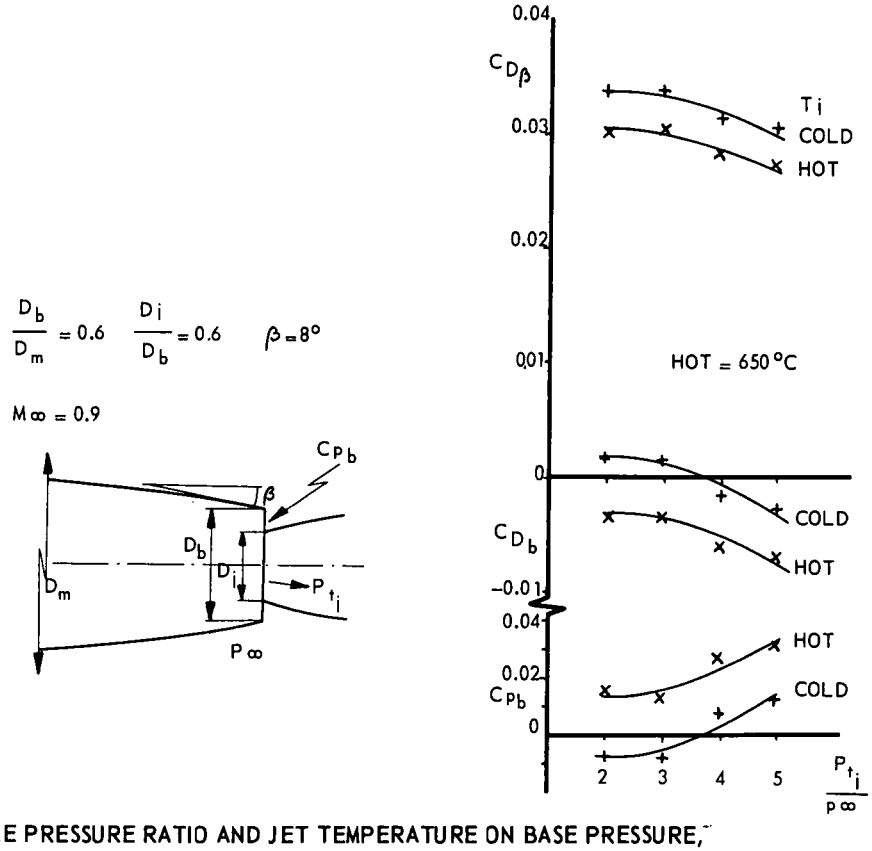

FIG. IV. 8a EFFECT OF NOZZLE PRESSURE RATIO AND JET TEMPERATURE ON BASE PRESSURE, BASE DRAG AND BOATTAIL DRAG

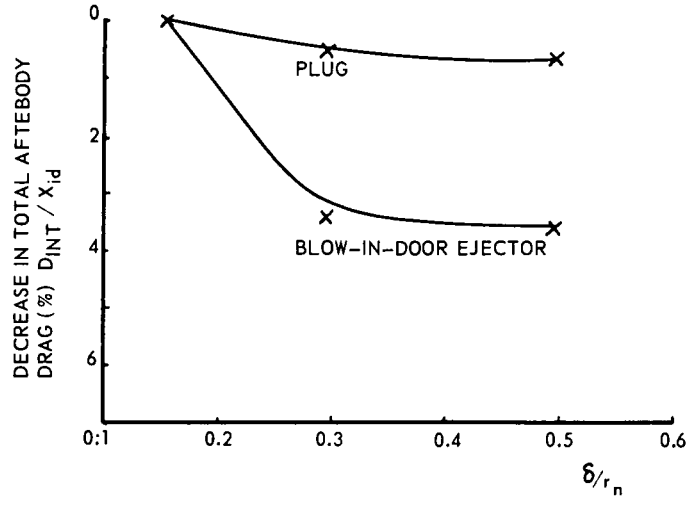

FIG. IV. 8b EFFECT OF BOUNDARY LAYER THICKNESS ON TOTAL INTERFERENCE DRAG

Another quantity that largely affects the base pressure is the amount of bleed or leakage through the nozzle leaves. Fig. IV.8c gives this effect as experienced and computed for a blunt base at supersonic speeds (Ref. C23).

In Ref. R5 large unsteady pressures are observed on the base of a cylindrical model due to the presence of a central jet (fig. IV.9). Though the steady component is already effected by the jet temperature, the average unsteady part must be strongly depended on jet velocity and therefore on temperature. This is concluded by the authors of Ref. R5 and hot jet simulation in wind tunnels is recommended for similar cases.

It should be noted that turbulent jet mixing is little influenced by Reynolds number effects since the characteristic mixing length is in first approximation proportional to the characteristic jet dimensions.

Summarizing the following can be concluded regarding the degree of jet simulation in transonic wind tunnels.

(a) For nozzle thrust coefficient assessment (internal and static) the geometry, nozzle pressure ratio and ratio of specific heats should be simulated as first parameters. This is also true for the secondary mass flow in case of ejector nozzles or nozzles with substantial cooling air. The secondary parameters are the total temperature, and internal flow distortions, also swirl, upstream of the nozzle.

(b) For almost inviscid jets where mixing has a secondary importance, the wave structure and stream line shapes, that is the initial inclination angle and wave reflection coefficients (Ref. F3) (both determining the plume shape), should be simulated regarding the influence on the external flow field. These parameters are determined by p_{t_j}/p_∞ , γ_j, M_j as well as by the free stream condition. The jet temperature yields a correction on the jet boundary due to mixing in which case the nozzle temperature ratio ($R_j T_{tj}/R_\infty T_{t_\infty}$) should be simulated as well.(If the jet becomes hotter, its suction action becomes less).

(c) In cases where jet mixing plays an important role on the external flow field, besides the nozzle pressure ratio nozzle, geometry, ratio of specific heats, the nozzle temperature ratio, secondary flows (if present), external boundary layer thickness and jet distortion should be simulated also. Scale effects due to turbulent mixing can be ignored.

(d) In case of unsteady jet phenomena, the jet temperature (or speed of sound) is a primary parameter besides the primary inviscid jet parameters. Also it may be very important to simulate the structural elastic constants.

4.1.4 WIND TUNNEL TESTING SCHEMES

The wind tunnel testing scheme for nozzle-afterbody performance assessment that one chooses to employ for a particular aircraft design depends primarily on the available test rigs and systems in the wind tunnel and on the stage of aerodynamic testing. In recent years the main transonic wind tunnel facilities have been equiped to perform powered nozzle testing. Usually each laboratory designed its own particular system that is flexible enough to test a variety of nozzle-afterbody combinations. These test rig designs were based on jet and nozzle parameters which were thought to be of first importance, as discussed in the previous section, on the other technical requirements, as will be discussed in the next section, and on the apparatus achievable in the wind tunnel within practical limits.

The next discussion concerns primarily the engine-airframe integrated systems (e.g. fighters). Similar techniques can be used for podded subsonic installations, but in those cases the jet influence on the wing or aftfuselage is of equal importance.

The nozzle-afterbody performance must be determined from wind tunnel measurements starting from aeroforce model drag data and the engine gross static thrust. The actual installed afterbody performance can be expressed as the difference between the installed gross engine thrust (F_{inst}) minus the installed afterbody drag ($D_{AB_{inst}}$). This quantity $(F-D_{AB})_{inst}$ should be as large as possible for maximum performance. It depends on the external parameters, such as Mach number (M_∞) and angle of attack (α), as well as on internal parameters such as engine r.p.m., degree of afterburning and exhaust area ratio. The engine parameters can be expressed in terms of the nozzle pressure ratio, temperature ratio, ratio of specific heats, geometry, etc. The engine static test bench gross thrust can be considered as the reference thrust F_{ref}, F_{st} (X_g in chapter III). The reference afterbody drag (D_{ABref}) can be determined by a model similar to the aeroforce model but with the afterbody only being metric. The afterbody drag is the drag on those parts of the afterbody which can be affected by the presence of the exhausting jet(s), such as inter- and outer-fairings, tailplanes, fuselage boat tail and base (if present). The metric line between the forebody and afterbody is generally somewhat halfway between the inlets and exhausts. Usually the drag on the external nozzle parts (D_n) is not included in the afterbody drag but is added to the nozzle losses. The external flow can also effect the internal nozzle thrust resulting in a thrust loss (ΔF_{inst}), also called the internal nozzle drag due to external flow. The interference drag is now generally defined as the difference between the net reference performance and the net installed performance of the nozzle and afterbody combination, that is

$$D_{int} = (F - D_{AB})_{ref} - (F - D_{AB})_{inst} \text{ or}$$

$$D_{int} = \Delta F_{int} + D_n + \Delta D_{AB} ,$$

since $\Delta F_{int} + D_n = F_{ref} - F_{inst}$

and $\Delta D_{AB} = D_{AB_{inst}} - D_{AB_{ref}}$.

Sometimes $F_{ref} - D_{int} \equiv F_{ref} - (\Delta F_{int} + D_n + \Delta D_{AB})$ is called the equivalent thrust.

FIG. IV. 8c EFFECT OF MASS INJECTION AT THE BASE ON THE BASE PRESSURE

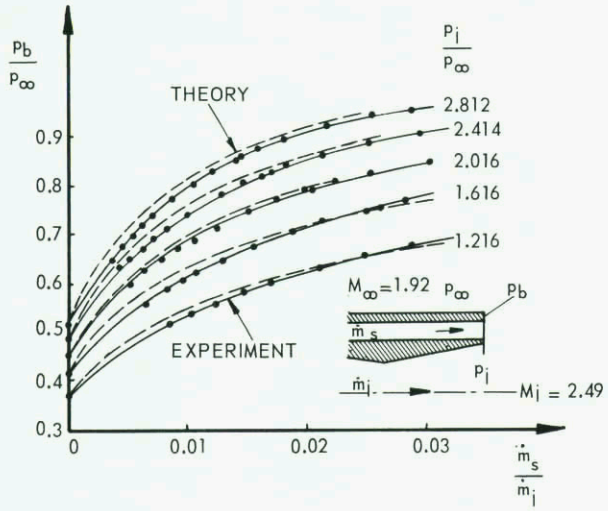

FIG. IV. 9 TIME AVERAGE AND UNSTEADY PRESSURES ON THE BASE OF A BLUFF AFTERBODY WITH JET SIMULATION

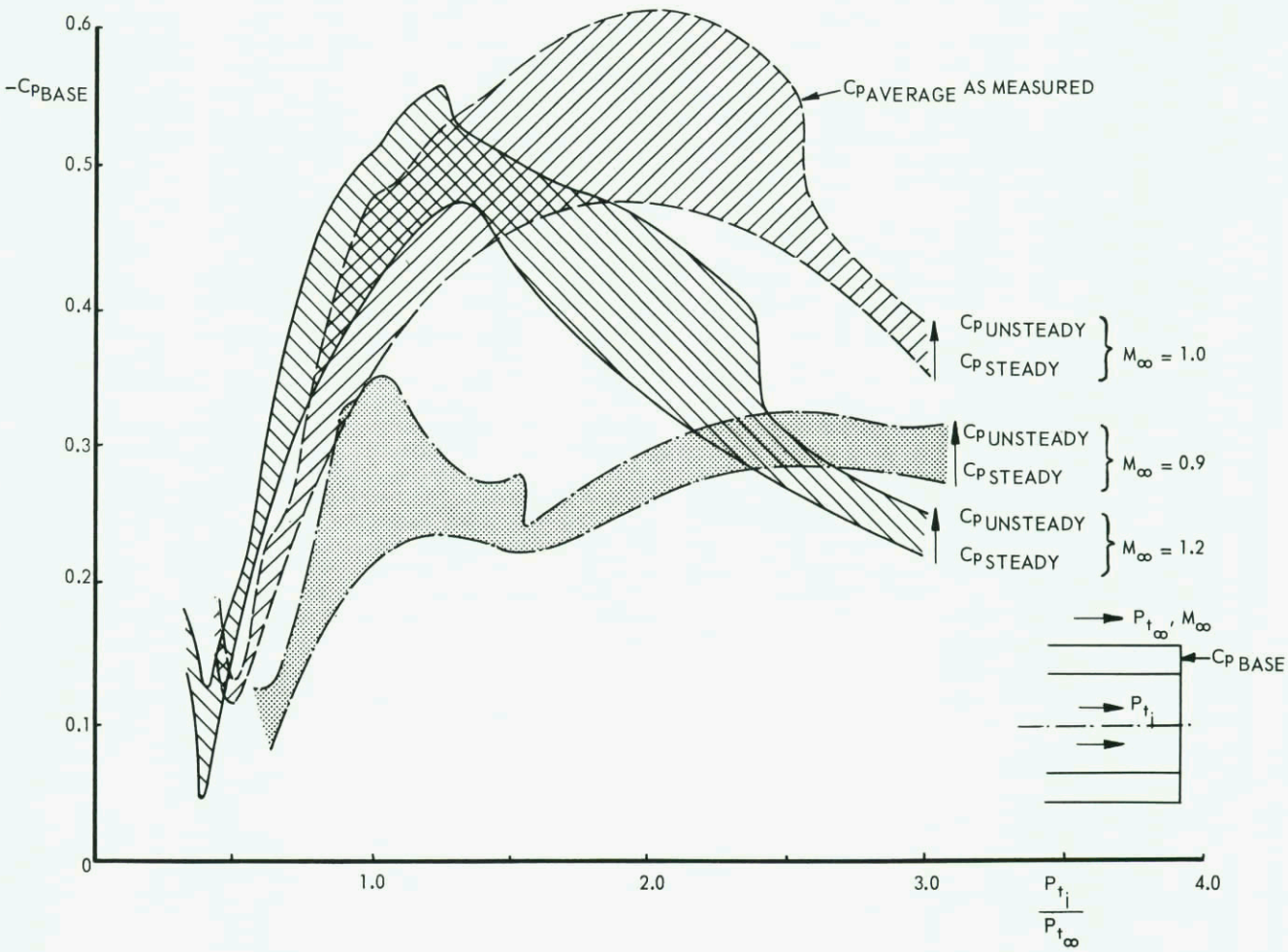

Overall installed performance (thrust minus drag) is:

$$(F\text{-}D)_{inst} = F_{ref} - D_{ref} - D_{int} .$$

This quantity should have a maximum value.
In an ideal testing scheme ΔF_{int}, D_n and ΔD_{AB} should be determined independently, sothat the optimization ($\min.D_{int}$) can be performed efficiently.

Fig. IV.10 illustrates the usual bookkeeping procedure for integrated nozzle-airframe systems where at the aeroforce model is supported by a sting located at the nozzles. Before the actual powered afterbody tests are performed an intermediate step is done at which the model is split into a forebody and an afterbody, the latter only being metric. The forebody is grounded and may be supported by a separate sting under the fuselage or at the wing tips. Also a half model support may be used if the exhausts are sufficiently free from the tunnel walls. For these tests the inlet is closed.

In fig. IV.10 the afterbody tests are performed with the complete exhaust model. However these tests can also be performed with an isolated nozzle test, if the powered test of the geometric similar afterbody is preceeded by an afterbody test. For this test the afterbody must have the same shape as the aeroforce model and must use a non-metric dummy sting at the location of the aeroforce model sting. This test yields the new reference afterbody drag $D_{AB_{ref}}$ for the actual powered afterbody/nozzle tests. The advantage and disadvantages of isolated nozzle tests have been described in the section 4.1.3.

The powered afterbody tests may use various schemes as is indicated in fig. IV.11. The first scheme (A) is the simpliest one and requires only one balance. The main disadvantages of this scheme are that optimization of the afterbody-nozzle combination is hard to achieve and that the afterbody drag is overshadowed by the large installed gross thrust which is an order of magnitude larger. The accuracy must be appropriate to the net thrust level while measuring gross thrust. This difficulty is overcome by the scheme in D where the entering jet momentum is subtracted from the total measured force of A, making possible the use of a more sensitive balance. However, in this case the effective flow area (A_i) can be assessed only with difficulty and also a sealing problem exists at this high pressure location. The schemes of fig. IV-11-B and -C are identical in practice and measure separately the installed gross thrust force and installed afterbody drag in series or in tandem respectively. The afterbody drag balance can be made more sensitive.

An alternate method to obtain the afterbody drag of simple models (e.g. axisymmetric) is to pressure tap the afterbody, which might also include a base. These pressures are integrated to obtain $D_{AB_{inst.p.}}$. Adding the calculated skin friction to this quantity yields $D_{AB_{inst}}$. This procedure is not recommended for the external nozzle drag of complicated afterbody shapes since in these cases large pressure gradients might exist yielding inaccurate date. However, some measurement of local pressure plotting and flow visualisation on afterbodies is useful in order to detect areas of drag increase and to make possible comparison with theoretical analysis.

In fig. IV.11 only the primary mass flow is indicated. If necessary secondary flow can also be introduced in a similar manner leading to less difficulties as the primary flow since the secondary mass flow is only a few percent of the total mass flow.

The mass flow can be controlled and metered outside the tunnel test section with a high degree of accuracy. Fig. IV.12 gives the sonic orifice method generally used for gaseous jet fluids. The discharge coefficients for sonic line curvature, boundary layer displacement effect and virial effect which are used are also given in fig. IV.12. The former two discharge coefficients are well covered in the literature (see for example Ref. C24, but not the discharge coefficient for the virial effect. This effect is usually neglected, but should be taken into account if the sonic orifice is operating at high pressures as it generally is the case. If the jet fluid or one of its components is a liquid an easy and accurate technique to control and meter the flow rate is the use of a cavitating venturi, which can be accurately calibrated. The flow rate of a cavitating venturi is proportional to the square root of the product of upstream pressure times the liquid density as long as the venturi back pressure is less than the maximum venturi recovery pressure.

The nozzle gross isentropic thrust (X_{id}) can be computed based on the measured mass flow rate and the nozzle one-dimensional ideal expansion from p_{t_j} to the ambient static pressure p_∞. In fact any of the theoretical isentropic thrust computations based on measured mass flow may be used as described in chapter III. In the real engine isentropic thrust computations the thermal real gas effects ($p = Z\rho RT$) are usually neglected, which can be justified, but the caloric real gas effects (C_v and $C_p \neq$ constant) are taken into account. However the model tests are sometimes performed at high pressure level in order to increase the model Reynolds number. In these cases the virial effect can not be ignored, particularly if a cold jet simulating fluid is used (see fig. IV.13). The gross thrust coefficient may be defined as

$$C_T = \frac{F}{X_{id}}$$

where F is the measured installed or static thrust and X_{id} the isentropic thrust for which the analytical procedure should be indicated. If secondary flow is supplied, the isentropic gross thrust is the sum of both isentropic thrusts, ($X_{idj} + X_{ids}$) :

$$C_{Ts} = \frac{F}{X_{idj}+X_{ids}}$$

where X_{idj} and X_{ids} are calculated from the primary nozzle pressure ratio plus $\dot{m}_j\sqrt{T_{t_j}}$ and the secondary nozzle pressure ratio plus $\dot{m}_s\sqrt{T_{t_s}}$ respectively. F is again the measured total thrust.

In practice it is convenient to work with primary flows only in the bookkeeping procedure even though secondary flows are present. This can be done by subtracting from the measured thrust with primary and secondary flows the ram drag of the secondary flow $\dot{m}_s V_\infty$ and base the thrust coefficient on the isentropic gross thrust of the primary flow only:

REFERENCE

INSTALLED

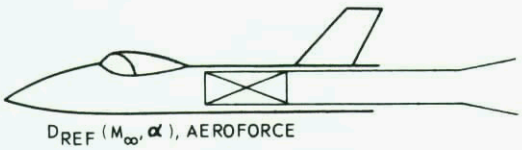

$D_{REF}\,(M_\infty, \alpha)$, AEROFORCE

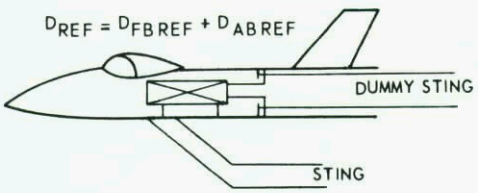

$D_{REF} = D_{FB\,REF} + D_{AB\,REF}$

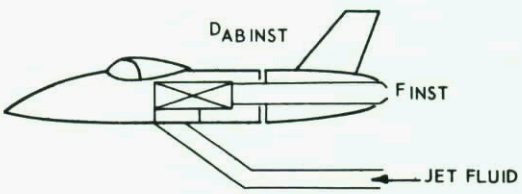

$F_{REF} = F_{ST}$ (R.P.M., A_{EX}, AFT. BURN)

STATIC NOZZLE THRUST

CHANGE IN DRAG : $\Delta D_{AB} = D_{AB\,INST} - D_{AB\,REF}$

CHANGE IN THRUST : $\Delta F_{INT} + D_N = F_{REF} - F_{INST}$

FIG. IV. 10 BOOKKEEPING PROCEDURE FOR INTEGRATED NOZZLE–AIRFRAME SYSTEMS

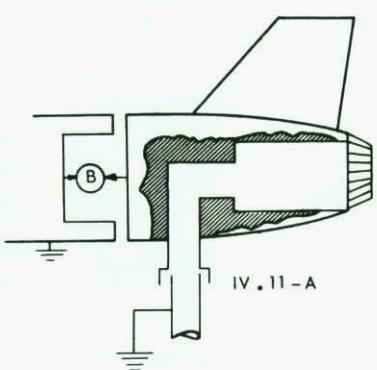

$B = (F - D_{AB})_{INST.}$

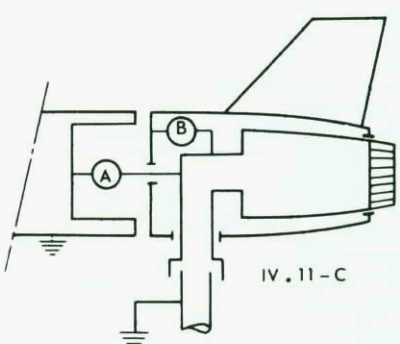

$B = D_{AB\,INST.}$

$A = (F - D_{AB})_{INST.}$

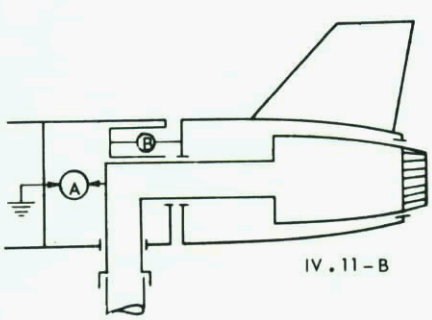

$B = D_{AB\,INST.}$

$A = F_{INST.}$

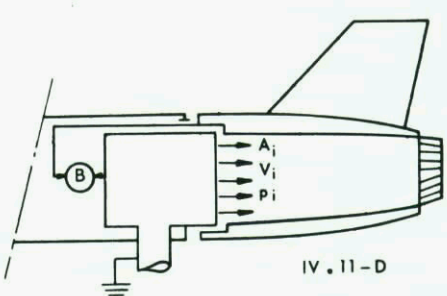

$B - (F - D_{AB})_{INST.} - (\dot{m} V_i + p_i A_i)$

CORRECTIONS REQUIRED FOR SPLIT PRESSURE , SEAL FORCES AND ANY MOMENTUM OF THE ENTERING JET SIMULATING MEDIUM.

FIG. IV. 11 WIND TUNNEL TESTING SCHEMES FOR INSTALLED AFTERBODY / NOZZLE PERFORMANCE DETERMINATION

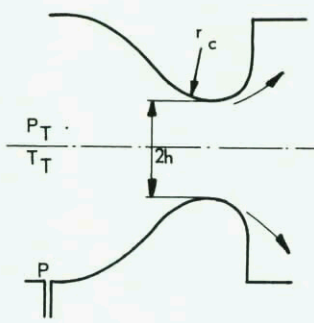

$$\dot{m} = \left\{ k \frac{P_T (\pi h^2)}{\sqrt{T_T}} \times C_{D_K} \times C_{D_\delta} \right\} \times C_{D_V}$$

P_T : TOTAL PRESSURE (DEDUCED FROM STATIC PRESSURE P).

T_T : TOTAL TEMPERATURE.

C_{d_K} : CORRECTIVE FACTOR (SONIC LINE CURVATURE).

C_d : CORRECTIVE FACTOR (BOUNDARY LAYER EFFECT).

C_{d_V} : CORRECTIVE FACTOR (VIRIAL EFFECT WITH RESPECT TO $\gamma \approx 1.4$).

$k : \left(\frac{2}{\gamma+1}\right)^{\frac{\gamma+1}{2(\gamma-1)}} \sqrt{\frac{\gamma}{R}}$

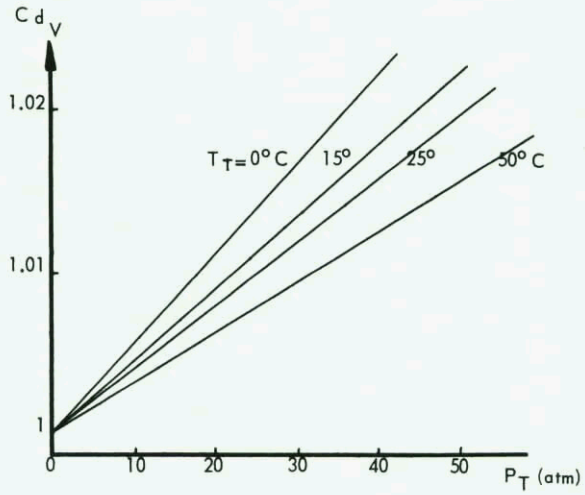

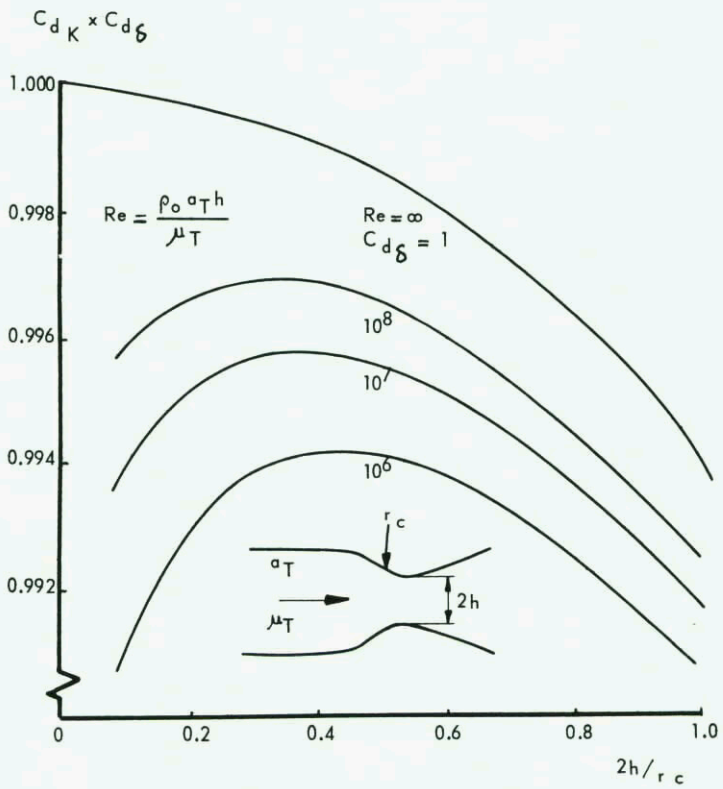

FIG. IV. 12 MASS FLOW MEASUREMENT BY THE SONIC THROAT METHOD

$$C_{Tx} = \frac{F - \dot{m}_s V_\infty}{X_{idj}} \quad .$$

The computed net thrust of the engine is then equal to

$$F_N = C_{Tx} X_{idj} - \dot{m}_j V_\infty$$

taking only into account the primary engine flows.

This procedure is also useful for direct comparison of the actual engine thrust with single nozzles on the static test bench.

Values of the model static thrust, which can be considered as the model reference thrust ($F_{st.model}$, $F_{ref.model}$), can be directly obtained from tunnel-off, jet-on measurements for the different nozzle operating conditions for purpose of determining the absolute installation effects:

$$F_{ref.model} = F_{st.model} = \frac{C_{Tref.model}}{C_{Tref.engine}} \frac{X_{id.model}}{X_{id.engine}} F_{st.engine} \qquad (F_{st.eng} = X_g)$$

where $C_{Tref} = \frac{F_{st}}{X_{id}}$ which should be the same for the model nozzle and the engine nozzle (attention must be exercised that X_{id} is computed in the same manner) or the difference must be traced by analytical procedures (Ref. C-24). If $\gamma_{jengine} = \gamma_{jmodel}$ and $(P_{tj}/p_\infty)_{model} = (P_{tj}/p_\infty)_{engine}$ for both primary and secondary flows) than

$$\frac{X_{id.model}}{X_{id.engine}} = (scale)^2 \frac{P_{tjmodel}}{P_{tjengine}} \quad .$$

If γ_j cannot be simulated in the wind tunnel than a small correction is required. The correction depends on whether the jet plume shape is correctly simulated, but not the jet momentum, or the jet momentum is simulated yielding a non-matched plume shape.

The difference between (jet-on, tunnel-off) and (jet-on, tunnel-on) thrust measurements yields:

$$(F_{ref} - F_{inst})_{model} = (\Delta F_{inst} + D_n)_{model} \ ,$$

i.e. the absolute nozzle installation drag, if the afterbody is measured separately. Since at some Mach number and simulated engine setting (r.p.m., A_{ex}), the ideal thrust and dynamic pressure are both proportional to the pressure level (for example, static pressure p_∞), the internal and external thrust losses (ΔF_{int} and D_N) can be correlated with the ideal thrust. Therefore $F_{inst}/X_{id} = C_{Tinst}$ is a meaningful quantity.

If the purpose of the afterbody tests is to compare the performance of different nozzle designs in the aircraft flow field, or even in an isolated test flow field, the simulation requirements for the jet properties are less pronounced. This method depends upon the difference between two tests on different nozzle configurations at the same free stream Mach number, nozzle expansion ratio and secondary air flow ratio. Then the comparison of installed gross thrust can be written as

$$\Delta F_{inst} = (C_{T_{inst}}' - C_{T_{inst}}'') \, X_{id} \ ,$$

the primes referring to the two different configurations. For $C_{T_{inst}}$ also $C_{T_{xinst}}$ can be written.

If the reference model utilizes a flow through inlet and exhaust, or a flow through nacelle, the reference afterbody drag or reference aft nacelle drag with natural flow must be determined including the natural flow jet effects on the afterbody and the natural flow thrust. These natural flow thrust minus drag term, as a function of Mach number and angle of incidence must be subtracted from the aeroforce model drag. This can be accomplished by measuring the forebody drag separately, as might be done in the inlet tests, or by measuring those values directly with a blowing reference afterbody and nozzle fed from the outside (inlet closed) for which the mass flow (cold air) is equal to the natural flow as might be done with one of the schemes of figure IV.11. The actual afterbody or nacelle aft configuration replaces in the next step the aeroforce configurations, at which the actual thrust and drag term are determined utilizing the proper jet simulation technique and one of the schemes of fig. IV.11.

In fig. IV.14a somewhat different scheme is indicated for a natural flow reference nacelle, where the D_{ref} is determined from wind tunnel-on and wind tunnel-off measurements with natural nozzle blowing. Since the natural flow nozzle is not necessarily choked, the internal thrust might be affected by the external flow yielding a wrong interpretation of D_{ref}. (Note, the notations are somewhat different as used otherwise).

In case of a fan engine with a podded installation the drag acting on the turbine cowl is sometimes called the scrubbing drag. This drag term can be compared with the external nozzle drag of an integrated system. In case of under-wing engine mounting the change in drag of the wing due to jet effects should be included in the bookkeeping procedure of thrust minus drag, same as the trim drag as resulting from lift distribution changes on the wing due to the jets.

In many publications the term base drag is found. This term is generally used if the drag on the base is determined by pressure plotting, as is done with aeroforce model or inlet model drag corrections. Since the base, if present, can either be considered as part of the afterbody or part of the nozzle, the base drag will be contained in the afterbody drag or nozzle drag terms if these terms are determined by force balance measurements .

4.1.5 JET SIMULATION TECHNIQUES

A GENERAL REQUIREMENTS

Apart from the jet parameter simulation requirements (see section 4.1.3) other general requirements exist with respect to model construction and wind tunnel operation. These requirements can be described

FIG. IV. 13 VIRIAL EFFECT ON NOZZLE THRUST FOR COLD AIR

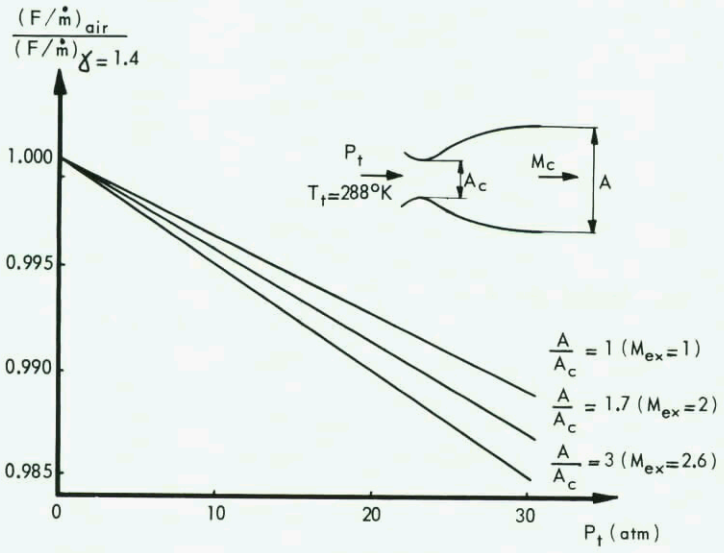

FIG. IV. 14 SCHEME FOR THRUST – DRAG MEASUREMENT UTILIZING A REFERENCE AND ACTUAL AFTERBODY

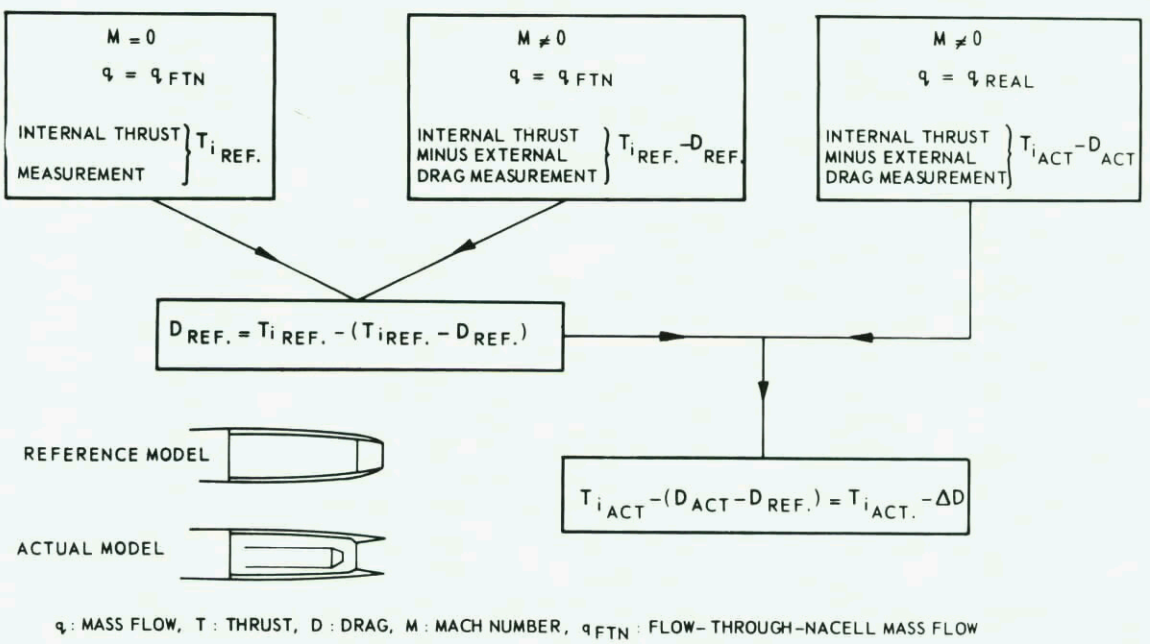

q : MASS FLOW, T : THRUST, D : DRAG, M : MACH NUMBER, q_{FTN} : FLOW-THROUGH-NACELL MASS FLOW

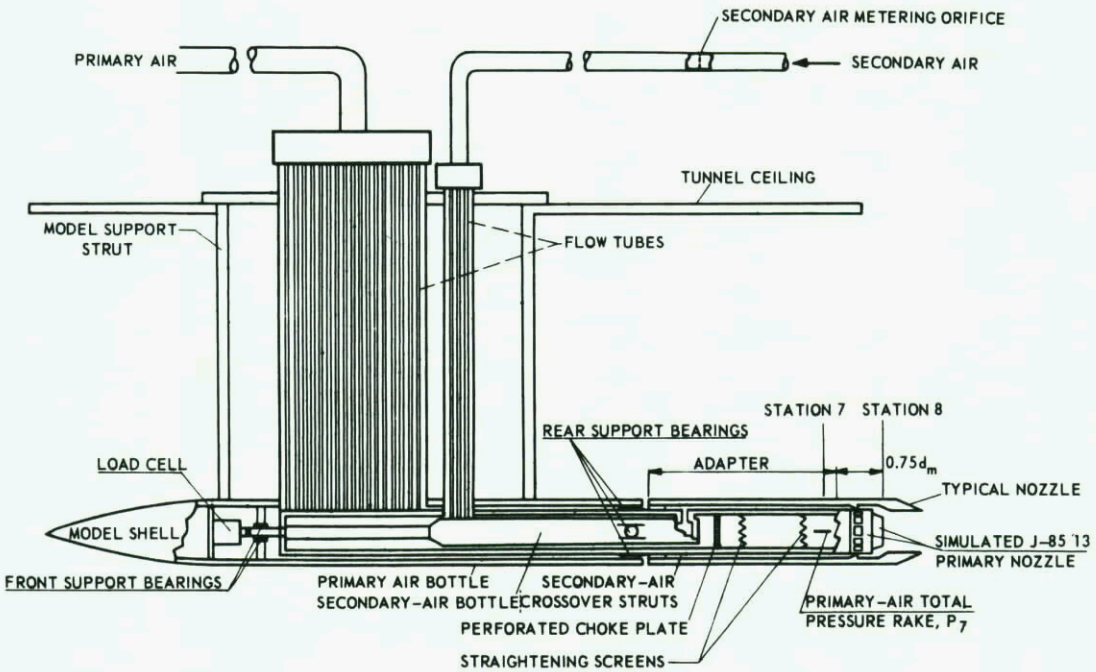

FIG. IV. 15 MODEL INTERNAL GEOMETRY AND THRUST MEASURING SYSTEM USING COLD AIR

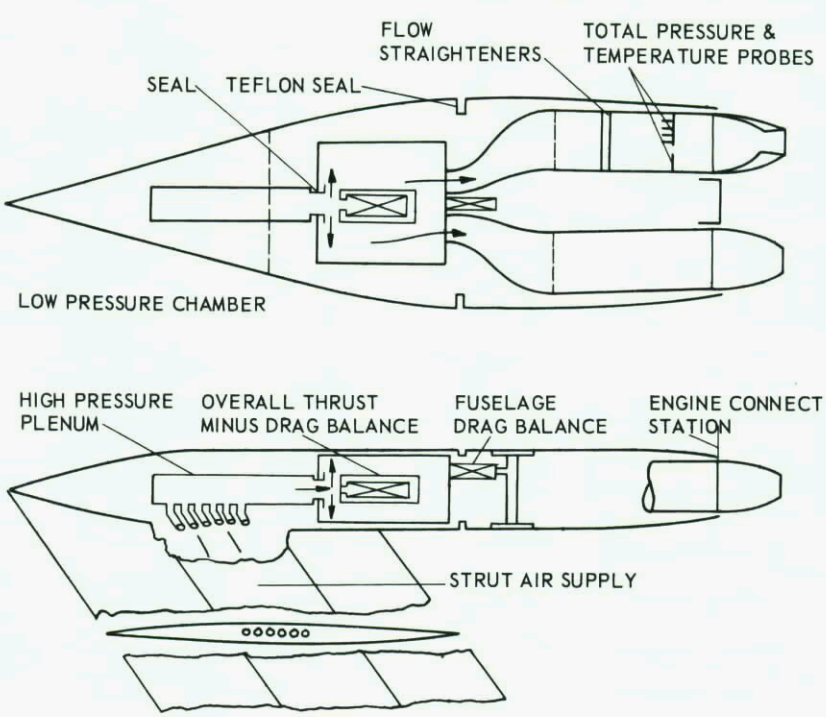

FIG. IV. 16 TANDEM, TURN JET ISOLATED NOZZLE TEST RIG

as follows.

(a) The feed pipes of the jet simulating fluid should be as thin as possible in order to avoid large aerodynamic interference of the supply duct and/or support system. This requirement calls for a dense fluid in the supply duct.
(b) If a thrust balance is used the system to bypass the balance without interference on the balance, should be as small as possible and/or operate at low pressures. This also calls for a dense fluid supply along the balance and/or low pressures.
(c) In order to keep the possible influence of the momentum of the entering fluid on the thrust balance reading as small as possible, this momentum should be a small fraction of the momentum of the exhaust jet. This calls for a dense fluid again.
(d) Within the balances, no temperature gradients should be generated due to heat flow from hot jet simulators, nor should the model deform by thermal stress.
(e) The operation of the simulator should be easily controllable, adjustable and accurately repeatable.
(f) The model and simulator design should be simple and cheap.
(g) The operation costs should be low.
(h) The operation should be safe, therefore the number of systems should be kept small.
(i) The jet flow should not contaminate the tunnel air of closed circuit tunnels, nor should explosive gas mixtures be accumulated in the tunnel.

B TECHNIQUES, ADVANTAGES AND LIMITATIONS

The techniques for jet simulation tests which have been utilized or suggested can be sub-divided in the following order:

- Cold gases.

Air or nitrogen are commonly used because of low costs, easy handling properties and reasonable gas properties for non-augmented engines (except for temperature). Cold gases give clean and continuous operation, and even with secondary flow simulation the plenum chamber of the simulator can be easily designed. However, the jet plume or jet momentum can not exactly be simulated, nor can the mixing process of ejector nozzles and along the jet boundary be simulated. Several exhaust nozzles may be required to obtain the desired entire range of pressure ratios at high jet pressure ratios. Scaling the real nozzle for complete expansion will result in under expanded scaled nozzle operation.
In order to keep the feed lines small the gas is supplied at high pressures, consequently large pressure drops in the ducts can be tolerated. The balance bypass system is generally quite voluminous and must be designed properly for detailed balancing if this system must be located inside the model. If the balance bypass system can be located outside the test section this problem can be avoided for example by utilizing long flexible hoses or pipes having a spring constant many orders of magnitude less than the spring constant of the balance. The gas must be supplied at right angles to the thrust axis. Right angle feed systems are mainly used for isolated model tests.
Fig. IV.15 shows an isolated nozzle system (Ref. H16) for which the necessary flexure in the axial direction is obtained by a number of feed pipes in the support strut, using the measuring arrangement of fig. IV.11.A, incorporating secondary air. In many models the stiffness perpendicular to the thrust axis is a hard requirement to meet. Therefore often extra support bearings or flexures are incorporated as seen in this figure.
In fig. IV.16 a tandem arrangement is sketched (fig. IV.11.C) for a twin nozzle isolated model arrangement where the balance bypass is within the model (Ref. M18). However, in this case no secondary air is provided.

A very popular arrangement for isolated nozzle support at transonic and supersonic speeds is the shaft method for which the nozzle is at the end of the shaft extending from the tunnel plenum chamber into the test section. The advantage is the complete omission of side supports; the limitation is the large boundary layer build up along the shaft in front of the nozzle and the impossibility of incidence variation. The influence of the shaft boundary layer can however be reduced by blowing or suction just upstream of the sensitive portion of the afterbody. Fig. IV.17 show such an installation with three jet fluxes available. The sealing is obtained by balancing rubber bellows. Also more details on data reduction and layout are given.

Fig. IV.18 depicts a simple nozzle test rig primarily for the purpose of gathering comparitive information useful to select a configuration rather than obtaining absolute datums. The tests are carried out: (a) without external flow to measure nozzle internal performance, and (b) with external flow to measure installed thrust minus drag. The latter tests are made with all the significant items which might contribute to the jet interference effects - boat tail, base area, tail surfaces, in the case of an afterbody - a wing and pylon in the case of a wing pod.

Fig. IV.19 represents another afterbody shaft mounted study rig in a transonic test section which is small with respect to the scale of the model (Ref. L.13). The aim of this rig is to study the afterbody performance of a podded fan engine installation by pressure plotting rather than by weighing, and to compare the results for the fan cowl with the pressure coefficients obtained from the inlet tests (as described in section 2.1.2-B.2). In order to obtain a representative flow around the model and provide a simulated reference upstream flow, the cylindrical shaft support has been smoothly faired to the external boat tail shape. However as is shown in fig. IV.20 the common portion in the pressure coefficient is present only at the lower Mach numbers, which is probably due to the fact that the flow field induced by the lip of the inlet is not reproduced in the afterbody test. Therefore the data should not be interpreted as an absolute value of the afterbody drag as determined from pressure integration and estimated skin friction drag. Consequently improvements of this test procedure must be made, for instance by a better representation of the shape of the streamline at the leading edge and by boundary layer control (as is done in ref. R.9).

Fig. IV.21 gives a layout of a side supported twin nozzle afterbody rig which can be installed in a transonic as well as in a supersonic wind tunnel. The rig, which carries models of 1/10 to 1/20 scale and uses air stored at 11 atmospheres, can be used to investigate nozzle-afterbody performance over a nozzle expansion range representative of turbo-jet and bypass engines. The scheme used is that of fig. IV.11A, incorporating secondary flow and tail planes at the metric afterbody. The forebody is non-metric and the strut is located at a typical wing location. The forebody is of reduced length making representative boundary layer thickness simulation possible at the metric line location, as is indicated in fig. IV.22, requiring, however, a careful design of the forebody contour. Detailed drawings of this test facility are given in fig. IV.23. The instrumentation layout is shown in fig. IV.24 A along with

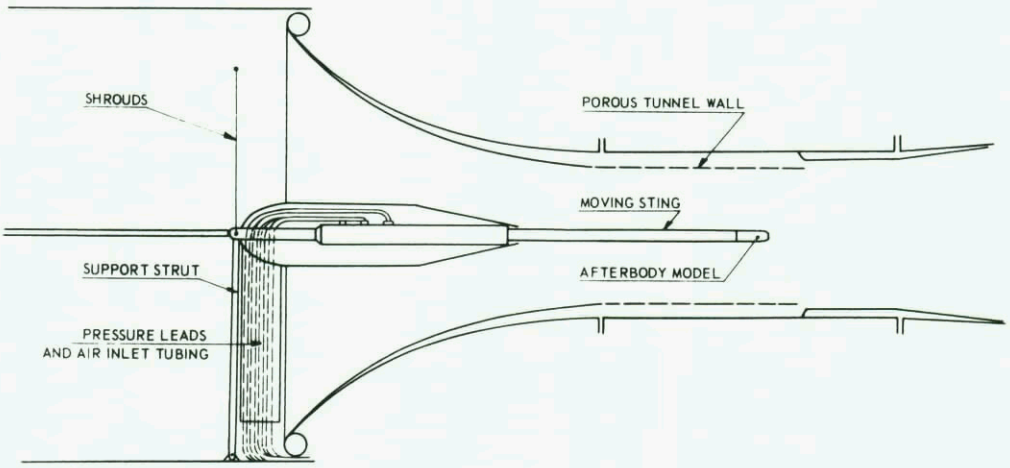

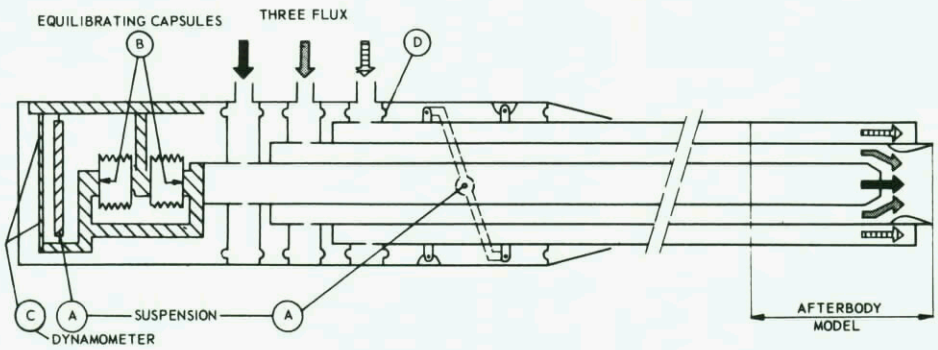

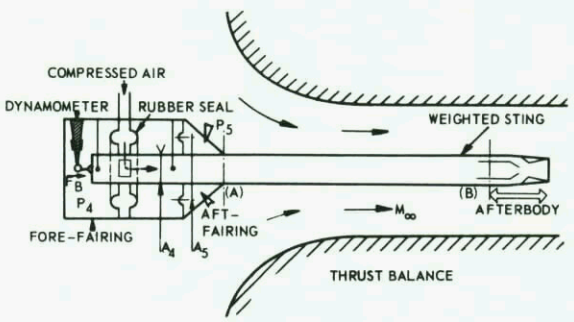

$$F_B + A_4 P_4 - (A_5 - A_4) P_5 + \text{MEMBRANES CORRECTIONS} = \text{FRICTION DRAG FROM (A) TO (B)}$$

MEASURED THRUST (P_4 : BALANCE INTERNAL PRESSURE; A_4 : EFFECTIVE AREA) (P_5 : AFT-FAIRING PRESSURE; $A_5 - A_4$: EFFECTIVE AREA) + AFTERBODY THRUST-MINUS DRAG

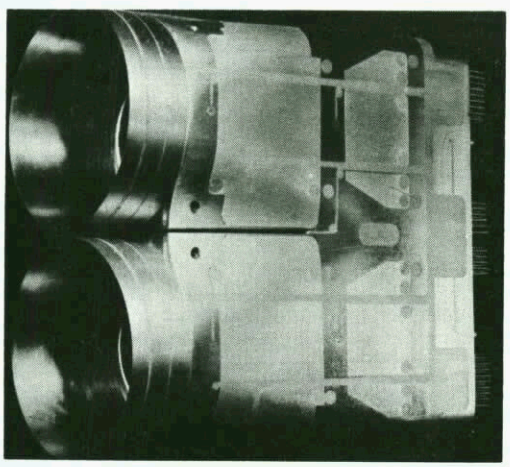

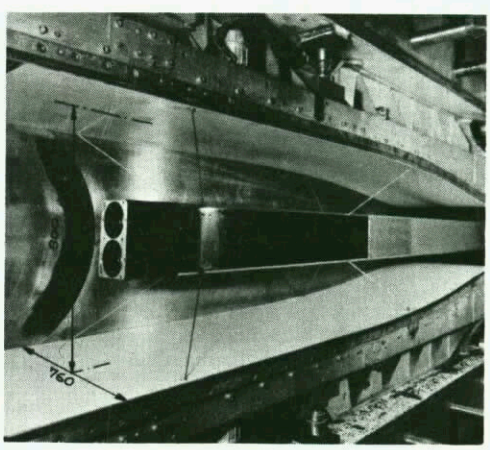

FIG. IV. 17 SHAFT MOUNTED AFTERBODY MODEL ARRANGEMENTS IN TRANSONIC AND SUPERSONIC WIND TUNNELS FOR THRUST-DRAG MEASUREMENTS

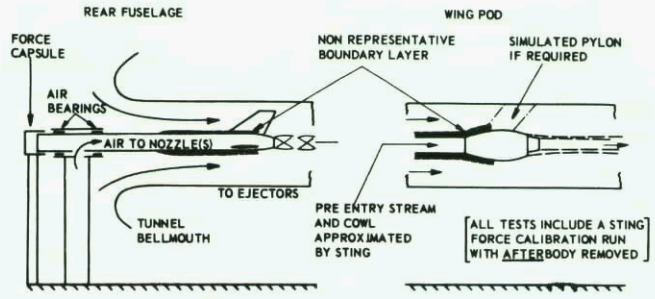

FIG. IV. 18 NOZZLE TEST RIG FOR REAR FUSELAGE AND WING POD MODELS

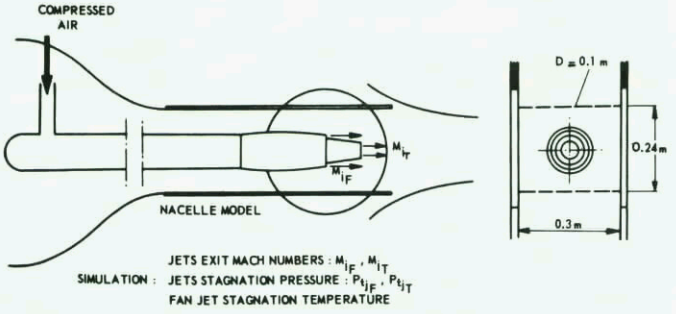

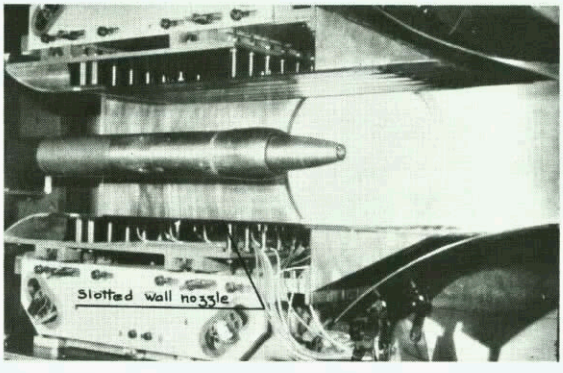

FIG. IV. 19 FAN ENGINE AFTERBODY TEST RIG IN TRANSONIC WIND TUNNEL

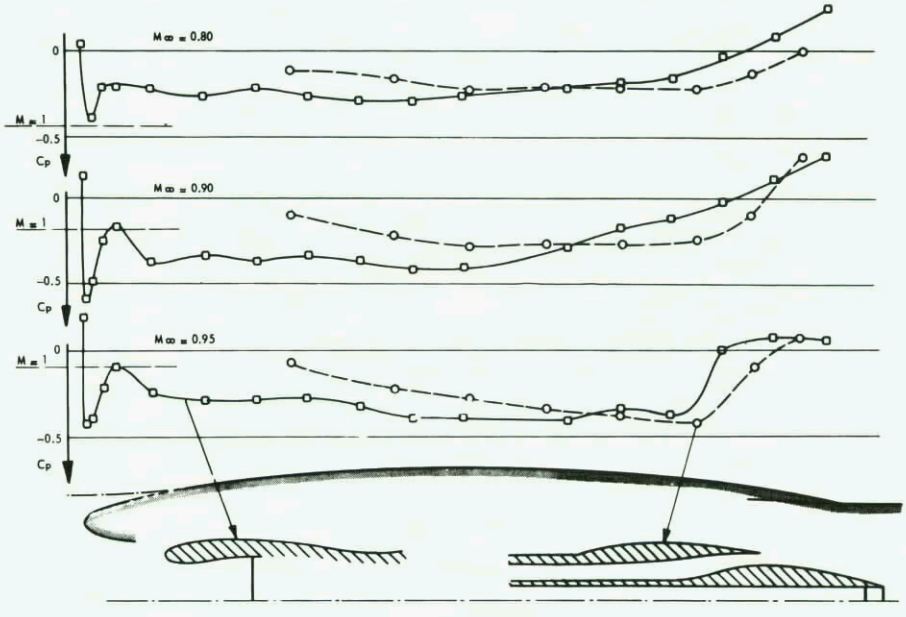

FIG. IV. 20 EXAMPLE OF PRESSURE COEFFICIENT ON A FAN COWL AS DERIVED FROM INLET AND FROM EXHAUST TESTS

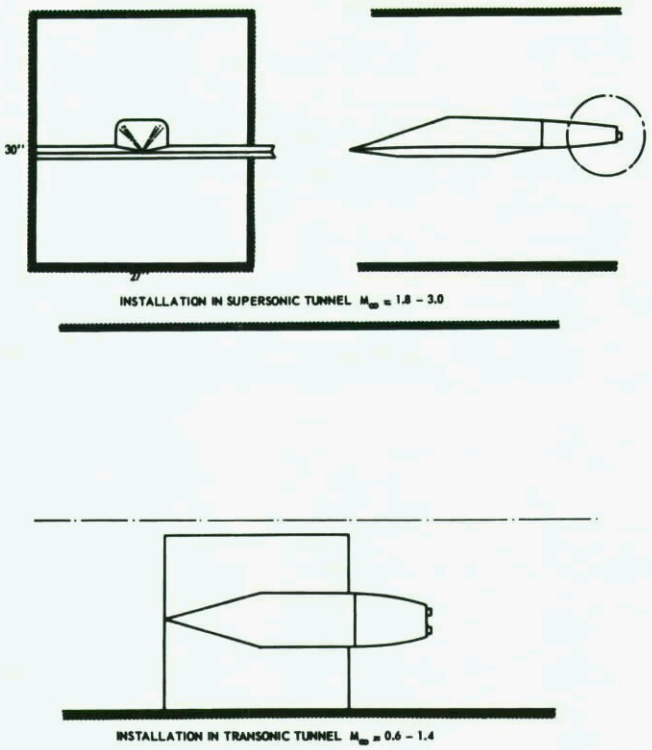

FIG. IV. 21 INSTALLATION OF A SIDE SUPPORTED TWIN NOZZLE AFTERBODY TEST RIG IN BOTH SUPERSONIC AND TRANSONIC WIND TUNNEL.

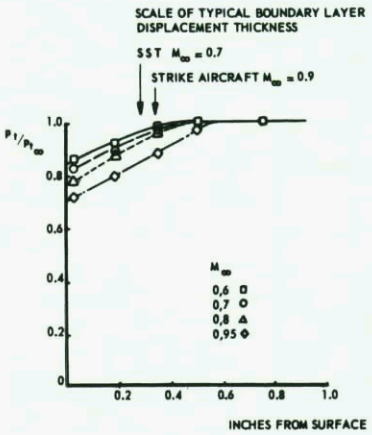

FIG. IV. 22 COMPARISON BETWEEN FULL SCALE BOUNDARY LAYER DISPLACEMENT THICKNESS AND MODEL BOUNDARY LAYER AT METRIC LINE (SEE FIG. IV. 21).

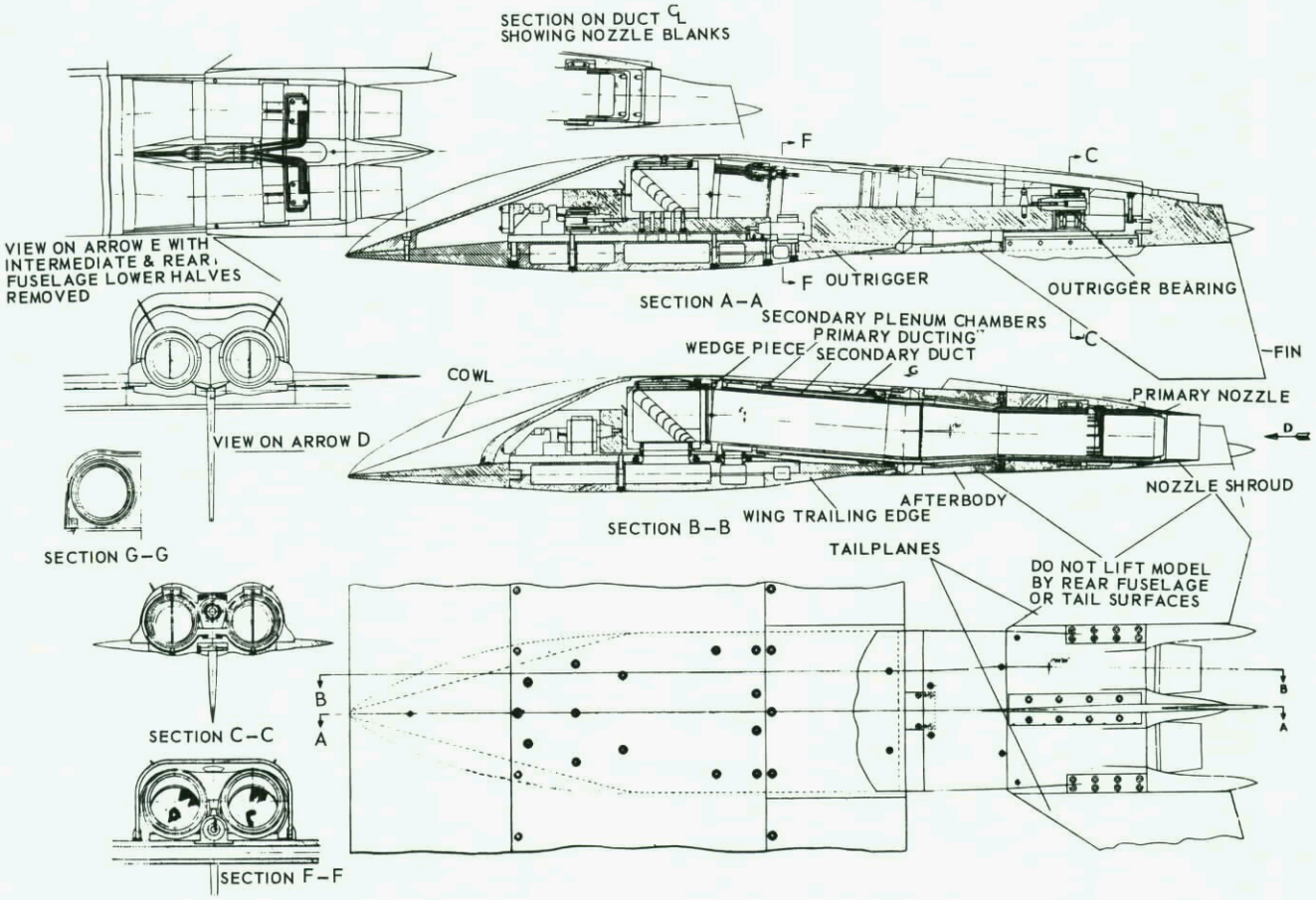

FIG. IV. 23 TYPICAL MODEL ASSEMBLED INTO RIG OF FIG. IV. 21

the line diagram for data reduction in fig. IV.24.B. The data reduction scheme results in various thrust coefficients (underlined) which depend each on the definition for the isentropic thrust and the associated deduced actual model thrust. Special attention has been directed to the mass flow and discharge coefficient determination. The mass flow is measured at a special discharge chamber in the supply line as indicated in fig. IV.24.A where the total pressure (p_m) and the bell mouth depression Δp_m are measured and used to define an accurate value for $\dot{m}\sqrt{T}$. The discharge coefficient relates to the ^{m}bell mouth Reynolds number and has been accurately determined against a known standard nozzle. The values of $\dot{m}\sqrt{T}$ for use in the nozzle requires correction for any total temperature change between the measuring bell mouth and nozzle plane. This can be an important item in relation to the required accuracy as 1 °/o temperature variation between the two stations gives 1/2 °/o variation in C_d. The secondary flow is measured separately in each duct by orifice plates. As is stated before, the significance of absolute discharge coefficients and thrust coefficients is subject to doubt since the rig values must be based on a defined nozzle pressure head. Also the flow distribution approaching the nozzle is likely to be very different.

If the engines are located in separate nacelles under the wings or at the aft-fuselage the semi-model test technique may be used sothat the air can be supplied through the wings and pylons to the nozzle. In this case the inlets will be faired if direct blowing is provided. Using engine simulators, such as small turbine-driven compressors, the inlet flow is also simulated partially. This technique will be discussed in chapter V. Fig. IV.25 gives a layout of a semi-model of a supersonic transport with a half-width of 0,5 m in a 1.7 x 1.7 m^2 tunnel. The system, which is under design has an external balance bypass air flow system, incorporating secondary flow also and faired inlets. The complete wing and nacelles are metric to a six component balance. It is expected that the external flow at the nozzle station can be simulated properly.

Cold gases other than compressed air or nitrogen for jet simulation in wind tunnels are proposed, since mixing air with multi-atomatic gases such as carbon dioxide or freon, the ratio of specific heats can be adjusted (Ref. T.1). By mixing a third light weight component such as He and/or H_2, the jet density can be simulated also. However, these techniques have not been used extensively due to costs, tunnel contamination and the possible accumulation of explosive or otherwise dangerous mixtures.

- Hot gases.

In practice the simulation of the exhaust jets by hot gases is performed using the decomposition of hydrogen peroxide, or by burning a liquid or gaseous fuel with air. The latter method can be used in conjunction with simple cold air simulation but is of course much more complicated since an additional ignition, fuel flow and control system must be provided. In order to keep the colling provisions and thermal flux requirements to a minimum, the heat must be generated just upstream of the nozzle, preferrably at the actual engine location. This will mean that the loading of the burner must be rather high, resulting in incomplete combustion and hence in unpredictable simulator performance. For this reason gaseous fuels, particularly H_2, are favourable, but are more dangerous with respect to leaks, then liquid fuels and will result in rather thick fuel lines. The fuels used are generally hydrogen, methane, propane, ethylene and liquid hydrocarbons, such as kerosine. The oxidizer is usually air or oxygen, with air being more favourable due to less costs and the required moderate temperatures. Usually the problem is not to meet the highest jet temperature requirements but rather the lower jet temperature. For lower temperatures the combustor must be designed such that burning takes place in the primary zone after which cooling air is added.

The main advantage of hot gases is the correct jet simulation properties, both $R_j T_j / R_\infty T_\infty$ and γ_j. Some advantage is obtained due to the reduced required mass flow and, hence, reduced supply ducts. For closed circuit wind tunnels intermittent jet operation is required, or else an exhaust gas collector must be provided for continuous operation.

Fig. IV.26.A depicts an axisymmetric hot isolated nozzle test rig of the shaft type in a transonic/supersonic wind tunnel (Ref. R.8). Also non-axisymmetric nozzle and afterbodies may be attached to the shaft which extends from the tunnel plenum chamber. The shaft is 10 cm in diameter and contains a propane burner and a downstream mixer for uniform temperature distribution at the nozzle entrance. The nozzle is fed by dry compressed air heated to 600° C maximum by propane burning. The range of obtainable jet temperature and ratio of specific heats is given in fig. IV.26.B. The combustion efficiency varies between 70 °/o and 90 °/o, the highest at the highest obtainable fuel-air ratio. The temperature distortion is less than 10 °/o. This rig has been developed and refined continuously over a period of years and, apart from Reynolds number effects, simulates flight conditions very closely. The approach boundary layer on to the afterbody is, however, too thick; no boundary layer control is provided.

For data reduction a thrust-minus-drag balance is provided together with pressure plotting along the afterbody and base. The primary pre-determined parameters (M_∞, p_{t_j}/p_∞, T_{t_j}/T_{t_∞}) then yields data on jet thrust, boat tail drag, skin friction drag, pressure drag and base drag of which the latter two terms can be obtained by pressure integration. The jet thrust and skin friction drag can then be determined after appropriate assumptions (for example estimation of skin friction drag, or assumed independence of external flow on jet thrust in choked nozzle operation).

The other way frequently used to generate hot exhausts gases is by decomposition of hydrogen peroxide in a catalyst pack producing hot steam/oxygen mixtures for which the temperature and composition depends on the peroxide concentration. It has the advantage that the ratio of specific heats and temperature of the decomposition products follow closely the values for turbojet engines as may be seen in fig. IV.27. Peroxide decomposition yields good plume shape and jet momentum simulation as well as simulation of the mixing process. The silver screen catalyst pack can generally be designed small enough to be located in the model and does not require more space than a scaled engine should. Due to the feed of cold peroxide the thermal effects have little influence on upstream components (i.e. balances).

Compared to the use of cold air the following numerical values show the use of hydrogen peroxide is very attractive from a model testing requirements point of view.

Density ratio $\rho_{H_2O_2} / \rho_{air} = 14$ (assumed 90 °/o H_2O_2 and compressed air at 80 atm.)

Supply mass ratio $\dot{m}_{H_2O_2} / \dot{m}_{air} = 0.46$.

Supply line diameter ratio $D_{H_2O_2} / D_{air} = 0.43$.

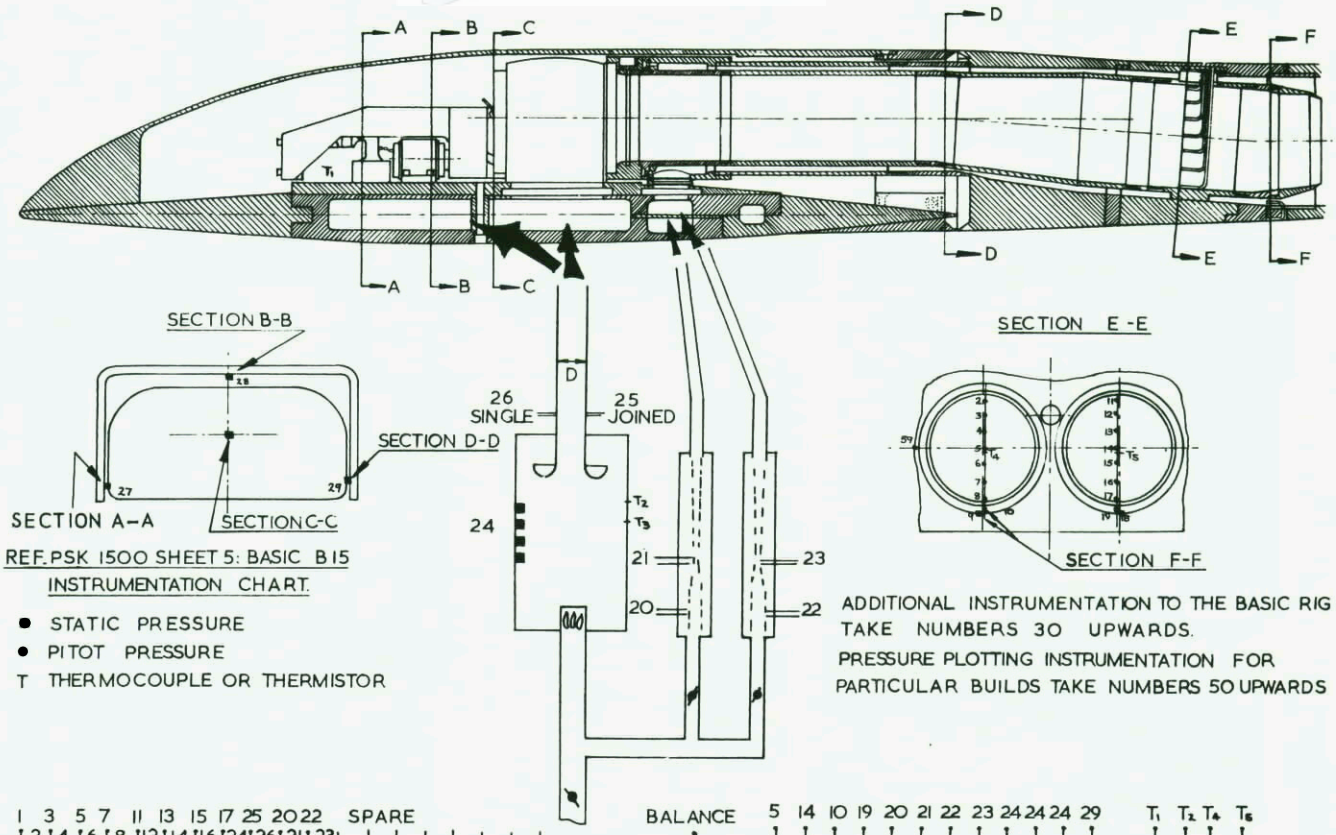

THE PROCESS OF CONVERTING A GIVEN BASIC MEASUREMENT FROM THE SIGNAL TO AN ABSOLUTE QUANTITY USING A ZERO MEASUREMENT, APPLYING CALIBRATION ETC. IS INDICATED BY ▼ FOR BASIC TUNNEL INSTRUMENTATION ▼ FOR MULTI CHANNEL DISCRETE RECORDINGS ▽ FOR SCAN DATA.

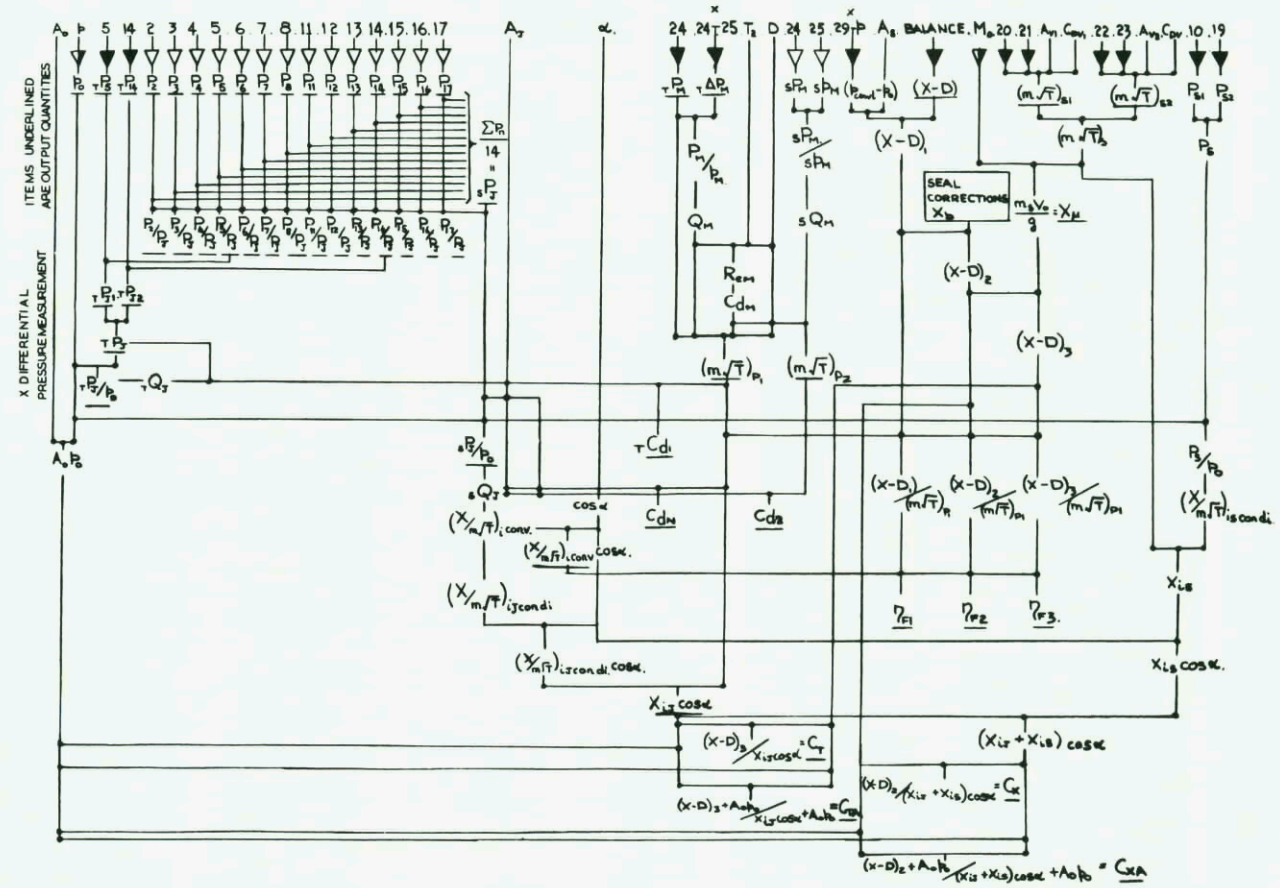

FIG. IV. 24 INSTRUMENTATION LAY OUT AND DATA REDUCTION SCHEME USED WITH FIG. IV. 23

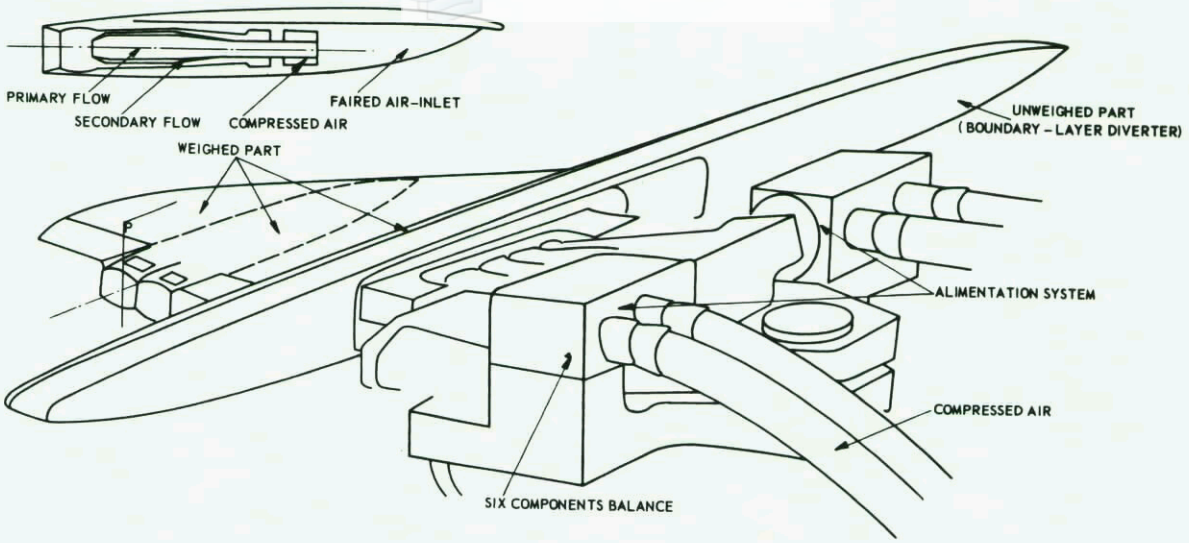

FIG. IV. 25 THRUST - DRAG TESTS ON A S.S.T. MODEL WITH INTEGRATED NACELLE (SCALE 1/25)

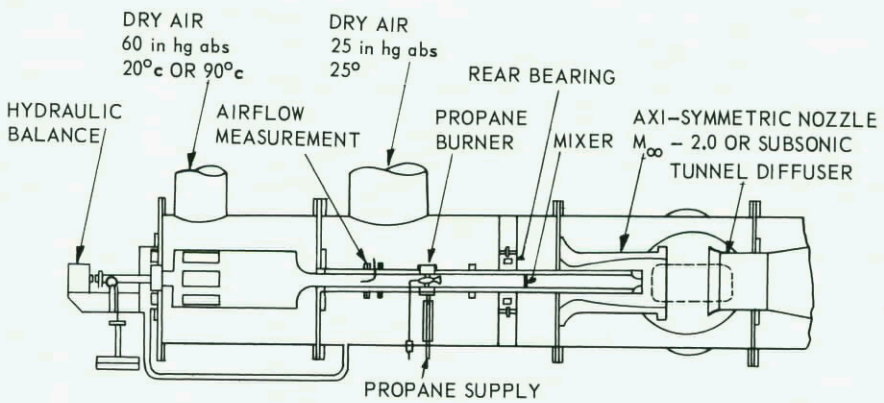

FIG. IV. 26a HOT AND COLD JET INTERFERENCE TUNNEL, SUPERSONIC AND TRANSONIC

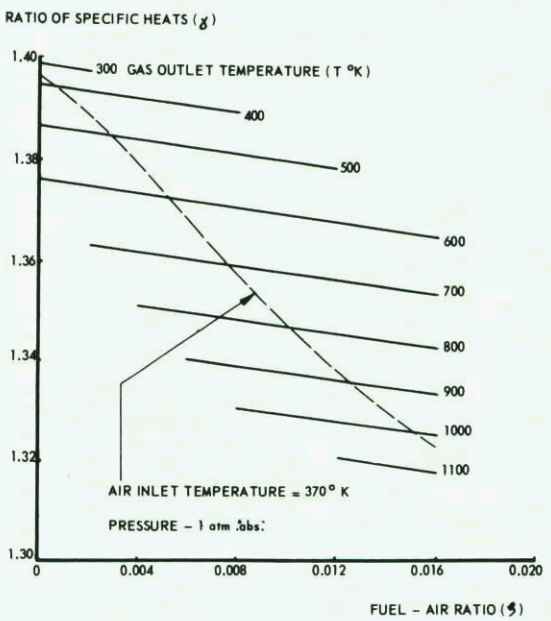

FIG. IV. 26b VARIATION OF RATIO OF SPECIFIC HEATS WITH TEMPERATURE AND FUEL-AIR RATIO FOR THE COMBUSTION PRODUCTS OF PROPANE - AIR MIXTURES

Supply line ultimate diameter ratio $D_{H_2O_2} / D_{air} = 0.26$.

Supply line stiffness ratio $D^3_{H_2O_2} / D^3_{air} = 0.08$.

Supply momentum ratio $(\dot{m}v_i)_{H_2O_2} / (\dot{m}v_i)_{air} = 0.08$.

Momentum ratio supply/exhaust H_2O_2 : $\dot{m}v_i / \dot{m}v_j = 0.023$.

air : $\dot{m}v_i / \dot{m}v_j = 0.28$.

This makes the use in complete afterbody model tests particularly suitable when incorporating thrust and drag balances in the model. The operation can easily be intermittent by opening and closing the supply flow. Mass flow control is easily and accurately achieved by a cavitating venturi, which also prevents chugging.

Since the feed lines are small, space is also available for secondary air flow supply as may be seen in fig. IV.28 for an isolated nozzle test (ref. N.6), using a two-balance system. Another balance system is shown in fig. IV.29 where the thrust balance and supply line to the simulator catalyst pack are integrated. The afterbody drag balance is concentric with the thrust balance, yielding a testing scheme similar to fig. IV.11.B. The balances of the system, so called ring balances, are very stiff with respect to side forces and axial forces, sothat small split lines between components of the model can be obtained. In spite of small displacement due to axial forces the output of this ring balance is relative large. Proved accuracy of this balance, electronic equipment included, is 0,25 % full scale. Temperature effects on the balance accuracy, caused by the hot simulator, are eliminated by cooling the contact surface between balance and simulator with water. During firing of the simulator, the balance and the front plate of the simulator are intensively cooled by the liquid hydrogen peroxide, which has an entrance temperature equal to the stagnation temperature of the tunnel air. More information on this technique can be found in Ref. B.1 and A.13.

Though this technique has several advantages from the wind tunnel testing point of view it also has drawbacks, of which the main draw back is the cleaning and passivation procedure of components in direct contact with the hydrogen peroxide in order to operate the facility savely. This requires a skilled operation team and a well-designed system. Fortunately dilution with only small amounts of water rapidly reduces the occurrance of fire and explosion hazards. The liquid and fumes are non-toxic. In closed circuit tunnels the humidity increases due to the large amount of steam in the jet and the tunnel air will rise in temperature. Therefore intermittent operation is required; blowing times between 4 sec. and 40 sec. are generally used. Several intermittent runs can be made before tunnel air exchange or tunnel drying is necessary due to increased humidity. Also short firing time is required due to limited catalyst pack life (one to 5 hours, depending on pack loading and peroxide concentration), which means in practice that the catalyst pack must be replaced a few times in a wind tunnel program. Another draw back may be the costs of H_2O_2, which is about ƒ 1.00/kg. Consequently this system will only be used in high quality wind tunnels and in wind tunnel programs for advanced aircraft design.

- Cold jet powered turbine engine.

The use of miniature cold jet powered turbine engines is rather new and requires special attention since the complete engine, inlet and nozzle are simulated. This technique will be discussed in chapter V. For completeness, some points of concern will be mentioned here. A miniature air or nitrogen powered unit contains a gas turbine driving a compressor. The inlet and exhaust flows can be simultaneously simulated to a large degree with this type of propulsion simulator.

Fig. IV.30 gives a sketch of the components. Part of the driving air can be extracted from the exit pipe flow and exhausted outside the test section in order to achieve proper inlet air flow ratio together with proper nozzle pressure ratio. This mixing of turbine gas and compressor discharge is not common currently; however, new simulators incorporate this feature. These simulators give continuous operation with controllable r.p.m. of the shaft resulting in varying net thrust. The main drawback is the high cost, including operation, extensive pressure instrumentation, and the extensive calibration required for the fan and exhaust mass flow and momentum evaluation. Previous bearings had only limited life. Provisions must be made to prevent turbine nozzle ice formation. The repeatability of thrust data has also led to difficulties and the accuracy obtainable from momentum calculation is limited. Better accuracies can be obtained by attaching the nacelle with the miniature turbo-fan engine to a balance.

C ACCURACIES

Apart from applied corrections to the wind tunnel data, one always should consider the obtained accuracy of the measurement. In general the measured thrust of standard nozzles show good agreement with the theoretical thrust if tested in the wind tunnel. The following general figures are quoted:

Tests in supersonic wind tunnel: $C_{T_A} = 1 \pm 0{,}1$ %.

Tests in transonic-subsonic wind tunnel: $C_{T_A} = 1 \pm 0{,}5$ %

Static tests : $C_{T_A} = 1 \pm 0{,}2$ %

where C_{T_A} is the determined vacuum gross nozzle thrust $(\dot{m}v_{ex} + p_{ex}A_{ex})$ divided by the corresponding theoretical isentropic value. For the succesful development of a new thrust balance, use of standard nozzles yields a reliable means to detect any defect which may occur.

The repeatability of thrust minus drag data if the measurements are performed with only one balance, is usually within 0,2 % for supersonic tests and less than 1 % for transonic tests. In general it can be said that the absolute achievable accuracy of strain gauge balances is better than 0,25 % full scale, making thrust minus drag evaluation within about 0,5 % possible. This closely meets the requirements as mentioned in section 4.1.1.

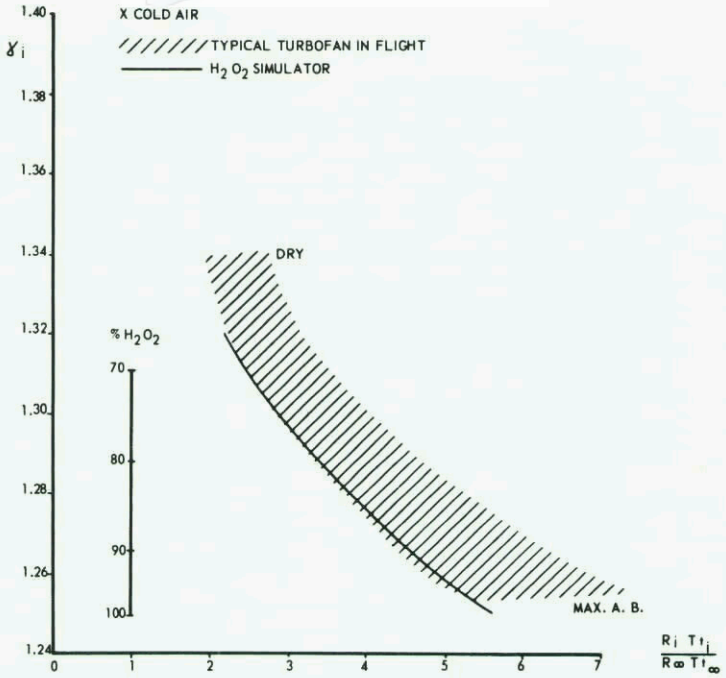

FIG. IV. 27 RATIO OF SPECIFIC HEAT VERSUS TEMPERATURE FOR TURBOJETS IN FLIGHT AND FOR DECOMPOSED HYDROGEN PEROXIDE IN WIND TUNNELS

FOREBODY ORDINATES			
Station, x, in.	Radius, r, in.	Station, x, in.	Radius, r, in.
2.000	0.490	20.000	3.080
5.000	1.140	20.900	3.127
8.000	1.700	23.500	3.220
11.000	2.175	26.000	3.250
14.000	2.565	47.125	3.250
17.000	2.865		

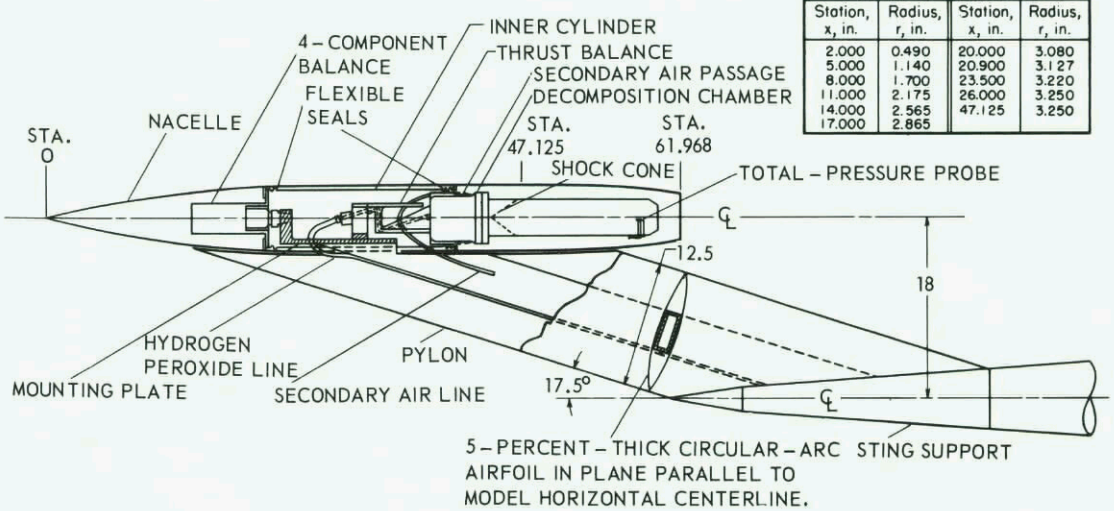

FIG. IV. 28 SKETCH OF PYLON – SUPPORTED NACELLE MODEL USING H_2O_2 AND SECONDARY FLOW (ALL DIMENSIONS IN INCHES)

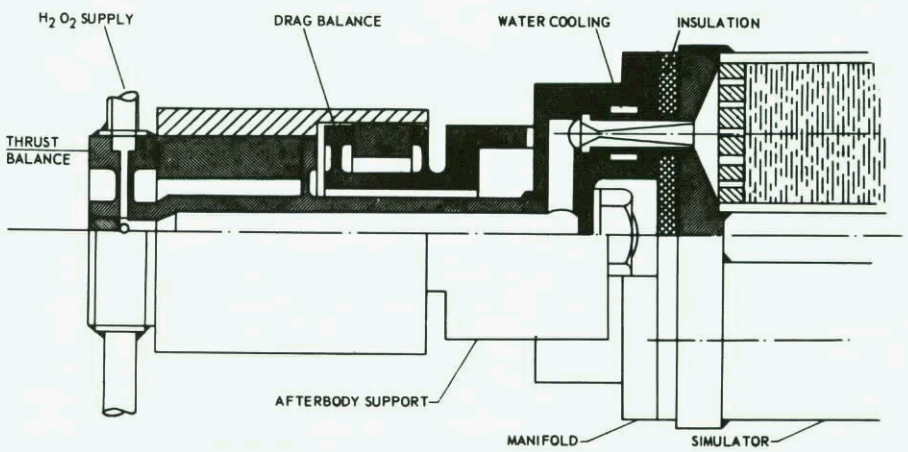

FIG. IV. 29 SKETCH OF DUAL BALANCE SYSTEM FOR THRUST AND AFTERBODY DRAG MEASUREMENT USING H_2O_2

4.1.6 CORRECTIONS

The results determined with the test techniques described in the former section, are normally published as they stand, either in the form of thrust and drag coefficients (based on maximum cross-sectional area) or as efficiencies (referred to the thrust of an isentropic nozzle with the same primary mass flow). Only those corrections, which have been established firmly in other wind tunnel investigations should be applied. When such corrections are made, a second set of data should also be compiled without the correction sothat a true representation of the particular correction may be evaluated by the "experienced" user. In any case the correction procedure should be clearly indicated.

If possible the experimental results should be compared with theoretical predictions. For the internal nozzle thrust predictions the methods as described in Ref. C.24 for example may be used if the ratio of specific heats are not matched in the wind tunnel test. If the nozzle in the wind tunnel model is designed for the γ of the simulating fluid in a similar manner as the actual nozzle is designed for the rear engine jet flow, the measured thrust coefficient as determined from the wind tunnel tests is directly applicable, except for a small correction for the discharge coefficient due to internal boundary layer effect. Consideration should however be paid to the fact that the ratio of specific heats increases during expansion and the rate of increase depends on the gas composition and temperature. Fig. IV.31 gives the increase in γ_j versus expansion ratio for actual turbine engine jets, the decomposition products of H_2O_2 and of cold air. Also the computation of the ratio of specific heats at high temperatures is not unique. The coefficient of isentropic expansion $\gamma = \left(\frac{\delta \ln p}{\delta \ln \rho}\right)_S$ (where p and ρ are normalised values of the total pressure and density of the gas mixture respectively, either frozen or in equilibrium) and the ratio of specific heats $\gamma = c_{p/c_v}$ may be used, as well as the computation from

$$\gamma = \frac{1}{1 - \frac{1}{\frac{d \sum_{i=1}^{n} x_i \, S_i^o/R}{d \ln T}}}$$

(where S_i^o = entropy of species i, x_i = mole fraction of species i of the gas mixture and R is the universal gas constant). The last equation is derived from the speed of sound definition. The latter method of equating γ is used in fig. IV.31. Computer programs for real gas properties are readily available.

For correction of the external afterbody drag two cases can be distinguished; namely, separated and non-separated external flows. If the flow remains attached until the nozzle edge in the wind tunnel test, it is not very likely that the flow will separate in flight, due to the relative thinner boundary layer at full scale. In those cases and for axisymmetric and clean afterbodies the correction on the pressure contribution due the boundary layer displacement thickness can be computed with modern transonic flow field analysis for the full scale and model case and compared with the experimental wind tunnel data, likewise the skin friction drag can be calculated. Such a technique is described in Ref. A.12 and is successful. In these computations the plume is introduced as a solid body with corrections for mixing along the jet boundary. These corrections give a displaced jet boundary with respect to the inviscid boundary depending on the estimated pumping action (momentum transfer) of the mixing process. Fig. IV.32 as given in ref. R.17 shows how the computed afterbody drag compares with the results from wind tunnel tests. If this correlation can be achieved, proper determination of corrections for scale effect should be possible.

In the case flow separation does occur in the wind tunnel at the afterbody no rules are available for proper correction methods, since the extent of the separated region can not be correlated with the scale and boundary layer characteristics. For separated flows isolated tests with limited forebody length yielding simulated relative boundary layer thicknesses probably will yield the best uncorrected results. If applicable the test data should be compared with the empirical afterbody drag estimation as given in Ref. M.10. If this estimation is close a hot jet correction factor (change of γ_j) may be computed for which the reliability should be checked.

If possible, the thrust and drag changes due to leakage of the nozzle leaves should also be determined, or estimated with as much precision as possible. Usually, however, the degree of leakage is not known and probably varies for all production nozzles.

In general it can be stated that only little is known of Reynolds number, boundary layer and mixing effect on the afterbody drag and nozzle thrust, except for some schematic configurations and that more work is needed in this area. These recommendations are complementary to the additional work needed on internal nozzle flow previously discussed in section 4.1.3.

4.1.7 FINAL REMARKS

A COMPARISON BETWEEN WIND TUNNEL DATA AND FLIGHT DATA

In order to obtain knowledge on an under-wing nacelle installation for a supersonic transport, a wind tunnel and free flight program has been carried out recently using an existing aircraft with delta wings (F-106) with auxiliary small jet engines (ref. C.25, M.20). Fig. IV.33 gives a compilation of comparisons between wind tunnel data and flight data concerning the afterbody drag and nozzle gross thrust. The 1/20 scale model tunnel data are obtained by simulating the jets with solid bodies. It is seen that the boat tail drag (determined from pressure integration) as experienced in flight is not predicted from wind tunnel measurements for the following reasons: (a) incomplete simulation of jet for complete model tests, (b) isolated nozzle tests are not adequate for the actual installed nozzle, and (c) separation on the model afterbody flow is more extensive than it is in flight. Also, the gross thrust coefficients of the three nozzle systems as tested are strongly affected by installation.

Further no data on nozzle thrust minus drag comparisons between wind tunnel and flight test are known to exist. Certainly the advantages of this type of data, even though after-the-fact, would be beneficial to the state-of-the-art in regards to future programs. Before the actual correlation of data, full scale versus wind tunnel, accuracy for both types of data should be subject to strict evaluation and interpretation prior to any conclusion. Predictions must be made before comparing flight test and wind tunnel data. As aircraft development programs proceed the configuration evolves and changes. By the time the actual aircraft flies there is little motivation to obtain wind tunnel data on an exact replica of the flight test aircraft. This fact hinders aircraft flight test and wind tunnel comparison and degrades usefulness of future tunnel programs. Correlation of flight test and wind tunnel data should be encouraged throughout the wind tunnel industry as a means of keeping abreast with current difficulties and improvements.

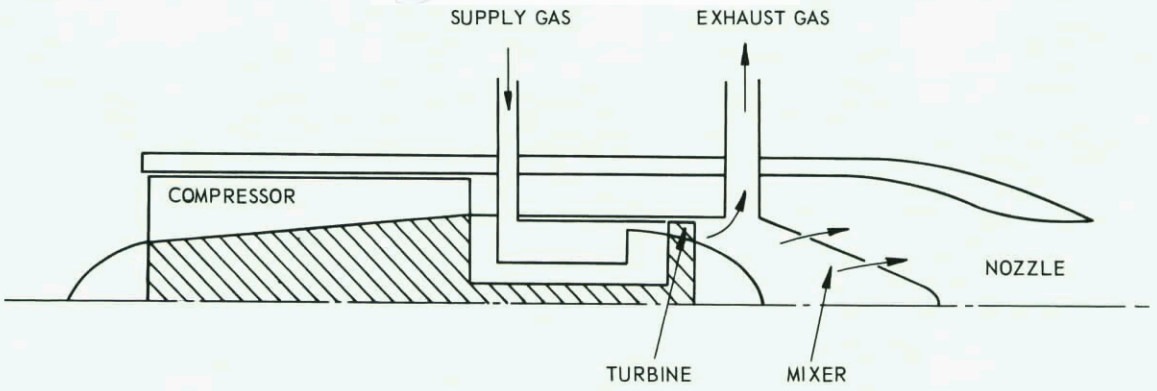

FIG. IV. 30 MINIATURE TURBINE DRIVEN ENGINE SIMULATOR

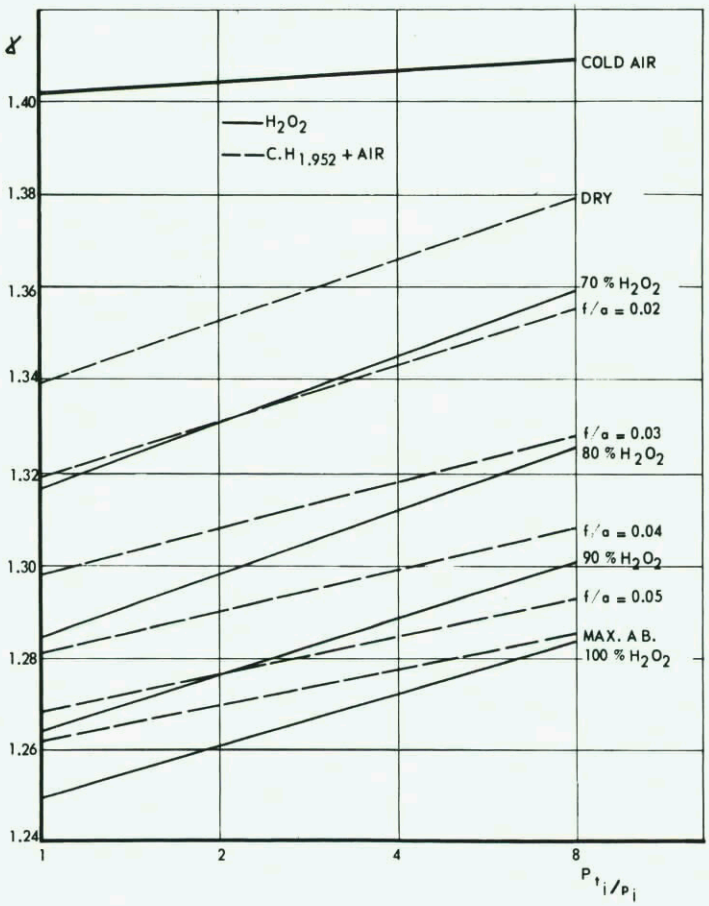

FIG. IV. 31 RATIO OF SPECIFIC HEATS AS A FUNCTION OF EXPANSION RATIO
(f/a = FUEL / AIR (MASS) RATIO)

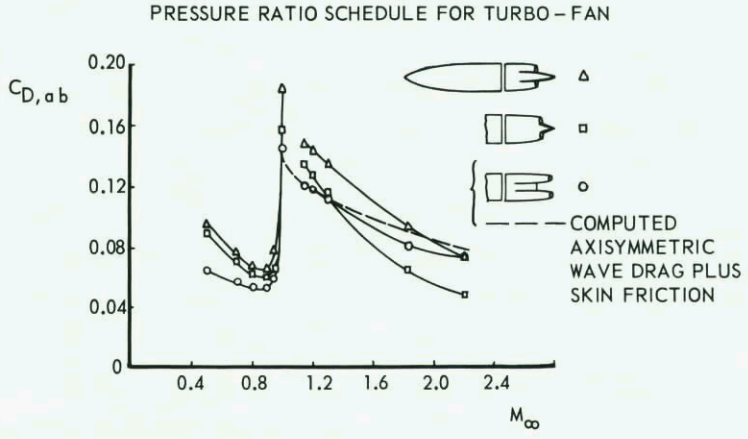

FIG. IV. 32 EFFECT OF JET – EXIT AXIAL LOCATION ON AFTERBODY DRAG
AND COMPARISON WITH COMPUTED DATA

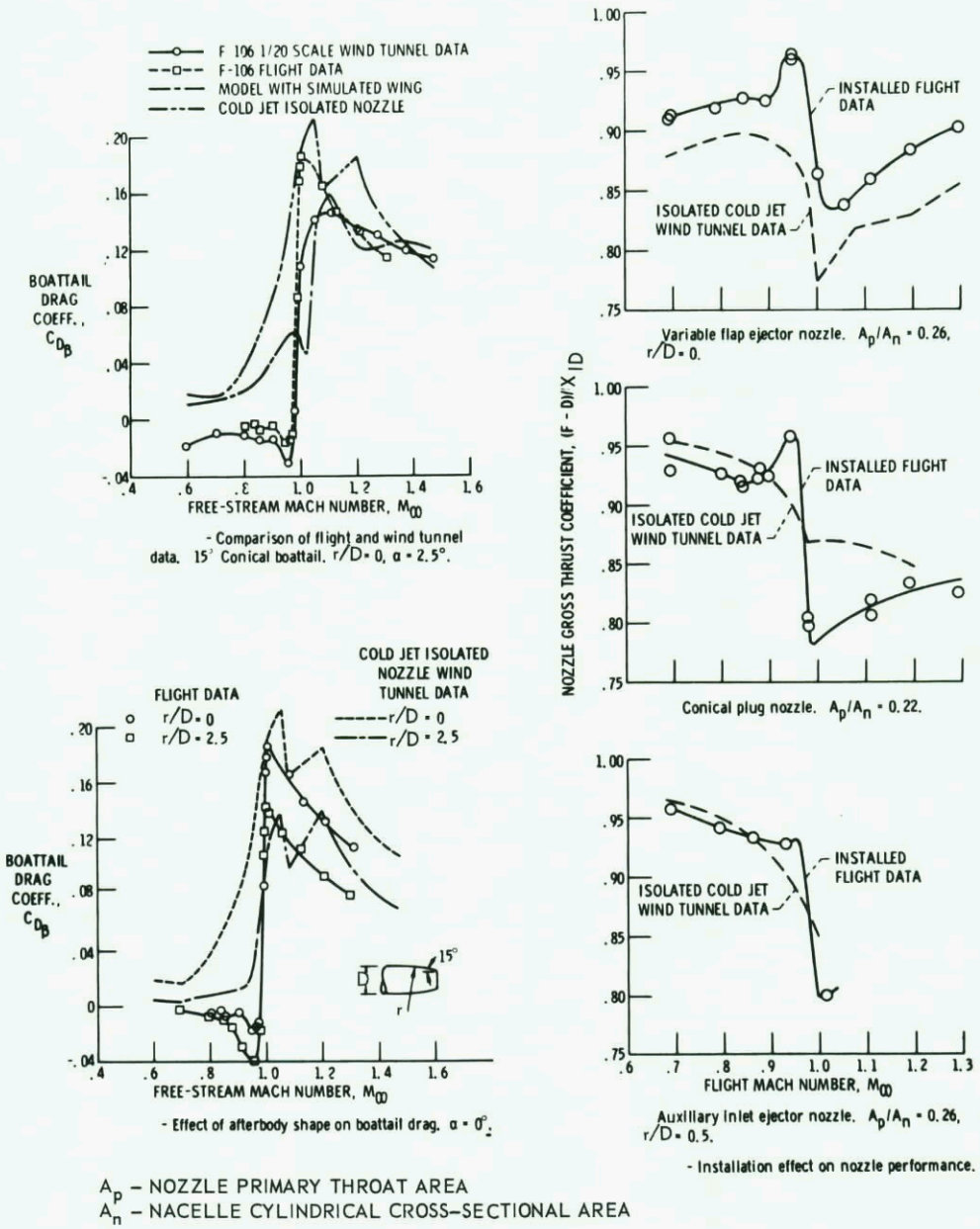

A_p – NOZZLE PRIMARY THROAT AREA
A_n – NACELLE CYLINDRICAL CROSS-SECTIONAL AREA

FIG. IV. 33 COMPARISON BETWEEN WIND TUNNEL DATA AND FLIGHT DATA ON AFTERBODY – NOZZLE PERFORMANCE OF SMALL ENGINES LOCATED UNDER THE AFT END OF THE DELTA WING OF A F – 106 AIRCRAFT

B NON-STATIONARY EFFECTS

As is noticed in fig. IV.9 large pressure fluctuations may be generated at the base and nozzle region at transonic speeds. For some nozzle systems, particularly the ejector type nozzles, interaction occurs between the internal flow, external flow, and the elastic nozzle leaves resulting in destructive instabilities.

Fixes have been obtained by trial and error, using common sense, and must be accomplished by aerodynamic means without deterioration of the nozzle performance (Ref. H.18). Little fundamental knowledge exists on this phenomenon. The problem is very complex since mutual interaction exists between the generated sound pressure field, mixing, vortex formation, separation (internal and external), geometry (sound reflection) and structural dynamic characteristics.

4.2 JET-AIRFRAME INTERFERENCE (EXCEPT THRUST-DRAG)

In many aircraft configurations the propulsive jets may influence the flow on nearby or far surfaces causing phenomena such as change in pressure distribution, shock wave-boundary layer interaction, flow separation, surface heating and unsteady loads. These interferences depend on the engine power setting. If these phenomena are expected to occur, wind tunnel tests with full nozzle blowing should be performed for assessing the increments (in lift, moment, drag) due to the jet interference. Fig. IV.34 gives a general impression how moment and lift increments due to jet effects can be determined. Normally the testing schemes are similar or even identical to the schemes for interference drag determination. During these tests the complete external flow should be simulated, hence isolated tests are not performed. This means that complete models or semi-models are used. Semi-models can be utilized if it is certain that the reflection plate boundary layer does not deteriorate the phenomena to be examined.

Since the jet interference phenomena and the testing techniques in the wind tunnel depend primarily on the aircraft configuration, the discussion in the following sections will take place according to the configuration catagory.

In these sections the problems will be formulated, and the applied techniques will be discussed.

4.2.1 SUBSONIC TRANSPORT

A WING MOUNTED FAN ENGINE

For these configurations the jet efflux considerably affects the local wing circulation and shock development due to the large mass flow and close position under the wing. Also the wing pressure field has a remarked influence on the flow in which the effluxes operate, affecting the shape of the sonic line and hence, altering the engine mass flow and net thrust. Therefore more attention must be paid now-a-days to these installations, than the formerly similarly installed turbo jets required.

The jet simulation parameters generally are the same as discussed in section 4.1.3. The main parameters are the jet plume shape, jet cell structure and wave reflections, which can be expressed in terms of nozzle pressure ratio and ratio of specific heats of the jet, assuming convergent nozzles only. However for these installations the far jet field is also important. Since the engine mass flow is relatively large the contraction or diversion of the effective jet stream as felt by the external flow due to the mixing effect may have a marked influence on the pressure distribution on the wing and fuselage, especially at transonic speeds. Simple analysis neglecting the kinetic energy of the flow with respect to the sensible enthalpy as a first approximation, shows that the jet mixing has a marked influence on the effective stream tube area, as may be seen in figure IV.35.A. In this figure n is the ratio of the free stream mass flow, that has been mixed with the jet flow, to this jet mass flow. It must be recognized, however, that at a given nozzle pressure ratio the nozzle mass flow $(A\rho)_j$ decreases as the square root of the $(RT)_j$ value at increasing jet temperature. This dependence on $(RT)_j$ mainly reduces the effect of jet temperature on the effective jet stream tube if the jet spreading were to be the same. Furthermore, it is well known that the temperature spreads faster due to turbulent mixing than the velocity (Ref. S.5 and S.7), which means that n should be larger than concluded from equal spreading characteristics. In general it can be stated that n depends on the detailed mixing of the jet with the external flow. Fig. IV.35.A can also be used for the effective jet stream tube near the core region of the jet. In that case the areas must be defined as indicated in the accompaning sketch, and n has an approximate constant value of the order unity, along the core region. Hence if $A_x/A_j < 1$ the jet acts as a suction region due to mixing. If $A_x/A_j > 1$ the external flow is deflected outward and the mixing acts as a source distribution along the jet boundary. In the latter case external gas heating is larger than external gas suction. The limit which the effective stream tube of the jet will obtain at long distances behind the exhaust ($n \rightarrow \infty$) is indicated in fig. IV.35.B.

Fig. IV.36 gives results of a more detailed analysis of the influence of the jet properties on the effective engine stream tube due to mixing. In this case the engine inlet mass flow is kept constant. The stream tubes have been calculated by assuming constant external pressure and turbulent or laminar mixing. Cases 1-1a, 2-3 represent tests where an engine simulator is used (as will be assumed in chapter V). Case 1 represents a turbojet and turbulent flow; Case 1a, the same case, but with a region of laminar mixing. Case 2 represents a bypass engine, and Case 3, an engine simulator where the mass flow of the nozzle is increased to satisfy the condition of equal exhaust area and Mach number, but with different temperature. Then the increase in mass balances the difference in temperature. The data of the engines are given in the figure. Case 4 is a through flow nacelle when the engine simulator is not used. Then the geometry of the engine cannot be simulated and the exhaust is much larger than required for simulation.

From preliminary studies (Ref. R.9), utilizing a shaft mounted fan engine nozzle (similar to fig. IV.19, but with boundary layer suction) blowing under a two dimensional wing, it is shown that the jet mainly influences the wing lower side pressure distribution. The differences in pressure distribution with respect to the isolated wing is, however, very large at both sides. From these tests it can be concluded that the reference aeroforce models tests should include the podded nacelles under the wing, either geometrically scaled such that the inlet mass flow is too small, or with increased exhaust such that the inlet mass flow is scaled. The main difficulty is how to represent the actual jet flow and not to disturb the effects of the inlet mass flow. Various approaches are in use, of which the most representative one is thatutilizing the small turbine driven jet simulators discussed in chapter V.

A cheaper but less representative way is the use of ejectors with multiple primary injection nozzles. This technique is however better suited for lifting fan engine representation of V/STOL models in wind tunnels. The main disadvantages of ejectors are the low secondary to primary flow ratios (of the order of

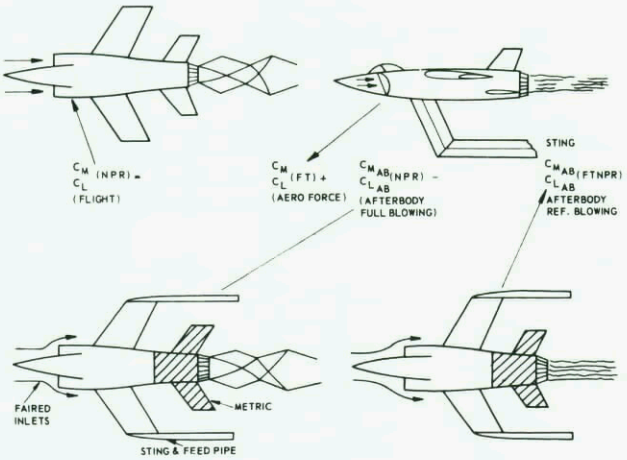

FIG. IV. 34 MOMENT AND LIFT INCREMENT DETERMINATION DUE TO JET EFFECTS

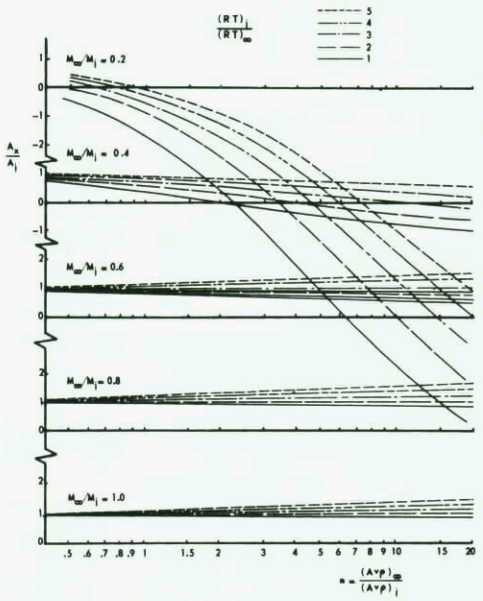

FIG. IV. 35a EFFECT OF MIXING RATIO N ON THE EFFECTIVE JET STREAM TUBE AT VARIOUS JET TEMPERATURES AND MACH NUMBERS (CONSTANT PRESSURE FIELD)

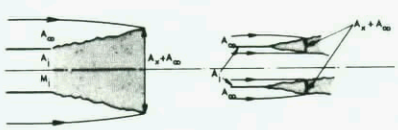

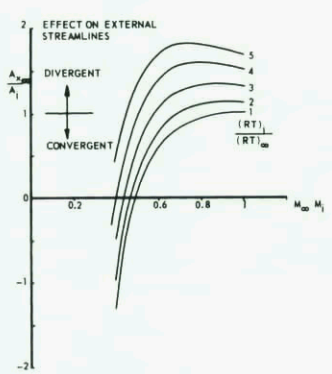

FIG. IV. 35b EFFECT OF JET TEMPERATURE AND MACH NUMBER ON THE FAR DOWN STREAM EXTERNAL FLOW FIELD

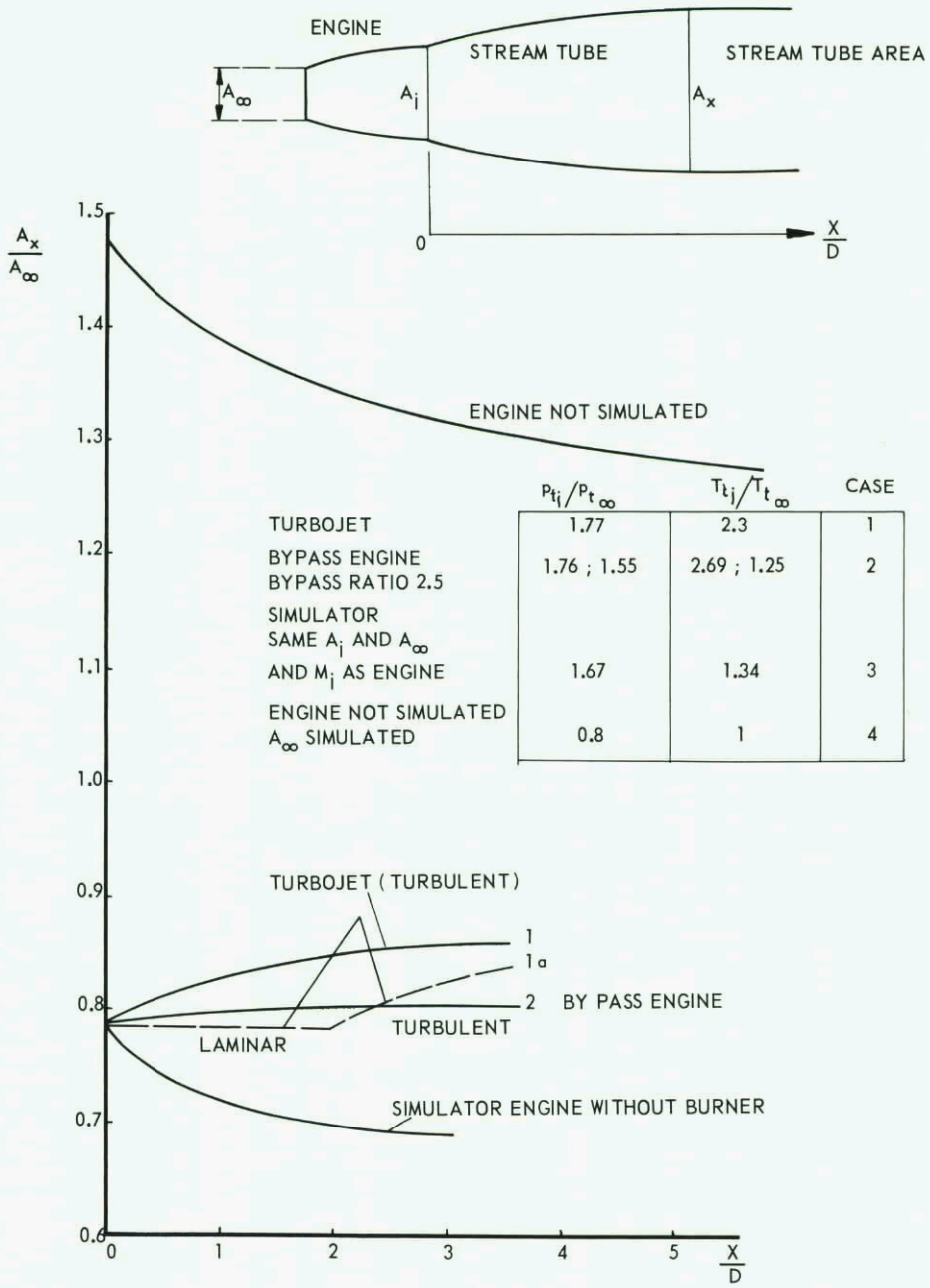

FIG. IV. 36 VARIATION OF JET ENGINE EFFECTIVE STREAM TUBE DUE TO MIXING

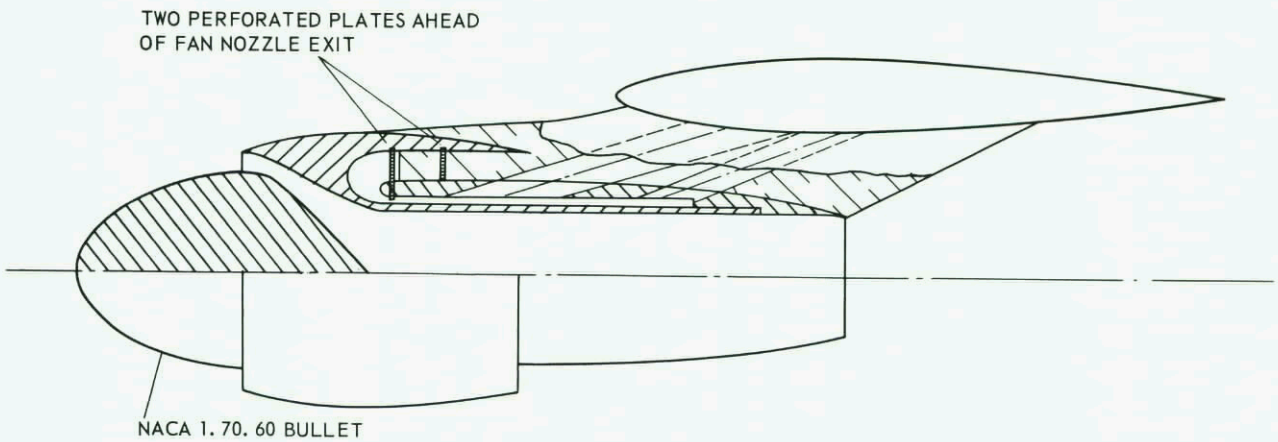

FIG. IV. 37 BLOWN FAN COWL MODEL INSTALLATION WITH PARTICAL INLET MASS FLOW SIMULATION

of 2 : 1), the difficulty of determining the secondary inlet flow under wind tunnel conditions, and the considerable flow distortions due to the primary jets in the exhaust jet.

The next step is to utilize direct blowing of the jets and do something with the inlet flow such that the external flow around the fan cowl is best represented. In general with fan engines the simulation of fan jet is much more important than the simulation of the primary jets. This had led to the technique of Ref. P.17 and shown in fig. IV.37. The bullet shaped body in the inlet simulates the approach stream line on the fan inlet lip. From the results as determined by pressure plotting it appeared that with respect to the reference flow through the nacelle the pressure distributions on the wing, pylon and fan and turbine cowl hardly changed by inserting the bullet and by blowing the fan jet as reference. By full blowing of the fan jet the pressure distribution on the lower side of the wing was affected markedly, as were the pressureson the turbine cowl. On the fan cowl only the pressure distribution at the aft end was affected by blowing. (Also the inlet lip suction changed somewhat, but this must be due to static pressure changes at the free flow turbine exhaust resulting in increased spillage).

The method of direct blowing of the fan and turbine jets with complete inlet fairing has the main advantage that both jets can be represented as accurately as possible, for example using for the fan jet cold or slightly heated air and for the hot turbine jet hydrogen peroxide. Fig. IV.38 depicts such a simulator, where, however, the purpose was to determine jet effects (also heating) on the tail planes of a small airliner with engine installation at the upper side of the wing.

In general for podded fan engines particularly for wing installed engines, three components can be distinguished, namely Inlet (I), Exhausts (E) and Wing plus pylon (W) for the mutual interference problem. The question for engine simulation in the wind tunnel can then generally be written as:

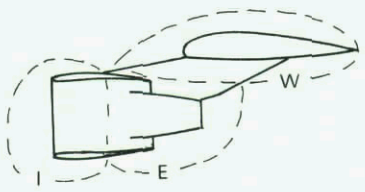

$$[(I + E) \rightarrow W] \stackrel{?}{=} [I \rightarrow W] + [E \rightarrow W]$$

where $[A \rightarrow B]$ means the effect of component A on B with respect to the reference conditions. Although not proven this question can be answered positive with good accuracy if one interference term on the R.H.S. is small with respect to the other one. From the tests as depicted in Ref. P.17 and the result shown in Fig. II.27 it can be concluded that the exhaust interference on the wing pressure distribution is many times larger than interference from completely or partially fairing the inlet. This means that addition of the interference effects is probably allowed. For the installed thrust-minus-drag evaluation the similar question

$$[(W + I) \rightarrow E] \stackrel{?}{=} [W \rightarrow E] + [I \rightarrow E]$$

must be answered. Also in this case separation can be allowed since from some examples it is indicated that $[I \rightarrow E]$ is very weak provided, the inlet fairing shape has been carefully determined.

With all these techniques semi-model measurements are more easily accomplished than complete, sting mounted model tests, and better accuracy is achieved due to the higher Reynolds number. The reflection plate boundary layer probably does not interfer significantly. Usually both pressure plotting and balance measurements are used. The better results are obtained if the engine simulator is separately weighed from the wing, with the metric line between simulator and wing being carefully chosen along the pylon.

In Ref. G.7 the engine simulators are separately mounted under a complete aircraft model in subsonic wind tunnel for jet interference measurements on the tail planes. Though not transonic, this work is mentioned here since it utilized a unique simulation technique as is shown in figure IV.39. The bypass jet is produced by an electric motor driven fan. The motor is located inside the nacelle driving the fan with a speed up to 30,000 r.p.m. For the turbine jet compressed air is used. In order to simulate the correct inlet mass flow an adequate quantity of air is sucked through a slot at the inlet tip. However, for transonic speeds the fan pressure ratio obtainable would not be sufficient and the heavy engine mounting struts could not be allowed.

B REAR FUSELAGE MOUNTED ENGINES

The aerodynamics of the afterbody of a fuselage containing the tail planes will be influenced by the jet efflux, either by direct impingement or by the constraint of the external flow. The influence of the engine on the wing pressure distribution is mainly caused by the inlet flow. The main phenomena caused by the exhaust jets can be a change in aircraft drag, change in angle of attack of the tail planes (hence causing change in pitching moment), surface heating (in case of direct impingement of the jets on for example brake flaps) and non-stationary aerodynamics (acoustic fatigue).

The basic measuring and jet simulation techniques as discussed in A, also apply in this case, but balance measurements seem to be more difficult. Half model techniques are not recommended, because the fuselage flow field is unrepresentative in the region of the jet interference with the rear fuselage due to the reflection plate boundary layer. Complete models require the use of wing stings and rear fuselage balances or pressure plotting. The air or jet fluid required for the jet simulators must be fed through the wings, fuselage and strut supports of the simulators to the nacelles, generally at high pressures. If balances have to be bypassed by the jet fluid the system must be located in the fuselage. However in most circumstances the simulators will be non-metric and the rear fuselage, tail planes, and/or tail brakes will be metric as far as the jet influence is expected.

Fig. IV.40 yields a cross-sectional view of a gasoline-air burner as used in a subsonic wind tunnel, simulating a low bypass jet engine installed at the fuselage aftend. The aim of the tests performed with simulator was to determine the forces (stationary and non-stationary) and heating of aft fuselage brake flaps under descent conditions. The jet flow could be well represented.

4.2.2 INTEGRATED AIRFRAME-ENGINE SYSTEMS

The main jet effects on the airframe aerodynamics occurs if the jet nozzle(s) are located upstream of the fuselage aftend and/or tail planes. If the nozzles form the fuselage aftend, the jet may cause effects on the fin and tail planes, for example separation due to pluming. The treatment of these latter cases is similar to that as discussed in the complete section 4.1. The jet simulation parameters are similar and the technique which must be followed to determine the lift and pitching moment increments are similar to those to determine the afterbody drag (see figure IV.34). In these cases the jet nozzle and engine simulator can be non-metric and the afterbody metric on a multi-component balance. Increment

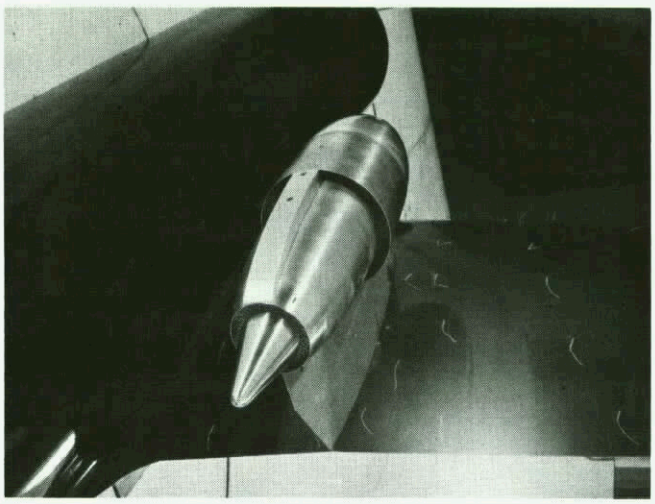

FIG. IV. 38 COLD FAN JET AND HOT TURBINE JET SIMULATOR WITH FAIRED INLET FOR DETERMINATION OF JET EFFECTS ON FLAPS AND TAILPLANES

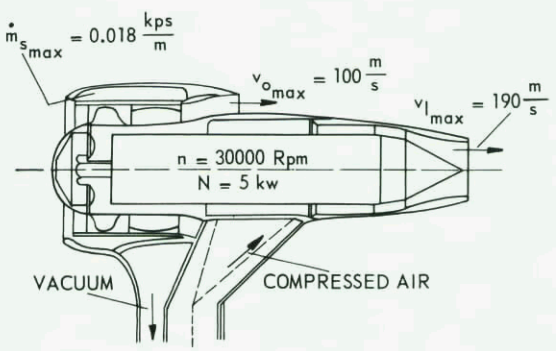

FIG. IV. 39 COMPLETE FAN ENGINE SIMULATOR FOR SUBSONIC USE

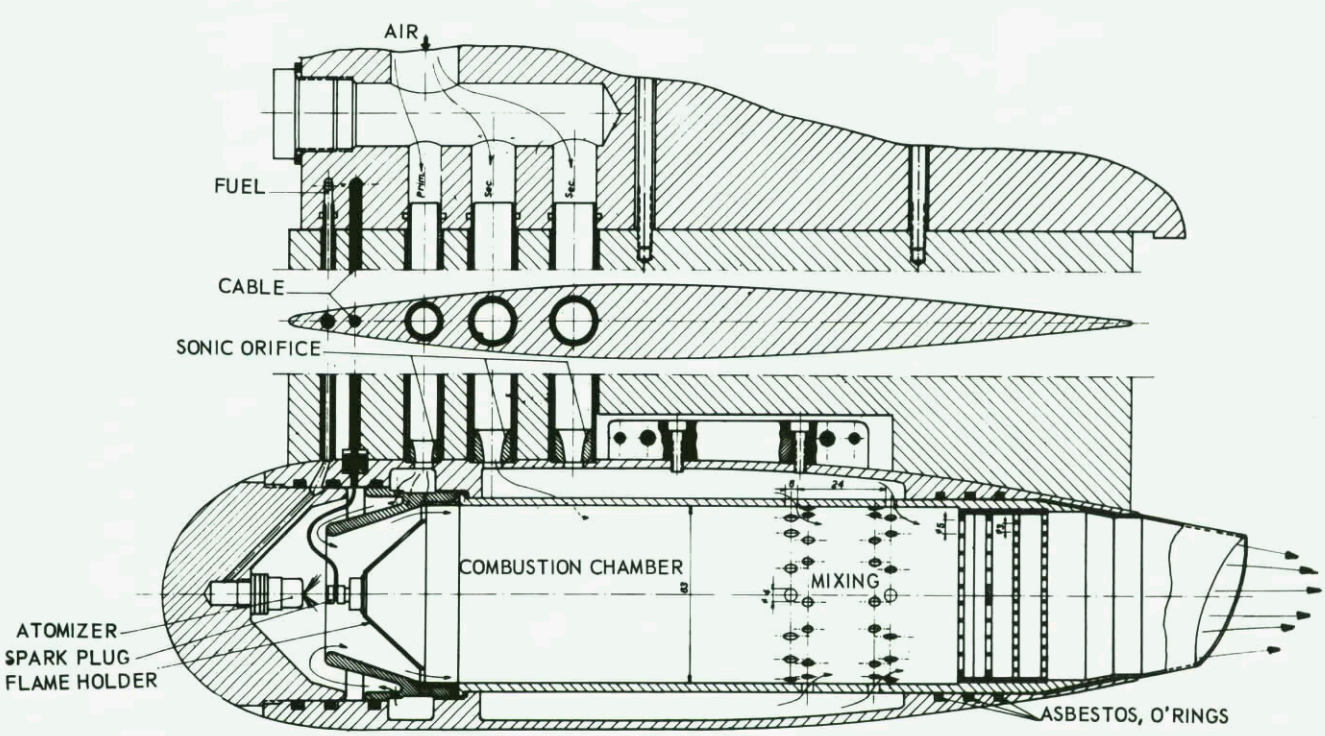

FIG. IV. 40 LOW BYPASS ENGINE SIMULATOR WITH GASOLINE BURNER; INLET FAIRED

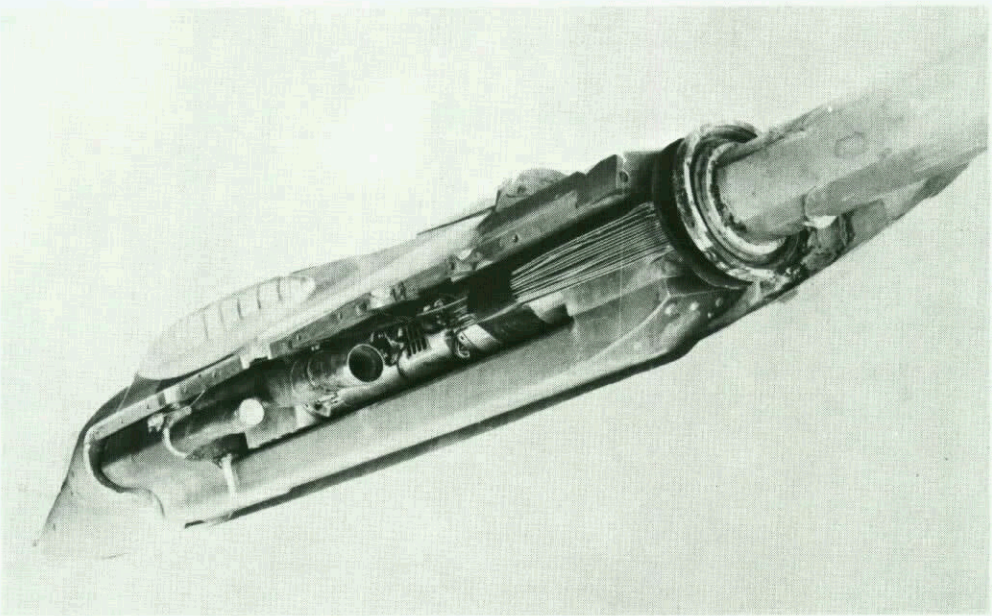

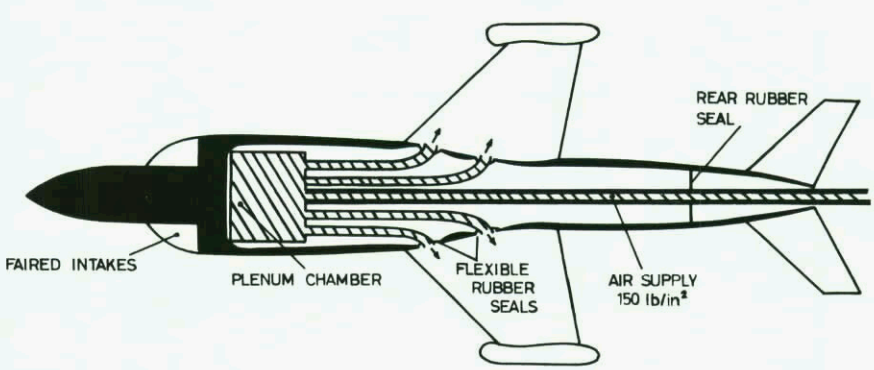

FIG. IV. 41 DIRECT BLOW FOUR, COLD JET EXHAUST SYSTEM, FAIRED INLETS

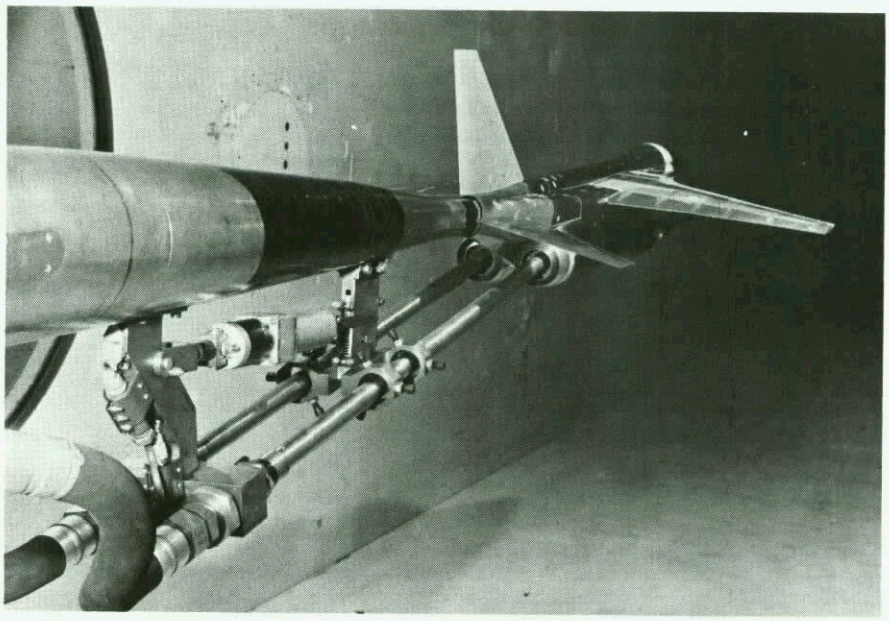

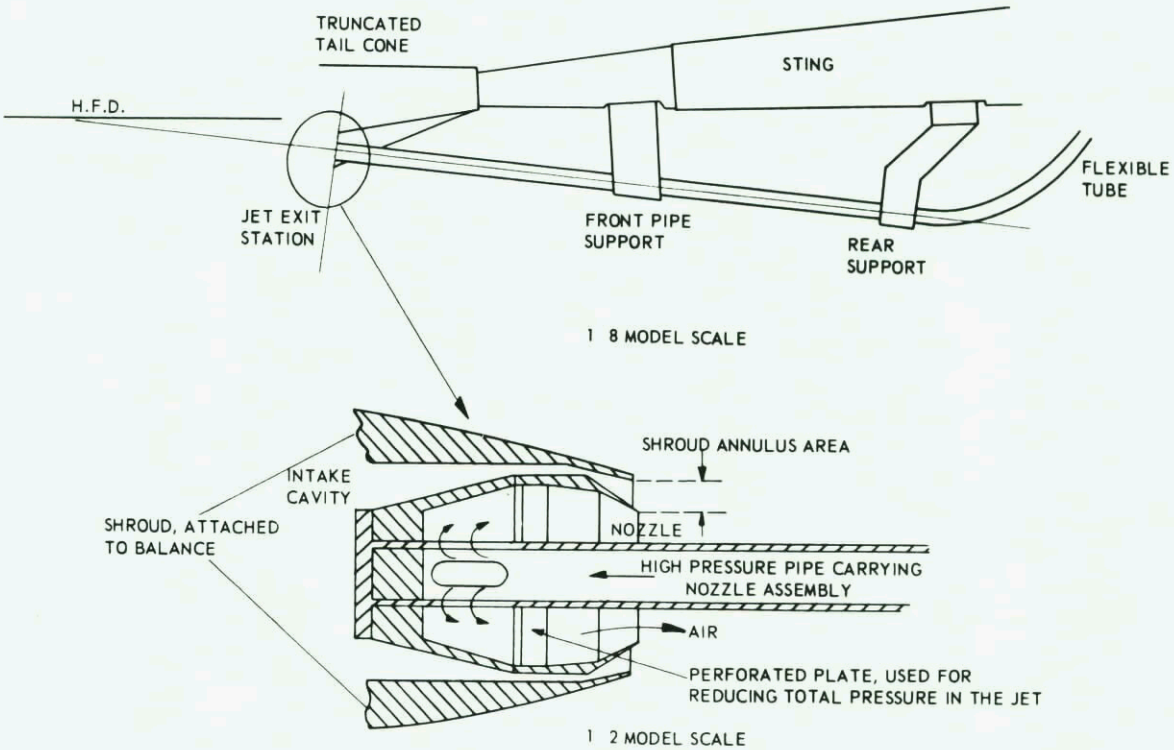

FIG. IV. 42 ARRANGEMENT FOR DUCTING HIGH PRESSURE AIR TO JET EXIT NOZZLES FOR TESTS WITH FAIRED INLETS

determination from pressure plotting is not very attractive due to the large pressure gradients at the fuselage aftend.

If the nozzles are upstream of the fuselage aftend the jets can have important effects on the afterbody and tail plane pressure distributions, and tail plane hinge moments and may cause acoustic fatigue in the rear aircraft structure. These effects may be particularly important when the jets are not aligned with the body axis. The jet parameters are similar as discussed before, jet plume shape and jet mixing are probably the main jet characteristics to be simulated. For non-stationary phenomena and surface heating, hot jet tests are required.

Fig. IV.41 depicts a direct cold air blowing system for exhaust jet flow simulation on a fighter type model. The model is mounted on a standard 6-component balance. Air which passes up the centre of the sting bypasses the balance through a parallel duct into a plenum chamber ahead of the balance. From this plenum chamber 4 ducts are fed rearwards into the exit nozzles of the mode. The whole of the blowing system is earthed and flexible seals are fitted between the model jet pipes and jet shrouds, and also between the model rear fuselage and sting. The latter seals being necessary to eliminate cross flows within the model. Seal constraint interference is measured by calibration with the model installed on the balance. Pressure constraints are obtained by section pressuring of the model. The direct air flow quantities were about 5 lbs/sec. at maximum pressure ratio. A faired inlet was used for these tests, with the effects of inlet spillage and a fully faired inlet being measured in a separate test. A major problem in these tests is the definition of the allocation of seal area between metric and non-metric model parts; small areas in this region can have significant effects on measured axial force.

Fig. IV.42 shows another useful way to simulate the initial part of the propulsive jet by cold air. The jet flow is brought up to the model in long thin pipes from behind the model of a strike-fighter aircraft. A six component balance measures all the forces on the model in the presence of the jet flow except, of course, the jet thrust and the nozzle base force. Pressures are measured in the balance cavity and in the cavity formed by the blanked-off intake duct. This blanked-off duct is ventilated to the annular "clearance" area between the earthed nozzles and the aircraft afterbody. This test was extended by measurements representing correct or partial inlet spillage with natural blowing exhausts either increased in area or geometrically scaled respectively. The object of this experiment was to obtain the effects of both intake spillage and jet pressure ratio on all the forces (6 components) measured on the same model. Variation of inlet flow and of jet pressure ratio were made separately. Care was taken to try to isolate the effect of variation of each of these and to minimise spurious effects caused by misrepresentation of the other variable occurring at the same time.

4.2.3 FINAL REMARKS

The results as obtained from models where the jet effects on the airplane flight characteristics are determined, are usually reported as they are obtained. If corrections are applied they are the same as those applied to other wind tunnel model tests. At the present time the scale effects on jet interference have not been evaluated. More work is needed in this area, because of incipient separation problems which are caused by jet effects and still little understood.

The required and achieved accuracies are usually in harmony with that obtained with complete model tests using internal balances. The main inaccuracies particularly a drag force stem from geometric modifications and from sealing corrections.

In the literature no data are available which give comparison between jet effects in the wind tunnel and jet effects in flight on airplane flight characteristics.

4.3 REFERENCES AND GENERAL BIBLIOGRAPHY (ALPHABETIC ORDER)

4.3.1 CATEGORY INDEX

External flow	0	no flow
	1	subsonic
	2	transonic
	3	supersonic
Jet flow	A	incompressible (subsonic)
	B	compressible (sonic or supersonic)
Configuration	I	smooth boat tail, no separation
	II	base, separation
Direction of jet	a	parallel to external flow
	b	makes angle to external flow
Number of jets	x	one jet (also more jets if no mutual interference)
	y	more jets
	Jets	general discussion of jets
	Jet simulation	general discussion of jet simulation in wind tunnels

Category	Author Index Symbols
OA ... x	C2, C3, C4, C5, G1, H1, H2, H3, K2, K3, L2, M2, S2, S3, S4, S5, W1, W2
OAIax	N5, S27
OA ,,, y	G1, K4, L2
OAIbx	E6, M11, W7
OAIIay	T5
Ob ... x	A2, A3, B1, C2, C6, E1, G1, G2, H2, H4, H5, H13, J2, J3, L3, L4, L5, L6, M3, M4, P2, P4, P5, R2, R3, R4, S21, V3, V4, W3, W4
OBIax	B18, J7, P15, R14, S20
OB ... y	C7, G1, H15, J4, M5, S23, V4, W12
OBIay	B18, E7
OBIbx	C16
OBIby	H10, R10
OBIIay	G6, L12
1AIax	F2, F3, H6, K2, M6, M7, P6, P7, P8, S1, S5, S6, S7, S8, S9, S10, S25, T3, U1, W5, W11, G7
IAIbx	F1, P9, S6, W7, W11, R15, W13, S29, G7
1AIby	E6, S19, W9
1AIIax	G5
1AIIbx	B2, J5, K5
1AIIby	O1
1BIax	B10, B18, G4, S20, W5, Z1, E7
1BIay	B18, J4, K11, R9, S17
1BIby	B14
1BIIax	C14, S11, W8, A12, M17, M19, C22
1BIIay	A8, A9, L12, W8, D5, M17, M19, C22
2AIax	H9, K6
2AIIay	K6, T5
2BIax	A5, B10, B18, C8, D4, H7, K7, K9, L7, M16, R1, S12, S20, H16, P17
2BIay	B8, K11, M13, S18
2BIbx	L8, N1, P9, S13
2BIby	B14, B15
2BIIax	A5, C8, C9, C10, C11, C15, C19, E2, G3, H7, H12, H16, K6, K10, L13, M8, M10, N1, N2, R5, R6, R8, S13, S14, S15, S16, W6, W8, A12, L15, W14, C22, H18, C23, C24, F3, N6, M20, C25
2BIIay	A8, A9, B19, G3, G4, K6, L14, M12, N2, W8, R17
2BIIbx	L8, N1, P9, S13
2BIIby	L8
3AIIax	C12
3BIax	A4, A5, B3, B4, B5, B6, B18, D4, E3, E4, K7, K8, K9, L3, L9, L10, L11, M4, M17, P2, P3, P10, P11, P12, P13, R4, S1, S20, V20, E7, C20, F4
3BIay	B18, H9, N3
3BIbx	B5, E5, P9, O2, C21, S28
3BIIax	A4, A5, B7, B8, B9, B13, B17, C12, C13, C14, C15, C19, D1, G3, H11, H12, J6, K10, N4, P2, P3, P14, R4, R8, R11, S22, W8, L17, C22, H18 ,B6
3BIIay	A7, A8, A9, A10, B19, C14, G3, G4, L14, M9, N3, N4, P3, S18, W8, M18, L16, C22, C23, C24
3BIIbx	H8, T4
Jets	A1, A6, B11, B12, C17, C18, D2, D3, H14, K1, M14, M15, P1, R7, R12, S24, R16, S30
Jet Simulation	A11, A13, B19, B20, C1, G4, J1, K11, L1, M1, P2, P3, R1, R13, S1, S19, S26, T1, T2, V1, W10, P16, M11, M18, W14, H17, M17, M19, S31

4.3.2 AUTHOR INDEX

A1	G.N. Abramovich	The Theory of Turbulent Jets. Cambridge MIT 1963	Jets
A2	T.C. Adamson and J.A. Nicholls	On the structure of Jets from Highly Under-expanded Nozzles into Still Air. Journal of Aerospace, Sc.Vol. 26 no. 1, 1959.	OBX
A3	A.R. Anderson and F.R. Johns	Characteristics of Free Supersonic Jets Exhausting into Quiescent Air. Jet Propulsion, vol. 20 no. 1, 1955.	OBX
A4	Anonymus	The Aerodynamics of Supersonic Powerplant Installations. Aircraft Engineering, Febr. 1969.	I 3B ax II
A5	R.C. Ammer and W.F. Punch	Variable-Geometry Exhaust Nozzles and their Effects on Airplane Performances. SAE paper, 680295.	I 2B ax 3 II
A6	G.N. Abramovich	An Investigation of the Turbulent Jets of Different Gases in a General Stream. Astronautica Acta, vol. 14, no. 3, March 1969.	Jets
A7	L.J. Alpinieri	Flow Separation due to Jet Pluming. AIAA Journal, vol. 4, no. 10, October 1966.	3BIIay
A8	J.L. Allen	Base Flow Aerodynamics of a Saturn-type Booster Stage at Mach numbers 0.1 to 2.0. NASA TN D 593, 1962.	1 2BIIay 3
A9	J.L. Allen	Base Heat Transfer, Pressure Ratio's and Configuration Effects Obtained on a $\frac{1}{27}$ Scale Model of the Saturn (C1) at Mach numbers from 0.1 to 2. NASA TN D 1566, 1963.	1 2BIIay 3
A10	R.H. Adams	Wind Tunnel Simulation of Rocket Vehicles in Flight with two-phase flow Rocket Plume. Journal Spacecraft Rockets, April 1967.	3BIIay
A11	Anonymus	Fan Jet Simulators. Tech. Development Inc., Dayton, Ohio. Data Sheet 1968.	Jet simulation
A12	R.S. Armstrong and S.R. Miller	Subsonic Aerodynamic Performance of Nozzle Installations in Supersonic Airplanes. Journal of Aircraft, vol. 5, no. 3, 1968.	$^{1}_{2}$BIIax
A13	Anonymus	Hot Jet Simulation Facility of N.L.R. Wind Tunnel. N.L.R. publication, March 1968.	Jet simulation
B1	D. Bershade and S.I. Pai	On Turbulent Jet Mixing in Two Dimensional Supersonic Flow. Journal of Applied Physics, Vol. 21, 1950.	OBX
B2	L.J.S. Bradbury and M.N. Wood	The Static Pressure Distribution Around a Circular Jet Exhausting Normally from a Plane Wall into an Airstream. RAE TN Aero 2978, 1964.	IA II bx
B3	W.E. Bresette	Some Experiments Relating to the Problem of Simulation of Hot Jet Engines in Studies of Jet Effects on Adjacent Surfaces at a Free Stream Mach number of 1.80. NACA RML56 E 07, 1956.	3BIax
B4	W.E. Bresette and A. Leiss	Investigation of Jet Effects on a Flat Surface Downstream of the Exit of a Simulated Turbojet Nacelle at a Free stream Mach number of 1.39. NACA RML55 L 13, 1956.	3BIax
B5	W.E. Bresette	Investigation of the Jet Effects on a Flat Surface Downstream of the Exit of a Simulated Turbojet Nacelle at a Free Stream Mach number of 2.02. NACA RML54 E05a, 1954.	3BI$^{a}_{b}$x
B6	W.E. Bresette and M.A. Faget	An Investigation of Jet Effects on Adjacent Surfaces. NACA RML55 E06, 1955.	3BIax
B7	E.L. Baughman and F.D. Kochendorfer	Jet Effects on Base Pressures of Conical Afterbodies at Mach 1.91 and 3.12. NACA RM E57, E06, 1957.	3BIIax

B8	M.A. Beheim, J.L. Klann and R.A. Yeager	Jet Effects on Annular Base Pressure and Temperature in a Supersonic Stream. NASA TR R-125, 1962.	3BIIax
B9	F.P. Boynton	Composition in the Far Field of a Rocket Jet Mixing with Air. Journal of Spacecraft, vol. 3, no. 6, June 1966.	3BIIax
B10	J.A. Beagley	Wind Tunnel Experiments on the Interference Between a Jet and a Wing at Subsonic Speed. AGARD CP.35, Transonic aerodynamics.	$^{1}_{2}$BIax
B11	B.J. Blaha and D.L. Dresnahan	Wind Tunnel Installation Effects on Isolated Afterbodies at Mach numbers from 0.56 to 1.5. NASA TM X-52581, 1969.	Jets
B12	D. Bechert	Zweidimensionale Strahl-Steuerung. Teil 1: Ein Ebener Freistrahl in einer Stationären Seitlichen Strömung. (Theorie). DLR FB 69-11, 1969.	Jets
		Teil 2: Ein ebener Freistrahl mit einer Schneide in Stationären Seitlichen Strömung. (Theorie) DLR FB 69-12, 1969.	Jets
		Teil 3: Ein Ebener Freistrahl in Stationären Seitlichen Strömung ohne und mit Schneide. (Messungen) DFR FB 69-13, 1969.	Jets
B13	J.E. Bowman and W.A. Clayden	Cylindrical Afterbodies in Supersonic Flow with Gas Injection. AIAA journal, vol. 5, no. 8, August 1967.	3BIIax
B14	J. Bärche und G. Kranz	Strahleinfluss an V/STOL Flugzeugen in Ubergangs- und Hochgeschwindigkeitsflug. Luft und Raumfahrttechnik, Band 15 no. 5, 1969, Mai.	$^{1}_{2}$BIby
B15	R.L. Berrier and O.C. Pendergraft Jr.	Transonic Aerodynamic Characteristics of Powered Models of Several Apollo Launch Escape Vehicle Configurations. NASA TN D 4843, 1968.	2BIby
B16	A.F. Bromm and R.M. O'Donnell	Investigations at Supersonic Speeds, of the Effect of Jet Mach numbers and Divergence Angle of the Nozzle upon the Pressure of the Base Annulus of a Body of Revolution. NACA RM L54I16, 1954.	3BIIax
B17	J.E. Bowman and W.A. Clayden	Boat Tailed Afterbodies at M = 2 with Gas Ejection. AIAA Journal, vol. 6 no. 10, Oct. 1969.	3BIIax
B18	J.F. Boytos	Gross Thrust Coefficient-Turbofan Engines. Journal of Aircraft, vol. 6, no. 6, Nov.Dec. 1969.	$^{0}_{1}$BIa$^{x}_{y}$ $^{2}_{3}$
B19	R.L. Berrier and F.H. Wood	Effect of Jet Velocity and Axial Location of Nozzle Exit on the Performance of a Twin Jet Afterbody Model at Mach numbers up to 2.2. NASA TND 5393, 1969.	Jet simulation $^{2}_{3}$BIIay
B20	M. Burnett	Development of a Hydrogen-Burning Annular Combustor for Use in a Miniature Gas Turbine. NASA CR 66362, 1969.	Jet simulation
C1	E.E. Covert	Jet Simulation in the Wind Tunnel. MIT Naval Supersonic Lab. TR 252, 1957.	Jet simulation
C2	W.L. Chow and H.H. Korst	On the Flow Structure within a Constant Pressure Compressible Turbulent Jet Mixing Region. NASA TND-1894, 1963.	$O^{A}_{B}x$
C3	Yih Chia-Shun	Temperature Distribution in a Steady Laminar Preheated Air Jet. Journal of Applied Mech., Vol. 17, no. 4, Dec. 1950.	OAx
C4	L.J. Crane and D.C. Pack	The Laminar and Turbulent Mixing of Jets of Compressible Fluid. Part 1: Flow far from the Orifice. Journal of Fluid Mech., Vol. 2 Part 5, July 1957.	OAx

C5	L.J. Crane	The Laminar and Turbulent Mixing of Jets of Compressible Fluid, Part II: The Mixing of Two Semi-Infinite Streams. Journal of Fluid Mech., vol. 3, Part 1, Oct. 1957.	OAx
C6	D.R. Chapman	Laminar Mixing of a Compressible Fluid. NACA TN 1800, 1949.	OBx
C7	J.M. Cubbage	Investigation of Exhaust Backflow from a Simulated Cluster of Three Wide-Spread Rocket Nozzles in a Near-Space Environment. NASA TND-3016, 1965.	OBy
C8	M.S. Cahn	An Experimental Investigation of Sting Support Effects on Drag and a Comparison with Jet Effects at Transonic Speeds. NACA RM L56 F 18a, 1956. NACA Report 1353, 1958.	$2B^{I}_{II}ax$
C9	J.M. Cubbage	Jet Effects on Base and Afterbody Pressures of a Cylindrical Afterbody at Transonic Speeds. NACA RM L 56, C 21, 1956.	2BIIax
C10	J.M. Cubbage	Jet Effects on the Drag of Conical Afterbodies for Mach numbers of 0.6 to 1.28. NACA RM L 57. B 21, 1957.	2BIIax
C11	J.M. Cubbage	Effect of Convergent Ejector Nozzles on the Boattail Drag of a 16^{o} Conical Afterbody at Mach numbers of 0.6 to 1.26. NACA RM L58 G25, 1958.	2BIIax
C12	W.L. Chow	On the Base Pressure Resulting from the Interaction of a Supersinic External Stream with Sonic and Subsonic Jets. Journal of Aerospace Sc. Vol. 26, No. 3, 1959.	3^{A}_{B}IIax
C13	E.M. Cortright Jr.	Some Aerodynamic Considerations of Nozzle-Afterbody Combinations. Aeron. Eng. Rev. Vol. 15, Sept. 1956.	3BIIax
C14	N. Charczenko and Cl. Hayes	Jet Effects at Supersonic Speeds on Base and Afterbody Pressures of a Missile Model having Single and Multiple Jets. NASA TN D-2046, 1963.	3BIIax 3BIIay
C15	D. Chamberlain	Measurement of Drag from Interaction of Jet Exhaust and Airframe. Journal of Aircraft, vol. 6, no. 2, March-April 1969.	$^{2}_{3}$BIIax
C16	M. Cox and W.A. Abbott	Jet Recirculation Effects in V/STOL Aircraft. Journal of Sound and Vibration, 1966 3(3) 396-406.	OBIbx
C17	S. Corrsin and M.S. Uberoi	Further Experiments on the Flow and Heat Transfer in a Heated Turbulent Air Jet. NACA TN 1865, 1949.	Jets
C18	E.B. Cook and J.W. Singer	Predicted Air Entrainment by Subsonic Free Round Jets. Journal of Spacecraft, vol. 6, no. 9, Sept. 1969.	Jets
C19	J.D.C. Coy	Thrust Augmentation of Rocket-Propelled Vehicles by Base Pressurization. AGARDograph 87, 1966.	$^{1}_{2}$BIIax 3
C20	P. Carrière	Recherches Récentes sur le Problème de la Pression de Culot. ONERA TP no. 18, 1963.	3BIIax
C21	L.J. Chrans and D.J. Collins	Stagnation Temperature and Molecular Weight Effect in Jet Interaction. AIAA Journal, vol. 8, no. 2, Febr. 1970.	3BIbx
C22	B.W. Corson and J.W. Schmeer	Summary of Research on Jet Exit Installation. NASA TM.X-1273, 1966.	$^{1}_{2}$BIIa$^{x}_{y}$ 3
C23	P. Carrière, M. Sirieix and J.H. Hardy	Problèmes d'adaption de Tuyères. AGARD, CP 34, 1968.	$^{2}_{3}$BIIax
C24	P. Carrière	Exhaust Nozzles. AGARD L.S. AGARDograph 12.	$^{2}_{3}$BIIax

C25	C.C. Crabs, E.O. Boyer and D.C. Mikkelson	Engineering Aspects and First Flight Results of the NASA F-106 Transonic Propulsion Research Aircraft. NASA TM.X-52559.	2BIIax
D1	M. Dryer and W.J. North	Preliminary Analysis of the Effect of Flow Separation due to Rocket Jet Pluming on Aircraft Stability During Atmospheric Exit. NASA-Memo 4-22-59E.	3BIIax
D2	H. Dissen und H. Schwantes	Versuchsanlage für Bodeneffectuntersuchungen bei Kurz- und Senkrechtstartern. D.L.R. Mitt.- 68-29, 1968.	Jets
D3	L.F. Donovan	Similarity Solution for Turbulent Mixing Between a Jet and a Faster Moving Coaxial Stream. NASA-TN D-4441, 1968.	Jets
D4	G.D. Dickie	Exhaust Nozzle Test Technique. AIAA paper 64-539, 1964.	1 2BIax 3
D5	W.M. Douglass	Aerodynamic Installation of High-Bypass-Ratio Fan Engines. SAE 660732, 1966.	1BIIay
E1	H.C. Eggers	Velocity Profiles and Eddy Viscosity Distributions Downstream of a Mach 2.2 Nozzle Exhausting into Quiescent Air. NASA TND-3601, 1966.	OBx
E2	K.D. Emmenthal	Basisdruck-Untersuchungen an Ebenen Gasstrahlen Unterschiedlicher Temperaturen und Geschwindigkeiten. DLR FB 65-59, 1965.	2BIIax
E3	G.W. Englert	Operational Method of Determining the Initial Contour of and Pressure Field about a Supersonic Jet. NASA TND-279, 1960.	3BIax
E4	G.W. Englert and R.W. Luidens	Wind Tunnel Technique for Simultaneous Simulation of External Flow Field About Nacelle Inlet and Exit Stream at Supersonic Speeds. NACA TN 3881, 1957.	3BIax
E5	F.E. Ehlers and T. Strand	The Flow of a Supersonic Jet in a Supersonic Stream at an Angle of Attack. Journal of Aerospace Sc.Vol. 25, No. 8, 1958.	3BIbx
E6	B. Ewald	V/STOL Windkanal. Messtechnik. Luftfahrttechnik und Raumfahrttechnik,Bd. 15 1969, Nr. 3, März.	$^{0}_{1}$AIb$^{x}_{y}$
E7	J.M. Eggers and M.C. Torrence	An experimental investigation of the Mixing of Compressible-Air Jets in a Co-axial Configuration. NASA TN D 5315, July 1969.	OBIay $^{1}_{3}$BIax
F1	H. Falk	The Influence of the Jet of a Propulsion Unit on Nearby Wings. NACA TM 1104, 1946.	1AI$^{a}_{b}$x
F2	W. Forstall, Jr. and A.H. Shapiro	Momentum and Mass Transfer in Co-axial Gas Jets. Journal of Applied Mechanics, Vol. 17 No.4, 1950.	1AIax
F3	A.E. Fuhs	Wave structure of Exhaust from Transonic Aircraft. Journal of Aircraft, in press 1971.	2BIIax
F4	R.A. Falanga	Exploratory Tests of the Effects of Jet Plumes on the Flow over Cone-Cylinder-Flare Bodies. NASA TN D-1000, 1962.	3BIax
G1	G.L. Gentry and R.J. Margason	Jet-induced Lift Loses on VTOL Configurations Hovering in and out of Ground Effect. NASA TN D3166, 1966.	OA$^{x}_{y}$ OB$^{x}_{y}$
G2	W.K. Greathouse	Preliminary Investigation of Pumping and Thrust Characteristics of Full size Cooling-Air Ejectors at Several Exhaust Gas Temperatures. NACA RM E54 A18, 1954.	OBx
G3	B.H. Goethert	Base Heating Problems of Missiles and Space Vehicles. ARS Reprint 1666-61, 1961.	$^{2}_{3}$BIIa$^{x}_{y}$
G4	W.K. Greathouse	Blending Propulsion with Airframe. Space/Aeronautics, Nov. 1968.	Jet simulation $^{2}_{3}$BIIay

G5	J.E. Green	Short Cowl Front Fan Turbojets; Friction Drag and Wall-Jet Effects on Cylindrical Afterbodies. RAE TR 67144, 1967.	IAIIax
G6	B.H. Goethert and R. Matz	Experimental Investigation of Base Flow Characteristics of Four Nozzle Cluster-Rocket Models. AGARDograph 87, 1966.	OBIIay
G7	W. Geissler and R. Wulf	Jet Simulation and Jet Interference Effects on Tail Planes. AGARD C.P. 71, 1970.	$1AI_b^x x$
H1	H.C. Hottel	Burning in Laminar and Turbulent Fuel Jets. 4th (Int.) Symposium on Combustion, 1953.	OAx
H2	C.C. Higgins and T.W. Wainwright	Dynamic Pressure and Thrust Characteristics of Cold Jets Discharging from Several Exhaust Nozzles Designed for VTOL Downwash Suppression. NASA TN D-2263, 1964.	$O_B^A x$
H3	J.O. Hinze and B.G. v.d. Hegge Zijnen	Transfer of Heat and Matter in the Turbulent Mixing Zone of an Axially Symmetrical Jet. Applied Scient. Review, Vol. A1.	OAx
H4	J. Hartmann and Fr. Lazarus	The Air-Jet with a Velocity Exceeding that of Sound. Phil. Magazin and Journal Sci.Ser. 7, Vol. 31, no. 204, 1941.	OBx
H5	A.G. Hammit	The Oscillation and Noise of an Over-pressure Sonic Jet. Journal of Aerospace Sc. Vol. 28, no. 9, 1961.	OBx
H6	Hung Wang and M.E. Childs	Two-Dimensional Turbulent Mixing Between a Free Stream and a Confined Parallel Slot Jet. Univ. of Washington, Trend in Engineering Oct. 1960.	1AIax
H7	B.Z. Henry and M.S. Cahn	Pressure Distributions Over a Series of Related Afterbody Shapes as affected by a Propulsive Jet at Transonic Speeds. NACA RM L 56 K05, 1957.	2BIax 2BIIax
H8	L.O. Hayman Jr. and R.W. Mc Dearmon	Jet Effects on Cylindrical Afterbodies Housing Sonic and Supersonic Nozzles which Exhaust against a Supersonic Stream at Angles of Attack from 90^o to 180^o. NASA TN D-1016, 1962.	3BIIbx
H9	J.S. Holdhusen and O.P. Lamb	Scale Model Studies of Exhaust Nozzle Performances. AIAA paper no. 66-641, 1966.	2AIax 3BIay
H10	C.C. Higgins, D.P. Kelly and T.W. Wainwright	Exhaust Jet wake and Thrust Characteristics of Several Nozzles designed for V.T.O.L. Downwash Suppression. NASA CR 373, 1966.	OBIby
H11	W.F. Hinson and R.J. Mc Ghee	Effects of Jet Pluming on the Static Stability of Five Rockets Models at Mach numbers of 4.5 and 6 and Static Pressure Ratios up to 26000. NASA TN D4064, 1967.	3BIIax
H12	M.H. Harries	Pressure on Asymmetric Base in a Transonic or Supersonic Free Stream in the Presence of a Jet. FFA report no. 111.	$^2_3$BIIax
H13	Herron, R.D.	Jet Boundary Simulation Parameter for Under-expanded Jets in a Quiescent Atmosphere. Journal of Spacecraft Rockets, Oct. 1968.	OBx
H14	R.W. Hensel	A Survey of Recent Developments in Wind Tunnel Testing Techniques at Transonic and Supersonic Speeds. AIAA Aerodynamic Testing Conference, Washington D.C., 1964.	Jets
H15	G.L. Herstine et al	Base Heating Experimental Program for Saturn S.IV Stage. IAS paper 30st Annual Meeting, N.Y. Jan. 1962.	OBy
H16	D.E. Harrington	Jet Effects on Boattail Pressure Drag of Isolated Ejector Nozzles at Mach number from 0.60 to 1.47. NASA TMX-1785, May 1969.	$2B_{II}^{I}ax$
H17	C.G. Hodge and V. Salemann	Aerodynamic Performance Testing Using Wind Tunnel Models and Blown Nacelle Engine Simulators. AIAA paper no. 68-396.	Jet simulation

H18	J.J. Horgan and D.B. Waring	Supersonic Nozzles. AGARD CP 34, 1968.	2_3BIIax
J1	F. Jaarsma	Het Gebruik van Waterstofperoxyde Raketmotoren voor Simulatie van Straalmotoren bij Windtunnel-modellen. NLR C-30, 1962.	Jet simulation
J2	N.H. Johannesen	Further Results on the Mixing of Free Axially Symmetrical Jets of Mach number 1.40. A.R.C. 20, 981. FM 2819, No. 88, 1959.	OBx
J3	N.H. Johannesen	The mixing of Free Axially Symmetrical Jets of Mach 1.40. R and M No. 3261, 1962.	OBx
J4	J. Jonas	On the Interaction Between Multiple Jets and an Adjacent Surface. Aeron. Engin. Review, Vol. 11, Jan. 1952.	OBy 1BIay
J5	R. Jordinson	Flow in a Jet Directed Normal to the Wind. Aeron.Res. Council, R and M No. 3074.	1AIIbx
J6	B.G. Jackson and N.L. Crabill	Free-Flight Investigation of Jet Effects at Low Supersonic Mach Numbers on a Fighter-Type Configuration Employing a Tail-Boom assembly. NACA RM L57 F19, 1957.	3BIIax
J7	J.J. Janos and F. Hoffman	Forces and Moments due to Air Jets exhausting parallel to large flat plates in a near vacuum. NASA TND-5147.	OBIax
K1	M.Z. Krzywoblocki	Jets-Review of Literature. Jet Propulsion Vol. 26, no. 9, 1956.	Jets
K2	A.M. Kuethe	Investigations of the Turbulent Mixing Region Formed by Jets. Journal of Applied Mechanics, Vol. 2, no. 3, Sept. 1935.	OAx 1AIax
K3	M.A. Koplin	Flow in the Mixing Region of a Jet. MIT Rep. ASRL TR 92-3, June 1962.	OAx
K4	R. Knystaunus	The Turbulent Jet from a Series of Holes in Line. The Aeronautical Quarterly, Vol. XV, Febr.1964.	OAy
K5	D.L.I. Kirkpatrick	Wind Tunnel Corrections for V/STOL Model Testing. University of Virginia, M Sc Thesis 1962.	1AIIbx
K6	A.G. Kurn	A Base Pressure Investigation at Transonic Speeds on an Afterbody Containing Four Sonic Nozzles and a Cylindrical Afterbody Containing a Central Sonic Nozzle. RAE TN Aero 2869, 1963.	$2^{A}_{B}II^{a}_{y}$
K7	H.H. Korst and W.L. Chow	Non-Isoenergetic Turbulent (P_{rt} = 1) Jet Mixing between two Compressible Streams at Constant Pressure. University of Illinois ME-TN-393-2 or NASA CR-419, 1966.	2_3BIax
K8	R. Kawamura	Reflection of a Wave at an Interface of Supersonic Flows and Wave Patterns in a Supersonic Compound Jet. Journal of Physical Soc. of Japan, Vol. 7 no. 5, 1952.	3BIax
K9	H.H. Korst and W.L. Chow	Compressible Non-Isoenergetic Two-Dimensional Turbulent (P_{rt} = 1) Jet Mixing at Constant Pressure-Auxiliary Integrals - Heat Transfer and Friction Coefficients for Fully Developed Mixing Profiles. University of Illinois, ME-TN-392-4, 1963.	3_2BIax
K10	H.H. Korst	Research on Transonic and Supersonic Flow of a Real Fluid at Abrupt Increases in Cross Section (With Special Consideration of Base-Drag Problems). Card N65-11440	2_3BIIax
K11	A.G. Kurn	A Further Wind Tunnel Investigation of Underwing Jet Interference. RAE.TR-69090, 1969.	1_2BIay Jet simulation
L1	A.G. De Louw	De Simulatie van Straalmotoren bij Windtunnel-proeven. NLR A.1559 nov. 1963.	Jet simulation

L2	H.C. Mc Lemore	Jet Induced Lift Loss of Jet VTOL Configurations in Hovering conditions. NASA TN D-3435, 1966.	OAx OAy
L3	E.S. Love and C.E. Grigsby	Some Studies of Axisymmetric Free Jets Exhausting from Sonic and Supersonic Nozzles into Still Air and into Supersonic Streams. NACA RM L54 L31, 1955.	OBx 3BIax
L4	E.S. Love and L.P. Lee	Shape of Initial Portion of Boundary of Supersonic Axisymmetric Free Jets at Large Jet Pressure Ratios. NACA TN 4195, 1958.	OBx
L5	E.S. Love, C.E. Grigsby, L.P. Lee and W.J. Woodling	Experimental and Theoretical Studies of Axisymmetric Free Jets. NASA TR R-6, 1959.	OBx
L6	W.T. Lord	On Axisymmetrical Gas Jets with Application to Rocket Jet Flow Fields at High Altitudes. RAE Report Aero 2626, 1959.	OBx
L7	G. Lee	An Investigation of Transonic Flow Fields Surrounding Hot and Cold Sonic Jets. NASA TND-853, 1961.	2BIax
L8	E.E. Lee and C.M. Willis	Interaction Effects of a Control Jet Exhausting Radially from the Nose of an Ogive-Cylinder Body at Transonic Speeds. NASA TND-3752, 1967.	$2B^{I}_{II}b^{x}_{y}$
L9	A. Leiss and W.E. Bresette	Pressure Distribution Induced on a Flat Plate by a Supersonic and Sonic Jet Exhaust at a Free-Stream Mach number of 1.80. NASA RM L56 I06, 1957.	3BIax
L10	E.S. Love	Initial Inclination of the Mixing Boundary Separating an Exhausting Supersonic Jet from a Supersonic Ambient Stream. NACA RM L55 J14, 1956.	3BIax
L11	E.S. Love	An Approximation of the Boundary of a Supersonic Axisymmetric Jet Exhausting into a Supersonic Stream. Journal of Aeronautical Science, Vol. 25, no. 2, 1958.	3BIax
L12	R.L. Lawrence	Afterbody Flow Fields and Skin friction on Short Duct Fan Nacelles. Journal of Aircraft, vol. 2, no. 4, July-Aug.1965.	O BIIay
L13	J. Leynart and G. Meauze	Quelques Problèmes Transoniques du Fuseau Moteur d'un Avion du Type "Airbus". AGARD CP 35 Transonic aerodynamics.	2BIIax
L14	H. Langfelder	Low-Drag Installation of Twin Propulsion Nozzles in the Rear of the Fuselage for Transonic and Supersonic Flight. AGARDdograph 103, part 1, 1965.	$\frac{2}{3}$BIIay
L15	J.A. Laughrey	Calculation of the Performance of Installed Exhaust Nozzles on Supersonic Aircraft. AIAA paper no. 69-428.	$\frac{2}{3}$BIIax
L16	J.P. Lamb, K.A. Abbud and C.S. Lenzo	A Theory for Base Pressure on Multi-nozzle Rocket Configurations. Journal of Spacecraft, vol. 7, no. 4, April 1970.	3BIIay
L17	J.P. Lamb and C.C. Hood	An Integral Analysis of Turbulent Re-attachment Applied to Plane Supersonic Base Flows. Journal of Engineering for Industry.	3BIIax
M1	C.A. Moreas, W.K. Hagginbothom, and R.A. Falange	Design and Evaluation of a Turbojet Exhaust Simulator Utilizing a Solid-Propellant Rocket Motor, for use in Free-Flight Aerodynamic Research Models. NACA RM L 5415, 1954.	Jet simulation
M2	D.R. Miller and E.W. Comings	Static Pressure Distribution in the Free Turbulent Jet. Journal of Fluid Mechanics, Vol. 3, Part 1 Oct. 1957.	OAx
M3	J.J. Mahoney	The Internal Flow Problem in Axisymmetric Supersonic Flow. Phil.Transact. of Royal Soc. Ser. A, Vol. 251, 1959.	OBx
M4	M. Moe and B.A. Troesch	Jet Flow with Shocks. ARS Journal, Vol. 30, May 1960.	OBx 3BIax

M5	E.D. Marion D.J. Daniels G.L. Herstine and G.W. Burge	Exhaust Reversal from Cluster Nozzles. A New Flow Model. ARS Reprint 2706-62.	OBy
M6	J.F.J. Maczyncki	A Round Jet in an Ambient Coaxial Stream. Journal of Fluid Mechanics Vol. 13, Part 4 1962.	1AIax
M7	B.R. Morton	Co-axial Turbulent Jets. International Journal of Heat and Mass Transfers, Vol. 5, Oct. 1962.	1AIax
M8	C.E. Mercer and L.B. Salters	Performance of a Plug Nozzle having a Concave Base with and without Terminal Fairings at Transonic Speeds. NASA TN D-1804, 1963.	2BIIax
M9	N.T. Murial and J.J. Ward	Base Flow Characteristics for Several Four- Clustered Rocket Configurations at Mach Numbers from 2.0 to 3.5. NASA TN D-1093, 1961.	3BIIay
M10	H. Mc Donald and P.F. Hughes	A Correlation of High subsonic Afterbody Drag in the Presence of a Propulsive Jet or Support Sting. Journal of Aircraft, Vol. 2, no. 3, May-June 1965.	2BIIax
M11	R.J. Margason and G.L. Gentry	Static Calibration of an Ejector Unit for Simulation of Jet Engines in Small-scale Wind Tunnel Models. NASA TN D-3867, 1967.	OAIbx
M12	D.L. Motycka and P.J. Skowronek Jr.	Performance Installation Effects for Nozzles Installed on a Twin-jet Fighter Airplane Model. SAE paper no. 680296, 1968.	2BIIay
M13	D. Migdal and W.K. Greathouse	Optimizing Exhaust Nozzle/Airframe Thrust Minus Drag. SAE paper no. 680294, 1968.	2BIay
M14	J.P. Moran	Similarity in High-altitude Jets. AIAA Journal vol. 5, no. 7, July, 1967.	Jets
M15	J.B. Miles	Similarity Parameter for Two-Stream Turbulent Jet-Mixing Region. AIAA Journal vol. 6, no. 7, July, 1968.	Jets
M16	C.A. de Moreas	Transonic Flight Test of a Rocket Powered Model to Determine Propulsive Jet Influence on Configuration Drag. NACA RM L54 D27, 1954.	2BIax
M17	D.G. Mobey	Jet Effects Measured on the Tail-plane of the Bristol 188 in Two Supersonic Wind Tunnels. RAE Techn. Memo Aero 1006, Aug. 1967.	3BIax
M18	D. Migdal E.H. Miller and W.E. Schnell	An experimental evaluation of exhaust nozzle/ airframe interference. AIAA paper no. 69-430.	Jet simulation $^{2}_{3}$BIIay
M19	E.H. Miller and D. Migdal	Subsonic Interference Characteristics of Single and Twin Jet Afterbodies. Journal of Aircraft vol. 7, no. 3 May-June 1970.	1BIIax 1BIIay Jet simulation
M20	D.C. Mikkelson and B.J. Blaka	Flight and Wind Tunnel Investigation of Installation Effects on Underwing Supersonic Cruise Exhaust Nozzles at Transonic Speeds. AGARD C.P. 71, Sept. 1970.	2BIIax
N1	H.T. Norton and J.M. Swihart	Effect of a Hot-jet Exhaust on Pressure Distributions and External Drag of Several Afterbodies on a Single Engine Airplane Model at Transonic Speeds. NACA RM L57 J04, 1958.	$2B^{I}_{II}$bx 2BIIax
N2	W.J. Nelson and W.R. Scott	Jet Effects on the Base Drag of a Cylindrical Afterbody with Extended Nozzles. NACA RM L58 A27, 1958.	$2BIIa^{x}_{y}$
N3	H.T. Norton W.E. Foss and J.M. Swihartn	An Investigation of Modified Clustered Jet- exit Arrangements at Supersonic Speeds. NASA TM X-540, 1961.	$3B^{I}_{II}$ay
N4	M.R. Nichols	Aerodynamics of Airframe-Engine Integration of Supersonic Aircraft. NASA TN D-3390, 1966.	$3BIIa^{x}_{y}$

N5	B.M. Nayar T.E. Siddon and W.T. Chu	Properties of the Turbulence in the Transition Region of a Round Jet. UTIAS TN no. 131, 1969.	0AIax
N6	H.T. Norton M.D. Cassetti and C.E. Miller	Transonic Off-design Performance of a Fixed Divergent Ejector Designed for a Mach number of 2.0. NASA TM X-165.	2BIIax
O1	J.H. Otis Jr.	Induced Interference Effects on a Four Jet VTOL Configuration with Various Wing Planforms in the Transition Speed Range. NASA TN D-1400.	1AIIby
O2	R.C. Orth J.A. Schetz and F.S. Billig	The Interaction and Penetration of Gaseous Jets in Supersonic Flow. NASA CR 1386, July 1969.	3BIbx
P1	S.I. Pai	Fluid Dynamics of Jets. D.v. Nostrand Co. Inc. N.Y., 1954.	Jets
P2	M. Pindzola	Jet Simulation in Ground Test Facilities. AGARDograph no. 79, 1963.	Jet simulation 0Bx $3B^{I}_{II}$ ax
P3	M. Pindzola and J.B. Delano	Wind Tunnel Testing of Propulsion Systems. AIAA 2nd Ann.Meeting, 1965, 65-477.	Jet simulation $3B^{I}_{II}a^{x}_{y}$
P4	D.C. Pack	A Note on Prandtls Formula for the Wave-Length of a Supersonic Gas Jet. Quarterly Journal on Mechanics and Applied Mathematics, Vol. III, pt. 2, 1950.	0Bx
P5	D.C. Pack	On the Formation of Shock-waves in Supersonic Gas Jets. The Quarterly Journal of Mechanics and Applied Mathematics, Vol. 1, 1948.	0Bx
P6	S.I. Pai	Two-dimensional Jet Mixing of a Compressible Fluid. Journal of Aeronautical Science, Vol. 16 no. 8, 1949.	1AIax
P7	S.I. Pai	Axially Symmetric Jet mixing of a Compressible Fluid. Journal of Aeronautical Science, Quarterly of Applied Mech., Vol. I, no. 2, 1952.	1AIax
P8	A. Pozzi	Viscous Jets from non Narrow Orifices. AIAA Journal, Vol. 2, no. 5, 1964.	1AIax
P9	S.I. Pai	Unsteady Three-Dimensional Laminar Jet Mixing of a Compressible Fluid. AIAA Journal, Vol. 3, no. 4, 1965.	1AIbx $2B^{I}_{II}$bx 3BIbx
P10	R.F. Peck	Jet Effects on Longitudinal Trim of an Airplane Configuration Measured at Mach numbers 1.7 and 1.8. NACA RM L54 J29a, 1955.	3BIax
P11	W.C. Pitts and L.E. Wiggins	Axial Force Reduction by Interference Between Jet and Neighbouring Afterbody. NASA TN D-332, 1960.	3BIax
P12	E. Pistolesi and M. Marini	Linearized Supersonic Flow of an Axisymmetric Jet in a Supersonic Stream. Institute of Aeron. University of Pisa, TR-2, 1962.	3BIax
P13	D.C. Pack	The Oscillations of a Supersonic Gas Jet Embedded in a Supersonic Stream. Journal of the Aeronautical Science, Vol. 23, no. 8, 1956.	3BIax
P14	R.H. Page and H.H. Korst	Non-Isoenergetic Turbulent Compressible Jet mixing with Considerations of its Influence on the Base Pressure Problem. Transact of 4th Miswestern Conf. on Fluid Mech. Purdue University, 1955.	3BIIax
P15	M. Pindzola and E.W. Henzel	High Altitude Jet Spreading and some Associated Interference Problems on Space Vehicles. AGARDograph 87, 1966.	OBIax

P16	J.C.J. Patterson	A Wind Tunnel Investigation of Jet-wake Effect of a High-bypass Engine on Wing-Nacelle Interference Drag of a Subsonic Transport. NASA 4693, 1968.	Jet simulation
P17	G. Pauley	Interim Note on Tests with a Wing-Mounted Fan Nacelle with the Fan Jet Simulated by Cold Air Blowing and Alternatively by a Gas Generator Shroud. A.R.C. C.P. No. 1111	2BIax
R1	J.F. Runckel and J.M. Swihart	A Hydrogen-Peroxyde Hot-Jet Simulation for Wind Tunnel Tests of Turbojet-Exit Models. NASA Memo 1-10-59L, 1959.	Jet simulation 2BIax
R2	J.A. Rietdijk	Metingen aan Vrije Supersone Stralen. Dissertatie TH-Delft, 1959.	OBx
R3	M.D. Rousso and F.D. Kochendorfer	Velocity and Temperature Fields in Cylindrical Jets Expanding from Choked Nozzles into Quiescent Air. NACA RM E51 F18, 1951.	OBx
R4	M.D. Rousso and L.E. Baughman	Spreading Characteristics of a Jet Expanding from Choked Nozzles at Mach 1.91. NACA TN 3836, 1956.	OBx 3BIax 3BIIax
R5	J.E. Rossiter and A.G. Kurn	Wind Tunnel Measurements of the Effects of a Jet on the Time Average and Unsteady Pressures on the Base of a Bluff Afterbody. RAE Report 65 187, 1965.	2BIIax
R6	J.F. Runckel	Preliminary Transonic Performance Results for Solid and Slotted Turbojet Nacelle Afterbodies Incorporating Fixed Divergent Jet Nozzles Designed for Supersonic Operation. NASA Memo 10-24-58L, 1958.	2BIIax
R7	J. Rom	Study of Similarity of High-Temperature, Turbulent Jets. AIAA Journal, Vol. 6, no. 7, July 1968.	Jets
R8	J. Reid	The Effect of Jet Temperature on Base Pressure. RAE TR 68176, July 1968.	$\frac{2}{3}$BIIax
R9	D.J. Raney A.G. Kurn and J.A. Bagley	Wind Tunnel Investigation of Jet Interference for Underwing Installation of High Bypass Ratio Engines. RAE TR 68049, 1968.	1BIay
R10	K.H. Rogers R. Lavi and G.R. Hall	Experimental Investigations of Ground-jet Suppression Fences for V.T.O.L. Aircraft Prepared Sites. Journal of Aircraft, vol. 6, no. 3, May-June 1969.	OBIby
R11	J. Reid and R.C. Hastings	The Effect of a Central Jet on the Base Pressure of a Cylindrical Afterbody in a Supersonic Stream. Aero.Res. Council R and M 3224/ARC 21796, 1961.	3BIIax
R12	H. Reichardt	Zur Problematik der Turbulente Strahlausbreitung in Einer Grundströmung. Max Planck Institut Götingen no. 35-1965.	Jets
R13	E. Riester	Temperaturanlauferscheinungen in Triebwerks-windkanälen. DLR Forschungsbericht 68-30, 1968.	Jet simulation
R14	E. Robert et J.P. Michard	Belatement de Jets dans le Vide. AGARDograph 87, 1966.	OBIax
R15	R. Rosen and L.A. Cassel	Secondary Jet Interaction with a Subsonic Mainstream. Journal of Aircraft vol. 7, no. 1, Jan. Febr. 1970.	1AIbx
R16	R.J. Reis P.J. Aucoin and R.C. Stechman	Prediction of Rocket Exhaust Flowfields. Journal of Spacecraft vol. 7, no. 2 Febr. 1970.	Jets
R17	J.F. Runckel	Aerodynamic Interference Between Exhaust Systems and Airframe. AGARD C.P. 71, 1970.	2BIIay
S1	J. Sedden and L.F. Nicholson	The Representation of Engine Airflow in Wind Tunnel Model Testing. RAE TN Aero 2371, June 1955.	Jet simulation 1AIax 3BIax

S2	W. Szablewski	Turbulente Ausbreitung eines Runden Heissluft-strahles in Ruhender Aussenluft. Ing. Archiv. XXX 1961.	OAx
S3	Sakae Yagi and Kenjiro Saji	Problems of Turbulent Diffusions in flame Jet. 4th (Int.) Symposium Combustion, 1953.	OAx
S4	W. Szablewski	Zur Theorie der Turbulenten Strömung von Gasen Stark Veränderlichen Dichte. Ingenieur Archiv. XX Band,Zweiter Heft, 1952.	OAx
S5	W. Szablewski	Asymptotische Gesetze der Turbulenten Ausbreitung von Heissluftstrahlen in Bewegten und Ruhenden Aussenluft. Zeitschrift Angew. Math. und Mech., Band 39, Heft 1/2. Jan./Febr. 1959.	OAx 1AIax
S6	H.B. Squire	Jet Flow and its Effect on Aircraft. Aircraft, Vol. XXII no. 253, 1950.	1AIax 1AIbx
S7	W. Szablewski	Turbulente Ausbreitung runden Heissluft-strahles in Bewegter Luft. Ingenieur Archiv. XXVI, 1958.	1AIax
S8	W. Szablewski	Turbulente Vermischung zweier ebenen Luft-strahle von fast gleicher Geschindigkeit und stark unterschiedlicher Temperatur. Ingenieur Archiv. XX Band zweiter Heft, 1952.	1AIax
S9	W. Szablewski	Turbulente vermischung ebener Heissluftstrahlen für den Unterschall Bereich. Ingenieur Archiv. XXV Band, Ersten Heft,1957.	1AIax
S10	B.S. Stratford Z.M. Jarvor and M. Smith	The Mixing between Hot and Cold Airstreams in a Centrifugal Field. Aeron. Research Council, Current Paper 793, 1965.	1AIax
S11	R.J. Salmi	Experimental Investigation of Drag of After-bodies with Exiting Jet at High Subsonic Mach Numbers. NACA RME 54I 13, 1954.	1BIIax
S12	J.M. Swihart and N.L. Crabill	Steady Loads due to Jet Interference on Wings, Tails and Fuselage at Transonic Speeds. NACA RM L57 D24b, 1957.	2BIax
S13	J.M. Swihart	Effect of Target-type Thrust Reverser on Transonic Aerodynamic Characteristics of a Single Engine Fighter Model. NACA RM L57 J16, Jan. 1958.	$2B^{I}_{II}$bx 2BIIax
S14	J.M. Swihart H.T. Norton and J.W. Schmeer	Effect of Several Afterbody Modifications Including Terminal Fairings on the Drag of a Single Engine Fighter Model with Hot Jet Exhaust. NASA Memo 10 -29- 58L, 1958.	2BIIax
S15	J.M. Swihart and C.E. Mercer	Investigations at Transonic Speeds of a Fixed Divergent Ejector Installed in a Single-Engine Fighter Model. NACA RM L57 L10a, 1958.	2BIIax
S16	J.M. Swihart C.E. Mercer and H.T. Norton	Effect of Afterbody-Ejector Configurations on the Performance at Transonic Speeds of a Pylon-Supported Nacelle Model Having a Hot-Jet Exhaust. NASA TN-1399, 1963.	2BIIax
S17	W.C. Swan	A discussion of Selected Aerodynamic Problems on Integration of Propulsion Systems with Airframe on Transport Aircraft. AGARDograph no. 103, 1965.	1BIay
S18	S. Sedden	Factors Determining Engine Installation Drag on a Subsonic and Supersonic Aircraft. AGARD CP9, part 1, 1966.	$2^{B^{I}_{II}}_{3}$ay
S19	U. Sacerdote	Techniques for the Simulation of Jet-lift Engines in Windtunnel Models of V/STOL Aircraft. AGARDograph no. 103, 1965.	Jet simulation 1AIby
S20	L.D. Smoot and W.E. Purcell	Model for Mixing of a Compressible Free Jet with a Moving Environment. AIAA Journal,vol. 5, no. 11, Nov. 1967.	0 1BIax 2 3
S21	J.W. Shirie	Length of the Supersonic Core in High-Speed Jets. AIAA Journal,vol. 5, no. 11,Nov. 1967.	OBx

S22	L.C. Squire	The Use of Excess Engine Exit Area over Intake Area to Reduce Zero-lift Drag at High Supersonic Speeds. The Aeronautical Quarterly, Aug. 1965.	3BIIax
S23	W.J. Sheeran and D.S. Dosangh	Observations on Jet Flows from a Two-dimensional, Underexpanded Sonic Nozzle. AIAA Journal, vol. 6, no. 3, March 1968.	OBx
S24	J.A. Schetz	Turbulent Mixing of a Jet in a Coflowing Stream. AIAA Journal, vol. 6, no. 10, Oct. 1968.	Jets
S25	W. Szablewski	Asymptotische Gesetze der Turbulenten Ausbreitung von Heissluftstrahlen in Bewegten und Ruhenden Aussenluft. Zeitschrift für Math. und Mech. Band 39 Heft 1/2, 1959.	1AIax
S26	W.J. Sheeran and K.C. Hendershot	Simulation of Earth Storable Liquid Biproppellants with Gaseous Reactants. Journal of Applied Mechanics, June 1969.	Jet simulation
S27	P.M. Sforza and G. Herbst	A study of Three-Dimensional, Incompressible Turbulent Wall Jets. AIAA Journal, vol. 8, no. 2, Febr. 1970.	OAIax
S28	J.A. Schetz	Interaction Shock Shape for Transverse Injection in Supersonic Flow. Journal of Spacecraft and Rockets, vol. 7, no. 2 Febr. 1970.	3BIbx
S29	J.G. Skifstad	Aerodynamic of Jets Pertinent to VTOL Aircraft (93 refs). Journal of Aircraft, vol. 7, no. 3. May-June 1970.	1AIbx
S30	J.A. Schetz	Unified Analysis of Turbulent Jet Mixing. NASA CR 1382.	Jets
S31	Salters Jr. and N.S. Chamaks	Studies on Flow Distortion in the Tailpipes of Hydrogen Peroxide Gas Generators Used for Jet Engine Simulation. NASA TM-X-1671, 1968.	Jet simulation
T1	K.E. Tempelmeyer	An Analytical Study of Hot Jet Simulation with a Cold Gas Mixture. AEDC-TN-58-54. Sept. 1958.	Jet simulation
T2	E. Thiel	Nachahnung der Triebwerkschubes bei Windkanal-Modellversuchen. WGLR-Bericht No. 1, 1963.	Jet simulation
T3	L. Ting	On the Mixing of Two Parallel Streams. Journal of Mathematics and Physics, Vol. 38, No. 3, 1959.	1AIax
T4	R.E. Tatro	The Spreading Characteristics of Choked Jets Exhausting into a Supersonic Stream. AEDC-TR-55-2, 1955.	3BIIbx
T5	W. Tabakoff and H. Sowers	Drag Analyses of Powered Nacelle Fan Jet Engine Model Test. Zeitschrift für Flugwissenschaften, April 1969, Heft 4.	$^{0}_{2}$AIIay
U1	S. Uchida	On Turbulent Free Mixing of Parallel Streams of Two Different Gases. PI BAL Report no. 635, 1961.	1AIax
V1	J. Vasiliu	Turbulent Mixing of a Rocket Exhaust Jet with a Supersonic Stream Including Chemical Reactions. Journal of Aerospace Science, Vol. 29, No. 1, Jan. 1967.	3BIax
V2	A.R. Vick E.H. Andrews Jr. J.S. Dennard and C.B. Craidon	Comparisons of Experimental Free-jet Boundaries with Theoretical Results Obtained with the Method of Characteristics. NASA TN D-2327, June 1964.	OBx
V3	A.R. Vick J.M. Cubbage and E.H. Andrews Jr.	Rocket Exhaust Plume Problems and Some Recent Related Research. AGARDograph 87, vol. 2, 1966.	OBx/y
W1	I. Wygnanski	The Flow Induced by Two-Dimensional and Asymmetric Turbulent Jets Issuing Normally from an Infinite Plane Surface. The Aeronautical Quarterly, Vol. XV, Part 4, Nov. 1964.	OAx

W2	I. Wygnanski and O. Haweleshka	Effect of Upstream Velocity Profile on the Free Mixing of Jets with Ambient Fluid. AIAA Journal, Vol. 5 no. 6, June 1967.	OAx
W3	C.J. Wang and J.B. Peterson	Spreading of Supersonic Jets from Axially Symmetric Nozzles. Jet Propulsion, Vol. 28, No. 5, 1958.	OBx
W4	W.R. Warren Jr.	The Static Pressure Variation in Compressible Free Jets. Journal of Aeronautical Science, Vol. 22, no. 3 1955.	OBx
W5	D.R. Willis and I. Glassman	The Mixing of Unbounded Co-axial Compressible Streams. Jet Propulsion, Vol. 27. Dec. 1957.	A 1BIax
W6	R. Wasko	Performance of Annular Plug and Expansion-Deflection Nozzles Including External Flow Effects at Transonic Mach Numbers. NASA TN D-4462, April 1968.	2BIIax
W7	J.T. Wareing	Consideration of V/STOL Downwash and the Ground Environment. SAE paper 680282, 1968.	0 1 AIbx
W8	J. Weir	Aircraft Performance Problems Associated with Engine and Intake Installation. AGARDograph no. 103, 1965.	1 2BIIa$^{x}_{y}$ 3
W9	J. Williams and M.N. Wood	Aerodynamic Interference Effects with Jet-lift Schemes on V/STOL Aircraft at Forward Speed. AGARDograph, no. 103, 1965.	1AIby
W10	J. Williams and S.F.J. Butler	Recent Developments in Low-speed Wind Tunnel Techniques for V/STOL and High-lift Model Testing. Zeitschrift für Flugwissenschaften, 13.Jahrgang, Heft 3, März 1965.	Jet simulation
W11	M.N. Wood and J.B.W. Howard	The Development of Injector Units for Jet-lift Engine Simulation on Low-Speed-Tunnel Models. RAE Techn. Report 65020, Febr. 1965.	1AIax 1AIbx
W12	J.P. Weidner and J.M. Cubbage	Base Pressures and Convective Heat Transfer Coefficients for Clustered Sonic Nozzles with Emphasis on Choked Exhaust Back Flow. NASA TN D-2929, 1965.	OBy
W13	J.C. Wu H.M. Mc Mahon D.K. Mosher and M.A. Wright	Experimental and Analytical Investigations of Jets Exhausting into a Deflecting Stream. Journal of Aircraft, vol. 7, no. 1 Jan.-Febr. 1970.	1AIbx
W14	F.A. Wilcox N.E. Samanich and B.J. Blaha	Flight and Wind Tunnel Investigation of Installation Effects on Supersonic Cruise Exhaust Nozzles at Transonic Speeds. AIAA paper no. 69-427, 1969.	2BIIax
Z1	V. Zakkay E. Krause and S.D.L. Loo	Turbulent Transport Properties for Axisymmetric Heteregeneous Mixing. AIAA Journal, vol. 2, no. 11, Nov. 1964.	1BIax

V COMPLETE ENGINE SIMULATION

In the previous chapters the inlets and exhausts are treated separately, following the usual procedure as performed in the wind tunnel testing program. However, the mutual possible interference between the inlets and exhausts has been mentioned occasionally, and doubt has been expressed if separate testing is allowed.

If a wind tunnel testing scheme is set up at which both the inlets and exhausts are simulated simultaneously, provision should be provided to add energy to the inlet air flow in the form of total pressure rise and preferably also in the form of a temperature rise (temperature rise only would yield ramjet conditions). This addition of energy can be either outside the wind tunnel test section or inside the model. Depending on the inlet mass flow and required pressure rise, it can generally be stated that the required power for pumping is very large (typically between 10 and 100 h.p.) which means that the location of the pumping system inside the model would be a considerable task, though not completely impossible. Two techniques are now available, ejectors and miniature gas turbine driven engine simulators, both based on gaseous driving fluids (air or nitrogen) which is expelled through the nozzle also. Use of electric power will yield voluminous motors. The system for which the pump system is located outside the tunnel test section can only be used if the air passages of the inlet flow can be made large enough to provide for the complete inlet mass flow. This means that this system cannot be used with podded engine installations since the pylon cross-sectional area is much less than the inlet area.

In this chapter the internal addition of energy system will be discussed first; the chapter will finish with some remarks on the external systems.

5.1 SYSTEMS WITH INTERNAL ADDITION OF ENERGY

The accompaning sketch depicts schematically the system with internal addition of energy where the primary driving fluid is expelled through the exhaust also, either mixed with the secondary flow or separated from the secondary flow in case of a fan engine simulator. If the tests are performed for thrust-drag determination or for engine-airframe interference determination, in both cases the secondary air flow must be measured (assuming the primary mass flow is measured adequately outside the test section) for correct inlet spillage and jet properties assessment. This means that careful calibration of the secondary mass flow (inlet mass flow) must be provided since the precise measurement of this quantity under wind tunnel model conditions is generally not possibly (see section 2.1.3).

As an intermediate step in the thrust minus drag assessment sometimes also the nacelle with engine simulator is measured under isolated conditions (e.g. free from the wing) at which the interference drag can then be defined as the difference in the isolated (nacelle free) wing or airplane drag plus the net nacelle force and the complete (with powered nacelles) aircraft drag.

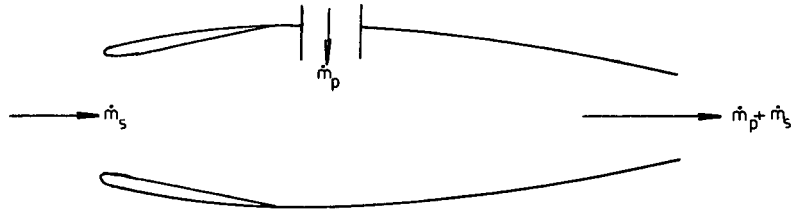

5.1.1 MINIATURE TURBINE DRIVEN ENGINE SIMULATORS

For a high bypass engine installed on a wing or rear fuselage in subsonic flow the performance engineer generally needs to know (a) the effect of the inlet and exhaust flow on the airframe aerodynamics, and (b) the effects of the wing flow field on the gross thrust of the nozzles and mass flow. Pressure ratios of the order of 1.7 are required to be simulated within the nacelle and this is not easily simulated by ejectors. Therefore miniature turbine driven engine simulators have recently been developed for wind tunnel use. These engine simulator units operate with a primary drive turbine using air (or N_2) at 25 atmospheres. This turbine drives a secondary duct fan (max. r.p.m. 80000) which gives a geometrically representative secondary air flow at the correct pressure ratio. The model is usually correctly scaled and only the unrepresentative features are γ, T and actual mass flow ratio. The inlet flow is less than the flight requirement but only about 15 °/o less and is within an acceptable limit above the spill drag margin. The primary gas generator flow is unrepresentative but is probably of little importance when surrounded by the secondary flow. Fig. V.1 shows such an unit installed in a nacelle under the wing (Ref. V.1).

A typical method in use with these currently available simulators will be described next. This method is perhaps the most advanced and logical which has been attempted with these simulated engines, in that the thrust of the individual nozzles is related to the conditions in that nozzle in the correct environment. Certain assumptions are made of necessity, and the value of any absolute answers is dependent upon prediction methods for external drag.

The degree of simulation can be described as follows:

(a) Fan pressure ratio is representative of full scale.

(b) Fan (secondary) nozzle can be sized correctly: thus with (a) fan nozzle exit conditions are correct in flow conditions and geometry. Distortion screens, detail struts and fairings can be incorporated within the nozzle in order to duplicate, as far as possible the exhaust flow characteristics of the full scale engine. In retrospect, it is evident that the failure to duplicate the nozzle radial total pressure profile, contributed to a discrepancy noted between model scale and full scale evaluations of the fan nozzle coefficients. At take-off power, for instance, the total pressure distortion $(P_{t_{max}} - P_{t_{min}}) / (P_{t_{av}} - P_{st})$ can typically be some 30 °/o for large bypass ratio engines (Ref.V.2).

(c) The whole of the inlet flow feeds the fan nozzle, thus the inlet is wrongly matched and therefore the performance and/or the geometry must be compromised, usually by cowl modifications.

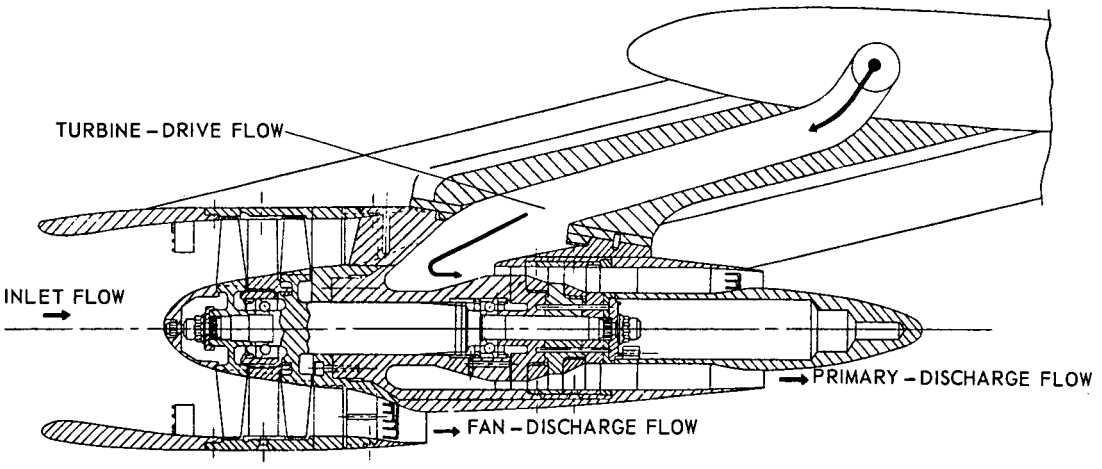

FIG. V. 1 CROSS – SECTIONAL VIEW OF A MINIATURE TURBO–DRIVER FAN SIMULATOR

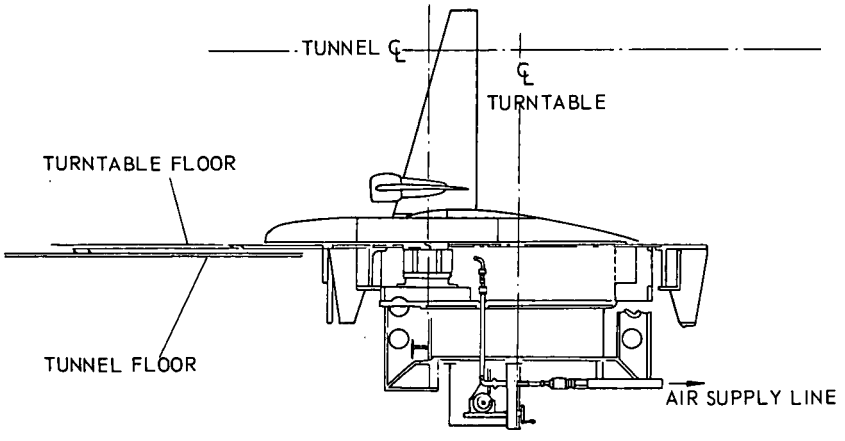

FIG. V. 2 SEMI–SPAN MODEL TUNNEL INSTALLATION WITH POWERED NACELLE

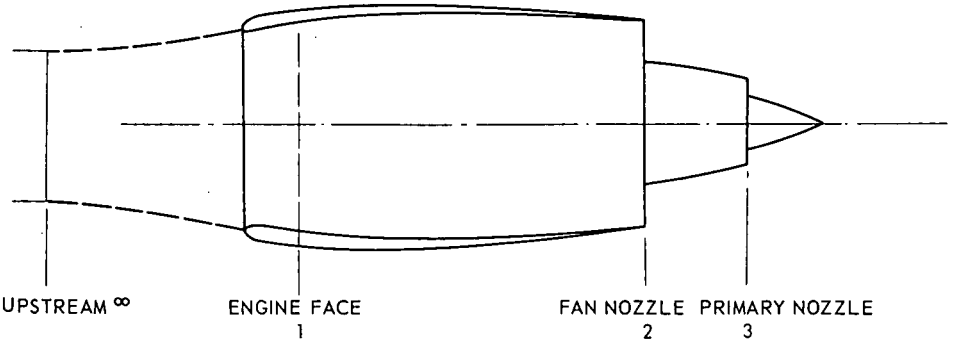

$\dot{m}$	MASS FLOW	
V	VELOCITY	
C_A	AREA COEFFICIENT	
C_V	VELOCITY COEFFICIENT	
X_g	GROSS THRUST	
H	TOTAL PRESSURE	FROM AREA WEIGHTED MEANS
p	STATIC PRESSURE	
T	TOTAL TEMPERATURE	
C_{d_1}	INLET MASS FLOW COEFFICIENT f (H_1/p_1 ONLY)	

SUBSCRIPTS

	NOTATIONS AS ABOVE
a	'ACTUAL'
m	MEASURED AT PARTICULAR STATION

FIG. V. 3 SCHEMATIC FAN ENGINE WITH NOTATIONS

(d) Primary nozzle is geometrically near correct, the pressure ratio is correct but very cold. Bypass ratio is 2 : 1 instead of 5 : 1. As the primary jet is shielded by the fan jet these effects should probably be unimportant as far as jet interference is concerned.

Usually the following testing is performed:

(a) Isolated engine on a balance without external flow with bellmouth for secondary mass flow calibration and some checks on (b) ,

(b) Isolated nacelle on balance with external flow for thrust calibration, and

(c) Nacelle(s) in position on metric model with balance measuring net forces on model, usually semi-span (Fig. V.2 from Ref. V.3).

The tests (a) or (a) and (b) can be replaced by "test bed" type calibration.

With respect to isolated tests it should be noted that the nacelle should be axisymmetric since a contoured nacelle in a uniform flow field would give unrealistic nacelle drag, that would not exist in the air plane flow field. This would result in apparent favourable interference effects. The installation criteria should be that the contoured nacelle operating in the airplane flow field should have essentially the same drag as an axisymmetric nacelle operating in the uniform field of the wind tunnel. Any drag increment due to improper contouring appears as interference drag and should be considered as an installation effect (Ref. V.4).

The following methods can be used to calculate thrust.

A. In this case an attempt is made to calculate the net standard installed thrust of the engines when installed on the "complete" model. Addition of this term to the balance measured overall drag gives an aircraft external drag. As the net standard definition of thrust is used any post exit thrust is in the external drag term.

The static test (a) yields a mass flow calibration of the fan face instrumentation (typically 28 pitots, 12 statics). A flow coefficient C_d, is calculated such that

$$\dot{m}_{1_a} = C_{d_1} \times \dot{m}_{1_m} \qquad \text{(see fig. V.3)}$$

where $\dot{m}_{1_a}$ is obtained from a calibrated bellmouth and $\dot{m}_{1_m}$ from area weighted mean total and static pressures and freestream total temperature at the fan.

When the nacelle is tested in isolation (test b) with external flow, pressure measurements can be made at the inlet, nozzle exits and on cowl external surfaces. The actual gross standard thrust for each nozzle is defined as

$$X_g = \dot{m}_m \, v_m \, C_A \, C_v^2 + (p_{ex} - p_\infty)A.$$

$\dot{m}_m$, v_m are determined from area weighted pressures (total and static) and total temperatures at the nozzle exit. C_A and C_v are area and velocity coefficients respectively. Obviously accurate mass flows must be used for the thrust calculations but it is also important that the same mass flow is used for the ram drag calculation as for the fan gross thrust. The inlet instrumentation is the best available (being more uniform than the nozzle) and so

$$\dot{m}_{1_a} = \dot{m}_{2_a} = C_{d_1} \times \dot{m}_{1_m} \quad \text{is taken} \quad (c_{f_1} \text{ being taken for the relevant value of } H_1/p_1)$$

An accurate determination of the primary mass flow can be made external to the model by a standard flow meter. In order to force the correct mass flow into the gross thrust equation above the flow coefficient can be written as:

$$C_A \times C_v = \frac{\dot{m}_a}{\dot{m}_m}$$

in other words

$$X_g = \dot{m}_a \, v_m \, C_v + (p_{ex} - p_\infty)A.$$

In order to determine these nozzle coefficients separately the primary nozzle C_A is taken from separate nozzle tests. Thus from the pressure, temperature and mass flow measurements the primary gross thrust X_{g_3} can be calculated. The measured balance drag D_{BAL} with the isolated nacelle model is given by

$$D_{BAL} = D_{EXT} + D_{RAM} - X_{g_2} - X_{g_3}$$

where the external drag D_{EXT} contains all terms such as axial pressure integrals, forebody spillage drag, skin friction drag and scrubbing drag. The ram drag can be calculated from freestream conditions and $\dot{m}_{1_a}$

Thus the secondary gross thrust X_{g_2} is determined if all the terms in D_{EXT} are estimable or calculable.

See for this procedure Ref. V.5 for example.

In the equations

$$C_{A_2} \times C_{v_2} = \frac{\dot{m}_{1_a}}{\dot{m}_{2_m}}$$

$$X_{g_2} = \dot{m}_{2_m} \times v_{2_m} \times C_A \times C_v^2 + (p_{ex_2} - p_\infty)A_2$$

C_A and C_v are the only two unknows. Only one of these coefficients can be used to calculate thrust in the aircraft configuration (test c) and C_A is chosen as it is conjectured that this is likely to vary the least. It is used as a function of fan pressure ratio and Mach number.

Then the net standard thrust can be calculated when the engines are used in the installed condition and this value added to the overall measured balance drag to give model external drag. This

external drag value will contain all the interference terms associated with both inlet and exhaust flows. It will also include the airframe on nacelle effects as well as the converse.

B. A similar series of tests can be conducted as in A, but interpreted differently. The static calibration (test a) is used to give a mass flow calibration but because no inlet instrumentation was available the fan nozzle instrumentation is used for the main fan mass flow measurement. The calibration is thus done in a test cell with the correct exit pressure. The calibration of the instrumentation is taken as a function not only of pressure ratio but also of corrected r.p.m., the latter because of swirl effects.

The thrust calibration with external flow (test b) is reduced as a thrust coefficient C_T defined as

$$C_T = \frac{-(D_{BAL} - D_{RAM})}{X_{g_2} + X_{g_3}}$$

2 and 3 referring to fan and gas generator flows respectively.

where the gross thrusts are calculated using corrected mass flows and are of the fully expanded type (isentropic thrust).

This thrust coefficient is used (as a function of power and M_∞) to correct full-model balance measurements (test c). As the thrust coefficient contains the isolated nacelle external drag the model data obtained only shows differences in relation to an isolated nacelle $X_g - D$ definition. Any adaption to full scale results must take allowance for the change in nacelle external drag between model and full scale.

C. An alternative method would be to use an altitude test cell type technique and measuring thrust with a balance (test a). The thrust in the installed condition could then be calculated in exactly the same way as the engine manufacturer guarantees thrust. In this way the effects of the engine are determined in a "legal" sense as long as the model engine behaves similarly from test bed to installed condition. This is basically similar to A, but does not allow for changes of thrust of the model engine in the airframe environment. There is evidence that this assumption is incorrect.

In all these methods it is necessary to measure "somewhere" the full scale engine performance in the airframe environment. Evidence on the model scale shows the fan nozzle flow distribution to be considerably influenced by the wing flow since in many instances the flight envelope of the airplane results in engine operation at jet pressure ratios less than critical for both the primary (turbine) and fan nozzles. Under these conditions the external pressures in the area local to the particular nozzle can alter the flow characteristics upstream of the nozzle. This can also occur for above critical nozzle operations for conical convergent nozzles due to sonic line locations as influenced by the external pressure field. These external pressures can be significantly different when the engine is installed close to the wing. When this happens the engine can be affected in two ways:
(a) the local pressure, if different from ambient at each nozzle exit plane, can cause the engine cycle to shift, and (b) the local back pressure can be affected.

Though this technique is very promising with the main features:
(a) yielding high degree of simulation, except for some increased inlet spillage and non-representative primary (turbine) jet temperature, and (b) similar installation procedures can be followed in the wind tunnel as the actual engine in the actual airplane, it has the main draw-backs that (a) it is expensive to operate, (b) it needs extensive control instrumentation for each engine, (c) it has little flexibility, each actual engine would require a different miniature turbine simulator, (d) the bearings have only limited life, (e) the repeatability is limited, (f) two equally manufactured simulators show different characteristics (as large as 5 °/o in net thrust, ref. V.4), and (g) the separation of various drag and thrust terms is very difficult and sometimes speculative, mainly due to the inaccurate assessment of the nozzle coefficients.

In general it can be stated that, using small turbine driven simulators, one gains in the degree of engine simulation with respect of techniques utilising direct nozzle blowing and direct inlet suction, but is adverse in obtainable accuracy of data assessment of each component. However, the use of these simulators is rather new, and could be much improved by further work.

5.1.2 EJECTORS

Ejectors do not contain rotating parts and are therefore much easier to manufacture and more flexible (not scale dependent) than turbine driven simulators. However, the secondary inlet mass flow is much less and the pressure ratio obtainable at the nozzle is usually limited. Furthermore large unrepresentative total pressure distortions due to the primary jets are hard to prevent. Since the ejector is a pure flow device its performance depends largely on the upstream and downstream conditions. The characteristics are usually quite different from the real engine. For these reasons the ejector is little used for thrust engine simulation; however, it is becoming popular for lift engine simulation in VTOL-aircraft, mainly due to the required low total pressure ratios in these cases. Since the ejector scheme is simple and cheap to operate it seems worthwhile to do more work in order to improve its characteristics.

Due to the large flow distortions in the exhaust jet caused by the primary jets, thrust measurements with ejectors are very unrepresentative and hence usually not performed. The system is however sometimes used for assessment of jet interference effects other than thrust minus drag. For example fig. V.4 shows an ejector system for inlet and exhaust flow simulation on a fighter type model. The model is mounted on a special 6-component balance. The high pressure blowing air is ducted below the balance to a plenum box from which it feeds into a peripheral ejector in each side duct. This ejector induces intake flow through the model boosting its total pressure and mass. This air is bifurcated to the two blowing nozzles on each side with appropriate internal control to give reasonable distribution. The final jet distribution is controlled by a splitter box. Special seals were developed for use between the metric air inlet and non-metric ejector box.
The ejector consists of an annular primary jet with an inner secondary inlet flow area. At the chosen design condition when operating in quiescent air conditions for each duct the primary flow was 1.65 lbs/secs, with a nozzle pressure of 4 atmospheres. The secondary or inlet flow was 0.85 lbs/secs.

For the front engine the nozzle distribution was relatively poor due to the short length. The rear nozzle distribution was good. The representation of total pressure ratio for the two nozzles was good and the inlet area ratio was 0.8 ejectors off, 0.65 ejectors on.

5.2 SYSTEM WITH EXTERNAL ADDITION OF ENERGY

As mentioned before the system for complete engine simulation with addition of energy outside the test

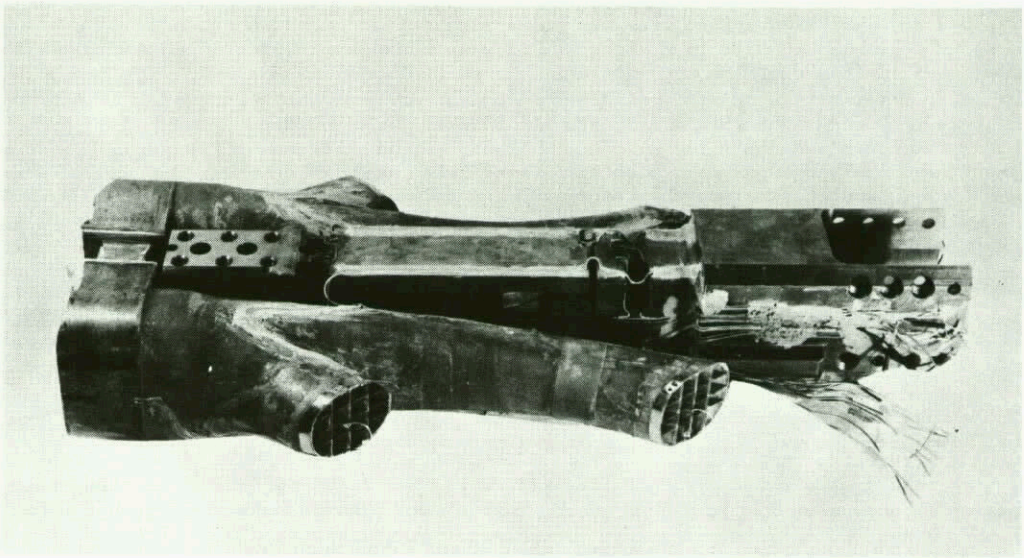

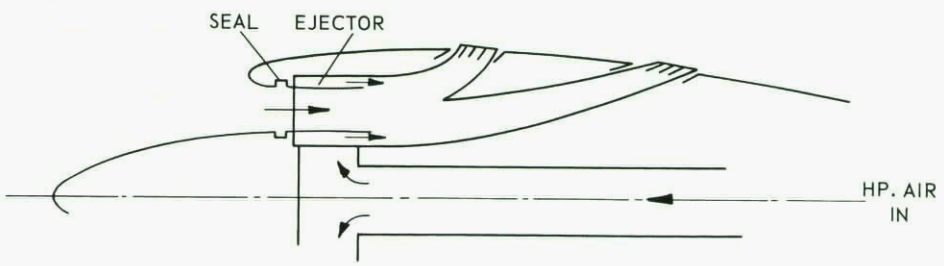

FIG. V. 4 AN EJECTOR SYSTEM FOR INLET AND EXHAUST FLOW.

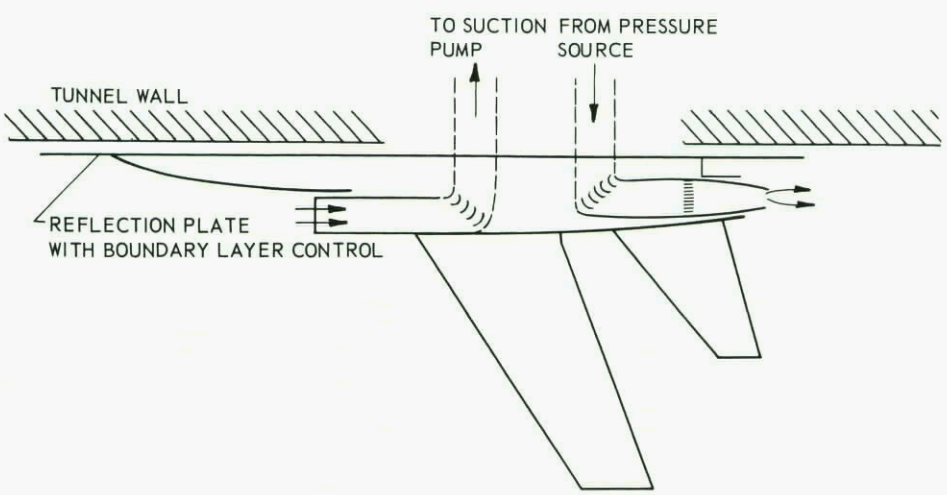

FIG. V. 5 SEMI – SPAN MODEL WITH DIRECT INLET SUCTION AND NOZZLE BLOWING

section can only be used if the air passages to the outside can be made large enough for the inlet mass flow without deteriorating the external flow. In practice this scheme can only be used with integrated engine-airframe systems, using the half model technique of a twin engine aircraft. Fig. V.5 depicts such a set up. However the main problem is the deteriorating effect of the reflection plate boundary layer, which probably can be kept under control for the inlet studies, but will have a disruptive effect on the phenomena looked for at the exhaust. From the point of view of engine interference testing this scheme is very attractive, and if ways could be found to omit the reflection plate boundary layer effects (shock wave-boundary layer interaction, separation, displacement, model boundary layer-plate boundary layer interactions) this method would certainly be used in the future. No examples are known which use this technique with good success.

Of course it is possible to use a combination of external and internal addition of energy, such that the inlet mass flow is scaled same as the temperature corrected exhaust flow, without the necessary use of the semi-model technique. Though this combination of techniques might show good promise, the complexity in manufacture, control and metering rises considerably.

5.3 FINAL REMARKS

The methods for correction are the same as required and/or as used for separate inlet and nozzle testing in transonic wind tunnels. In general less care can be devoted for correct inlet and exhaust simulation and precise measurements of mass flows and forces components in case of internal addition of energy.

Besides the problems concerning engine-airframe interference the wind tunnel experimentalist faces also the usual other wind tunnel problems such as Reynolds number effects at transonic speeds, support interference, the difference in aeroelastic effects of the model and the actual aircraft, non-stationary effects, tunnel wall effects, making the total problem even more difficult. These latter effects are outside the scope of this report, but it can be stated that recent theoretical analysis, which are possible with large high speed computers, make inviscid subcritical interference and deformation predictions possible so that the influence of disturbing effects can be assessed and corrections can be applied. Work along these lines should be encouraged.

5.4 REFERENCES

V-1 J.C. Patterson, Jr. — A wind tunnel investigation of jet-wake effect of a high bypass engine on wing-nacelle interference drag of a subsonic transport. NASA TN D-4693, Aug. 1968.

V-2 D.T. Poland and J.C. Schwanebeck — Turbo-fan thrust determination for the C-5a. AIAA 70-611, June 1970.

V-3 S.E. Aldridge and J.L. Nye — Experimental results of high bypass ratio turbo-fan and wing aerodynamic interference. AGARD C.P. 71, Sept. 1970.

V-4 H.R. Welge and J.R. Ongarato — Powered engine simulator procedures and experience for the DC-10 wing engine at high subsonic speeds. AIAA 5th Aerodynamic testing conference, Tullahoma, May 1970.

V-5 W. Tabakoff and H. Sowers — Drag analysis of powered nacelle for jet engine model tests. Zeitschrift für Flugwissenschaften, April 1969.

APPENDIX

QUESTIONNAIRE

"ENGINE AIRPLANE INTERFERENCE IN TRANSONIC TESTS"

In all points distinction should be made between engines in pods (usually airliners, freighters and large bombers) and integrated airframe-engine configurations (usually fighters).

1 INLETS

1.1 INFLUENCE OF INLET MASS FLOW ON EXTERNAL AERODYNAMICS AND MEASURED FORCES (concerning pressure distributions on nacelles and lifting surfaces, lift, drag, moments, etc.) at transonic speeds.

1.1.1 GENERAL

a Circumstances for which complete inlet mass flow duplication in transonic wind tunnels is necessary.
b Circumstances for which partial inlet mass flow can be allowed.
c Circumstances for which the inlet can be completely faired.
d Specific information that can be obtained from a, b and c.

1.1.2 COMPLETE INLET MASS FLOW

a Techniques used or required for complete inlet mass flow simulation in transonic wind tunnels.
b Advantages and limitations of these techniques.
c Testing technique for determining the external aerodynamic coefficience (C_ℓ, C_m, C_p, etc.).
d Obtainable or required accuracies.

1.1.3 PARTIAL INLET MASS FLOW AND COMPLETE INLET FAIRING AT TRANSONIC SPEEDS

a Rules used.
b Basis of the rules.
c Techniques used.
d Corrections required or introduced for reduction of the wind tunnel data (C_ℓ, C_m, C_p etc.).
e Basis and justification of these corrections.
f Techniques used or required to determine these corrections.
g Expected or required accuracy.

1.1.4 BLEED AIR AND SPILLAGE

a Simulation of bleed air or spillage from inlet mass flow (influence on external air flow).
b Corrections on external flow in case of no complete simulation of spillage and bleed air.
c Basis of such corrections and justification.
d Expected or required accuracy.

1.1.5 CORRECTIONS FROM WIND TUNNEL MODEL TO FULL SCALE (SCALE EFFECTS, REYNOLDS NUMBER)

a Corrections required or used taking into account scale effects, if not yet involved in earlier corrections.
b Expected or required accuracy.

1.1.6 EXPERIENCE ON DATA EVALUATION FROM WIND TUNNEL MEASUREMENTS AND FREE FLIGHT MEASUREMENTS.

1.2 INTERNAL INLET FLOW DETERMINATION IN TRANSONIC WIND TUNNEL TESTS

1.2.1 TECHNIQUES FOR INLET MASS FLOW SIMULATION

a Techniques used or required to achieve complete inlet mass flow simulation till compressor entrance.
b Advantages and/or limitation of these techniques.
c Required overall accuracies.

1.2.2 EXTERNAL FLOW FIELD SIMULATION

a Degree of external flow field simulation for measuring the internal flow field properties.
b Justification of the technique used in case of no complete external flow field simulation.

1.2.3 MEASURING TECHNIQUES

a Techniques used or required to determine the inlet duct internal flow properties (pressure recovery, internal drag etc.).
b Corrections necessary for these techniques.
c Basis and justifications of these corrections.
d Achieved and required accuracies.

1.2.4 SCALE EFFECTS

a Corrections introduced or required to reduce the wind tunnel data to full scale.
b Basis of these corrections.
c Expected or required accuracy of these corrections.

1.2.5 SPILLAGE AND BLEED AIR

a Corrections introduced on the internal inlet flow if spillage and bleed air from the inlet are not completely simulated.
b Justification and basis of these corrections.
c Scale-effects for not complete bleed air and spillage simulation.

1.2.6 COMPARISON BETWEEN WIND TUNNEL TESTS AND FLIGHT DATA

2 ENGINE THRUST

2.1 ENGINE THRUST DEFINITIONS (gross and net).

a Engine thrust definitions as specified by engine companies.
b Advantages and limitations of these definitions.

2.2 TECHNIQUES
a Techniques for measuring and/or determining actual engine thrust.
b Advantages and limitations of these techniques.

2.3 CORRECTIONS
a Corrections for differences between aircraft inlet air flow properties and test cell inlet flow properties.
b Corrections for differences between measured thrust and thrust definitions due to different nozzle conditions.
c Corrections for different altitude conditions.
d Corrections for auxillary power and air take off.
e Basis and justifications of these corrections.
f Overall required and obtained accuracy of the thrust definition.

3 EXHAUSTS

3.1 ENGINE GROSS THRUST MINUS DRAG AT TRANSONIC SPEEDS
a Required or obtained overall accuracy of thrust-drag.

3.1.1 ISOLATED NOZZLE TESTS VERSUS COMPLETE MODEL TESTS
a Advantages and limitations of isolated nozzle tests.
b Advantages and limitations of complete model nozzle tests (also inlet flow).

3.1.2 WIND TUNNEL TESTING SCHEME (ISOLATED AND COMPLETE AIRCRAFT MODEL)
a Testing schemes required or used to obtain thrust-drag performance from wind tunnel data and thrust definition.
b Definition of various thrust and drag terms for various nozzle configurations (reference thrust, static thrust, internal nozzle drag, external nozzle drag, base drag, afterbody drag, reference drag, interference drag).
c Techniques used to determine the various thrust-drags terms.
d Required and achieved accuracies for determination of these terms.

3.1.3 JET SIMULATION IN WIND TUNNELS
a Jet simulation for which thrust-drag terms.
b Requirements for jet simulation parameters (jet pressure ratio, jet temperature ratio, secondary air, specific heats, jet inhomogeneities).
c Jet simulation techniques.
d Limitations and advantages of these techniques.

3.1.4 CORRECTIONS
a Corrections for no external flow field simulation (isolated tests).
b Corrections for thrust-drag terms that do not require jet simulation.
c Corrections for no complete jet simulation in terms where jet effects may be expected.
d Corrections for scale effects.
e Justification and basis of these corrections.
f Required or achieved accuracies of these correction.

3.1.5 COMPARISONS BETWEEN WIND TUNNEL DATA AND FLIGHT DATA

3.2 JET-AIRFRAME INTERFERENCE AT TRANSONIC SPEEDS (EXCEPT THRUST-DRAG)

3.2.1 CIRCUMSTANCES FOR JET-AIRFRAME INTERFERENCE (suction, heating, shock waves).
a Jet simulation required or used.
b No jet simulation required or used.
c Justification.

3.2.2 TECHNIQUES
a Wind tunnel test techniques to measure jet interference.
b Achieved and/or required accuracies.

3.2.3 JET PARAMETERS
a Required or used jet simulation parameters.
b Justification of these parameters.

3.2.4 CORRECTIONS
a Corrections for no jet simulation.
b Corrections for partial jet simulation.
c Corrections for scale effects.
d Basis and justifications of these corrections.
e Required and/or achieved accuracies of these corrections.

3.2.5 COMPARISONS BETWEEN WIND TUNNEL DATA AND FLIGHT DATA

PART III

WALL CORRECTIONS FOR AIRPLANES WITH LIFT IN TRANSONIC WIND TUNNEL TESTS

by

R.Monti

Istituto di Aerodinamica, Universita Degli Studi
Piazzale Tecchio, 80125 Napoli, Italia

ABSTRACT

This part of the Report summarizes the technical information supplied as written contributions or in oral discussions by the Members of the Ad Hoc Committee.

After some preliminary remarks on wall interference corrections in transonic tests, the different answers to the A.G.A.R.D. Questionnaire are presented in Section 2 together with the main points made by the Committee Members as representatives of the different countries. A number of general agreements among the Committee Members are stated which indicate the state-of-the-art of transonic wind tunnel corrections.

Section 3 illustrates the work presently under progress in the Nato Countries which have interest in the field. A number of programs are being carried out which consider some of the problems in transonic wind tunnel testing; a coordination of these programs would be highly desirable in order to reach more efficiently some of the common goals of the national researches already in progress.

Section 4 summarizes the discussions and the conclusions of the Committee on the problems which appear to be most important for future research. Problems are briefly reviewed and research areas are indicated for which the Committee agreed an international program will be most profitable.

A list of References, in alphabetical order, is provided which includes the works referenced by all the different groups participating in the Committee.

1. INTRODUCTION

In general the aim of any test in a wind tunnel is the prediction of the performance and of the aerodynamic characteristics of an aircraft by means of experimental data obtained on a model geometrically similar to the aircraft.

Due to the inevitable constraints posed by the limited size of wind tunnels it is not possible to reproduce exactly all the conditions of an unconstrained flow over a body. Of course the zero constraint free flight conditions will be asymptotically approached in a wind tunnel when the model size becomes less and less compared with the tunnel size. On the other hand, for a given tunnel size, it is generally desiderable to test the largest possible models. This is mainly due to considerations of a faithful reproduction of the real configuration, a better simulation of internal aerodynamics and of the surface conditions; sometimes aeroelastic deformations of the model put another lower limit to model size especially when trying to simulate the free flight Reynolds number.

Since none of the conceivable wind tunnels is able to perfectly simulate the free flight conditions, one must deduce that corrections should be made to the experimental data obtained in all the wind tunnels.The ideal corrections should be such as to restore around the model the flow field which has been altered by the presence of the wind tunnel walls. At each point of the flow field, velocity (in magnitude and in direction) and pressure should be corrected in order to get the true flight values; in this way one would obtain on the model a pressure distribution (and aerodynamic forces) equal to that of free flight.

The three possible configurations for wind tunnels are: 1) the open jet, 2) the closed jet and 3) the partially open (or ventilated) type.

In subsonic open-jet wind tunnels the stream-lines bulge out around the model similar to their behaviour in free flight; but the free jet is surrounded by a chamber in which the static pressure is constant. Therefore in the jet itself the undisturbed free stream pressure is established in a lateral distance which is one half of the jet width; in free flight, on the contrary, the undisturbed pressure is attained only at an infinitely large distance from the model. This means substantially different flow field conditions; in particular the stream lines in the open jet will be more highly curved, and the mean velocities smaller than in free flight.

In a subsonic closed wind tunnel with straight walls the streamlines will follow the model contour near the model surfaces and will become completely straight at the walls. This means reduction of the bulging and a reduced curvature of the streamlines as compared with the free flight conditions and consequently larger mean velocities.

Since many of the wall interference effects for the open and for the closed wind tunnel are of opposite sign it may be possible to eliminate, or at least to reduce, the wall interference effects in a partially open tunnel. This is the reason why the ventilated tunnels are widely used for subsonic, transonic and supersonic speeds. In theory at given free flight conditions, for instance at a given Mach number and Reynolds number, it should in principle be possible to find correct aerodynamic characteristics by the use of ventilated walls with variable permeability along the tunnel axis. It will not be possible however to remove all types of wall interference at different flow conditions by a wall of uniform permeability along the test section; corrections for interference effects are therefore needed also for the ventilated walls.

In general the test section geometry for minimizing subsonic wall interference is different from the geometry used at supersonic flow conditions (i.e. cancellation of the shock waves and expansions arriving at the walls which would otherwise be reflected back into the model).

In transonic flows where both these types of interference are present, the situation is more complicated and the problem more difficult.

The boundary interference problem is intensified at transonic high-lift and maneuvering conditions. Blockage and circulation effects will require proper accomodation of the highly deflected wake. At the same time the transonic buffet and flutter boundaries may become obliterated in the presence of the high turbulence levels coupled with the intense noise field.

The difficulties involved in correcting wind tunnel data account for the extreme attitude of some people: if strong doubts exist on wall corrections, and if these are not small because of the large blockage and high lift, it may be better to make direct calculations of the aerodynamic characteristics instead of wind tunnel tests plus a number of (non-reliable) calculations of the data corrections.

Historically, the problem of tunnel boundary interference has been approached in two distinct ways:
1) theoretical calculation of the interference effects and subsequent correction of the data, and
2) empirical development of walls which show as little interference as possible. Substantial progress has been achieved on each approach individually, although little effort has been made to combine them into a unified program.

The major effects caused by wind tunnel wall interference may be separated and divided into blockage, down wash, buoyancy and streamline curvature.

The blockage consists of a variation of the tunnel cross sectional area due to the model volume (solid blockage) and to the model wake (wake blockage); it affects the velocity, static pressure, the dynamic pressure and all the aerodynamic coefficients. The blockage is caused by the reaction of the tunnel walls on the displacement of the flow by the model (volume and wake). In general the result is a velocity increment at the model centre station and a variation of the static pressure along the test section.

The downwash, or lift interference, is caused by the reaction of the walls on the flow deflection produced by the model; it is important for the induced lift and must be taken into account when measuring the lift coefficient and moment coefficient for models with tail.

The buoyancy is due to the longitudinal pressure gradient which may already be present in the empty tunnel or may be due to: solid and to wake blockage, the induced lift or a non symmetrical test set up. This term mainly affects the drag coefficient.

The streamline curvature may be induced either by the tunnel geometry (empty tunnel) or may be produced by the induced lift. This effect has a direct influence on moment, drag and lift coefficients. The streamline curvature may cause an effective change of the angle of attack at the horizontal tail position which will

therefore be different from the induced angle of attack at the wing: this requires an additional correction to the moment coefficient.

It is generally accepted that these major effects, to a first approximation, can be considered as independent and additive so that, for instance, the blockage effect can be calculated at zero model lift and viceversa.

The wind tunnel types used in transonic testing have had generally two configurations: 1) the slotted (or perforated) walls type originally designed to minimize subsonic wall interference and 2) the perforated-walls type designed to cancel shock waves at supersonic conditions. The permeability of this second kind of wind tunnel wall is much higher than that for minimum transonic wall interference so that they very often behave as open jet tunnels when operating subsonically. For this type of tunnel one could adopt formulae which give corrections to the subsonic open jet wind tunnel; however in situations where the model and/or the lift are rather large the accuracy of these corrections would be questionable.

In a class by itself, and offering a new dimension in minimizing wall interference over the full transonic regime, is the variable porosity wall. As described in Ref.36, the wall porosity to minimize interference effects on, say, lift at a given Mach number has been experimentally established by comparison with tests in a much larger wind tunnel. It appears, however, that the porosity to minimize lift interference is not necessarily optimum for drag and pitching moment measurements. Although the variable porosity approach to minimizing wall interference is successful and highly promising,there is still a question of whether or not empirically determined porosity setting is in principle superior to or more refined than the alternative of applying empirical correction factors to data obtained at fixed porosity.

2. SURVEY ON WIND TUNNEL WALL INTERFERENCE

At the present time there is a renewed interest in transonic testing especially for high lift and/or maneuvering vehicles with close design margins; in addition the increased size of airplanes and the consequently increased flight Reynolds number implies the construction of larger models. Furthermore it appears necessary to test the transonic airfoils up to the stall because of the need of new airfoil shapes which can be adapted to both high speed cruise and high lift coefficient manouvers.

Larger models and high lift models mean large disturbances in wind tunnel flow fields and make it mandatory to adopt reliable corrections for the aerodynamic characteristics of the model. These considerations led the AGARD to make a survey among the NATO Countries on the subject. The purpose of the survey is:

"The wall interference in transonic tests is well understood for the case of zero lfft; however, when the airplane has significant lift the interaction between the airplane and permeable walls is not uniquely determined. The air that flows through the permeable walls is not symmetrical about the airplane. The control of this flow affects the measured force coefficients of the airplane. The purpose of the Ad Hoc Committee is to investigate such effects".

Even though the purpose of the AGARD survey should have been confined to the wind tunnel wall interference for models with high lift in transonic condition, the survey also gave results on subsonic wall interference and on models at low lift.

In fact a number of important points came out of the discussions and of the contributions presented by different countries which are not strictly related to real transonic conditions ($0.9 \leq M \leq 1.3$) but more to high subsonic flow conditions ($.5 \leq M \leq .9$). These contributions were included because transonic wind tunnel flows are not always completely understood so that often experimenters do not make wall interference corrections to the wind tunnel data. For subsonic or supersonic wind tunnel flows, theories are a little better established, a number of corrections formulae are available in the literature and experimental data exist with which theories and other experiments can be compared. In the absence of any more specific information the present tendency is to extrapolate the subsonic wind tunnel correction techniques to transonic regimes.

2.1 AGARD QUESTIONNAIRE

The AGARD Questionnaire is reproduced below for ease of reference:

QUESTIONS

1. What corrections are introduced on the measured coefficients in order to predict airplane performances at angle-of-attack?

2. What control is used in the air flowing through the permeable walls in order to have the correct lift representations?

   A. Is the pressure of each wall controlled independently?

   B. Is the air discharged downstream in the test section or diffuser?

   C. Is the pressure distribution at the wall measured?

   D. Is there any experimental indication of the effect on lift and drag due to change of mass-flow flowing across the porous or slotted walls?

3. What are the basic theoretical and experimental reasons for the selection of the method used?

4. What consideration is given to tunnel turbulence? (Added to some questionnaires).

The answers to the first two points of the Questionnaire are summarized in Table I and Table II (°).The other two questions plus some other points related to the subject problems are briefly discussed and reported below.

(°) The Tables are similar to those presented by Mr.J.Jones to the Ad Hoc Committee General Discussion on Wall Correction.

FRANCE

The main transonic facilities are the S1, S2, S3 tunnels at Modane, the S3 and R1 at Chalais Meudon (ONERA) and the $\Sigma 4$ at St.Cyr (Institute Aerotechnique); they have perforated walls (2 or 4) and different permeabilities (from 6.5% to 21%). In general there seem to be no empty tunnel pressure gradients and therefore no correction for buoyancy deriving from this effect is actually needed.

The maximum blockage ratio of 1% is generally adopted which reduces the correction requirements.

Up to the present time, transonic results obtained in French tunnels have received no wall corrections; the reason is the absence of a reliable theoretical approach to the interference of ventilated walls. This is the motivation for the extensive and systematic researches which are being carried out on different wind tunnel facilities in France, as illustrated in the next Section reporting on the work in progress.

GERMANY

At the Porz-Wahn wind tunnel, tests have been performed with wing area ratios of 5% up to an angle of attack of 15° (with a wall permeability of 6% and holes inclined at 60°) and corrections have been estimated according to Ref.27.

In the Transonic-Wind-Tunnel of AVA generally no corrections for wall-interference are applied. This assumption is reasonable however if the models used are small enough. Three-dimensional models should have blockage less than 1% and a wing area less than 5% of test section area.

Two-dimensional models which are supported at the side walls of the test section and which have therefore a span of 1 m should have a wing chord less than 15 cm. If these limits are exceeded, corrections are calculated and reported for information only, together with the measured coefficients, since wall corrections are uncertain for these flow conditions. These wall corrections are calculated by the linear theory described in Ref.27.

In the wind tunnel at the Technical University of Berlin the air suction was varied but very little influence on the lift and drag was found. For Mach numbers somewhat above 1, the suction effect seems to be within the scatter of the data.

THE NETHERLANDS

All information and answers have been obtained from National Aerospace Laboratory N.L.R.,Amsterdam, as Dutch airplane manufacturers and airlines do not at present have any requirements or experience concerning wind tunnel wall interference.

The answers are based on experience obtained in two transonic facilities: The Pilot Tunnel (PT) and the High Speed Tunnel (HST).

A clear division is made between the high subsonic regime ($.5 \leq M \leq .9$) and the genuine transonic regime ($.9 \leq M \leq 1.3$).

In the real transonic regime N.L.R.cannot supply useful information on wind tunnel wall interference. No corrections are applied, and no experimental investigations on interference effects have been made to determine any kind of wall interference control.

In the high subsonic regime no corrections for wall interference are applied, as certain experiments have indicated that blockage is generally very small, whereas there is no conclusive information with respect to the magnitude of lift interference.

For the large tunnel, blockage ratios have been less than.1%. In special cases, however, corrections have been applied by employing semiempirical correction factors. For instance, for 2-dimensional airfoils a number of corrections have been calculated for : 1) solid blockage (58) (to tunnel speed, static pressure,temperature, dynamic pressure) 2) downwash due to lift (empirically) (to incidence angle and to drag coefficient) and 3) streamline curvature (to incidence angle, lift coefficient, moment coefficient and drag coefficient).

Some tests have been carried out in order to determine empirically the parameters K and P which appear in the linearized boundary conditions for the perturbation velocity potential when an equivalent homogeneous boundary is assumed to replace the real slotted (or perforated) wall (27). The values of K and P, determined by the method of Ref.14, were used to compute correction factors which did not match with the fully empirically determined correction factors. The equivalent homogeneous boundary condition however cannot be assumed for the case where significant model lift exists.

The wall pressure distribution has been measured during the tests of models at increasing angles of attack; when the model had significant lift (about 6° of incidence) a variation of pressure distribution was detected.

U.K.

The work done in the U.K.has been oriented towards using the ventilated tunnel in a closed wall condition as a method of defining a fully corrected set of data. Or alternatively, for two dimensional tunnels the most up-to-date theory is used as a datum for correction methods. These results are then compared with data obtained in the ventilated section and correction coefficients are obtained which follow the theoretical methods . This technique is used up to M=0.88 beyond which the methods of Ref.62 are used, again empirically factored from experimental data with models of varying sizes.

It is considered that a general theory giving correction formulae must always be adjusted by empirical factors to allow for the many variables existing in each tunnel. Participation in International programmes with exchange of models is contemplated.

U.S.A.

Test agencies generally do not apply wall interference corrections to the measured performance of a model at angle-of-attack as long as the model size is well within their standards for negligible interference. However, at nearly all installations, studies are in progress to examine further the validity of this practice. At the present time no one method provides acceptable corrections to all aerodynamic data. Comparati-

ve data from different facilities on the same or similar models provide some insight into the problem. However, the results are often beclouded by differences that are attributed to sources other than wall effects.

Two cases are reported of correction tests made in wind tunnels for which the permeability of the walls is designed for supersonic shock cancellation (from 19% to 22%); in these cases the subsonic corrections for an open jet seem to give satisfactory results.

Variation of wall porosity is the only control that is applied to reduce wall interference; it provides a first order correction to the slope of the lift versus angle-of-attack curve. Second order peculiarities test section walls will provide the correct lift representation at high angles-of-attack.

Regarding the question of the discharge of the plenum air there seems to be a variety of plumbing configurations which appear to be equally successful.

For tunnels which were designed to minimize subsonic wall interference the corrections required are generally small and of questionable validity in the general case and consequently are usually neglected as long as the model blockage is low (say 1%). As an example it has been established experimentally that lifting models of 0,7% blockage (or less) in a test section of 6% permeability experience errors due to the wall interference that are of the same order of magnitude as the experimental errors.

The second class of test sections (i.e.the perforated wall type designed to attenuate the shock waves in the transonic regime) exhibit a permeability much higher than that for minimum wall interference at subsonic speeds. However for these tunnels the linearized theory correction for an open jet test section provides an acceptable correction to the measurements. These corrections have been validated by comparative tests in larger wind tunnels having minimal interference effects. However in any new situation such as high lift, large models etc. the accuracy of the corrections would be highly questionable and must normally be established by comparison with similar tests in large scale facilities.

As for any type of wind tunnel flow, turbulence is of concern, and attempts in varying degrees are made to minimize the turbulence level. The ventilated walls of transonic tunnels tend to increase the fluctuation level, the increase being much greater for perforated walls. One study indicates pressure fluctuations of 3 to 4 psf (at q = 1000 psf)- for a perforated wall and a much lower level (of 1 psf) for a slotted wall. Although the results are not qualified as to the character of the fluctuations it may be expected that the differences are attributed to sound (pressure fluctuations) generated at the perforated wall.

2.2.- Conclusions from the answers to the Questionnaire

From the direct answers and from the different opinions manifested in answering the Questionnaire a number of conclusions can be drawn which give a precise idea about the state of the art of the wind tunnel interference problems in the various NATO Nations:

- Ventilated wall wind tunnels of both the slotted and perforated type are presently used in transonic testings
- Test sections (with two and four ventilated walls) with constant permeability are generally adopted
- There is generally a single plenum chamber around the test sectinn; plenum pressure control is used to establish a desired test section Mach number and there is no independent control of pressure or of mass flow through each wall
- There is a lack of confidence in analytical corrections for ventilated wall interference in transonic testings
- The pressure at the wall is generally not measured during the tests; difficulties exist in the measurement of pressure on slotted and perforated walls
- Attempts to correct wind tunnel (at high subsonic conditions) have been made based on separating the different effects due to blockage, lift and streamline curvature (Table II)
- Experimenters recognize that whenever significant lfft is present the boundary conditions at the walls can be more complicated even at high subsonic conditions
- Solid wall and open jet data are sometimes used as reference
- General practice is to reduce the blockage ratio as much as possible. Maximum blockage ratio of 1% (for 3-D models) seems to be accepted by everybody even in the presence of high lift.
- Everybody seems to be concerned with turbulence level in transonic wind tunnels: the turbulence is actually increased because of the slots or because of the perforations at the walls. However no systematic study and experiments have yet been performed in order to quantify the effect of the turbulence level in tunnel testing. Usually the turbulence has been reduced to the lowest possible level.
- Extensive and time consuming researches on empirical correction factors are not generally carried out in large facilities due to the usual stringent time requirements of the aircraft model tests themselves.
- Common practice is to obtain empirical corrections by comparing wind tunnel results with so called "interference free" data, taken in larger facilities with much smaller blockage ratios. Frequently, however, reliable interference-free data is not available and this creates problems in the determination of an empirical correction factor.

3. WORK IN PROGRESS

The answers to the AGARD questionnaire point out the lack of reliable wall interference corrections to experimental transonic wind tunnel data. The need for an improved situation was strongly felt by all the countries operating transonic wind tunnels and this gave rise to a number of programs to consider some of the main problems related to transonic wind tunnel testing. These program, reported to the Committee, are briefly summarized below.

FRANCE

Work is in progress at Dassault along two lines: 1) Study of an appropriate wall permeability which makes the blockage effect negligible and 2) Adoption of a rather large permeability, which makes the flow behave as a free jet, and appropriate correction of the results for this case. The experimental part of the program is being carried out on the wind tunnel $\sum 4$ at St.Cyr (Institute Aerotechnique).

In some wind tunnel experiments the so-called separation parameter was introduced which appears to be a convenient parameter for the study of the interference effects at high angles of attack. In fact when the flow separates on the model the effective blockage is strongly influenced; preliminary experiments showed that if due account is given to this effect rather good correlations are obtained.

ONERA, in cooperation with the French Government Air Technical Service, has initiated in the national trasonic installations, two experimental programmes expected to furnish some information from which it should be possible to refine the basic rules for transonic wind-tunnel design and for wall corrections, and also to justify some theoretical approaches.

The work is related to three dimensional and also to two-dimensional models because more basic experimental researchcon transonic airfoil sections is still needed in order to improve both the wings for future generation of military and civil aircraft and the performance of rotors (and propellers) for future high-speed V/STOL configurations.

The experimental approach is based on the analysis of the data obtained in a given wind-tunnel with similar models at various scales, i.e. at different blockage ratios; this is expected to give - by extrapolating down to the "zero-scale" - some empirical correction laws to be applied to "large models". The wall porosity is also varied; looking at the variation of a chosen parameter as a function of the wall porosity, for various model scales, should indicate the true value of this parameter, and, consequently, the corrections to be introduced for a given combination of porosity and model-scale (investigated parameters can be: minimum drag, lift gradient, shock-wave location etc.). This kind of approach however is complicated by the Reynolds number effects; for this reason systematic investigations are carried out in variable density tunnels, where different scales can be compared to determine the wall effects, whilst the Reynolds number is kept constant by stagnation pressure adjustment.

The artificial tripping of the transition, and its influence on the results obtained with models of different scale is also investigated, it is hoped that a tripping method can be defined, which will yield the same results at low Reynolds number as those obtained at high ones with natural transition.

1) Two dimensional wing sections

It has appeared necessary to test two-dimensional transonic aerofoils up to and above the stall, with a view to developing new aerofoil shapes suitable for both high-speed cruise and high lift coefficients (manouvering limit of airplanes, stall limit of the retreating blade of a rotor). The selected "calibration" section is of the standard type: NACA 0012. The profile has been subjected to a number of tests, but with some disparate results especially at conditions where a combinatinn of Mach number and high angles of attack gives a supercritical flow on the upper surface. The tests for this aerofoil are carried out in two blow-down variable density tunnels of ONERA:

- S3 at Modane (0.78 x 0.56 m^2; max stagnation pressure = 4 atm.)
- R1 at Chalais-Meudon (0.2 x 0.07 m^2; max. stagnation pressure = 9 atm.)

Both have perforated walls (normal holes); the wall porosity can be widely varied for the investigation of this parameter. Models with many pressure taps have been constructed at three scales to investigate the blockage effect (2.4% - 6%); integrating the measured pressures gives the normal and axial forces and the moment; wake surveys permit the total drag to be derived.

The Reynolds number effects on the maximum lift coefficient for Mach numbers from 0.3 to about 1 is investigated in a rather wide range ($7 \times 10^6 \leq Re \leq 15 \times 10^6$). Adjustment of the stagnation pressure helps to test the different scale models at the same Reynolds number, and, as a result, to eliminate the Reynolds number effect from the wall interactions study.

The experiments made at Chalais-Meudon (RICh) are designed to provide data on wall interference and to correlate with the theoretical analysis presented in Ref.27.

The main difficulty when one wants to correct data for wall interference according to Ref.27 is the lack of the knowledge of the porosity parameter P which is a function of wall geometry (and flow conditions). Different ways of measuring the porosity parameter have been suggested (51) (59) which have not been considered suitable by the experimenters. Furthermore large uncertainties exist about the viscosity effects in the holes (and in the slots). The method adopted is an indirect one: the intefference corrections are experimentally determined and compared with the theoretical values: from the matching of the two a porosity parameter is found. In particular the determination is made according to the Mach number correction based on the location of the shock wave appearing on the NACA profile (tested with three different chord lengths at zero angle of attack); this method has been followed because it appears that the shock wave location is one of the most sensitive parameters to the Mach number in the test section.

For a permeability of 12.5% the shock location does not change, at a given Mach number ($.8 \leq M \leq .95$), for the three different blockage ratios corresponding to the three model sizes; it is assumed that the Mach number correction is zero in these conditions. Comparing theoretical predictions and experimental data, a plot of the porosity parameter versus wall permeability (0 - 12%) is found which seems to be relatively constant with Mach number.

These effective porosity values have been used to calculate the theoretical corrections to the lift curve slope. Only preliminary results have been obtained (at low Mach number $M \simeq 0.4$) from which one may conclude that corrections to lift seems to be as good as the blockage corrections except at the maximum value of the lift coefficient.

A number of experiments made in the S3 tunnel at Modane show an unfavorable Reynolds number effect on the maximum lift coefficient which appears to decrease when going from Reynolds numbers of 1.8×10^6 to 5.3×10^6 in transonic flows: however more information is needed about this effect expecially at Reynolds numbers of the order of those obtained in cruise flight ($Re \simeq 40 \times 10^6$).

2) Three dimensional tests

Two programs are in progress on 3 - D geometries.

In the first program, tests at transonic speeds of complete aeroplane models (at 5 different scales) of a modern subsonic transport, in the Mach 0.85 class, are being made in 4 French transonic wind tunnels (at Modane, Chalais-Meudon and at St.Cyr).

The purpose of this program is to:

a) Investigate the possibility of defining wall corrections suitable for tests carried out on larger models than currently in use (the use of a larger model increases the Reynolds number and the realistic representation of details of the project configuration).

b) Systematically investigate the influence of the Reynolds Number on the aerodynamics of a project (longidunal and lateral stability, drag components, onset of transonic troubles, maximum lift versus Mach number, etc.).

c) Calibrate the French transonic tunnels, and make the necessary improvements required to improve the accuracy of the results for the users.

d) Extend this calibration operation to facilities in other countries, to facilitate comparisons of results obtained in specific projects launched within the framework of multinational civilian and military programs.

The second program considers bodies of revolution to study the blockage effects in the same transonic tunnels on axisymmetric models of an "equivalent" area to the complete aeroplane models (area rule). This program is aimed at finding :

a) the corrections to be made as a function of the blockage and porosity ratios;
b) the perturbations due to the shock-waves reflection onto the model from the walls for Mach number $M \simeq 1$ for various model scales and porosities in a given tunnel;
c) the comparison of results obtained for various tunnel height/span ratios and for different turbulence levels.

Preliminary results have been presented on the influence of the blockage ratio in the wind tunnel with a 21% permeability and on the influence of the porosity ratio (for a blockage of 0.59%).

THE NETHERLANDS

Work is in progress at NLR along the lines of an indirect determination of the wall interference effects in slotted tunnels. A method has been developed, applicable to all types of wind tunnels with ventilated top and bottom walls (either slotted or perforated), by which it is possible to determine the overall wall interference effect on the drag coefficient of 2-dimensional airfoil profiles.

The so called drag-balance method is based on the equation:

$$C_{d_p} + C_{d_f} + \Sigma C_{d_i} = \lambda C_{d_w}$$

where C_{d_p} is the profile drag coefficient from model surface pressure measurements, C_{d_f} is the skin friction drag coefficient from theoretical calculations using the measured surface pressure distribution, ΣC_{d_i} is the sum of all drag increments due to wall interference and λ is a correction factor on C_{d_w} for blockage interference (Ref.81) C_{d_w} is the total drag coefficient from total head wake measurements.
The overall wall interference effect C_{d_i} is made up of various buoyancy components related to solid blockage, wake blockage, upwash, streamline curvature, sidewall induced static pressure gradient, separation etc. Using the theoretical approach of the linearized homogeneous equivalent boundary condition one can calculate these various buoyancy components for given values of the wall geometry parameter K and the ventilation porosity parameter P (or rather β/P where β = the Prandtl factor $\sqrt{1 - M^2}$, see Ref.27 and 60).

By equating the measured values of ΣC_{d_i} with the calculated values as a function of K and β/P for a given flow condition, one obtains the appropriate K and β/P values.

Application of this method on a set of 2-dimensional models (including lifting and non-lifting models with peaky pressure distribution) over a wide range of Mach number and incidence has given satisfactory results (83). It was found that the method yields results with reasonable accuracy (in the order of 10 dragcounts or better) up to the point where a large supersonic flow region has developed over the model, terminated by a fairly strong shock.

The characteristic wall parameters K and β/P of the wind tunnel were found to be essentially constant up to this point.

Investigations are presently made on the influence of chord to tunnel height ratio c/h, Reynolds number and the pressure distribution on these wall parameters.

It should be pointed out that even though the value of the wall parameters might be a function of the absolute Reynolds number, the drag-balance method when properly applied is essentially independent of the Reynolds number.

U.K.

Groups in the U.K.tend to approach the problems of wall interference mainly from the empirical point of view.

It is in general considered unwise to rely theoretical ventilated wall interference corrections because of the particular characteristics of each transonic facility.

Better confidence is shown in using the transonic tunnels with temporarily closed walls to derive corrected

results for this simpler wall geometry and then to compare these results with those obtained in ventilated (perforated) walls. This procedure can be applied up to M = .88 for standard bodies (wings or body + wings) and 0.75% blockage. The main contribution to the correction for the drag coefficient C_D seems to be the blockage buoyancy for the case of zero lift.

The Mach number correction due to the solid blockage is negligible in the large ARA tunnel for $M \leq .86$. The curvature effect is also considered and found to be negligibly small.

U.S.A.

Many researches are presently under progress in different areas related to transonic wind tunnel testings. In nearly all installations, studies are made to examine the validity of the practice of not applying any wall interference correction if the model size is smaller than a given fraction of the wind tunnel area, independent of the magnitude of the model lift.

In Ref.69 a program, similar to that presently in progress in France, is illustrated which collects data taken in different facilities on a scale model of the C5-A aircraft.

Studies are being made of transonic tunnel turbulence : the turbulence is particularly important in high speed wind tunnels for the study of buffet problems, flutter, inlet buzz and other dynamic phenomena. Even though the role of the free stream turbulence in boundary layer transition has been recognized, its effect has not been explicitely analyzed in transonic wind tunnel testing. It appears necessary that turbulence level be mentioned as an integral part of any aerodynamic test program.

Preliminary exploitation of variable porosity walls seems to indicate a possible way of obtaining interference free data in a particular Mach number range. In fact it has been shown that is is not possible, for instance, to eliminate pitching moment interference simultaneously with lift interference when using walls with uniformly distributed porosity. However, some recent unpublished data obtained at the AEDC indicates that possibly this can be accomplished by using streamwise distribution of porosity and this concept may develop into a third generation wall. A perforated wall has been developed (59) to cancel these model-induced disturbances and thus provide interference - free flow at only one specific Mach number; however, a variable-porosity wall (23) (37) can provide practically interference-free flow throughout the Mach number range from 1.05 to 1.40.

In addition a study is being made of the possibility of changing the wall effective porosity by means of a combination of permeable wall and plates which are located at different distances from the perforated walls in the plenum chamber; different pressure conditions at the wall can therefore be established along the test section due to the variable gap.

Another source of interference effects influencing the data obtained from wind tunnel model tests arises from the need to support the model firmly throughout a range of model attitudes relative to the moving airstream. The presence of a model support system near the model, as well as possible modifications to the model contour which may be necessary for support attachment, introduce extraneous aerodynamic forces giving model results that differ from those of the free-flight aircraft. The magnitude and nature of these interference effects is a function of the support systems design and size relative to the model, the geometric modifications to the model, the wind tunnel test conditions, and the specific model configuration.

The only support system capable of giving completely interference-free data would be one of the force field type such as the magnetic model support system. In the United States, work of this concept has been performed at the Massachusetts Institute of Technology (67), the University of Virginia, and the Arnold Engineering Development Center. The tunnels using magnetic model supports are relatively small, and are used mostly for fundamental research programs. The direct application of magnetic model support technology to large scale development tunnels has not yet proved feasible, but such an approach could theoretically eliminate the support interference problem.

In the classical case of geometrically similar shapes of different scale, a matching of Reynolds number and Mach number will result in proportionate scaling of flows about the shapes and corresponding duplication of the aerodynamic forces and moments coefficients. In the practical case, however, Reynolds number matching of flight conditions in existing wind tunnels is unattainable for a large class of airplanes of present and future interest. To cope with this problem, the aerodynamicists must devise means of simulating the effects of flight Reynolds number and methods for accurate extrapolation of wind tunnel test results to flight conditions.

Because of the current lack of facilities to provide flight Reynolds numbers recent emphasis has been on trying to artificially achieve correct flow simulation on models in wind tunnels using the present state-of-the-art techniques to account for Reynolds number effects. The customary approach is to fix boundary layer transition on the model, particularly winged configurations, near the leading edge where it would occur naturally on the airplane in flight. By this procedure, laminar separation (aft to the fixed transition) unrepresentative of flight conditions is avoided.

One rational approach to develop a wind tunnel test technique for simulating full-scale flows over airfoils with shock-induced separations is based on experimentation at the Langley Research Center and is reported in Ref.20. This technique involves locating the boundary-layer trip aft of the leading edge at such a position, that, at the wind tunnel test conditions. the resulting turbulent-boundary-layer thickness at the trailing edge is similar to that which would be experienced at flight conditions.

The investigation was conduced using a two-dimensional model spanning the wind tunnel test section.

There is an effort underway at the Arnold Engineering Development Center to develop techniques for simulating the flow over sensitive airfoils such as that used on the C-141. In addition, efforts are currently underway at the Langley Research Center to apply the technique of Ref.20 to three-dimensional swept wings, although only limited success has been achieved to date. Another approach being investigated at the Ames Research Center, in cooperation with the Air Force Flight Dynamics Laboratory and the Lockheed-Georgia Company, involves the use of a large swept constant-chord wing-panel model of a C-141 wing section. The objective of this approach, which has not yet proved successful because of model and support interference effects, is to determine the effect of Reynolds number, up to approximate flight values, on the two-dimensional characteristics of swept wing sections subject to shock-induced separation.

4. GENERAL DISCUSSION AND CONCLUSIONS

A number of topics have been examined by the Commitee in the plenary discussion held in Florence (Italy) and the different opinions have been compared. The field of interest of the original AGARD Questionnaire has been somewhat broadened; extended discussions led to the observations and recommendations contained in the second part of the Final Report prepared by the Chairman of the Ad Hoc Committee Prof.A. Ferri.

The main topics on which some general agreement was reached, are: 1) Better Criteria for Blockages 2) Availability of reliable experimental data for tunnel calibration 3) Theoretical investigation of wall interference 4) Reynolds number effect 5) Turbulence effects.

1) All the experimenters who have not carried out extensive wall interference tests on their tunnels (very often in the more important facilities there is little time available to improve test techniques) try to minimize the model blockage ratio defined as the ratio of the maximum cross sectional area of the model to the tunnel test section cross sectional area. The generally accepted maximum value of the blockage ratio is about 1%, within this maximum it is common for no correction for wall interference to be applied to the experimental data. Some tunnels however have established experimentally their own level of interference corrections by comparative methods. In 3-D tunnels blockages of .5% to 1% generally mean models which span .5 to .7 of the tunnel width (depending on the model aspect ratio); at these conditions only a small increase of the model size beyond the limiting 1% seems to be possible. On the contrary in 2-D tunnels it is important to be able to increase the model size to increase Reynolds numbers and to simplify pressure plotting techniques.

If the above mentioned blockages are meaningful for models at small angle of attack, they may have no physical meaning in the presence of high lift and flow separation; in these cases one should more properly refer to lift or to separation blockages. It seems very important to have an experimental way of checking if the effective blockage is actually small enough for negligible wall intefference effects.

A possible and practical diagnostic means could be to monitor pressure at the test section wall during the run; practical difficulties may exist for pressure measurement on ventilated walls (especially perforated walls), but the method seems to be worth exploring.

A practical criterion could be the formulation of a unique parameter, which combines solid and wake (or separation) blockages plus model lift, defining an "effective" blockage (function of wall geometry and test conditions); an upper limit of this parameter could then practically ensure wall interference-free data. It may prove more difficult (if possible at all) to establish corrections to other wind tunnel data as a function of this one unique parameter.

2) A need for reliable interference-free data is strongly felt both for 2-D and for 3-D models in transonic wind tunnel calibration. Common practice is to extrapolate wind tunnel data taken at different blockage ratios, down to zero blockage conditions. This implies a large number of tests in different wind tunnels (or preferably in the same wind tunnel with different models); a number of difficulties still exist for ensuring the same test conditions (model accuracies, Reynolds number, unit Reynolds number, aeroelastic effects) and sometimes the validity of the extrapolation does not hold down to zero blockage.

An international program is desirable for: the exchange of data, definition of calibration models (similar national programs have already been initiated in France and in USA as reported in Section 3), definition of the tests and collection of model flight data (interference free); when all these information will be available it will be possible to undertake systematic and extensive studies on third generation (variable permeability) walls.

3) Wall interference corrections are available by a linearized theory and superposition of image singularities for a model with lift. The following points should be considered: first, the theory will not be valid approaching Mach number one; second, if the flow distortion is large (because of significant lift or large separation) one cannot expect the linearized theory to hold because of violation of the small perturbation assumptions and because of the shape of the vortices generated by 3-D models; third, so called homogeneous wall boundary conditions (replacing both slotted and perforated wall) does not seem to hold for highly distorted flows.

Extensive discussion was made on two possible lines of research to improve the present situation of the wall interference: 1) studying variable porosity wall from both a theoretical and an experimental point of view as a possible method of reducing the wall interferences, 2) considering well-defined and simple boundary conditions (open jet and closed wall wind tunnel) which are amenable to more reliable analysis for furnishing wall interference data corrections.

The first approach deals with very complex boundary conditions which should minimize the wall interferences; however these conditions further complicate the analytical treatment of the problem. The second approach, on the opposite tries to deal with simpler boundary conditions, involving larger wall interference, which however could be more easily computed by theoretical analyses.

4) The problem of the Reynolds number effect and its simulation in wind tunnels is very important and justifies very extensive research efforts. Artificial transition and devices for tripping boundary layer transition, turbulent boundary layer separation and its influence on shock wave locations and unit Reynolds number effects are all problems which can invalidate wind tunnel tests, if not properly accounted for. The C-141 airplane wind tunnel test data in the low transonic regime was cited as an example where artificial boundary layer tripping in the wind tunnel, at Reynolds numbers lower than free flight, caused a turbulent boundary layer separation, and the shock, at a point forward of where it would naturally occur in free flight. This gave a consequent change in the centre of lift which had an important effect on airplane trimming and air loads.

The need exists to investigate models (particularly 2-D models) in very large, high pressure facilities in order to survey the entire spectrum of Reynolds number effects and to establish criteria for the Reynolds number simulation in transonic wind tunnels.

5) The effect of tunnel turbulence has been examined and discussed. Contributions presented showed that in general very little is known of this item.

Even if there seems to be a general agreement that the tunnel turbulence length scale and magnitude may have relevant effects on the experimental data of the models, not very much has been done at present. Generally the turbulence characteristics of the facilities have not been analyzed and it is not clear how the turbulence is affected by the geometry of the wind tunnels. It would be very interesting to make a systematic study of how different types of turbulence can affect transonic wind tunnel data; tests are to be devised at different turbulence scales in the same facility but at the same time there appears to be an urgent need for an extensive collection of data on this subject.

It would be advisable that the turbulence characteristics of the tunnel should be measured and provided together with all sets of experimental data.

REFERENCES

1. ACUM, W.E.A. :"Note on the evaluation of solid-blockage corrections for rectangular wind tunnels with slotted walls". R. and M. No. 3297 (1962)
2. ALLEN,H.J. and VINCENTI, W.G. :"Wall Interference in a two-dimensional flow wind tunnel, with consideration of the effect of compressibility". NACA Rep. 782 (1944)
3. AOYAMA, K. and WU,J. :"On Transonic Flow field Around Tangent Ogive Bodies" AIAA Paper No. 70-189, January 1970
4. BALDWIN, B.S. Jr, TURNER, J.B. and KNECHTEL, E.D. :"Wall Interference in Wind Tunnels with slotted and porous Boundaries at Subsonic Speeds" NACA T,N, 3176 (1954)
5. BOEL, J. and ERDMANN, S.F. :"The NLL transonic and supersonic wind tunnel facilities, with reference to their use for research and development testing" NLL Report MP. 183, presented at AGARD-STA W.T. Panel Meeting 1959
6. BOLTZ,F.W., KENYON, G.C. and ALLEN, C.Q. :"The Boundary Layer Transition Characteristics of Two Bodies of Revolution, a Flat Plate, and an Unswept Wing in a Flow-Turbulence Wind Tunnel" NASA TN D-309
7. BOROVIK, Y. :"Corrections de blocage et corrections de parois en souffleries avec parois perforées"- Avions MARCEL DASSAULT - DOC. Aéro No. 1135 Avril 1970 - Non publié
8. BOSSEL, H. :"Flow Studies and Turbulence Measurements in the Hesse 6-Inch Supersonic Wind Tunnel " Report No. AS-67-2, February, 1967, College of Engineering, University of California, Berkeley, California
9. BURG, K. :"Schallnahe Profilumstromungen in blockierten Kanal" Acta Mechanica 5 (1968) S. 213-236
10. CAHILL, J.R. and STANEWSKY, E. :"Wind Tunnel Tests of a Large Chord, Swept Panel Model to Investigate Shock-Induced Separation Phenomena" AFFDL-TR-69-78. Prepared by Lockheed-Georgia Co., October 1969
11. CAHN, M. :"An Experimental Investigation of Sting-Support Effects on Drag and a Comparison with Jet Effects at Transonic Speeds" NACA RM L56F18a, September 24, 1956
12. CARTER, E.C. :"Some Measurements of the Interference of a Sting Support on the Pressure Distributions on a Rear Fuselage and Tailplane at Subsonic Speeds" ARA Wind Tunnel Note No. 67, October 1967
13. CARTER E.C. :"Some Measurements of Porous Tunnel Wall Interference in the A.R.A. 8'x9' Tunnel" ARA Report 19- Paper to be presented at the 35th Meeting of the Supersonic Tunnel Association at L.T.V. Aerospace Corporation, Dallas, Texas - March 1971
14. CHEN, C.F. and MEARS,J.W. :"Experimental and theoretical study of mean boundary conditions at perforated and longitudinally tunnel walls". AEDC T.R. 57-20 (1957)
15. CHEVALIER, J.P. :"Téchnique et résultats d'essai dans le domaine des vitesses transoniques". Colloque International de Mécanique, Poitiers - 1950 PST No. 250
16. CHEW, W.L. :"Experimental and theoretical studies on three-dimensional wave reflection in transonic test sections" PART III, AEDC TN 55-44 (1956)
17. DAVIS, D.D. and MOORE, D. :"Analytical study of blockage-and lift-interference corrections for slotted tunnels obtained by the substitution of an equivalent homogeneous boundary for the discrete slats NACA R.M. L53E07^{b} (1953)
18. ENTHOVEN, M.E.E. :"Determination of wall interference effects in the NLR Pilot Tunnel". To be published as NLR Technical Report, 1971
19. ERDMANN, S.F. and de VICQ, R.F. :"Short Review on Wind Tunnel Facilities of the N.L.R." N.L.R. Internal Note GC. 47, 1964
20. ERICSSON, L.E. and REDING, J.P. :"Aerodynamic Effects of Bulbous Bases" LMSC-4-17-68-4, November 1968
21. ESTABROOKS, B.B. :"Tests on Sting-Support Interference Conducted in the Transonic Model Tunnel - Phase III" AEDC-TN-55-29, October 1955
22. EVANS, J.Y.G. :"Corrections to velocity for wall constraint in a 10x7 feet rectangular tunnel" ARC Random 2662-1949
23. FELIX, A.R. :"Variable Porosity Walls for Transonic Wind Tunnels" NASA TM-X-53295, pp. 54-58 (N66-35551)
24. FLAX, A.H., ROSS,I.G. ,KELSO, R.S., WILDER, J.G. :"Development and Operation of the C.A.L.- Perforated-Throat Transonic Wind Tunnel Transonic Testing Techniques (A Symposium)" I.A.S. National Summer Meeting-Los Angeles - June 24, 1954
25. GANZER,U. :"Eichversuche in ILTUB - Transonic - Windkanal" Fortschr. - Ber. VDI-Z Reihe 7, Nr. 22
26. GARNER, H.C. :"Lift Interference on Three-dimensional wings" AGARDograph 109, S.75-218 (1966)
27. GARNER, H.C. and ROGERS, E.W.E., ACUM, N.E.A. and MASKELL, E.C. :"Subsonic wind tunnel wall corrections" AGARDograph 109 (1966)
28. GOETHALS R. and MENARD,M. :"Contribution à l'étude de l'aile portante en fluide compressible" - Publication Scientifique et Technique No. 299 du Ministére de l'Air - Paris (1955)
29. GOODMAN T.R. :"The Porous Wall Wind Tunnel - Part II - Interference Effect on a Cylindrical Body in a Two Dimensional Tunnel at Subsonic Speed"- Cornell Aeronautical Laboratory - Report No. AD 594-A-3- November 1950
30. GOODMAN, T.R. :"The Porous Wall Wind Tunnel Part III - The Reflection and Absorption of Shock Waves at supersonic speeds" Cornell Aeronautical Laboratory Report - No. AD 706-A-1 November 1950

31. GOTHERT, B. :"Berich 127 der Lilienthal Geselschraft fur Luftfahrforshung" Berlin 1940 pp. 97-101
Traduction française due S.D.I. No. 3693, Ministère de l'Armement - Paris 1946
Traduction du NACA TM 1105

32. GOTHERT B. :Forschungsbericht No. 1216 - D.V.L. Institut fur Aerodynamik Berlin - Adlershof May 1940
Traduction française du S.D.I. No. 3803 - Ministère de l'Armement Paris
Traduction du NACA TM 1300 - Wind Tunnel correction at High Subsonic speeds particularly for an Enclosed circular Tunnel

33. GOTHERT, B. :"Transonic Wind Tunnel Testing - AGARDograph no. 49 (1961)

34. HART, R.G. :"Effects of Stabilizing Fins and a Rear-Support Sting on the Base Pressures of a Body of Revolution in Free Flight at Mach Numbers from 0.7 to 1.3" NACA RM L52E06, September 12, 1952

35. HOLDER,D.R. :"Upwash Interference on Wings of Finite Span in a Rectangular Wind Tunnel with closed side walls and porous - Slotted Floor and Roof"A.R.C. and M 3395 London (1965)

36. JACOCKS, J.L. :"An Evaluation of Interference Effects on a Lifting Model in the AEDC-PWT 4 Foot Transonic Tunnel" AEDC TR 70-72, 1970

37. JACOCKS, J.L. :"Reduction of Wall Interference Effects in the AEDC PWT 1 - Foot Transonic Tunnel with Variable Perforated Walls" AEDC TR 69 -86 , April , 1969

38. JUNGLUTH, H. :"Experimentelle Untersuchungen der schallnahen, ebenen Unstromung einer welligen Wand im blokkierten Kanal. Dissertation an der Universitat Karlsruhe, Nov. 1969

39. KASSNER, R.R. :"Subsonic Flow over a Body Between Porous Walls" WADC Tech. Report-52-9 (1952)

40. KLANN, J.L. and HUFF, R.G. :"Experimental Investigation of Interference Effects of Lateral Support Struts on Afterbody Pressures" NACA RM E56C16 , May 14, 1956

41. KURN,A.G. :"Drag Measurements on a Series of Afterbodies at Transonic Speeds Showing the Effect of Sting Interference" RAE Technical Report No. 66298 September, 1966

42. LO, C.F. and OLIVER, R.H. :"Subsonic lift interference in a wind tunnel with perforated walls" J.of Aircraft, vol. 7, No. 3 May-June 1970, pp. 281-283

43. LOEVE, W. :"On the subsonic Wall interference Effects in the H.S.T. of the N.L.R." N.L.R. TM T. 167, 1967

44. LORENZ, MEYER, W. :"Theor. und. exper. Bestimmung von Windkanalkorrekturen fur den transsonischen Windkanal bei dreidimensionalen Modelen." AVA Bericht 69 A 17

45. LOVE, E.S. :"A Summary of Information on Support Interference at Transonic and Supersonic Speeds" NACA RM L53K12, January 12, 1954

46. LUDWIEG, H. :"Windkanalkorrekturen bei kompressibler Sromung, Gottingen Monographie $D_3$4.2 (1947)

47. LUDWIEG, H. :"Windkanalkorrekturen bei kompressibler Sromung" Gottingen Mongraphie D_3 4.2 (1947)

48. LUMLEY, J.L. :"Passage of a Turbulent Stream Through Honeycomb of Large Length-to-Diameter Ratio" ASME-JOBE, June 1964

49. MACKRODT, P.A. :"Windkanalkorrekturen bei Messungen an 2-dimensionalen Profilen in transsonischen Windkanal der AVA Gottingen, AVA Bericht 69 A 01

50. MAGNUS, R. and YOSHIRARA, H. :"Inviscid Transonic Flow Over Airfoils" AIAA Paper No. 70-47, Jan.970

51. MAEDER, P.F. :"Investigation of the boundary condition at a perforated wall" Techn. Rep. WT 9, Brown University - May 1953

52. MAEDER, P.F. :"Theoretical investigations of subsonic wall interference in rectangular slotted test sections" T.R. WT 11 Division of engineering, Brown University (1953)

53. MAEDER, P.F., ANDERSON, G.F. and CARROLL, J.B. :"Experimental investigation of subsonic wall interference in rectangular slotted test sections" Tech. Rep. W.T. 16, Division of Engineering, Brown University (1955)

54. MAEDER, P.F. and WOOD, A.D. :"Transonic Wind Tunnel Test Seetion-ZAMP Vol. VII 1956, pp. 177-212

55. MORKOVIN, M.V. :"Critical Evaluation of Transition from Laminar to Turbulent Shear Layers with Emphasis on Hypersonically Traveling Bodies" AFFDL-TR 68-149, March 1969

56. PANKHURST, R.C. and HOLDEN, D.W. :"Wind tunnel technique" Pittman and Sons, Ltd.London 1952

57. PATE, S.R. and SCHUELER, C.J. :"Radiated Aerodynamic Noise Effects on Boundary-Layer Transition in Supersonic and Hypersonic Wind Tunnels" AIAA Journal, vol,7, No.3 March 1969

58. PEARCEY, H.H. et al. :"Some Effects of Wind Tunnel Interference Observed in Tests on Two-Dimensional Aerofoils at High Subsonic and Transonic Speeds" AGARD Report 296, 1959

59. PINDZOLA, M. CHEW, W.L. :"A Summary of perforated wall wind tunnel studies at the Arnold Engineering Development Center" AEDC TR 60-9 August 1960

60. PINDZOLA, M. , LO C.F. :"Boundary Interference at subsonic speeds in wind tunnels with ventilated walls" AEDC TR 69.47 May 1969

61. POPE A. :"Wind Tunnel Testing"

62. ROGERS, E.W.E. :"Blockage effects in closed or open tunnels"
AGARDograph 109, S. 279-340 (1966)

63. ROGERS, E.W.E. :"Wall interference in tunnels with ventilated walls"
AGARDograph 109, S 341-430, Aerodynamic Division NPL Teddington (1966)

64. SCHILLING, B.L. - WRIGHT, R.H. :"Calculated wind tunnel boundary lift interference factors for rectangular perforated test sections"
NASA TN D 5635 - January 1970

65. SIVIER , K.R. and BOGDONOFF, S.M. :"The Effect od Support Interference on the Base Pressure of a Body of Revolution at High Reynolds Numbers" Princeton University Report No. 332, AFOSR TN 55-301, October 1955

66. STAFF N. L.R. Fluid Dynamics Division - Aerodynamics at N.L.R.

67. STEPHENS, T. :"Summary of the Design of a Magnetic Suspension and Balance System for the Aeronautical Research Laboratories" ARL 69-0019 January 1969

68. THOM, A. :"Blockage corrections in a closed high speed tunnel, R. and M. No. 2033 (1943)

69. TREON, S.L. STEINLE, F.W. , HOFSTETTER, W.R. and HAGERMAN J.R. :"Data Correlation from Investigations of a High Subsonic Speed Transport Aircraft Model in Three Major Transonic Wind Tunnels" presented at A.I.A.A. Aircraft Design and Operations Meeting, Los Angeles, Calif. July 1969, AIAA Preprint No. 69-794 July, 1969

70. TUNNEL, P.J. :"An Investigation of Sting Support Interference on Base Pressure and Forebody Chord Force at Mach Numbers from 0.60 to 1.30" NACA RM A54K16a, January 28, 1955

71. VAYSSAIRE J.C. :"Corrections de blocage et corrections de parois en fluide compressible" Avions MARCEL DASSAULT - DOC. Aéro No. 1035 Janvier 1970 Non publié

72. VAYSSAIRE, J.C. :"Introduction à l'étude des souffleries dont les interactions de parois sont nulles ou négligeables" Avions MARCEL DASSAULT DOC. Aéro No. 1133 Mai 1970 Non publié

73. VAYSSAIRE J.C. :"Nouvelle méthode de calcul de correction des résultats d'essais en soufflerie basse vitesse (corrections de blocage et corrections de parois)" l'Aeronautique et l'Astronautique PARIS 1969 n. 15 pp. 55 - 67 n. 16 pp.45-57

74. WAGNER, R.D.; MADDALON, D.V. WEINSTEIN, L.M. and HENDERSON, A. Jr. :"Influence of Measured Free Stream Disturbances on Hypersonic Boundary Layer Transition" AIAA Paper 69-704, 1969

75. WEIRICH, P.H. :"Experimentelle Untersuchungen schallnaker, ebexner Profilumstromungen im blockierten Kanal" Mitteilungen des Instituts fur Stromungslehre und Stromungsmaschinen der Techn. Hochschule Karlsuhe, Heft 6, Juni 1967 S.1-17

76. WOODS L.C. :"On the theory of two dimensional wind tunnels with porous wall" Australia Proc. Roy. Soc. A 233 pp. 74 - 90 (1955)

77. WRIGHT R.H. :"The effectiveness of the transonic wind tunnel as a device for Minimizing tunnel boundary interference for model test at transonic speeds" AGARD Report 294 (1959)

78. WRIGHT R.H. and SCHILLING B.L. :"Approximation of the Spanwise Distributions of Wind tunnel boundary interference on Lift of Wings in rectangular perforated wall test sections" NASA TR 285 (May 1968)

79. ZIEREP, J. :"Die quergestellte platte bei schallanstromung" Acta Mechanica 9 (1970), S. 137-141

80. ZIEREP J. :"Der Kopfwellenabstand bei einem spitzen, schlanken korper in schallnaher uberschallnstromung" Acta Mechanica 5 (1968) S. 204-208

81. ZIEREP J. :"Ein Ahnlichkeitsgesets fur den Kanalwandeinfluf fur alle Geschwindigkeitsbereiche" Acta Mechanica 6 (1968) S. 113-114

82. ZONARS, D. :"Large Angle of Attack Model Sting Interference Effects at Transonic Speeds" AGARD Report 301, March 1959

83. ZWAANSVELD, J. :"Dragbalance Method for Determining the Wall Interference in 2-Dimensional Test Sections with Ventilated Walls in a Subsonic Compressible Flow" TR 70055 L.I.

84. ZWAANSVELD, J. :"Principal Data of the NLL Pilot Tunnel" - NLL Report MP 185, 1959.

AKNOWLEDGMENTS

The author wishes to thank all the members of the Ad Hoc Committee on "Engine Airplane Interference in Transonic Tests and Wind Tunnel Wall Interference for Airplane with Lift" for supplying the information contained in this Report. In particular the author wishes to thank the Reviewer, Mr. E.C. Carter, Mr. M.E.E. Enthoven and Mr. J. Jones for their very useful cooperation.

TABLE I

Transonic Wind Tunnels Characteristics

COUNTRY	WIND TUNNEL	INDEPENDENT CONTROL PRESSURE OF EACH WALL ?	AIR DISCHARGED DOWNSTREAM INTO TEST SECTION ? (OR DIFFUSER?)	IS PRESSURE DISTRIBUTION AT WALL MEASURED ?	EXPERIMENTAL EFFECT OF CHANGE OF FLOW THROUGH WALLS ON LIFT AND DRAG ?
FRANCE ONERA	RICH CHALAIS-MEUDON	NO	YES	NO	NO
GERMANY	AVA GOTTINGEN (UNIV.BERLIN-ILTUB)	NO NO	YES YES	NO YES	NO LIMITED-INCONCLUSIVE
THE NETHERLANDS	NLR PILOT NLR HIGh SPEED	NO NO	YES YES	YES NO	NO NO
USA NASA AMES	11' x 11' 14' x 14' 6' x 6' 2' x 2'	NO NO YES NO	YES + PARTIAL AIR REMOVAL YES NO INTO DIFFUSER YES + PARTIAL AIR REMOVAL	NO NO NO NO	NO NO ΔC_L = .001 For Δp = 1PSF NO
LANGLEY	16' (Octagonal TS) 8' Pressure	NO NO	YES + PARTIAL AIR REMOVAL YES + PARTIAL AIR REMOVAL	NO NO } CALIBRATION ONLY	NO NO
LEWIS	8' x 6'	NO	YES + PARTIAL AIR REMOVAL	NO CALIBRATION ONLY	NO
MARSHALL	14"	NO	NO	NO	NO
USAF AEDC	16' x 16' 4' x 4' 1' x 1'	NO NO NO	YES YES + PARTIAL AIR REMOVAL YES	NO NO NO } CALIBRATION ONLY	NO NO NO
CORNELL	8'	NO	YES + PARTIAL AIR REMOVAL	NO	YES LIMITED
U.K.	ARA 9' x 8' TRANSONIC	NO	PLENUM SUCTION INTO DIFFUSER	CALIBRATION ONLY	YES LIMITED

TABLE II

Wall Interference Corrections

S (SLOTTED) ; P (PERFORATED)

SUB. ($.5 \leq M \leq .9$); TRANS. ($.9 \leq M \leq 1.3$)

COUNTRY	FACILITIES	POROSITY (amount, No. of walls, type)	SOLID BLOCKAGE		WAKE BLOCKAGE		DOWNWASH		BUOYANCY		STREAM LINE CURVATURE	
			SUB.	TRANS.	SUB.	TRANS.	SUB.	TRANS.	SUB.	TRANS	SUB.	TRANS
FRANCE	ONERA	6% - 20% 2P - 4P	NO MODEL SIZE RESTRICTED		NO MODEL SIZE RESTRICTED		NO (SMALL)		YES TUNNEL EMPTY		NO	
GERMANY	AVA GOTTINGEN (3D)	6% - 4P	YES REF. 25		YES REF. 25		YES REF. 25		YES WAKE BLOCKAGE		YES REF. 25	
	UNIV.BERLIN (ILTUB)	6% MAX. - 4P - 2P	NO	NO	NO	NO	YES REF. 54	NO	NO	NO	NO	NO
	MAX-PLANCK INST.	- 2S	NO	NO	NO	NO	NO	NO	NO	NO	NO	NO
THE NETHERLANDS	NLR PILOT	4.3% - 2S	NO GENERALLY (SMALL) (EMPIRICAL-2D)	NO (NO RELIAB METHODS)	NO (SMALL)	NO (NO RELIAB METHODS)	NO GENERALLY (EMPIRICAL-2D)	NO (NO RELIAB METHODS)	YES TUNNEL EMPTY	NO	NO GENERALLY (EMPIRICAL-2D	
	NLR HIGH SPEED	7% - 2S	REF. 56				REF. 25		NO SOLID OR WAKE BLOCKAGE		REF. 25	
U.S.A.	GOVERNMENT LABORATORIES	GENERALLY ABOUT 6% } 2-S, 4-P, 4-S/P	NO GENERALLY MODEL SIZE RESTRICTED 0-5-1,0% BLOCKAGE		NO GENERALLY MODEL SIZE RESTRICTED		NO GENERALLY MODEL SIZE RESTRICTED		YES TUNNEL EMPTY NO SOLID OR WAKE BLOCKAGE		NO GENERALLY MODEL SIZE RESTRICTED	
	3 INDUSTRY WIND TUNNELS	19%-22%	NO MODEL SIZE RESTRICTED		NO MODEL SIZE RESTRICTED		2-OPEN JET CORRECTIONS TO M = 0.75 1-EMPIRICAL				NO MODEL SIZE RESTRICTED	
U.K.	ARA TRANSONIC	22% 4P	NO MODEL SIZE $\leq 0.8\%$	THEORY FOR $0.88 \leq M \leq 1$	NO		50% OF OPEN TUNNEL VALUE (MEASURED)		YES - EMPTY TUNNEL (CALIBRATION) YES-BLOCKAGE (MEASURED)		NO ALMOST ZERO (MEASURED)	

NATIONAL DISTRIBUTION CENTRES FOR UNCLASSIFIED AGARD PUBLICATIONS

Unclassified AGARD publications are distributed to NATO Member Nations through the unclassified National Distribution Centres listed below

BELGIUM
General J.DELHAYE
Coordinateur AGARD – V.S.L.
Etat-Major Forces Aériennes
Caserne Prince Baudouin
Place Dailly, Bruxelles 3

CANADA
Director of Scientific Information Services
Defence Research Board
Department of National Defence – 'A' Building
Ottawa, Ontario

DENMARK
Danish Defence Research Board
Østerbrogades Kaserne
Copenhagen Ø

FRANCE
O.N.E.R.A. (Direction)
29, Avenue de la Division Leclerc
92, Châtillon-sous-Bagneux

GERMANY
Zentralstelle für Luftfahrtdokumentation
und Information
Maria-Theresia Str. 21
8 München 27
Attn: Dr Ing. H.J.RAUTENBERG

GREECE
Hellenic Armed Forces Command
D Branch, Athens

ICELAND
Director of Aviation
c/o Flugrad
Reykjavik

ITALY
Aeronautica Militare
Ufficio del Delegato Nazionale all'AGARD
3, Piazzale Adenauer
Roma/EUR

LUXEMBOURG
Obtainable through BELGIUM

NETHERLANDS
Netherlands Delegation to AGARD
National Aerospace Laboratory, NLR
Attn: Mr A.H.GEUDEKER
P.O. Box 126
Delft

NORWAY
Norwegian Defense Research Establishment
Main Library, c/o Mr P.L.EKERN
P.O. Box 25
N-2007 Kjeller

PORTUGAL
Direccao do Servico de Material
da Forca Aerea
Rua de Escola Politecnica 42
Lisboa
Attn: Brig. General Jose de Sousa OLIVEIRA

TURKEY
Turkish General Staff (ARGE)
Ankara

UNITED KINGDOM
Ministry of Technology Reports Centre
Station Square House
St. Mary Cray
Orpington, Kent BR5 3RE

UNITED STATES
National Aeronautics and Space Administration (NASA)
Langley Field, Virginia 23365
Attn: Report Distribution and Storage Unit

* * *

If copies of the original publication are not available at these centres, the following may be purchased from:

Microfiche or Photocopy

National Technical
Information Service (NTIS)
5285 Port Royal Road
Springfield
Virginia 22151, USA

Microfiche

ESRO/ELDO Space
Documentation Service
European Space
Research Organization
114, Avenue de Neuilly
92, Neuilly-sur-Seine, France

Microfiche

Ministry of Technology
Reports Centre
Station Square House
St. Mary Cray
Orpington, Kent BR5 3RE
England

The request for microfiche or photocopy of an AGARD document should include the AGARD serial number, title, author or editor, and publication date. Requests to NTIS should include the NASA accession report number.

Full bibliographical references and abstracts of the newly issued AGARD publications are given in the following bi-monthly abstract journals with indexes:

Scientific and Technical Aerospace Reports (STAR)
published by NASA,
Scientific and Technical Information Facility,
P.O. Box 33, College Park,
Maryland 20740, USA

United States Government Research and Development Report Index (USGDRI), published by the Clearinghouse for Federal Scientific and Technical Information, Springfield, Virginia 22151, USA

Printed by Technical Editing and Reproduction Ltd
Harford House, 7-9 Charlotte St, London. W1P 1HD